2019

Molecular Characterization of Novel Mutations in Fanconi Anemia Patients

Kimberly Rickman

MOLECULAR CHARACTERIZATION OF NOVEL MUTATIONS IN FANCONI ANEMIA PATIENTS

A Thesis Presented to the Faculty of

The Rockefeller University

in Partial Fulfillment of the Requirements for

the degree of Doctor of Philosophy

by

Kimberly Rickman

June 2019

MOLECULAR CHARACTERIZATION OF NOVEL MUTATIONS IN FANCONI ANEMIA PATIENTS

Kimberly Rickman, Ph.D.

The Rockefeller University 2019

Fanconi anemia (FA) is a rare disorder that is characterized by bone-marrow failure in the first decade of life, developmental abnormalities, and predisposition to malignancies. The majority of patients have mutations in one of the 22 known FA genes, while a small number of patients have not been assigned to a complementation group. FA proteins are required for the proper repair of DNA interstrand crosslinks (ICL), a deleterious type of DNA damage that covalently binds DNA strands. We have used Whole Exome Sequencing (WES) in conjunction with cell-based assays to determine disease-causing mutations in a subset of patients enrolled in the International Fanconi Anemia Registry (IFAR) who are not assigned to a known complementation group. In this thesis, we present three cases that were the focus of study.

We describe a new FA complementation group identified in a patient presenting with typical FA features and deficiency of the ubiquitin-conjugating enzyme (E2), UBE2T. No pathogenic gene variants were identified by WES, but RNA sequencing (RNA-seq) uncovered a significant decrease in UBE2T transcript, and western blot confirmed deficiency of UBE2T protein. Sanger

sequencing of genomic DNA revealed a large paternal deletion and maternal duplication resulting from *Alu*-mediated recombination. In the absence of UBE2T, the patient cells are defective for FA pathway activation and are hypersensitive to crosslinking agents. These cellular defects are complemented by expression of wild type *UBE2T* demonstrating that deficiency of the protein UBE2T causes this individual's FA.

WES of a sibling pair with FA revealed biallelic mutations in *FANCD1/BRCA2*. Both siblings presented with multiple developmental abnormalities at birth, but did not develop any early childhood malignancies or hematological abnormalities typically associated with the *FANCD1* complementation group. FANCD1/BRCA2 is best known for its role in homologous recombination directed repair of DNA double strand breaks, a function also required during the repair of ICLs. Each sibling inherited a LOF BRCA2 mutation in *trans* to a missense mutation of the BRCA2 DNA binding domain. Evaluation of BRCA2 DNA binding domain mutations revealed that this domain is important for replication fork protection, and to a lesser extent canonical homologous recombination.

FA is a very heterogeneous disorder and as a consequence of overlapping clinical features, patients may be misdiagnosed with FA *in lieu* of another DNA repair or replication deficiency. Besides identifying FA mutations, we have

identified non-FA patient enrolled in the IFAR. This individual has a defect in resolving DNA replication stress that presented in childhood as tri-lineage bone marrow failure, facial dysmorphia, and small stature. Our analysis demonstrated that the patient cells lack the hallmarks of FA, but are defective for cellular resistance to DNA replication stress.

ACKNOWLEDGEMENTS

I would first like to thank my advisor Dr. Agata Smogorzewska for the wonderful opportunity to pursue my thesis research in her laboratory. I appreciate the tremendous amount of time and energy she has spent mentoring me over the years, from which I have greatly benefited.

I am grateful for my Faculty Advisory Committee, Dr. Hironori Funabiki, Dr. Jean-Laurent Casanova, and Dr. Christopher Park, who have been generous with their time, given advice, and shared their expertise year after year. I would like to thank Dr. Alberto Ciccia for accepting the invitation to be the external examiner on my committee.

I am thankful to the Rockefeller Dean's office and Tri-Institutional MD-PhD program office for their support. A special thank you to Olaf Anderson and Ruthie Gotian who have offered encouragement and advice through the years.

I would also like to acknowledge past and present Smogorzewska laboratory members. A special thank you to Frank Lach for all that he does to keep the laboratory running and for sharing his expertise in gene mutation analysis and chromosomal breakage. I would like to thank Anderson Wang, Sunandini Sridhar, and Liz Garner for their assistance in learning molecular biology techniques when

I joined the laboratory. I would like to acknowledge Ray Noonan for working with me to optimize efficient CRISPR/Cas9 gene editing to generate many cell lines for these studies and for his assistance with experiments. I thank Ryan White for sharing his expertise in flow cytometry and lively discussions.

I thank my fellow grad student and labmate, Brooke for being an amazing colleague and friend through the years. I am appreciative of all our scientific as well as non-scientific talks. I am grateful for the support of my family and friends. I would like to express my gratitude to my husband David for his unwavering support and encouragement throughout the years.

TABLE OF CONTENTS

LIST OF TABLES

LIST OF FIGURES

LIST OF ABBREVIATIONS

3HB	three-helix bundle
53BP1	Tumor suppressor p53 binding protein 1
9-1-1 complex	Rad9-Hus1-Rad1 complex
aa	Amino acid
ACTH	Adrenocorticotropic hormone
AML	Acute myeloid leukemia
APIM	AlkB homolog 2 PCNA-interaction motif
ATM	Ataxia-telangiectasia mutated
ATR	Ataxia-telangiectasia and Rad3-related
ATRIP	ATR-interacting protein
BLM	Bloom syndrome RecQ like helicase
BMF	Bone marrow failure
BMT	Bone marrow transplant
BRCA	Breast cancer susceptibility protein
BRCA1	Breast cancer susceptibility protein 1
BRCA2	Breast cancer susceptibility protein 2
$BRCA2^{mut}$	BRCA2 patient cell line
BrdU	Bromodeoxyuridine
BRIP1	BRCA1 interacting protein C-terminal helicase 1
C-terminus	Carboxyl-terminus

CADD	Combined annotation dependent depletion
Cas9	CRISPR associated protein 9
cDNA	Complementary DNA
CFS	Common fragile sites
CHK1	Checkpoint kinase 1
CHK2	Checkpoint kinase 2
CldU	5-Chloro-2'-deoxyuridine
CMG complex	Cdc45/Mcm2-7/Gins complex
CNS	Central nervous system
CNV	Copy number variant
CPT	Camptothecin
CRISPR	Clustered regularly interspaced short palindromic repeats
CtIP	Ct-BP-interacting protein
DBA	Diamond-Blackfan anemia
DBD	DNA binding domain
DKC	Dyskeratosis congenita
DDR	DNA damage response
DEB	Diepoxybutane
DIG-TMP	Digoxigenin-trimethylpsoralen
DNA-PKcs	DNA-dependent protein kinase, catalytic subunit
DNA2	DNA replication helicase/nuclease 2
DR-GFP	Direct repeat fluorescent protein

DSB	DNA double strand break
dsDNA	Double stranded DNA
DSS1	Decreased sperm survival 1
EM	Electron microscopy
ETAA1	Ewing's tumor-associated antigen 1
EV	Empty vector
EXO1	Exonuclease 1
FA-A	Fanconi anemia complementation group A
FA-D1	Fanconi anemia complementation group D-1
FA-like	Fanconi anemia-like
FAAP100	FA core complex associated protein 100
FAAP24	FA core complex associated protein 24
FAN1	FANCD2/FANCI-associated nuclease 1
FANCA	Fanconi anemia complementation group A
FANCB	Fanconi anemia complementation group B
FANC	Fanconi anemia complementation group C
FANCD1	Fanconi anemia complementation group D1
FANCD2	Fanconi anemia complementation group D2
FANCE	Fanconi anemia complementation group E
FANCF	Fanconi anemia complementation group F
FANCG	Fanconi anemia complementation group G
FANCI	Fanconi anemia complementation group I

FANCJ	Fanconi anemia complementation group J
FANCL	Fanconi anemia complementation group L
FANCM	Fanconi anemia complementation group M
FANCN	Fanconi anemia complementation group N
FANCO	Fanconi anemia complementation group O
FANCP	Fanconi anemia complementation group P
FANCQ	Fanconi anemia complementation group Q
FANCR	Fanconi anemia complementation group R
FANCS	Fanconi anemia complementation group S
FANCT	Fanconi anemia complementation group T
FANCU	Fanconi anemia complementation group U
FANCV	Fanconi anemia complementation group V
FANCW	Fanconi anemia complementation group W
G2-phase	Gap 2 phase
GH	Growth hormone
gnomAD	Genome Aggregation Database
GVHD	Graft versus host disease
HBOC	Hereditary breast and ovarian cancer
HDR	Homology directed repair
HJ	Holliday junction
HR	Homologous recombination
HU	Hydroxyurea

ICL	Interstrand crosslinks
ID2	FANCI/FANCD2
IdU	5-Iodo-2'-deoxyuridine
IFAR	International Fanconi Anemia Registry
IR	Ionizing radiation
KIN	Karyomegalic interstitial nephritis
LCL	Lymphoblastoid cell line
LIG4	DNA Ligase 4
LMNA	Lamin A
LOF	Loss of function
LUC	Luciferase
MMC	Mitomycin C
MRN	MRE11-RAD50-NBS1
N-terminus	Amine-terminus
NAHR	Non-allelic homologous recombination
NBS1	Nijmegen breakage syndrome 1
NEIL3	Nei like DNA glycosylase 3
NHEJ	Non-homologous end joining
NLS	Nuclear localization signal
OB1	Oligonucleotide/oligosaccharide-binding fold 1
OB2	Oligonucleotide/oligosaccharide-binding fold 2
OB3	Oligonucleotide/oligosaccharide-binding fold 3

PALB2	Partner and localizer of BRCA2
PARPi	PARP inhibitor
PB	Peripheral blood
PCNA	Proliferating cell nuclear antigen
PCR	Polymerase chain reaction
PDA	Patent ductus arteriosus
PFAS	Phosphoribosylformylglycinamidine synthase
PI3K	Phosphoinositide 3-kinase
PIKK	Phosphoinositide 3-kinase (PI3K) related kinases
PIP Box	PCNA-interacting protein box
POLδ	DNA-polymerase delta
POL ε	DNA-polymerase epsilon
POLξ	DNA-polymerase zeta
$RAD50^{mut}$	RAD50 patient cell line
RFWD3	Ring finger and WD repeat domain 3
RNAi	RNA interference
RNAseq	RNA sequencing
RPA	Replication protein A
RT q PCR	Quantitative reverse transcription PCR
S-phase	Synthesis-phase
s.d.	Standard deviation
SCC	Squamous cell carcinoma

SCE	Sister chromatid exchange
SDS	Shwachman-Diamond syndrome
sgRNA	Single-guide RNA
shRNA	Short hairpin RNA
siRNA	Small interfering RNAs
$SLX4^{mut}$	SLX4 patient cell line
ssDNA	single stranded DNA
TBI	Total body irradiation
TLS POL	Translesion synthesis polymerase
TMP	Trimethylpsoralen
Ub	Ubiquitin
UBE2T	Ubiquitin conjugating enzyme E2 T
UV	Ultraviolet light
VSD	Ventricular septal defect
VUS	Variant of unknown significance
WES	Whole exome sequencing
WGS	Whole genome sequencing

Chapter 1: Introduction

1.1 DNA replication and genome maintenance

1.1.1 Cell division and replication

For growth and development, cells must undergo cellular reproduction by which the parental cell divides resulting in two genetically identical daughter cells. This requires that the genetic material is precisely duplicated. High fidelity DNA replication is important for cell viability and normal function, and it also prevents mutations and tumorigenesis. The DNA replication machinery, a large multiprotein complex termed the replisome, initiates replication from many places in the eukaryotic genome called replication origins during the S-phase of the cell cycle. At the very basic level, the eukaryotic replisome consists of the Cdc45, MCM2-7, and Gins (CMG) helicase, DNA polymerases, PCNA sliding clamps, primase, and single stranded binding protein RPA (O'Donnell et al., 2013). During replication, the CMG helicase unwinds the DNA duplex and the DNA polymerases synthesize nucleotides along the template parental strand.

During replication, the replisome may encounter many obstacles that pose a risk to precisely copying the genetic material. Cellular responses have evolved to manage replication stress imposed by these obstacles and work to ensure that the genome is fully and accurately reproduced each cell cycle. Cells can also incur damage that is repaired outside of S-phase that can result from normal cellular metabolism or insults from exogenous sources. Repair of these DNA lesions requires many dedicated pathways.

1.1.2 DNA damage response

Damaged DNA must be repaired to ensure integrity of the genetic material to ensure normal function and prevent tumorigenesis. The cellular DNA damage response (DDR) primarily depends on the activation of three phosphoinositide 3-kinase (PI3K) related kinases (PIKK), ATM, ATR, and DNA-PK (Blackford and Jackson, 2017).

DNA-PKcs and ATM activation

The DNA-PKcs and ATM kinase are both involved in signaling and directing repair of DNA double strand breaks (DSB). DNA-PKcs serves as a regulator of DNA repair by non-homologous end joining (NHEJ) and is recruited to DSBs by Ku proteins where it becomes activated and undergoes auto-phosphorylation (Figure 1.1A) (Kienker et al., 2000; Kurimasa et al., 1999). DNA-PKcs binds and stabilizes broken DNA ends to prohibit end-resection and promote NHEJ. NHEJ is the primary repair pathway of DSBs outside of S/G2 phases (Ciccia and Elledge, 2010). DSB repair by NHEJ involves the ligation of the broken ends of DNA and is generally efficient, but is an error-prone repair pathway when DNA ends are joined irrespective of homology (Blackford and Jackson, 2017).

ATM has a more global role in the repair of DSB. ATM is recruited to DSBs through interaction with NBS1, a part of the MRE11-RAD50-NBS1 (MRN) complex

(Figure 1.1B). Activated ATM initiates a signaling cascade that promotes DNA repair activation, chromatin signaling, apoptosis, senescence, and transcription (Blackford and Jackson, 2017; Matsuoka et al., 2007). At DSBs, ATM promotes end-resection to channel repair to the homologous recombination (HR) pathway. Due to crosstalk in DSB repair, ATM activation can contribute to promoting a minority of repair events by NHEJ (Blackford and Jackson, 2017; Ciccia and Elledge, 2010). However, during S/G2 phase of the cell cycle the homologous sister-chromatid is available as a repair template, and homology directed repair predominates.

ATR activation

The ATR kinase is activated in response to DNA replication stress (Figure 1.2). Replication stress is defined as the slowing or stalling of the replication fork (Zeman and Cimprich, 2014). The replisome may encounter many obstacles such as damaged DNA template, difficult to replicate regions (repetitive DNA sequences), active transcription machinery, RNA-DNA hybrids, DNA-protein structures, and secondary DNA structures that all cause replication stress (Zeman and Cimprich, 2014). Activation of oncogenes and rapid cell proliferation also generate replication stress (Ahuja et al., 2016; Neelsen et al., 2013; Zeman and Cimprich, 2014). These obstacles ultimately cause slowing of the DNA polymerases and activation of the ATR kinase.

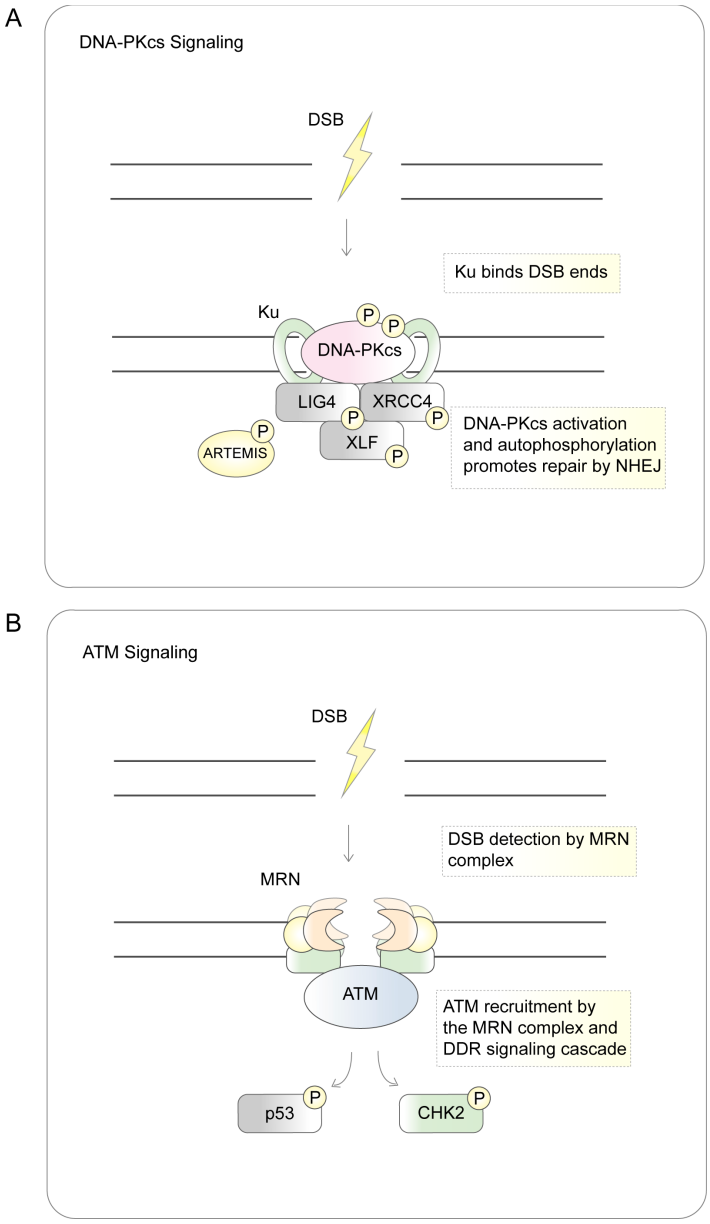

Figure 1.1 Activation of the DDR kinases DNA-PKcs and ATM.

(A) DNA-PKcs is recruited to DSBs by the Ku heterodimer and becomes activated. DNA-PKcs stabilizes the DNA ends and undergoes auto-phosphorylation that permits end processing by ARTEMIS. NHEJ repair factors LIG4/XRCC4 and XLF, promote the ligation of the DNA ends. (B) ATM is recruited to DSBs by the MRN complex. ATM is activated resulting in a signaling cascade that promotes DSB repair by HR and activation of p53 and CHK2. Consequences of the ATM signaling cascade include DDR activation, chromatin signaling, regulation of transcription, senescence, and apoptosis.

The generation of single stranded DNA (ssDNA) at stressed replication forks serves to recruit the ATR interacting protein (ATRIP) (Saldivar et al., 2017; Zou and Elledge, 2003). ATRIP binding facilitates the association of ATR; however, ATR activation requires the binding of an activator protein, either TOPBP1 or ETAA1 (Kumagai et al., 2006). The RAD9-RAD1-HUS1 (9-1-1) checkpoint complex binds at the ssDNA-dsDNA junction and recruits TOPBP1 which directly interact with ATRIP-ATR (Mordes et al., 2008; Zou and Elledge, 2003). ETAA1 binds RPA on ssDNA where it then can activate ATR by association with the ATRIP-ATR complex (Bass et al., 2016; Haahr et al., 2016).

Once activated, ATR phosphorylates downstream targets including the CHK1 kinase to promote the DNA damage response (Blackford and Jackson, 2017; Liu et al., 2006; Sorensen et al., 2004). The ATR kinase modulates the response to replication stress by activating and recruiting DNA repair machinery to DNA lesions, preventing new origin firing, and promoting replication fork stability and processing so that replication may resume (Saldivar et al., 2017). In the absence of ATR, replication stress leads to extensive ssDNA formation resulting in RPA exhaustion and DNA breakage (Toledo et al., 2013). Improper response to replication stress can result in replication fork collapse. In the absence of ATR activity, the replisome components are stable; however, the proteome at the stalled fork is altered reflecting the requirement of ATR activity for modulating effectors of the replication stress response to prevent fork collapse (Dungrawala et al., 2015).

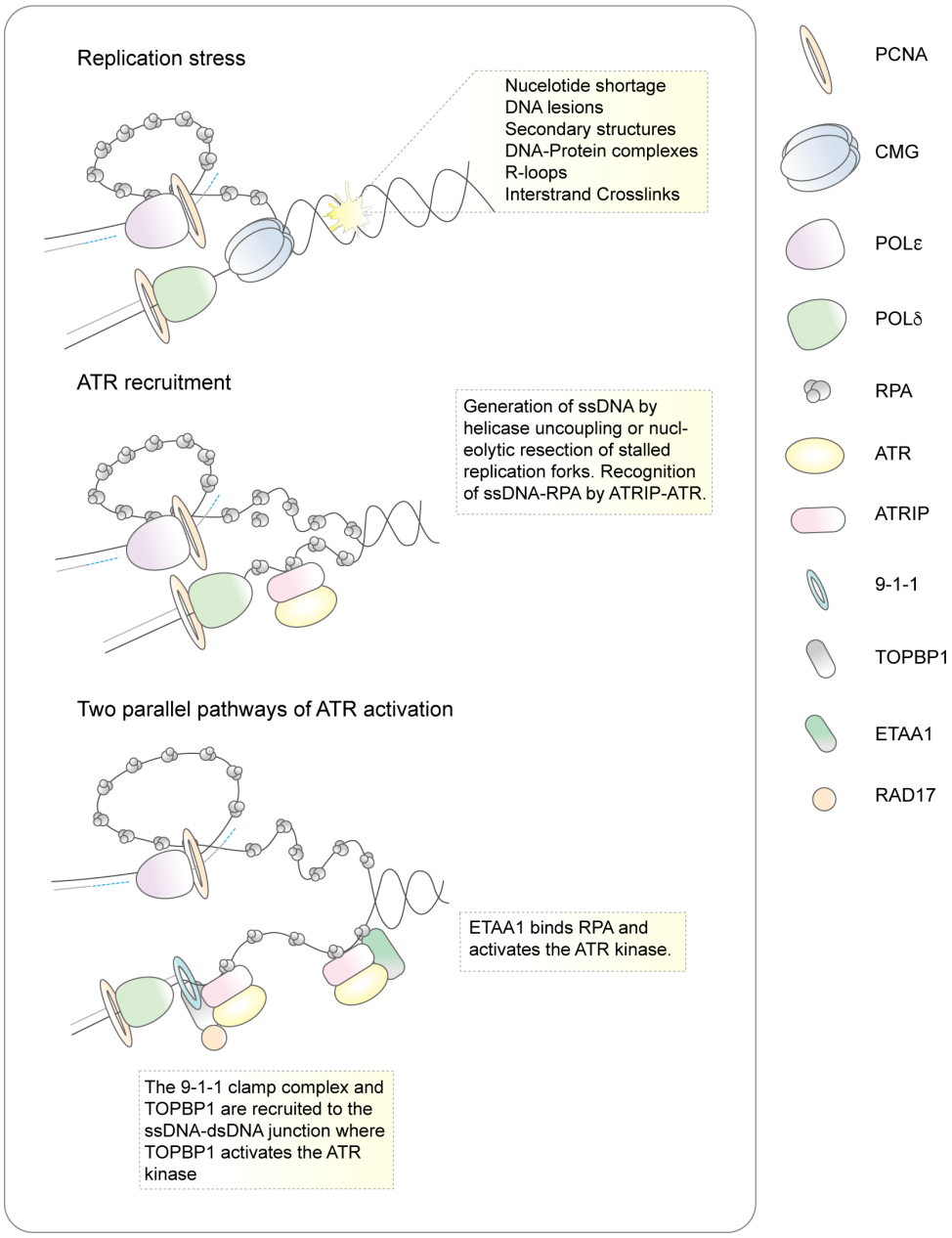

Figure 1.2 Replication stress and ATR activation.

The generation of ssDNA at stressed replication forks serves to recruit ATRIP through ssDNA bound RPA. ATRIP binding facilitates ATR association, but ATR activation requires the binding of an ATR activating protein, TOPBP1 or ETAA1. The 9-1-1 checkpoint complex binds at the ssDNA-dsDNA junction and recruits TOPBP1. ETAA1 interacts with RPA where it interacts with the ATRIP-ATR complex. Once activated, ATR phosphorylates downstream targets including the CHK1 kinase to promote the DNA damage response.

1.2 Fanconi anemia/BRCA DNA repair pathway

The Fanconi anemia (FA) pathway is responsible for resolving interstrand crosslinks (ICLs), deleterious DNA lesions that covalently link the two DNA strands impeding transcription and replication. During DNA replication, ICLs cause replication fork stalling resulting in checkpoint and FA pathway activation (Figure 1.3) (Garcia-Higuera et al., 2001; Knipscheer et al., 2009). FANCM function is important for efficient checkpoint-signaling by ATR; an activity that extends to ICL repair where FANCM is reported to promote ATR activation by regulating RPA recruitment at ICLs (Collis et al., 2008; Huang et al., 2010; Schwab et al., 2010; Singh et al., 2013). ATR activation results in phosphorylation of the FA factors FANCA, FANCG, FANCD2, and FANCI (Ho et al., 2006; Ishiai et al., 2008; Wang, 2008; Wilson et al., 2008). Removal of ICLs is a multistep process requiring activation of the FA core complex (composed of FANCA, FANCB, FANCC, FANCE, FANCF, FANCG, FANCL, FANCM, and their interacting factors), nucleolytic processing at the lesion, translesion synthesis (TLS) past the DNA crosslink adduct, and homologous recombination.

A key step in ICL repair is the core complex-mediated monoubiquitination of FANCD2 and FANCI at K561 and K523, respectively (Garcia-Higuera et al., 2001; Smogorzewska et al., 2007a; Timmers et al., 2001; Walden and Deans, 2014). Ubiquitin transfer requires the activity of an E1 ubiquitin-activating enzyme, an E2 ubiquitin-conjugating enzyme, and an E3 ubiquitin-ligating enzyme (Hershko

and Ciechanover, 1998). The FANCL subunit of the FA core complex is the E3 ubiquitin-ligase that monoubiquitinates FANCD2 and FANCI (Meetei et al., 2003a). UBE2T is the E2 ubiquitin-conjugating enzyme and its interaction with FANCL is required for monoubiquitination of FANCD2 and FANCI (Alpi et al., 2008; Hira et al., 2015; Hodson et al., 2014; Longerich et al., 2009; Machida et al., 2006; Rajendra et al., 2014; Rickman et al., 2015; Sato et al., 2012).

Monoubiquitinated FANCD2 and FANCI form a heterodimer (ID2 complex) that is recruited to chromatin and is required for the downstream processing of the ICL. Nucleolytic unhooking of the crosslink is dependent on FANCP/SLX4 and FANCO/XPF (Kim et al., 2011; Kim et al., 2013; Klein Douwel et al., 2014; Niedernhofer et al., 2004). Unhooking of the ICL enables translesion bypass on one strand and double strand break (DSB) repair by homologous recombination (HR) on the second strand (Howlett et al., 2002; Litman et al., 2005; Long et al., 2011; Xia et al., 2007).

The current working model of interstrand crosslink repair has been corroborated by studies in *Xenopus* egg extracts where replication intermediates of plasmids carrying a site-specific ICL (pICL) can be analyzed synchronously (Zhang and Walter, 2014). Repair in this system is replication dependent and results in ATR activation and monoubiquitination of FANCI and FANCD2 (Raschle et al., 2008). In this model of ICL repair, two replication forks converge on the pICL,

one of the leading strands is extended to within one nucleotide of the lesion, and dual incisions that require XPF are made on either side of the lesion generating a double strand break (Klein Douwel et al., 2014; Raschle et al., 2008; Zhang et al., 2015). In the absence of the I/D2 complex repair of the pICL is defective and no incisions are made (Knipscheer et al., 2009). Translesion synthesis restores the adduct containing strand while RAD51-mediated HR is required to repair the incised DNA ends (Long et al., 2011; Raschle et al., 2015). Synthesis across from the lesion and extension requires a replicative polymerase and a complex of Rev1 and POLξ respectively (Budzowska et al., 2015; Raschle et al., 2008).

An alternative repair pathway of ICLs described from *Xenopus* egg extract studies utilizes the NEIL3 DNA glycosylase. In this model, dual forks converge on the pICL and NEIL3 cleaves a N-glycosyl bond of the psoralen crosslink to release the ICL without incising the DNA (Semlow et al., 2016).

The dual fork model proposed from *Xenopus* egg extract studies is performed on a 6-kb plasmid that guarantees that the replication forks, in this limited space, will converge (Raschle et al., 2008; Zhang and Walter, 2014). However, in mammalian cells distance between origins is much greater and single fork collisions with ICLs may occur. How repair may be similar or different from converging forks is unclear. One proposed mechanism of single fork collisions is ICL traverse. Using DNA-fiber techniques to examine fluorescently labeled ICLs,

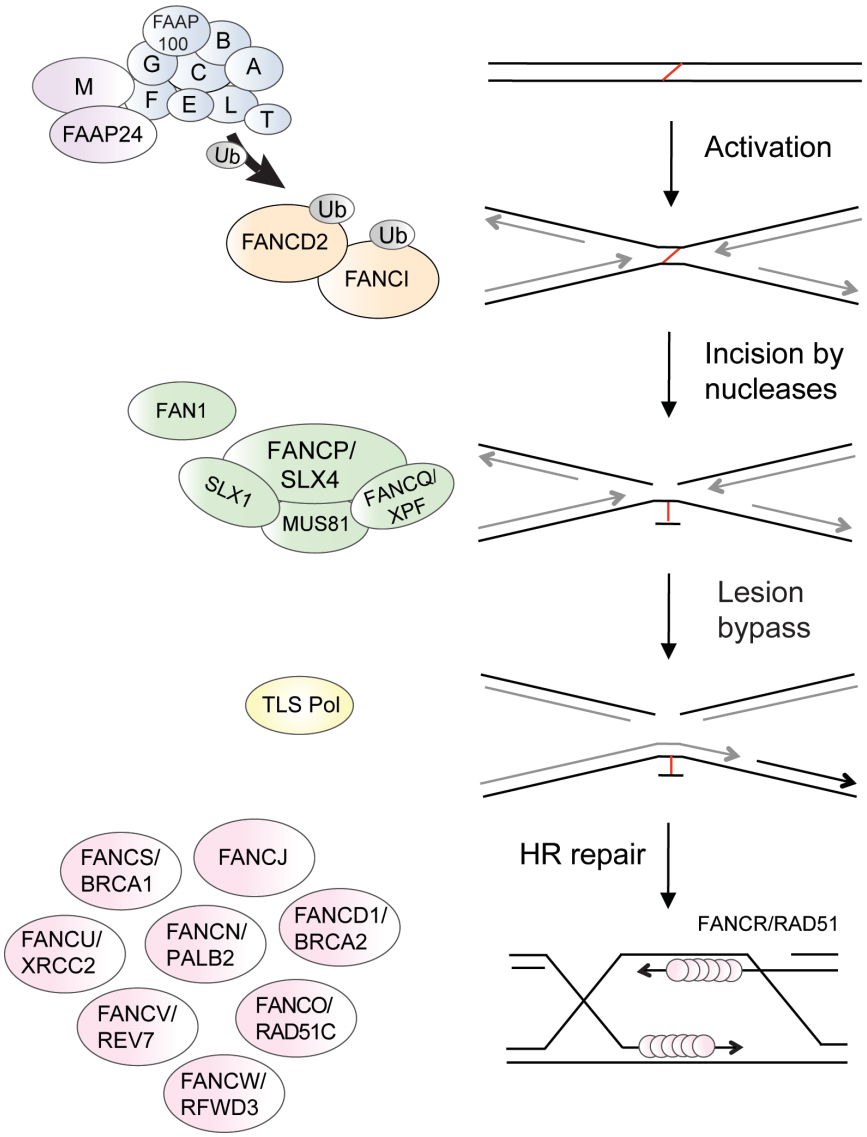

Figure 1.3 Fanconi anemia pathway.

The FA pathway is responsible for resolving DNA interstrand crosslinks (ICLs) that impede DNA replication. Stalling of replication machinery at ICLs results in the activation of the FA pathway. The activated FA core complex composed of 8 FA proteins, FANCA, FANCB, FANCC, FANCE, FANCF, FANCG, FANCL, and FANCM, monoubiquitinates FANCI and FANCD2 via the E3 ubiquitin ligase activity of FANCL and E2 ubiquitin-conjugating enzyme FANCT/UBE2T. The ubiquitinated FANCI and FANCD2 complex orchestrates downstream processing of the ICL, which entails unhooking by nucleolytic processing of the lesion, translesion bypass, and homologous recombination.

it was discovered that in 60% of ICL containing species, lesion bypass occurred without ICL unhooking. ICL traverse required the activity of FANCM (Huang et al., 2013).

In both the ICL traverse and glycosylase studies, psoralen based ICLs were used. NEIL3 mediated repair does not occur on cisplatin based ICLs largely used in other Xenopus studies These data suggest that ICLs produced endogenously or by exogenous chemicals may be repaired by many different pathways and repair mechanisms identified using specific crosslinking agents may not apply to all types of ICLs.

1.3 Disorders of interstrand crosslink repair

1.3.1 Fanconi anemia

Fanconi anemia (FA) is a rare disorder with an incidence of 1/100,000 that results when genes important for resolving DNA interstrand crosslinks are mutated (Kottemann and Smogorzewska, 2013). FA is a heterogeneous disorder characterized by developmental abnormalities, bone marrow failure (BMF), predisposition to solid tumors and leukemia, and cellular hypersensitivity to crosslinking agents (Auerbach, 2009; Nalepa and Clapp, 2018). FA patient mutations have been identified in 22 *FANC* genes, *-A, -B, -C, -D1 (BRCA2), -D2, -E, -F, -G, -I, -J (BRIP), -L, -M, -N (PALB2), -O (RAD51C), -P (SLX4), -Q (XPF), -R (RAD51), -S (BRCA1), -T (UBE2T), -U (XRCC2), -V (REV7*), and -*W (RFWD3)* (Bagby, 2018; Wang and Smogorzewska, 2015). FA is largely inherited in an autosomal recessive manner; however, there are exceptions, *FANCB* is X-linked

and *FANCR* is autosomal dominant (Ameziane et al., 2015; Meetei et al., 2004; Wang et al., 2015). A minority of FA patients still have unknown causative gene mutations.

Patients with FA may present at birth with a spectrum of developmental malformations that range in severity including short stature, renal dysplasia or ectopia, craniofacial abnormalities, radial ray malformations, VATER association, central nervous system defects (CNS), café-au-lait spots, cardiac defects, or gastrointestinal or genitourinary malformations (Alter and Rosenberg, 2013; Nalepa and Clapp, 2018; Stivaros et al., 2015). FA patients often present with BMF in the first decade of life with a median age of seven years old. Some patients will present with acute myeloid leukemia (AML) or myelodysplastic syndrome (Auerbach, 2009). Endocrine dysfunction including growth hormone (GH) deficiency, abnormal glucose metabolism, dyslipidemia, hypothyroidism, hypogonadism, and infertility are frequent in individuals with FA (Petryk et al., 2015). FA patients also develop solid tumors at an increased incidence. Head and neck squamous cell carcinoma (SCC) and anogenital SCC incidence are elevated 500-700 fold in individuals with FA (Kutler et al., 2003; Nalepa and Clapp, 2018).

Diagnosis of FA is based on chromosomal breakage tests of peripheral blood (PB) samples or lymphocytes exposed to either the crosslinking agent diepoxybutane (DEB) or mitomycin C (MMC) (Auerbach, 2009; Auerbach and

Wolman, 1976). FA patient cells show increased chromosomal breakage levels when treated with these genotoxic agents compared to normal cells. Somatic mosaicism of the hematopoietic compartment can occur in FA resulting in partial or full rescue of chromosomal breakage (Gregory et al., 2001; Lo Ten Foe et al., 1997; Soulier et al., 2005; Waisfisz et al., 1999). Patient fibroblasts can be tested in individuals with suspected mosaicism or those post hematopoietic stem cell transplant to confirm diagnosis.

Exogenous compounds, many common chemotherapeutics, such as mitomycin C (MMC), diepoxybutane (DEB), cisplatin, psoralen, and nitrogen mustards can generate DNA ICLs. The endogenous source of DNA ICLs has been an intense area of study and current models provide evidence that naturally occurring biological metabolites such as aldehydes are suspected to generate ICLs *in vivo* (Garaycoechea et al., 2012; Hira et al., 2013; Langevin et al., 2011; Oberbeck et al., 2014; Ren et al., 2013; Ridpath et al., 2007).

Karyomegalic Interstitial Nephritis (KIN) is a second disorder of ICL repair. Although patient cells are sensitive to ICLs the disease is distinct from FA. KIN is an autosomal recessive disorder that results from mutations in Fanconi anemia-associated nuclease 1 (*FAN1*). *FAN1* was discovered as an interactor of the FA pathway, is recruited to ICLs by the ID2 complex, and may have a specific role in the nucleolytic processing of the DNA lesion (Kratz et al., 2010; Liu et al., 2010;

MacKay et al., 2010; Smogorzewska et al., 2010). KIN is characterized by tubular degeneration, fibrosis, and karyomegally in the kidney that results in end stage kidney disease (Zhou et al., 2012). The discovery that *FAN1* mutations do not result in FA was surprising, but recent studies have demonstrated that FAN1 has roles outside of the FA pathway and cells deficient for FAN1 have a milder sensitivity to ICLs than FANC protein deficiency (Thongthip et al., 2016; Zhou et al., 2012).

1.3.2 Homologous recombination deficient FA subtypes

The Fanconi anemia repair pathway requires HR factors for proper ICL repair. A number of proteins mutated in FA, FANCD1/BRCA2, FANCN/PALB2, FANCJ/BRIP1, FANCQ/RAD51C, FANCR/RAD51, and FANCS/BRCA1, are known for their importance in facilitating HR (Howlett et al., 2002; Litman et al., 2005; Rahman et al., 2007; Sawyer et al., 2015; Vaz et al., 2010; Xia et al., 2007). In contrast to other FA subtypes, carriers of single allele mutations in many of these genes (-D1, -N, -J, -Q, and –S) are predisposed to breast and/or ovarian cancers (Bryant et al., 2005; Patel et al., 1998; Rahman et al., 2007; Ratajska et al., 2012; Wong et al., 2011).

FA patients with biallelic mutations in complementation groups *FANCD1/BRCA2* or *FANCN/PALB2* present with a more severe clinical phenotype than those in other complementation groups; developing embryonal malignancies

and acute myeloid leukemia (AML) early in childhood (Alter et al., 2007; Tischkowitz and Xia, 2010). Medulloblastoma and Wilms tumor are the predominant solid tumors of the *FANCD1/BRCA2* and *FANCN/PALB2* complementation group (Alter et al., 2007; Tischkowitz and Xia, 2010).

Biallelic *FANCS/BRCA1* mutations have only recently been described in a limited number of patients. All individuals display a number of congenital abnormalities typical of FA, but no bone marrow failure. Two female individuals identified with biallelic *FANCS/BRCA1* mutations each developed cancer, ovarian and breast, in their 20s. Both of these *BRCA1/FANCS* individuals carried loss of function (LOF) mutations in *trans* to a hypomorphic missense allele (Domchek et al., 2013; Sawyer et al., 2015). In two other families, homozygous LOF mutations have been identified and the children display congenital abnormalities characteristic of FA and one child presented with neuroblastoma at the age of 2 (Freire et al., 2018; Mehmet Demirel, 2016).

FA patients with biallelic *FANCO/RAD51C* mutations present with an FA-like syndrome; characterized by developmental abnormalities and intermediate chromosomal breakage, but no bone marrow failure (Vaz et al., 2010). Similarly, monoallelic dominant negative *FANCR/RAD51* mutations result in an FA-like syndrome characterized by mild chromosomal breakage levels, defects in ICL repair, but no bone marrow failure or cancer (Ameziane et al., 2015; Wang et al.,

2015). Examination of *FANCR*/*RAD51* patient cells revealed intact HR activity likely accounting for the absence of early childhood malignancies associated with *FANCD1* and *FANCN* complementation groups.

1.4 BRCA2 in homologous recombination and cancer susceptibility

1.4.1 BRCA2 structure and function

The identification of the BRCA breast cancer susceptibility genes was pursued on the observation that there was familial clustering of highly penetrant and autosomal dominant breast cancer (King, 2014). Shortly after the discovery of *BRCA1* and *BRCA2,* the generation of mouse models for each, demonstrated that homozygous inactivation of either gene is embryonic lethal and that these genes are essential (Hakem et al., 1996; Liu et al., 1996; Sharan et al., 1997). *BRCA1* and *BRCA2* deficient cells display spontaneous chromosomal aberrations and hypersensitivity to genotoxic agents including DSBs induced by ionizing radiation (IR) (Chen et al., 1998; Connor et al., 1997; Deng and Scott, 2000; Patel et al., 1998; Sharan et al., 1997; Shen et al., 1998). Both BRCA1 and BRCA2 were identified as interactors of the RAD51 recombinase and found to be important for the repair of DSBs by homology directed repair (Chen et al., 1998; Moynahan et al., 1999; Moynahan et al., 2001; Scully et al., 1997; Sharan et al., 1997; Snouwaert et al., 1999).

BRCA2 is a large protein composed of 3418 amino acid (aa) residues and a molecular weight of 390 kDa. At the N-terminus BRCA2 interacts with PALB2 through aa 21-39. BRCA2 has eight BRC repeats composed of aa 1009-2083 that bind to RAD51 (Roy et al., 2012). The BRCA2 DNA binding domain (DBD) is composed of five domains, a helical domain, three oligonucleotide/oligosaccharide binding (OB) folds (OB1/OB2/OB3), and a Tower domain (Yang et al., 2002). The Tower domain is composed of a 130 aa structure of anti-parallel helices that extend out from the OB2 domain and are supporting a three-helix bundle (3HB) (Yang et al., 2002). The BRCA2 DBD binds ssDNA and dsDNA, but the binding preference is for ssDNA tails in the context of dsDNA. This DNA binding activity is dependent on OB2, OB3, and the Tower domain. 3HB domains generally recognize dsDNA so the Tower domain in conjunction with the OB folds may provide recognition of dsDNA/ssDNA junctions (Jensen, 2013; Yang et al., 2002). The small peptide protein DSS1 binds BRCA2 though interaction with the helical domain, OB1, and OB2 (Yang et al., 2002). An NLS and additional RAD51 binding domain are located at the C-terminus (Roy et al., 2012).

1.4.2 Canonical homologous recombination pathway

To initiate DSB repair by HR, BRCA1 localizes to breaks to promote end-resection and the generation of 3' ssDNA overhangs (Jasin and Rothstein, 2013). End resection is modulated by the competing factors 53BP1-Rif1 and BRCA1-CtIP. 53BP1-Rif1 favors end-protection and the NHEJ pathway of DSB repair while

BRCA1-CtIP promotes end-resection and HR (Bunting et al., 2010; Di Virgilio et al., 2013; Escribano-Diaz et al., 2013). Pathway choice by these factors is modulated by chromatin modifications and cyclin dependent kinases to promote HR during S/G2 phases (Nielsen et al., 2016; Tang et al., 2013). The deletion of *53BP1* in *BRCA1* deficient cells rescues HR defects (Bunting et al., 2010). Similarly, deletion of *53BP1* rescues the embryonic lethality of homozygous *BRCA1* mice and suppresses tumor formation (Cao et al., 2009). These data suggest that the primary role of *BRCA1* is pathway choice and to promote end-resection for repair by HR.

The MRE11-RAD50-NBS1 (MRN) complex and the CtIP endonuclease initiate symmetrical end-resection of the DSB in the 3' to 5' direction (Figure 1.4). Longer 3' ssDNA tails are generated by more extensive resection by either the EXO1 exonuclease or the BLM-DNA2 helicase nuclease complex in the 5' to 3' direction (Gravel et al., 2008; Mimitou and Symington, 2008; Sartori et al., 2007; Symington, 2014; Zhu et al., 2008). The ssDNA overhangs are coated by RPA, which is replaced by RAD51 nucleofilaments prior to HR.

PALB2 is a BRCA1 and BRCA2 interacting partner required for proper RAD51 filament formation (Xia et al., 2006). BRCA1 promotes BRCA2 localization to DSBs through the mutual interaction of PALB2 (Sy et al., 2009; Zhang et al., 2009a; Zhang et al., 2009b). While BRCA2-PALB2 interact irrespective of cell

cycle, the BRCA1-PALB2 interaction is inhibited by ubiquitination outside of S/G2 phase. Deubiquitination of PALB2 results in the BRCA1-PALB2-BRCA2 interaction and permits BRCA2 recruitment to DSBs (Orthwein et al., 2015).

BRCA2 is required for displacing the ssDNA binding protein RPA from the 3' overhangs and loading RAD51 nucleofilaments (Jensen et al., 2010; Yang et al., 2005). RAD51 nucleofilaments invade the sister chromatid to perform homology search. The homologous DNA is then used as a template for precise DNA repair (Jasin and Rothstein, 2013; Jensen et al., 2010). Following strand invasion and DNA synthesis, double Holliday junctions (HJ), are dissolved by either the BLM/TOPOIIIa/RMI1-RMI2 (BTR) complex or resolved by nucleolytic processing by GEN1 or the SLX4-SLX1/MUS81-EME1 complex (Sarbajna and West, 2014).

1.4.3 BRCA1 and BRCA2 in cancer susceptibility

Heterozygous germline *BRCA1* or *BRCA2* mutations predispose individuals to hereditary breast and ovarian cancer (HBOC) and to a lesser extent pancreatic, prostate, and other cancers (Prakash et al., 2015). Carriers of *BRCA1* mutations largely experience increased risk of female breast and ovarian cancer. *BRCA2* mutation carriers are predisposed to female and male breast cancer, ovarian, pancreas, and prostate cancers (Attard et al., 2016; Rustgi, 2014; Venkitaraman, 2014). The estimated life-time risk for ovarian cancer by the age of 70 for *BRCA1*

Figure 1.4 Double strand break repair by homologous recombination.

Homologous recombination mediated repair of DSBs requires the formation of 3' ssDNA overhangs. The MRE11-RAD50-NBS1 (MRN) complex senses DSB and with the CtIP endonuclease initiates DNA end resection. The EXO1 exonuclease or the BLM-DNA2 helicase nuclease complex are responsible for more extensive resection. BRCA2 loads and stabilizes RAD51 nucleofilaments on the ssDNA overhangs displacing the ssDNA binding protein RPA. RAD51 nucleofilaments invade the sister chromatid to perform homology search. DNA synthesis can proceed utilizing homologous DNA for precise repair.

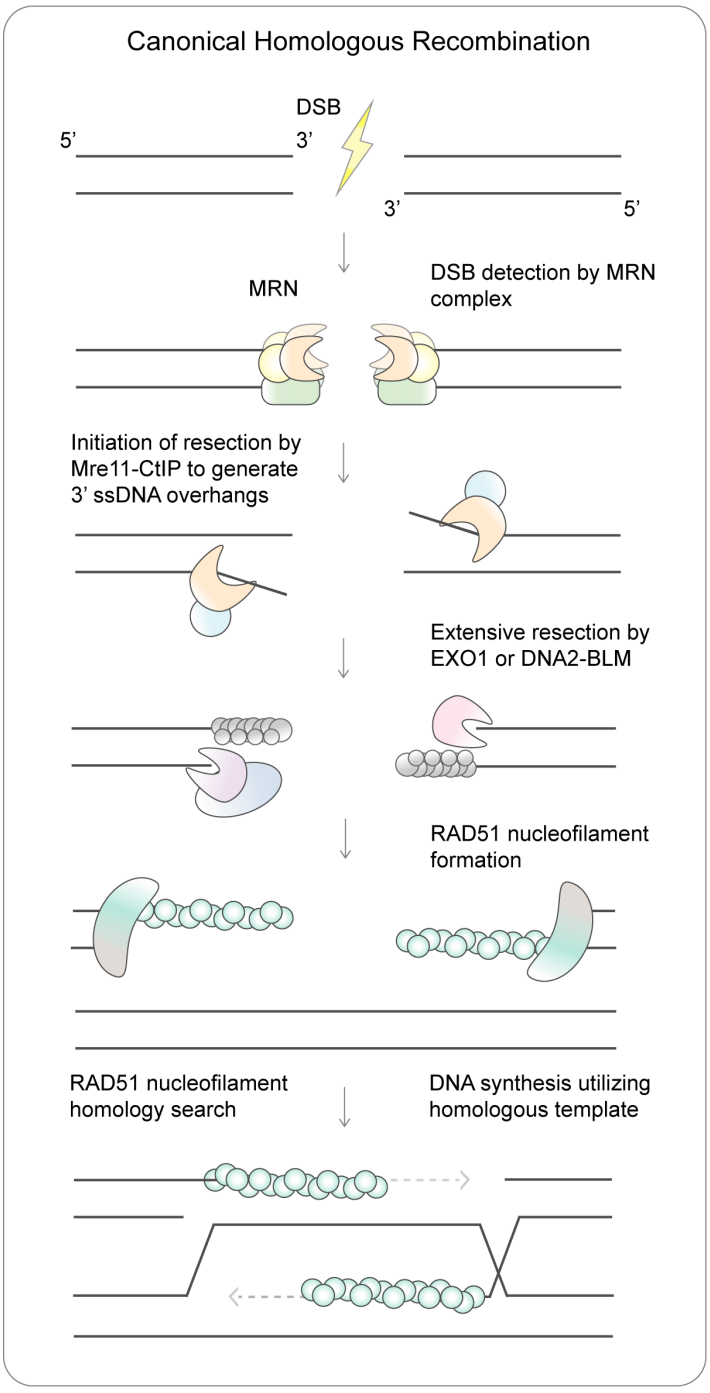

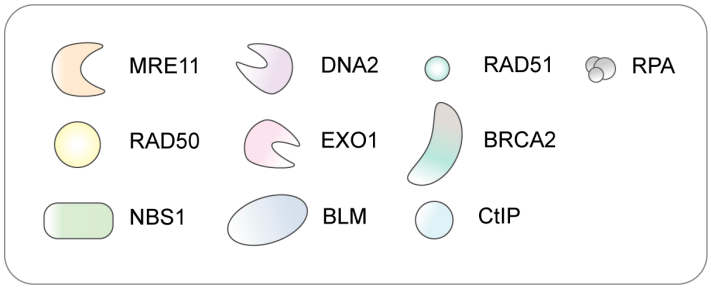

and *BRCA2* carriers is 57-65% and 45-55% respectively (Nielsen et al., 2016). *BRCA1* carries have a higher lifetime risk of ovarian cancer at 39-44% by the age of 70 compared to *BRCA2* carriers' lifetime risk of 11-18% (Nielsen et al., 2016). *PALB2* carriers also have an increased lifetime risk of breast cancer of 35% with no significant increase in ovarian cancer (Nielsen et al., 2016; Rahman et al., 2007). *BRCA* mutations account for approximately 25% of HBOCs, and the list of associated candidate HBOC genes is growing, but for the majority, more information is required to determine if they pose a significant risk.

Cells null for *BRCA1* or *BRCA2* are generally nonviable and deficiency of either protein is embryonic lethal (Feng and Jasin, 2017; Gowen et al., 1996; Hakem et al., 1996; Ludwig et al., 1997). However, in the context of malignancy, *BRCA1* and *BRCA2* loss of function (LOF) tumors do arise when the wild type (WT) allele becomes mutated. These cancer cells have acquired the ability to handle high levels of replication stress despite *BRCA1* or *BRCA2* deficiency. Current treatment regimens such as radiation therapy, cisplatin, and PARP inhibitor (PARPi) take advantage of loss of HR in these malignancies. Understanding the mechanism of how these factors work to suppress tumorigenesis will be informative for hereditary tumors, but also sporadic tumors that display what has been termed *BRCAness*. *BRCAness* describes tumors that have characteristics of *BRCA1* or *BRCA2* LOF but do not result from germline mutation. *BRCAness* can arise via somatic mutation or silencing of either gene,

mutations in other genes in the HR network, or other undefined mechanisms (Lord and Ashworth, 2016).

PARP inhibition in combination with *BRCA1* or *BRCA2* deficiency is synthetically lethal making PARP inhibitor (PARPi) therapy an attractive treatment option for hereditary BRCA cancers. PARPi has shown efficacy in treating *BRCA1* or *BRCA2* mutated tumors (Farmer et al., 2005, Bryant et al 2005., Lord et al 2015). Like with most therapies, advanced cancers acquire chemo-resistance. A clinically confirmed mechanism of chemotherapy resistance in *BRCA1/2* tumors is acquisition of secondary mutations that restore BRCA1/2 activity providing resistance to platinum based and PARPi therapy (Barber et al., 2013; Edwards et al., 2008; Norquist et al., 2011; Sakai et al., 2008; Swisher et al., 2008). Other mechanisms of resistance have been investigated for BRCA1/2 cancers including loss of 53BP1, REV7, or PARP1 activity, drug efflux transporters, and restoration of replication fork protection (Jaspers et al., 2013; Patch et al., 2015; Pettitt et al., 2013; Ray Chaudhuri et al., 2016; Rottenberg et al., 2008; Xu et al., 2015).

PARPi synthetic lethality has been attributed to a few proposed mechanisms: (1) the persistence of single strand breaks (SSBs), that once encountered during replication results in replication fork collapse and DSB generation that would require canonical homology directed repair (HDR) and (2) the “trapping” of PARP1 on DNA by inhibiting auto PARylation activity that would

release the protein, generating a protein-DNA lesion during replication (Lord and Ashworth, 2017). The role of PARP1 in promoting nascent strand degradation by MRE11 in BRCA deficient cells adds further complexity to the mechanism of PARPi lethality and acquired chemoresistance (Ding et al., 2016).

1.5 The role of BRCA2 in replication fork protection

1.5.1 Homologous recombination independent function of BRCA2 in replication fork protection

Outside of its role in HR mediated DSB repair, *BRCA2* function is required to protect stalled replication forks (Figure 1.5). By studying DNA replication at the single molecule level (DNA fibers), the Jasin laboratory discovered that BRCA2 protects stalled replication forks from nucleolytic processing by the MRE11 nuclease. Importantly, this activity appeared to be independent of the canonical HR function of BRCA2. The study identified the BRCA2 S3291A mutant as a separation of function mutant, which permitted the uncoupling of the two roles of BRCA2 in HR and replication fork protection (Schlacher et al., 2011). BRCA2 Ser3291 is a cyclin-dependent kinase phosphorylation site that regulates the C-terminal interaction of BRCA2 and RAD51 (Esashi et al., 2005). The C-terminal interacting domain of BRCA2 is hypothesized to stabilize RAD51 nucleofilaments on ssDNA and upon phosphorylation of Ser3291 this interaction is lost (Davies and Pellegrini, 2007). The S3291A BRCA2 mutant is proficient for HDR activity, but is

unable to protect against nascent strand degradation by MRE11 (Feng and Jasin, 2017; Schlacher et al., 2011).

In the absence of BRCA2, newly synthesized ssDNA at stalled replication forks is not protected and undergoes extensive degradation that is reported to result in increased chromosomal aberrations (Schlacher et al., 2011). The BRCA2 C-terminal interaction and stabilization of RAD51 on the nascent ssDNA is required for replication fork protection. In support of this conclusion, disruption of RAD51 nucleofilaments by expression of the BRC4 peptide results in nascent strand degradation. Conversely, overexpression of a RAD51 mutant, K133R, that forms stable nucleofilaments due to loss of ATPase activity required for dissociation from DNA, renders replication forks resistant to degradation (Schlacher et al., 2011).

Furthermore, depletion or inhibition of RAD51 has been shown to also result in nascent strand degradation at stalled replication forks and cause replication fork restart defects (Hashimoto et al., 2010; Petermann et al., 2010; Taglialatela et al., 2017). However, the role of RAD51 recombinase in replication fork protection has been disputed due to conflicting results among studies. In other studies, RAD51 depletion does not result in nascent strand degradation at stalled replication forks (Feng and Jasin, 2017; Lemacon et al., 2017; Mijic et al., 2017; Thangavel et al., 2015). Different thresholds of RAD51 activity may account for these discrepancies, which may be in part due to a newly described BRCA2 independent role of RAD51

in replication fork reversal (discussed below) identified by electron microscopy (EM) analysis of replication fork intermediates by (Lemacon et al., 2017; Mijic et al., 2017).

Following the discovery that BRCA2 and RAD51 are required for the protection of stalled replication forks, other proteins in the DNA damage response pathway were also found to have a role including BRCA1, RAD51 paralogs, FA proteins including FANCA and FANCD2, BOD1L, Abro1, RECQ1, and WRNIP1 (Higgs et al., 2015; Leuzzi et al., 2016; Schlacher et al., 2012; Somyajit et al., 2015; Xu et al., 2017).

1.5.2 BRCA2 independent role of RAD51 in replication fork reversal

Replication forks that slow and stall can undergo remodeling into a reversed replication fork structure. Reversed forks are formed when the parental DNA strands reanneal and nascent DNA strands anneal forming a “regressed arm” and a joint molecule resembling a Holliday junction. Replicating cells display a baseline level of reversed replication forks that is increased upon exogenous genotoxic stress to a wide array of agents including topoisomerase inhibitors, DNA interstrand-crosslinking agents, DNA synthesis inhibitors, alkylating agents, and UV (Berti et al., 2013; Ray Chaudhuri et al., 2012; Zellweger et al., 2015). Additionally, EM analysis suggests that cells undergoing rapid proliferation utilize replication fork slowing and fork reversal as a means to protect against genomic

instability produced by endogenous replication stress (Ahuja et al., 2016). There is evidence to support fork reversal as a mechanism to protect against genomic instability as it may guard against extensive ssDNA generation, provide DNA repair machinery access to the damaged template, or promote lesion bypass (Betous et al., 2012; Cortez, 2015; Couch et al., 2013; Ray Chaudhuri et al., 2012; Zellweger et al., 2015). However, reversed replication forks are also a substrate liable to nuclease processing and DSB formation (Couch et al., 2013; Neelsen et al., 2013; Schlacher et al., 2011; Schlacher et al., 2012; Ying et al., 2012).

EM analysis of replication fork intermediates from BRCA2 depleted cells shows a decrease in reversed replication fork intermediates. The levels of reversed replication fork species are rescued by MRE11 inhibition (Lemacon et al., 2017; Mijic et al., 2017). Interestingly, in BRCA2 deficient cells, reversed replication fork intermediates are detected at normal levels at early time points after replication stress but then decrease due to MRE11 dependent nucleolytic processing (Lemacon et al., 2017). These data along with observations from DNA fiber analysis suggest that BRCA2 protects reversed replication fork structures from nucleases.

Analysis of replication fork species by EM in RAD51 depleted cells also shows a decrease in reversed replication forks (Kolinjivadi et al., 2017; Mijic et al., 2017; Zellweger et al., 2015). Unlike BRCA2 depleted cells, the reversed

replication fork levels in RAD51 depleted cells are not rescued by MRE11 inhibition (Mijic et al., 2017). Levels of reversed replication forks in BRCA2 deficient cells are not rescued by RAD51 depletion or with concomitant MRE11 inhibition despite rescue of nascent strand degradation at stalled replication forks (Mijic et al., 2017). Conclusions from this work are that BRCA2 and RAD51 are both important for protecting reversed replication forks by stabilization of RAD51 nucleofilaments, while RAD51 may perform an additional independent function in promoting replication fork reversal. These data suggest a model by which depleting RAD51 prevents replication fork reversal and averts the formation of a substrate for MRE11 degradation in the absence of BRCA2/RAD51 nucleofilament formation.

A RAD51 dominant negative separation of function mutant, T131P, identified in an individual with Fanconi anemia-like syndrome is proficient for HDR but deficient for replication fork protection (Mijic et al., 2017; Wang et al., 2015). The *RAD51-T131P* mutant does not form stable nucleofilaments due to hyperactive ATPase activity (Wang et al., 2015). The *RAD51-T131P* mutant cells undergo MRE11 dependent nascent strand degradation at stalled replication forks (Mijic et al., 2017). Reversed replication fork species are also decreased in *RAD51-T131P* cells but are rescued by MRE11 inhibition (Mijic et al., 2017). The *RAD51-T131P* cells are heterozygous and express RAD51 mutant protein at a ratio of 1:5 to WT (Wang et al., 2015). The RAD51 activity presumably is enough to support replication fork reversal, but not the formation of stable RAD51

nucleofilaments that can protect the reversed replication fork from MRE11 degradation.

The differences in the reporting of the requirement of RAD51 for protecting against nascent strand degradation may be due to the extent that RAD51 is depleted or inhibited. The use of the BRC4 peptide or B02 inhibitor, like *RAD51-T131P,* may prohibit stable RAD51 nucleofilament formation leaving DNA vulnerable to nuclease degradation but still leave enough RAD51 activity for replication fork reversal (Schlacher et al., 2012; Taglialatela et al., 2017). The formation of stable RAD51 nucleofilaments may not be required for replication fork reversal activity, but is required for protection of the regressed fork from nucleolytic activity (Kolinjivadi et al., 2017; Mijic et al., 2017).

EM analysis of replication fork structures has largely focused on reversed replication forks, but other intermediates have also been identified. *RAD51* and *BRCA2* depletion in *Xenopus* egg extracts results in replication fork intermediates with increased ssDNA at the fork and behind the fork (Hashimoto et al., 2010; Kolinjivadi et al., 2017). MRE11 inhibition rescues ssDNA gaps behind the fork but not the increased ssDNA at the fork junction (Hashimoto et al., 2010; Kolinjivadi et al., 2017). Replication forks with ssDNA at the junction may be intermediates that proceed replication fork reversal; however, levels in BRCA2 and RAD51 depleted extracts appear to be similar despite the perceived independent role of RAD51 in

fork reversal (Kolinjivadi et al., 2017). Cells treated with genotoxic agents also show increased regions of ssDNA behind the fork and at the fork (Zellweger et al., 2015). While unprotected reversed replication forks are targeted by MRE11, internal ssDNA gaps behind the fork are also MRE11 substrates, and further understanding of the role of BRCA2/RAD51 fork protection in preventing their generation is needed.

1.5.3 Nuclease processing at stalled replication forks in *BRCA2* deficient cells

Restoring replication fork protection in *BRCA2* deficient cells has been an intense area of research that has largely focused on prohibiting processing by MRE11. MRE11 travels with the replisome and its recruitment to chromatin is enhanced by exogenous replication stress (Dungrawala et al., 2015; Mirzoeva and Petrini, 2003; Robison et al., 2004). The presence of MRE11 at the replisome following replication stress is PARP1 dependent, important for Chk1 signaling, and replication fork restart (Bryant et al., 2009; Lee and Dunphy, 2013; Olson et al., 2007; Trenz et al., 2006). While MRE11 is required for the processing of stalled replication forks, aberrant activity at unprotected stalled replication forks in *BRCA1* and *BRCA2* deficient cells contributes to increased genomic instability (Ray Chaudhuri et al., 2016; Schlacher et al., 2011; Schlacher et al., 2012; Ying et al., 2012). In BRCA2 deficient cells treated with genotoxic agents, MRE11 inhibition reduces genomic instability providing evidence that replication fork protection may

be an important mechanism for resistance to DNA damage (Ray Chaudhuri et al., 2016; Schlacher et al., 2011).

Despite the hypersensitivity of *BRCA1* and *BRCA2* deficient cells to PARPi, deficiency of PARP1 protects against nascent strand degradation of stalled replication forks by preventing MRE11 recruitment (Bryant et al., 2009; Ding et al., 2016; Ray Chaudhuri et al., 2016; Ray Chaudhuri et al., 2012). Recent work has demonstrated that MRE11 recruitment to sites of replication stress is also dependent on PTIP and the associated methyltransferases MLL3/MLL4, the chromatin remodeler CHD4, and RAD52 (Mijic et al., 2017; Ray Chaudhuri et al., 2016). Depletion of these factors rescues nascent strand degradation in *BRCA* deficient cells similar to MRE11 inhibition. Similarly, the decrease in reversed replication fork intermediates in *BRCA2* deficient cells treated with genotoxic agents are rescued by RAD52 inhibition or depletion of PTIP (Lemacon et al., 2017; Mijic et al., 2017). These data suggest that deficiency of PARP1, MLL4, PTIP, CHD4, or RAD52, in *BRCA1* or *BRCA2* deficient cells rescues nascent strand degradation by prohibiting MRE11 fork processing (Mijic et al., 2017; Ray Chaudhuri et al., 2016).

Recent studies extend the resection of unprotected nascent DNA at stalled forks to EXO1 and CtIP. Depletion of EXO1 or CtIP rescues nascent strand degradation in *BRCA2* deficient cells (Lemacon et al., 2017). Similarly, knockdown

of EXO1 rescues reversed fork levels that are decreased in BRCA1/2 deficient cells treated with replication stress inducing drugs (Lemacon et al., 2017). A clear role for DNA2 in the processing of stalled replication forks in *BRCA* deficient cells has not been determined. Lemacon *et al* found that DNA2 depletion does not rescue nascent strand degradation in BRCA2 deficient cells. On the contrary, Chaudhuri *et al* show that in *BRCA2* deficient B-cells DNA2 inhibition is epistatic with MRE11 in the rescue of nascent strand degradation. It is unclear what accounts for the difference in the requirement of DNA2 for nascent strand degradation in BRCA2 deficient cells, but the studies use different cell types and assess the role of DNA2 using two different methods, by siRNA depletion and small molecule inhibitor (Lemacon et al., 2017; Ray Chaudhuri et al., 2016). Further investigation will be required to determine the dependency of DNA2 in nascent strand degradation of BRCA2 deficient cells. The implication of EXO1 and CtIP leaves us to contemplate a model of resection similar to DSB end resection at unprotected regressed forks. In the absence of *BRCA2,* resection may be initiated by CtIP and MRE11 followed by more extensive processing by EXO1. Although it is also possible that the nucleases have different substrates at stalled replication forks.

Figure 1.5 BRCA2 and RAD51 mediated replication fork protection

Replication fork reversal is proposed to be a global response to replication stress that requires RAD51-mediated fork reversal. When a replication fork encounters replication stress the generation of ssDNA may serve to promote replication fork reversal that entails the annealing of the nascent strand DNA and reannealing of the parental DNA strands. This process requires RAD51 in a BRCA2 independent process. To prevent nuclease degradation, RAD51 must be loaded and stabilized on the nascent DNA by BRCA2.

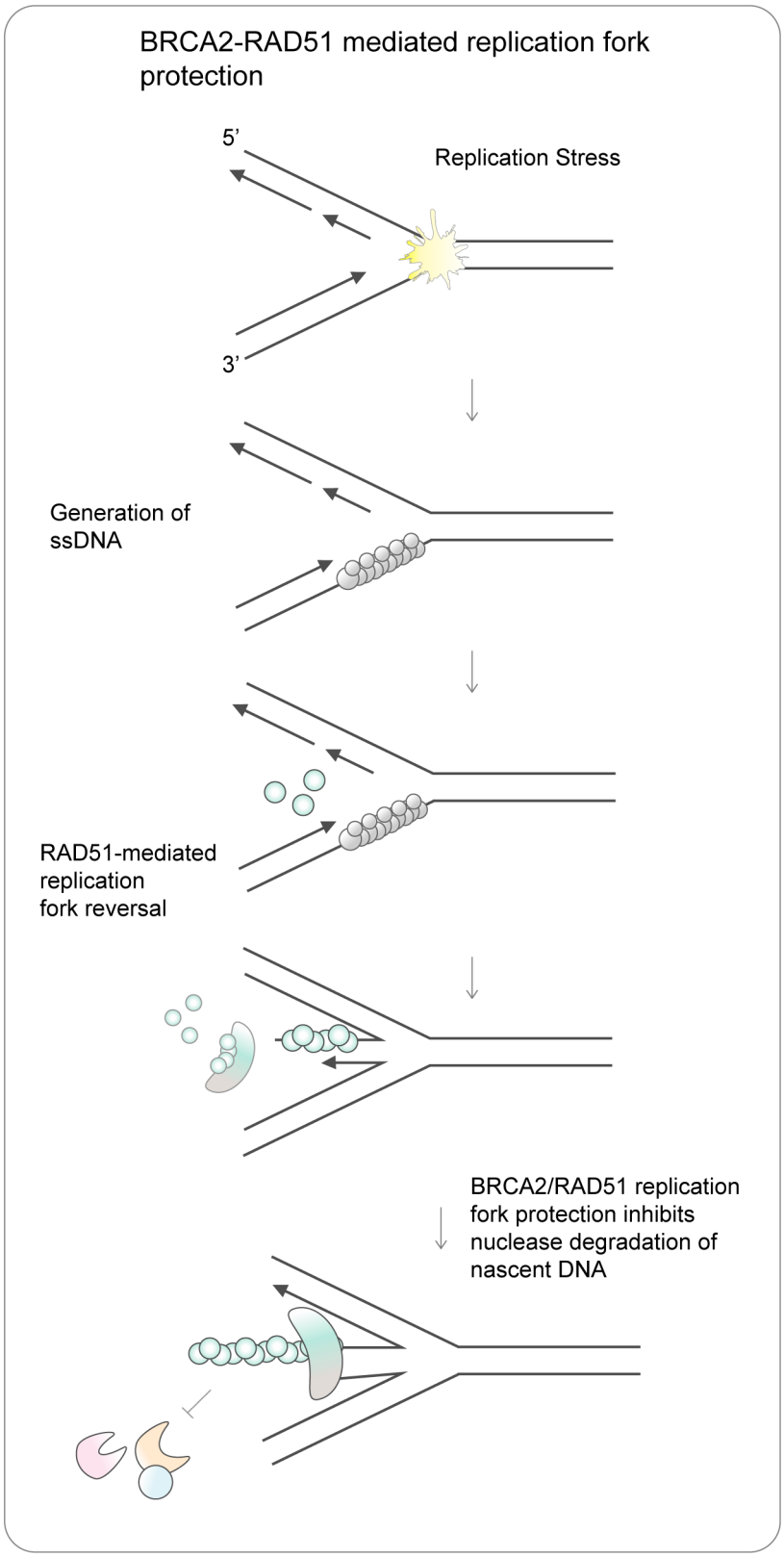

1.5.4 DNA translocases in replication fork protection and processing

Similar to RAD51 depletion in BRCA2 deficient cells, depletion of any of the three ATPase dependent DNA translocases of the SNF2 family of chromatin remodelers, SMARCAL1, ZRANB3, or HLTF, rescue resection of nascent strand DNA by loss of replication fork reversal. These related proteins have been shown to have similar fork remodeling activity *in vitro*. SMARCAL1 demonstrates affinity for DNA fork structures and catalyzes activity promoting strand annealing, fork regression, and branch migration (Betous et al., 2012; Ciccia et al., 2012; Yusufzai and Kadonaga, 2008). ZRANB3 and HLTF also catalyze replication fork reversal *in vitro* (Ciccia et al., 2012; Yuan et al., 2012; Yusufzai and Kadonaga, 2010).

These translocases have been found to associate with the replication fork; however, how they each associate with the fork is different (Figure 1.6). SMARCAL1 travels with the replication fork and becomes further enriched following replication stress through interaction with RPA. (Bansbach et al., 2009; Betous et al., 2012; Ciccia et al., 2009; Dungrawala et al., 2015; Kolinjivadi et al., 2017; Postow et al., 2009; Yuan et al., 2009). SMARCAL1 interaction with RPA is important for providing substrate specificity to promote replication fork reversal and prevent activity during normal DNA replication (Betous et al., 2013). ATR phosphorylation of S652 of RPA bound SMARCAL1 has been shown to be important for regulating its activity at the replication fork (Couch et al., 2013).

HLTF and ZRANB3 have been shown to interact with PCNA. HLTF contains a RING finger domain and a N-terminal HIRAN domain (Poole and Cortez, 2017). HLTF acts as ubiquitin ligase to polyubiquitinate PCNA in a MMS2-Ubc13 dependent manner (Motegi et al., 2008; Unk et al., 2008). *In vitro* studies indicate the HIRAN domain of HLTF recognizes the 3' end of the leading strand to promote replication fork reversal (Kile et al., 2015). Upon replication stress, ZRANB3 is recruited to DNA through a PCNA-interacting protein (PIP) box and an AlkB homolog 2 PCNA-interaction motif (APIM) to PCNA (Ciccia et al., 2012; Weston et al., 2012; Yuan et al., 2012). ZRANB3 contains a NPL4 zinc finger (NZF) motif that preferentially binds K-63 poly-ubiquitinated PCNA and is required for its localization to sites of replication stress (Ciccia et al., 2012; Vujanovic et al., 2017).

In the absence of any of the three translocases, SMARCAL1, ZRANB3, or HLTF, cells become hypersensitive to replication stress inducing agents and have increased genomic instability (Bansbach et al., 2009; Ciccia et al., 2009; Taglialatela et al., 2017). Likewise, translocase activity must be carefully regulated to prevent inappropriate fork reversal and breakage. Overexpression of SMARCAL1 increases ssDNA and DNA damage (Bansbach et al., 2009). Similarly, in ATR inhibited cells, excessive ssDNA is generated in part due to aberrant SMARCAL1 activity (Couch et al., 2013). Inappropriate SMARCAL1 activity generates intermediates that have been shown to be acted on by SLX4 coupled nucleases and CtIP (Couch et al., 2013).

Despite similar biochemical activity, SMARCAL1 and ZRANB3, do not act redundantly as increased DNA damage accrues upon depletion of both proteins (Ciccia et al., 2012). This may be attributed to synergistic functions at replication forks, different roles and replication fork substrates, or roles outside of more global replication fork remodeling. SMARCAL1 activity is also important for replication through difficult to replicate telomeric sequences, a function not attributed to ZRANB3 or HLTF (Poole et al., 2015).

Recent work has further expanded the role of SMARCAL1, ZRANB3, and HLTF to replication fork reversal *in vivo*. Depletion of SMARCAL1, ZRANB3, and HLTF results in decreased detection of reversed replication fork intermediates by EM (Vujanovic et al., 2017). Depletion of any of any of these three translocases rescues nascent strand degradation at forks defective for BRCA2 replication fork protection. This is thought to occur by preventing replication fork reversal, a substrate for MRE11 (Kolinjivadi et al., 2017; Taglialatela et al., 2017; Vujanovic et al., 2017). SMARCAL1 depletion in BRCA1, BRCA2, or FANCD2 deficient cells rescues degradation of nascent DNA at stalled replication forks (Kolinjivadi et al., 2017; Taglialatela et al., 2017). Similarly, depletion of ZRNAB3 or HLTF in BRCA1 or BRCA2 deficient cells rescues nascent strand degradation (Mijic et al., 2017; Taglialatela et al., 2017).

The overall impact of rescuing nascent strand degradation in replication fork protection deficient cells by depletion of these translocases is unclear, as depletion on their own increases DNA damage and current findings are contradictory. In one study, DNA damage is reduced by ZRANB3 depletion in BRCA deficient cells, with no further rescue observed with co-depletion of SMARCAL1 (Taglialatela et al., 2017). While another study observes rescue of nascent strand degradation by ZRANB3 depletion, but increased genomic instability (Mijic et al., 2017). These two studies analyzed different cell types under different conditions of damage, hydroxyurea (HU) versus camptothecin (CPT), likely in part contributing to the observed differences. Replication fork reversal is a response to many types of DNA damage, so moving forward it is of interest to clarify how each of these translocases respond to specific types of damage and if they work cooperatively or have distinct roles at different replication fork substrates (Zellweger et al., 2015).

1.5.5 Deficiency of RADX, a RAD51 effector protein, rescues nascent strand degradation in *BRCA2* deficient cells

RADX is a single stranded DNA binding protein recently identified as being enriched at replication forks following replication stress (Figure 1.7) (Dungrawala et al., 2017). RADX has sequence similarity to RPA and binds through three RPA-like OB folds. RADX is recruited to replication forks where it modulates the RAD51 recombinase (Dungrawala et al., 2017). In the absence of RADX, increased levels of RAD51 accumulate at stalled replication forks while BRCA2 levels are

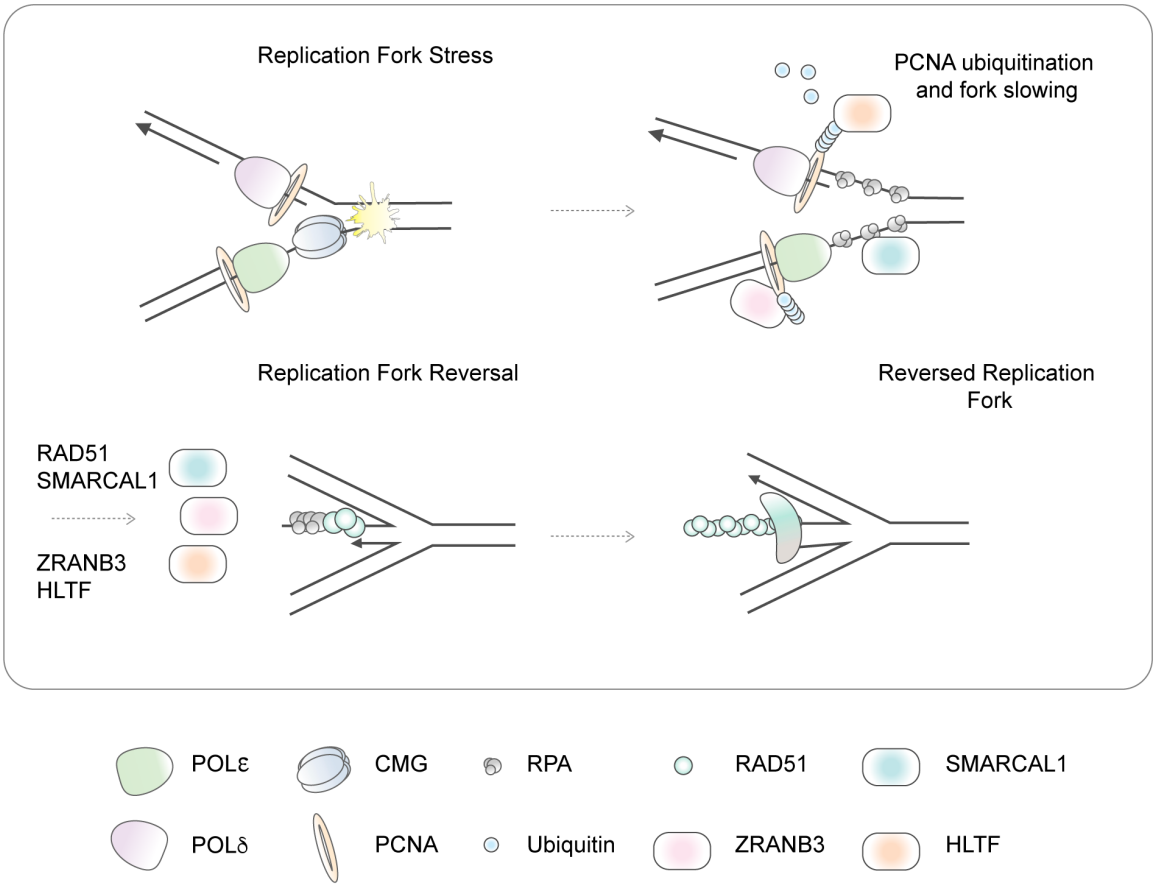

Figure 1.6 Replication fork reversal mediated by the SNF2 family translocases SMARCAL1, ZRANB3, and HLTF.

Replication fork reversal is mediated by the SNF2 family chromatin remodelers SMARCAL1, ZRANB3, and HLTF. HLTF is important for the polyubiquitination of PCNA that serves as a platform for recruitment of ZRANB3. SMARCAL1 is recruited to the replication fork through interaction with RPA. How these translocases remodel the replication fork and whether they work synergistically to reverse replication forks is unclear and needs further investigation.

unaffected. Conversely RADX overexpression results in a decrease in RAD51 recruitment to stalled replication forks (Dungrawala et al., 2017).

Depletion of RADX results in increased DNA damage and DSB formation and slowed replication fork progression (Dungrawala et al., 2017; Schubert et al., 2017). These defects are rescued by co-depletion of RAD51. Similarly, depletion of replication fork remodelers, SMARCAL1 and ZRNAB3, or the MUS81 nuclease rescue DSBs in RADX depleted cells. These data suggest that in the absence of RADX, hyperactivity of RAD51 interferes with normal replication and promotes inappropriate replication fork remodeling that results in DSBs mediated by MUS81 (Dungrawala et al., 2017).

RADX levels must be carefully controlled as overexpression also increases DNA damage. RADX overexpression increases nascent strand degradation at stalled replication forks, which likely is the result of antagonizing the protective RAD51 nucleofilament. Conversely, depletion of RADX rescues nascent strand degradation but not HDR defects in *BRCA2* deficient cells. In BRCA2 depleted cells, some RAD51 nucleofilament formation may occur in the absence of RADX antagonism, which may be significant enough to protect the nascent DNA from degradation (Dungrawala et al., 2017). RADX depletion also increases BRCA2 deficient cells resistance to PARPi (Dungrawala et al., 2017). This presents the tradeoff of RADX inhibition to promote replication fork protection in BRCA2

deficient cells versus the possibility of inappropriate fork reversal promoted during replication that may result in DSBs. Increased viability of BRCA2 deficient and RAD51 depleted U2OS cells to genotoxic agents by RADX inhibition suggest restoration of replication fork protection is more important.

Another effector protein of RAD51 is FBH1, a 3'-5' DNA helicase of the UvrD family that contains an F-Box domain, a PIP box, and APIM (Bacquin et al., 2013; Kim et al., 2002). FBH1 negatively modulates RAD51 through its E3 ubiquitin ligase activity that preferentially targets K58/64 of RAD51 (Chu et al., 2015; Kim et al., 2002). Unlike RADX, FBH1 depletion in *BRCA2* deficient cells does not rescue replication fork protection (Higgs et al., 2015; Leuzzi et al., 2016). However, FBH1 depletion in cells deficient for either BOD1L or WRNIP1, two other replication fork protection factors, does rescue nascent strand degradation at stalled replication forks (Higgs et al., 2015; Leuzzi et al., 2016). Further investigation is required to understand the differences in fork protection and antagonism by all of these factors.

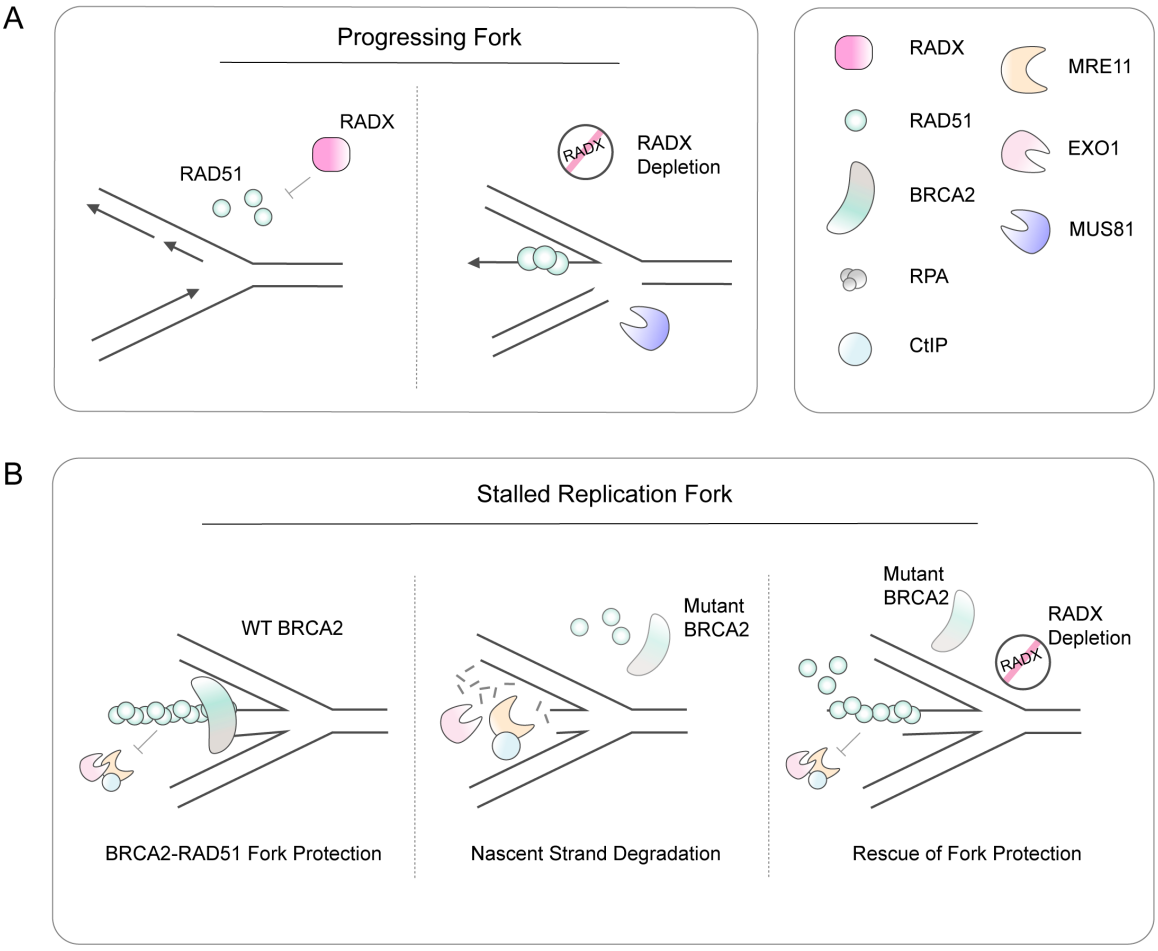

Figure 1.7 RADX modulates RAD51 activity at replication forks

(A) The proposed model of RADX activity is to regulate RAD51 activity at the replication fork to prevent unnecessary RAD51 association and fork reversal during normal DNA replication progression. Upon RADX depletion there is increased genomic instability and DSBs that may be the result of inappropriate fork remodeling leading to increased fork cleavage and collapse. (B) The depletion of RADX in BRCA2 deficient cells rescues nascent strand degradation at HU stalled replication forks. Removal of RADX antagonism of RAD51 may permit rescue of RAD51 fork protection and prevent degradation by nucleases.

1.5.6. MUS81 cleavage of stalled replication forks in *BRCA2* deficient cells

MUS81 has previously been described as the nuclease responsible for the DSBs formed during replication stress that results in replication fork collapse. However, MUS81 is also important for replication fork restart and depletion of MUS81 increases chromosomal aberrations in cells challenged by replication stress (Franchitto et al., 2008; Hanada et al., 2007; Pepe and West, 2014; Regairaz et al., 2011). MUS81 activity is responsible for breakage at late replicating regions in the genome also known as common fragile sites (CFS). However, without MUS81 processing CFSs can cause greater genomic instability during mitosis (Naim et al., 2013; Ying et al., 2013). Controlled DNA breakage by MUS81 is a necessary compromise to promote genome stability and resume replication at stalled forks. However, in the case of oncogene-induced DNA replication stress, when the cell cycle is deregulated, there is increased MUS81 dependent DSB formation that contributes to increased genome instability (Murfuni et al., 2013; Neelsen et al., 2013).

MUS81 depletion prevents DSB formation in BRCA2 deficient cells, but does not rescue nascent strand degradation. Prevention of nascent strand degradation by MRE11 or EXO1 deficiency also decreases DSB formation in BRCA2 deficient cells (Lemacon et al., 2017). This places MUS81 activity and breakage downstream of MRE11 and EXO1 processing. (Lemacon et al., 2017). Reversed replication fork intermediates, visualized by EM, are rescued by

depletion of MUS81 in BRCA2 deficient cells, but these replication fork intermediates appear to have a ssDNA flap (Lemacon et al., 2017). The ssDNA flap intermediate may be the product of MRE11 or EXO1 processing and the substrate for MUS81 cleavage (Lemacon et al., 2017).

Another study identified EZH2, a histone methyl transferase, as important for promoting MUS81 processing of stalled replication forks in BRCA2 deficient but not BRCA1 deficient cells (Rondinelli et al., 2017). The same study found that MUS81 depletion rescued replication fork degradation in BRCA2 deficient cells which is in contrast to Lemacon *et al's* findings. EZH2 co-depletion with MRE11 further augmented fork protection, suggesting a separate mechanism from MRE11 recruitment by MLL3/MLL4/PTIP (Rondinelli et al., 2017).

Replication fork restart in BRCA2 deficient cells is defective in the absence of MUS81 (Lemacon et al., 2017). Similarly, EZH2 inhibition results in reduced replication fork restart in BRCA2 deficient cells (Rondinelli et al., 2017). DSBs generated in BRCA2 deficient cells, following replication fork stress, are transient and return to control levels (Lemacon et al., 2017). Inhibition of nucleases in BRCA2 deficient cells rescues nascent strand degradation and breakage, but also result in defects in replication fork restart. It is possible that processing of reversed replication forks by nucleases is required for replication fork restart and that DNA breakage is a transient repair intermediate of this process.

1.6 Objectives

The objective of this thesis was to investigate novel genes mutated in FA families that have not been assigned to one of the known FA complementation groups. To achieve this objective, families that fit this criterion were identified from the International Fanconi Anemia Registry (IFAR) and were evaluated by Whole Exome Sequencing (WES) and cell-based assays. Examination of patient-derived cells for hypersensitivity to drugs that generate ICLs and other DNA damaging agents demonstrated that despite the overlap in clinical features they behaved differently suggesting the patients do not harbor mutations in the same gene. I will present three cases identified from the IFAR that were the focus of study in this thesis.

The first case, the subject of Chapter 2, is the identification of biallelic *UBE2T* mutations as causing a new subtype of FA in an individual with typical FA features. Pathogenic mutations were not identified by WES, but a large duplication and a large deletion were detected by sequencing of the UBE2T locus upon discovery of a significant decrease in *UBE2T* transcripts by RNA sequencing (RNAseq). Analysis of cells deficient for UBE2T demonstrated it is the primary E2 of the FA pathway and is required for monubiquitination of the ID2 complex.

The second case, the subject of Chapter 3, is the unexpected identification of compound heterozygous biallelic *FANCD1/BRCA2* mutations in a sibling pair that does not display the typical clinical findings of this complementation group. Their atypical presentation had previously precluded their screening for the *FANCD1* complementation group. The objective of this study was to determine the function of the DBD of BRCA2 that is mutated in this family in order to better understand the functions of BRCA2 and the consequences its disruption has on human diseases such as FA and HBOC. The work herein determined that the BRCA2 DBD is required for replication fork protection and to a lesser extent HR.

The third and final case, the subject of Chapter 4, describes an individual enrolled in the IFAR that cellular characterization revealed to not have defects in ICL repair. Due to the heterogeneous nature of FA, defects of other pathways important for DNA repair or replication can have overlapping clinical features leading to misdiagnosis. Cellular analysis revealed no classic hallmarks of FA, but defects in the cellular response to DNA replication stress. The genetic basis of disease in this individual is still under investigation.

The identification of novel inherited DNA repair disorders increases our understanding of the cellular networks working to maintain genome integrity, preserve normal cellular function, and protect against tumorigenesis. These are

networks that work in all human cells to assure normal function, so the implications of these studies go beyond the rare diseases studied.

Chapter 2: Deficiency of UBE2T causes a new subtype of Fanconi anemia and is the primary E2 ubiquitin-conjugating enzyme necessary for FANCD2 and FANCI ubiquitination

2.1 Introduction

A key step in the repair of ICLs is the monoubiquitination of FANCD2 and FANCI at residues K561 and K523 respectively. Site specific mutagenesis of either of these lysine residues results in failure of FANCD2 and FANCI to be ubiquitinated and recruited to ICLs (Garcia-Higuera et al., 2001; Smogorzewska et al., 2007b). FANCD2 and FANCI monoubiquitination requires an intact FA core complex that acts as an E3 ubiquitin ligase with FANCL as the catalytic subunit (Hodson et al., 2014; Meetei et al., 2003a). The E2 ubiquitin-conjugating enzyme UBE2T was identified as an interactor of FANCL by a yeast two-hybrid screen (Machida et al., 2006). Depletion of UBE2T results in defective ubiquitination of FANCD2, loss of FANCD2 recruitment to foci after DNA damage, and cellular sensitivity to ICLs (Alpi et al., 2008; Machida et al., 2006). Here we describe a new FA complementation group identified in a patient enrolled in the International Fanconi Anemia Registry (IFAR) presenting with typical FA features and deficiency of the ubiquitin-conjugating enzyme (E2), UBE2T.

2.2 Results

2.2.1 Presentation of Fanconi anemia patient of unknown complementation group

The subject of study was identified as a participant enrolled in the International Fanconi Anemia Registry (IFAR) diagnosed with FA of unknown complementation group. The patient was born premature at 36 weeks gestation weighing 3lbs 7oz and measuring 16.5 inches long in the 3rd percentile. At birth the subject presented with bilateral radial aplasia and absent thumbs, microcephaly,

micrognathia, café au lait spots, ventricular septal defect (VSD), patent ductus arteriosus (PDA), and absent left kidney. At birth the patient had thrombocytopenia that resolved in subsequent days. There was family history of Thalassemia, but no history of early onset cancer or bone marrow failure.

The patient was clinically diagnosed with Fanconi anemia at birth. Cytogenetic studies were performed at the Laboratory of Human Genetics and Hematology at The Rockefeller University Hospital and showed elevated chromosomal breakage in peripheral blood (PB) samples treated with the DNA crosslinking agent diexpoxybutane (DEB). Initially, breakage levels of PB collected at 2 days old displayed significantly elevated chromosomal breakage levels at 5.8 breaks per cell in 85% of the cell population. Decreasing breakage levels over time demonstrated the development of somatic mosaicism in the hematopoietic compartment, a phenomenon seen in a small subset of FA patients (Table 2.1) (Gregory et al., 2001; Lo Ten Foe et al., 1997; Soulier et al., 2005; Waisfisz et al., 1999).

The patient is seen at Cincinnati Chidlren's hospital for bone marrow testing annually. Our most recent blood counts for age 16 years old report a hemoglobin of 13.9, platelet count of 202,000, and white blood cell count of 6.6 (absolute neutrophil count mildly decreased at 0.79 and an elevated absolute lymphocyte count of 5.6). Peripheral blood smear shows moderate neutropenia and microcytic

Table 2.1 Chromosome breakage analysis of subject's peripheral blood samples treated with DEB

Age, Report Date	# DEB treated cells analyzed	Mean chromosome breaks per cell/ percent of cells with breaks
2 days, 11/30/98	20	5.8, 85%
10 days, 11/30/98	10	7.1, 80%
1 years, 11/06/98	10	7.5, 80%
6 years, 05/22/05	15	4.1, 47%
6 years, 10/05/05	50	0.08, 8%
6 years, 10/10/05	40	0.28, 17.5%
16 years, 4/18/15	50	0.32,18%

red blood cells consistent with thalassemia trait. Bone marrow biopsy demonstrates mild hypocellularity for age in the 35-45% range with trilineage hematopoiesis. Chromosome studies show a normal 46, XY karyotype. To date there is no evidence of abnormal clonal cells, MDS, or leukemia in this patient.

The patient has a history of normal Adrenocorticotropic hormone (ACTH) and Growth Hormone (GH) stimulation. The patient takes thyroid replacement therapy for hypothyroidism. Cardiac evaluation by ECG was normal and echocardiogram reveals a normal heart with normal valve anatomy and function. The patient has a solitary kidney and normal renal function with a creatinine value of 0.57. The patient at 16 years of age, performed well in school with no known learning disabilities, and is generally active. The patient has bilateral conductive hearing loss and uses hearing aids. The patient's height remains below the 5th percentile and most recent bone age was slightly greater than chronological age.

2.2.2 Cellular phenotype of Fanconi anemia cell line of unknown complementation group

To support the elevated chromosomal breakage levels identified in early PB tests and diagnosis of FA, we analyzed patient derived fibroblasts (RA2627). RA2627 fibroblast are hypersensitive to crosslinking agents MMC and DEB in survival assays (Figure 2.1A-B). Chromosomal breakage levels are elevated in RA2627 fibroblasts treated with DEB as compared to BJ wild type fibroblast, although slightly lower than FA-A patient cells (RA3087) (Figure 2.1C-D). RA2627

cells are deficient for FANCD2 monoubiquitination (Figure 2.1E) while the lymphoblastoid cell line (LCLs) (RA2946), derived from blood that showed mosaicism, displayed normal FANCD2 monoubiquitination, consistent with genetic reversion (Figure 2.1F). By immunofluorescence, FANCD2 foci were not observed in RA2627 cells following 24-hour treatment with MMC (Figure 2.1G). These data demonstrate that the subject's fibroblasts display deficiency of FA pathway activation, consistent with either the deficiency of the FA core complex, one of the associated proteins, or the ID2 complex, whereas the subject's LCLs are phenotypically reverted consistent with mosaicism observed in the subject's blood.

2.2.3 Whole exome sequencing and high-resolution array comparative genomic hybridization

High-resolution array comparative genomic hybridization (aCGH) of genomic DNA from the subject's fibroblasts and peripheral blood samples did not detect deletions or duplications in the known FA genes. Whole exome sequencing (WES) of DNA derived from proband LCLs and parental peripheral blood samples was performed. Analysis of WES data revealed a single *FANCA* mutation, c.2574C>G/p.Ser858Arg, previously described in FA (Tamary et al., 2000; Wijker et al., 1999). A second mutation in FANCA was not identified, but detection may not be possible in DNA derived from a revertant cell line. Normal levels of FANCA were detected by western blot in RA2627 cells (Figure 2.2A) and overexpression of wild type *FANCA* in RA2627 failed to rescue the monoubiquitination defect of

Figure 2.1 Characterization of cell lines from an individual with FA under study.

(A-B) MMC and DEB cell survival assays of the subject's RA2627 fibroblasts in comparison to *FANCA*-mutant (RA3087) and BJ wildtype fibroblasts. Cells were treated in triplicate with increasing concentration of MMC or DEB. Cell numbers were determined after 7 days and normalized to untreated control to give percent survival. Error bars indicate s.d. (C) Example of metaphase spread of RA2627 following 0.1 ug/ml DEB treatment. Inset images highlight radial chromosomes. (D) Quantification of chromosome breaks of DEB treated BJ, *FANCA*-mutant, and RA2627 fibroblasts. Mean breaks per cell were 0.19, 7.5, and 3.3 respectively (E-F) Western blot with FANCD2 antibody of BJ, RA2627 proband fibroblasts, and *FANCA*-mutant fibroblasts or non-FA control RA2987 lymphoblasts, RA2946 proband lymphoblasts, and *FANCA*-mutant lymphoblasts. Cells were cultured with or without 1 μM MMC for 24h. (G) FANCD2 foci formation following treatment with or without 1 μM MMC for 24h.

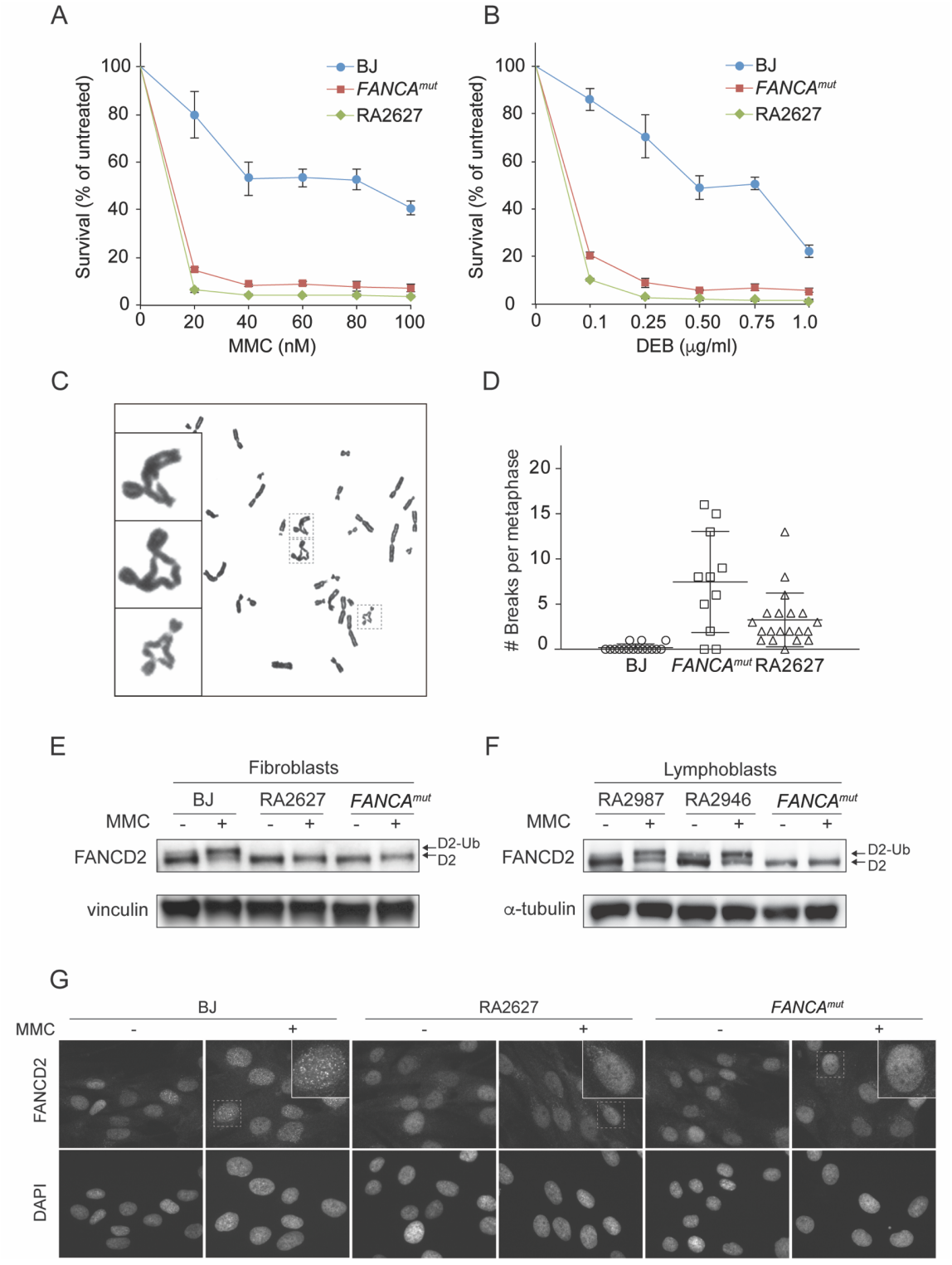

FANCD2 and FANCI excluding *FANCA* as a causative gene in this cell line (Figure 2.2C). WES analysis identified no other mutations in reported FA genes.

2.2.4 Identification of biallelic *UBE2T* mutations in the subject

RNA sequencing (RNA-seq) was performed on RA2627 fibroblasts to assess altered transcript levels that might indicate functionally significant gene mutations not captured by WES. Compared to a non-FA patient cell line (RA3380), a marked reduction in *UBE2T* was detected, but not in any of the known FA genes (Figure 2.3A). Decreased *UBE2T* transcript levels were confirmed by RT-qPCR (Figure 2.3B) and UBE2T protein was undetectable in RA2627 fibroblast lysates by western blot analysis (Figure 2.3C). Interestingly, UBE2T transcript and protein were present at near normal levels in proband LCLs (RA2946) (Figure 2.3D) supporting the presence of a genetic reversion in the hematopoietic compartment.

Sanger sequencing of genomic DNA and cDNA from proband primary fibroblasts (RA2627), parental peripheral blood, and LCLs revealed compound heterozygous mutations in *UBE2T*, a large paternally derived deletion and maternally derived duplication (Figure 2.4).

The paternally derived deletion, g.202332626_202341295del, appears to have resulted from recombination of two *AluYa5* repeats within the *UBE2T* gene (Figure 2.5). The paternally derived deletion was uncovered by genomic sequencing of the proband and parental DNA. Genomic deletion was suspected

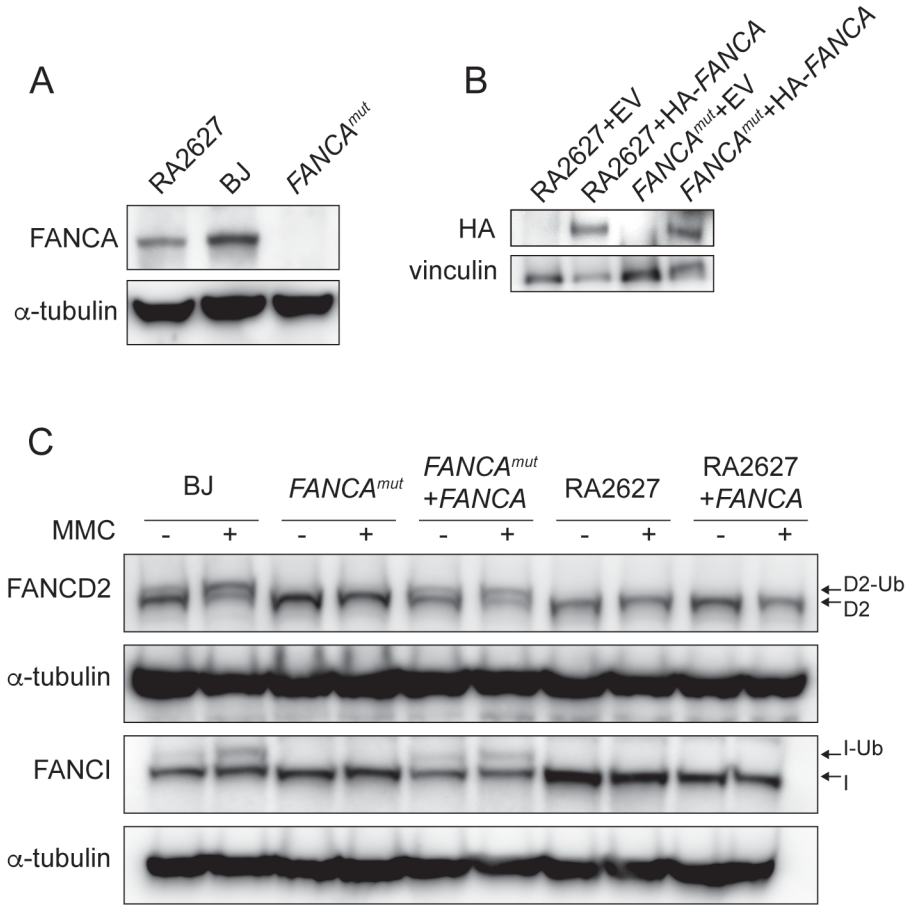

Figure 2.2 FANCA cDNA fails to complement RA2627 FANCD2 and FANCI monoubiquitination defect.

A) Western blot with FANCA antibody of RA2627, BJ, and *FANCA*-mutant fibroblasts. (B) Expression of wild type HA-FLAG tagged *FANCA* cDNA or empty vector control (EV) in RA2627 and *FANCA*-mutant fibroblasts. (C) Western blot with FANCD2 and FANCI antibody of *FANCA* complemented cells.

based on the inheritance of an informative polymorphic marker rs14451 (exon2) detected in WES of the proband and parental DNA. Somatic mosaicism of the proband LCLs complicated interpretation of WES data; however, the homozygous presence of rs14451 in the paternal data and absence in proband data suggested hemizygosisty for the proband in this region even in the revertant LCLs. PCR and Sanger sequencing of the UBE2T locus confirmed this finding and revealed additional informative markers rs10753914 (IVS1) and rs788801 (IVS6). The proband is hemizygous for the rs10753914 (IVS1) SNP, but heterozygous for the downstream rs788801 (IVS6) SNP suggesting break boundaries for the indel. A long range genomic PCR using primers flanking these markers failed to amplify the predicted 10,120bp product, but a smaller amplicon of ~1500 bp was present in the proband and the father but not the mother or non-FA control (Figure 2.5A). Sanger sequencing of this smaller PCR product confirmed a large genomic deletion, g.202332626_202341295del, in the proband and father likely resulting from *Alu-Alu* mediated non-allelic homologous recombination (NAHR) between two *AluYa5* repeats within the UBE2T gene. The sequence intervening IVS1 *AluYa5* and IVS6 *AluYa5* and one *Alu* is lost in the paternally derived allele resulting in an 8670bp deletion (Figure 2.5B). The resulting single *AluYa5* sequence is bordered by IVS1 on the 5' side and IVS6 on the 3' (Figure 2.5C). This deletion is expected to be a null allele, as it results in the loss of a majority of the gene including the start codon.

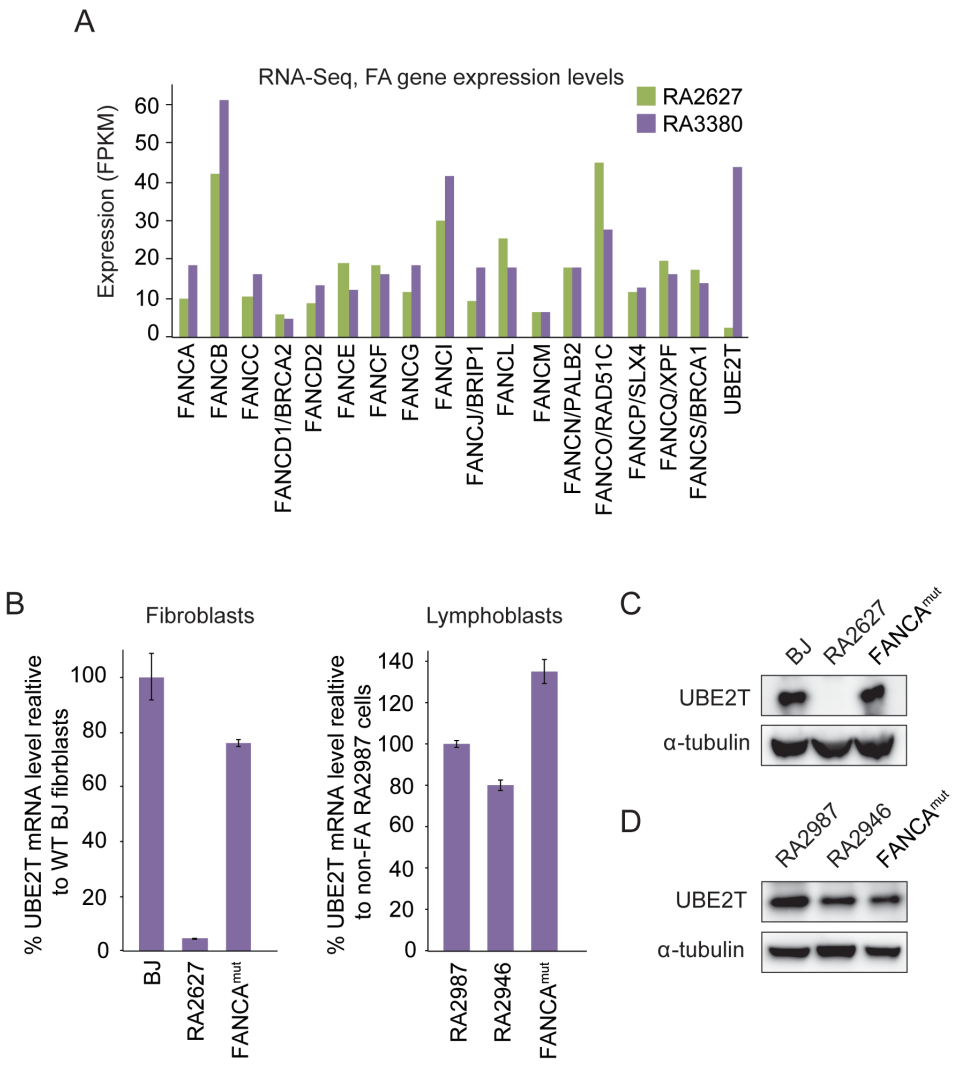

Figure 2.3 UBE2T is deficient in RA2627 cells.

(A) Comparison of normalized RNA-seq expression, Fragments Per Kilobase of transcripts per Million reads (FPKM), of known FA genes and *UBE2T* for RA2627 and non-FA control RA3380 primary cells. (B) RT-quantitative PCR of *UBE2T* expression levels in RA2627 fibroblasts (left) and RA2946 lymphoblasts (right) in comparison to wild type control and *FANCA*-mutant cells. Error bars indicate standard error of three replicates. (C-D) Western blot with UBE2T antibody.

The maternal duplication, g.202332626_202341295dup, also appears to be mediated by *Alu* recombination. The maternally derived mutation consists of a large duplication of the genomic region between the two *AluYa5* repeats (Figure 2.4 and Figure 2.6). Analysis of *UBE2T* cDNA revealed a unique Exon6-Exon2 junction suggesting a genomic duplication of a region of *UBE2T* (Figure 2.6A). This unique junction, was also identified in the genomic DNA from proband fibroblasts and mother's LCLs using PCR and Sanger sequencing (Figure 2.6B). The region following exon 6 was found to contain IVS6 sequence flanking the 5' of the *AluYa5* repeat and IVS1 sequence flanking the 3' of the repeat, and was confirmed by cloning. This is likely a duplication event mediated by *Alu* recombination (Figure 2.6C).

Cloning of cDNA from proband fibroblasts revealed a transcript containing the hypothesized duplication c.-64_468dup (dupEx2_6) (Figure 2.6A and C). In this transcript, exon 6 is spliced to the duplicated exon 2. Inclusion of the noncoding region from exon 2 results in a frameshift and a premature stop codon. The c.-64_468dup transcript can be detected at very low frequency in RA2627 cells and is likely degraded by nonsense-mediated decay due to the premature stop codon. If any transcript is translated, it may produce a residual amount of the predicted protein p.A157Cfs*7. PCR analysis of gDNA demonstrates that the maternally derived mutation is absent in the RA2946 LCLs (Figure 2.6D). This indicates that

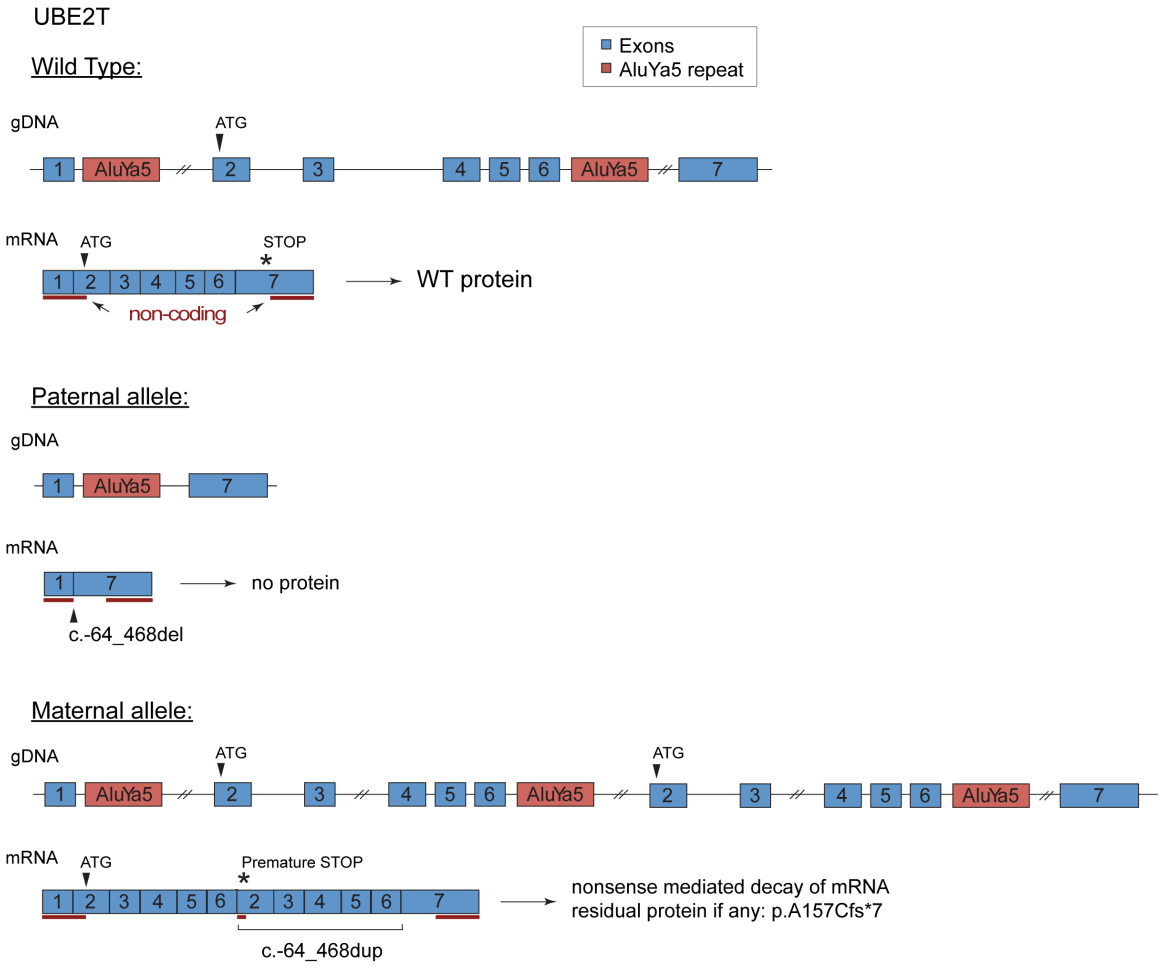

Figure 2.4 UBE2T deficiency is the result of *AluYa5* mediated non-allelic homologous recombination.

Schematic of the paternally derived deletion and maternally derived duplication resulting from *Alu-Alu* mediated non-allelic homologous recombination (NAHR) of *AluYa5* repeats present in IVS1 and IVS6 of the *UBE2T* gene. For the paternal allele, recombination resulted in the loss of the intervening sequence and one *AluYa5* repeat (8,670bp). For the maternal allele, recombination resulted in the insertion of another *AluYa5* repeat and duplication of the sequence between the *Alu* repeats.

Figure 2.5 Identification of paternally-derived deletion resulting from *AluYa5* mediated non-allelic homologous recombination.

A) PCR to identify mutations in UBE2T in the indicated cell lines and parental peripheral blood (PB) samples. RA2627 are proband-derived fibroblasts and RA2946 are proband LCLs. The expected PCR product amplifying with primers 474Fwd and 479Rev is 10,120bp. The large amplicon PCR failed, but a smaller amplicon of ~1,500bp was identified in the proband and father but not the mother and non-FA control. Asterisk denotes non-specific bands. (B) Schematic of *UBE2T* indicating the location of PCR primers 474Fwd and 479Rev and the span of PCR amplicons. Recombination between the *AluYa5* sites results in an 8,670bp deletion that yields the smaller 1,450bp PCR products. (C) Chromatograms displaying sequencing results of the 1,450bp PCR product. *UBE2T* IVS1 borders the 5' *AluYa5* sequence and the 3' *AluYa5* sequence is bordered by IVS6. The sequence intervening the *Alu* repeats and one *AluYa5* repeat has been deleted.

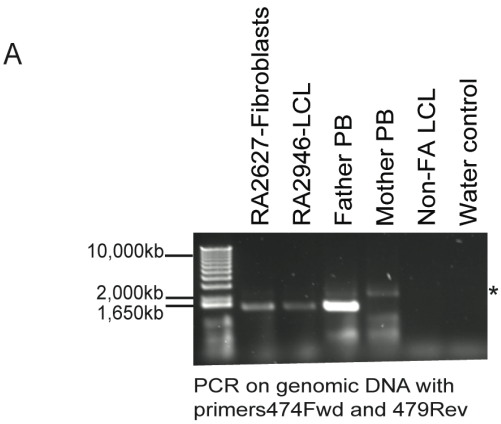

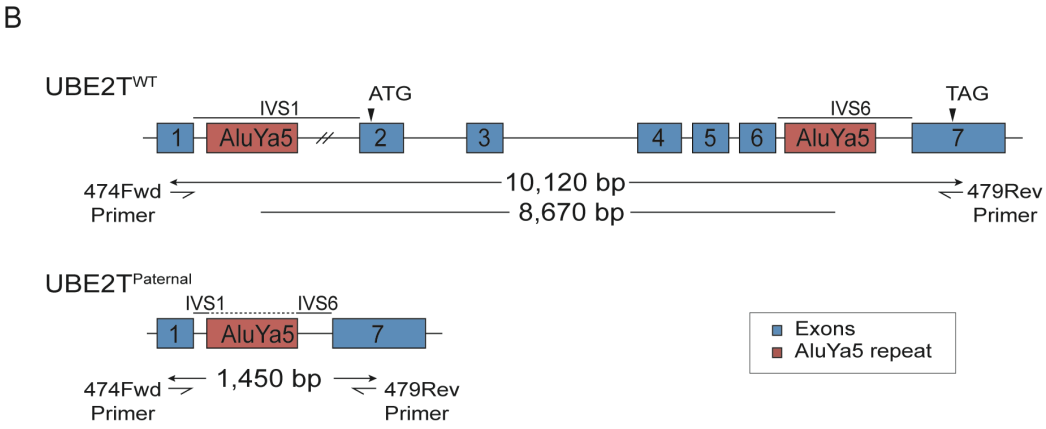

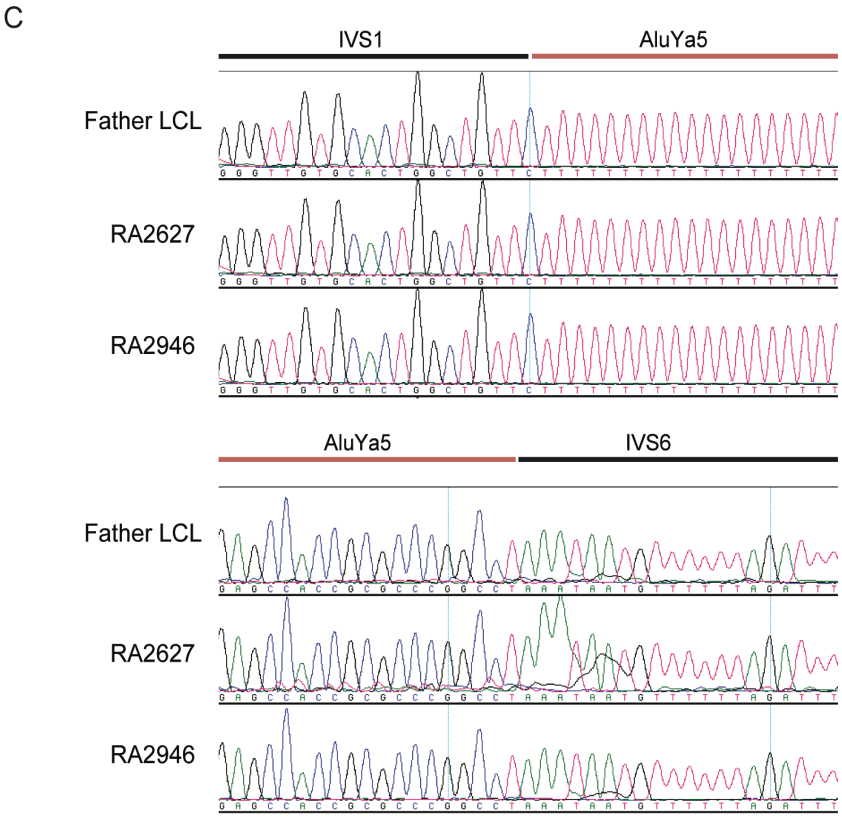

Figure 2.6 Identification of maternally-derived duplication mutation resulting from *AluYa5* mediated non-allelic homologous recombination.

(A) Examination of RT-PCR products amplified with primers 474Fwd and 479Rev yielded the maternal duplication transcript that is 1,250bp in length. Chromatograms depict the Exon6-Exon2 and Exon6-Exon7 junctions present in this mRNA transcript. (B) Analysis of genomic DNA for *Alu* mediated duplication. PCR using 509Fwd and 538Rev primers results in a 1,128bp PCR product in proband fibroblasts and maternal LCLs. Chromatograms display PCR sequencing demonstrating that *UBE2T* IVS6 borders the 5' *AluYa5* sequence and the 3' *AluYa5* sequence is bordered by IVS1. The sequence between the *Alu* repeats and one *AluYa5* repeat has been duplicated. (C) Schematic of *UBE2T* indicating location of PCR primers and span of amplicons for genomic and cDNA assays. (D) 1,128bp PCR product that is specific to the maternal duplication (509Fwd and 538Rev primers). Analysis of gDNA from fibroblasts, LCLs, and PB from the proband compared to maternal and paternal gDNA.

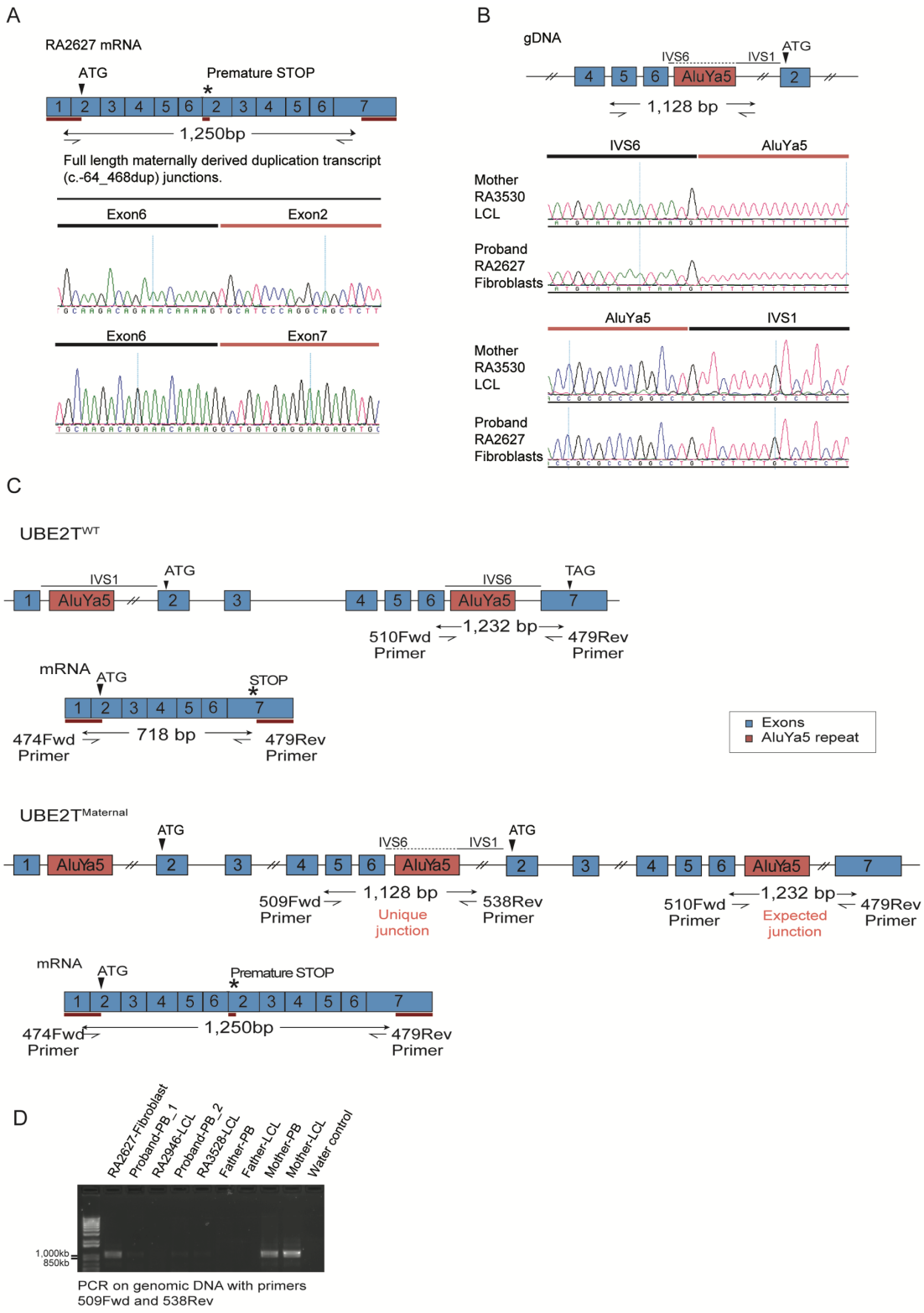

the expression of wild type UBE2T in the proband blood may be due to recombination of the maternally derived allele to restore the WT sequence.

2.2.5 Complementation of RA2627 cellular defects by wild type UBE2T expression

To prove that UBE2T deficiency is the cause of the subject's FA, we introduced wild type *UBE2T* into RA2627 fibroblasts and assayed for rescue of FA phenotypes. Overexpression of UBE2T rescued cellular hypersensitivity to crosslinking agents MMC, DEB and cisplatin (Figure 2.7A-C). UBE2T expression restored monoubiquitination of FANCD2 and FANCI (Figure 2.7D) and FANCD2 foci following treatment with MMC (Figure 2.7G). Analysis of cell cycle distribution following treatment with MMC revealed an accumulation of RA2627 cells in G2 that was rescued by UBE2T overexpression to the levels observed in wild type BJ cells (Figure 2.7E). These results confirm that deficiency of UBE2T results in Fanconi anemia-T complementation group.

2.2.6 The primary role of UBE2T is in ICL repair

To determine if UBE2T is important for resistance to other types of damage, RA2627 cells were tested for sensitivity to other genotoxic agents. RA2627 cells were not found to be sensitive to UV, IR, CPT, HU, or the PARP inhibitor olaparib (PARPi) (Figure 2.8A-F). These results are in contrast to previously reported UV and HU sensitivity of UBE2T deficient DT40 cells (Kelsall et al., 2012). These data suggest that UBE2T does not have a major role in responding to DNA lesions or

Figure 2.7 UBE2T cDNA complements RA2627 hypersensitivity to crosslinking agents and monoubiquitination of FANCD2 and FANCI.

(A-C) Complementation of MMC, DEB, and cisplatin sensitivity of proband fibroblasts (RA2627). Error bars indicate s.d. (D) Western blot analysis with FANCD2 and FANCI antibody of *UBE2T* complemented cells with 1 μM MMC treatment for 24h. (E) Complementation of cell cycle defect after 45 nM MMC treatment. Cells were treated with drug and cultured for 48 h before analysis. (F) Expression of wild type HA-FLAG tagged *UBE2T* cDNA or empty vector control (EV) in RA2627 fibroblasts. (G) FANCD2 foci formation of complemented cells following treatment with or without 1μM MMC for 24h.

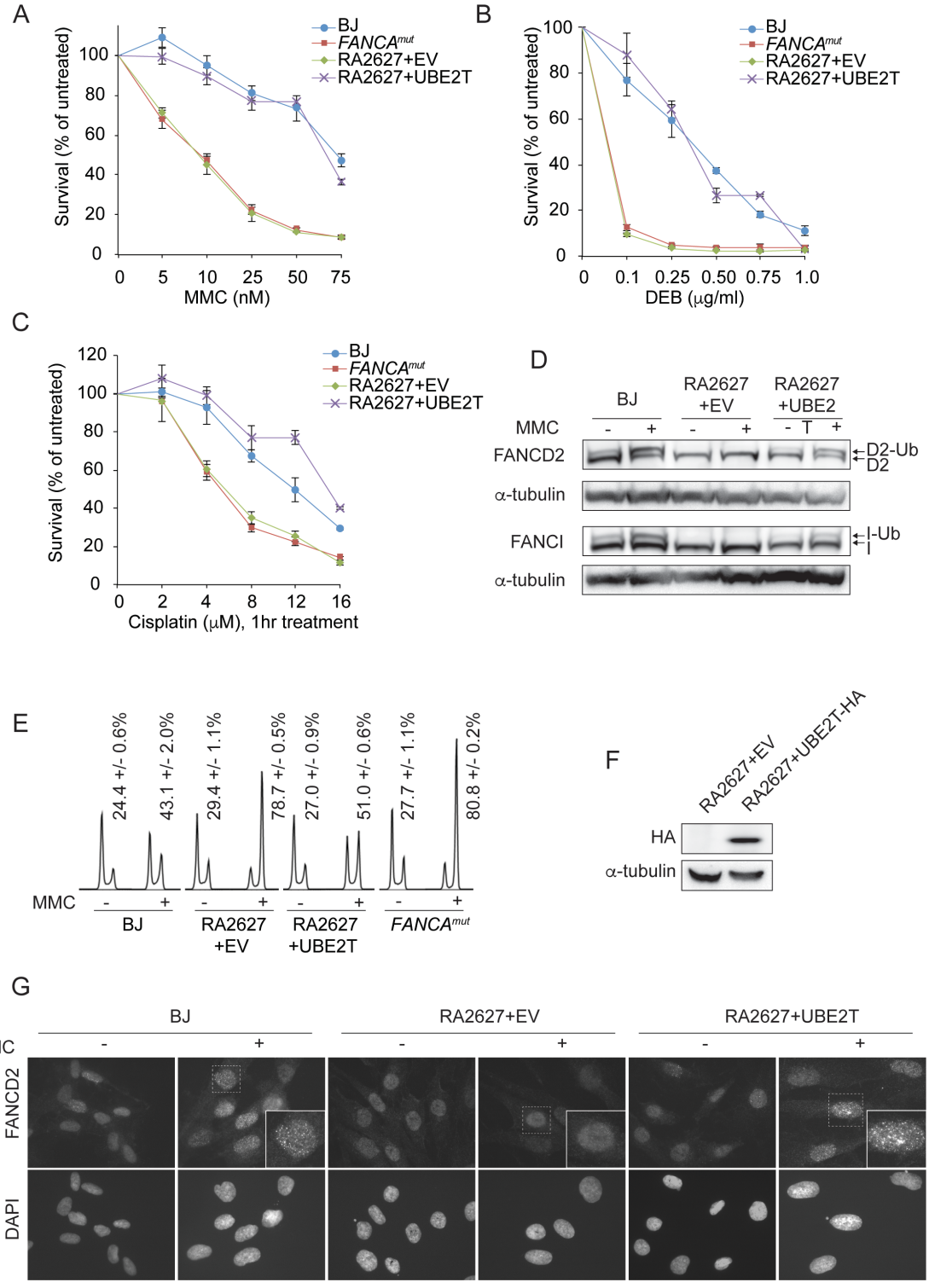

replication stress produced by these agents and its primary function is in ICL repair.

2.2.7 A potential a mechanism of FA pathway regulation through UBE2T

While our manuscript was in press, Hira *et al.*, published the identification of two individuals with compound heterozygous *UBE2T* mutations. Both individuals harbored different LOF mutations in *trans* to a N-terminal aa substitution p.Q2E (Hira et al., 2015). The Q2E substitution replaces a polar aa with an acidic residue and results in decreased FANCL binding and reduction in ID2 ubiquitination (Hira et al., 2015).

Analysis of the *S. pombe* E1-E2 structure of Uba1-Ubc15 shows that acidic residues of the N-terminus may reduce E1-E2 binding and that introduction of negative charge at the N-terminus also reduces E1-E2 interaction. Similarly, phosphorylation of the N-terminal of Ub E2s may also serve to regulate the E1-E2 interaction and a number of Ub E2s have serine/threonine phosphorylation sites in the N-terminal region (Lv et al., 2017). The UBE2T N-terminus contains a protein kinase C (PKC) consensus sequence and can be targeted by basophilic kinases on Ser5 *in vitro* (Lv et al., 2017). The structure of UBE2T and the FANCL RING domain demonstrates that the RING domain is also in proximity to UBE2T Ser5 suggesting that phosphorylation would disrupt the E1 as well as the E3 interaction (Hodson et al., 2014; Lv et al., 2017).

Compared to unmodified wild type UBE2T protein, phosphorylated Ser5 (pSer5) and the phosphomimetic mutant S5D have severely diminished monoubiquitination activity *in vitro*. Similarly, the Q2E substitution disrupts E1-E2 thioester transfer and monoubiquitination of FANCD2 (Lv et al., 2017). To determine the consequences phosphorylation may have *in vivo,* we overexpressed the UBE2T S5D phosphomimetic mutant in UBE2T deficient RA2627 fibroblasts (Figure 2.9A). The Q2E substitution was also overexpressed for comparison. Both S5D and Q2E showed significant defects in monoubiquitination of FANCI and FANCD2 by western blot and foci formation following treatment with mitomycin C (MMC) (Figure 2.9B-D). The S5D and Q2E mutants did not fully rescue sensitivity to MMC by cell survival assay (Figure 2.9E). In contrast, the S5A phosphomutant rescues monoubiquitination of FANCD2/I, FANCD2 foci formation, and hypersensitivity to MMC (Figure 2.9G-H). The pSer5 was undetectable in cell lysates using a phospho specific antibody and by mass spectrometry. However, the S5A phosphomutant is able to fully rescue the defects of the UBE2T deficient cells suggesting the S5D phosphomimetic is not a non-specific disruption of the E1-E2 or E2-E3 interaction. These data demonstrate that phosphorylation of the N-terminus in UBE2T may serve to regulate E1-E2 and E2-E3 interactions, but more investigation and identification of a responsible kinase would be required to determine if this is an important mechanism of regulation of the FA pathway. Additionally, in light of these findings, we predict that the patient Q2E mutation

Figure 2.8 UBE2T does not have a major role in repair of other types of DNA damage.

(A) UV treated cell survival assay of the UBE2T complemented pair of RA2627 fibroblasts compared to BJ wild type fibroblasts depleted of XPF. (B) Western blot of XPF levels for cells used in A. (C) IR cell survival assay of RA2627 fibroblasts in comparison to *RAD50* patient fibroblasts ($RAD50^{mut}$). (D-E) Camptothecin (CPT) and PARP inhibitor olaparib (PARPi) cell sensitivity assays comparing RA2627 fibrobalsts to a patient *SLX4* fibroblast cell line ($SLX4^{mut}$). Patient *SLX4* complemented pair are transduced with wild type *SLX4* cDNA or empty vector (EV). (F) Cell survival assay to hydroxyurea (HU) of RA2627 cells compared to BRCA2 patient fibroblast cell line ($BRCA2^{mut}$). Error bars indicate s.d.

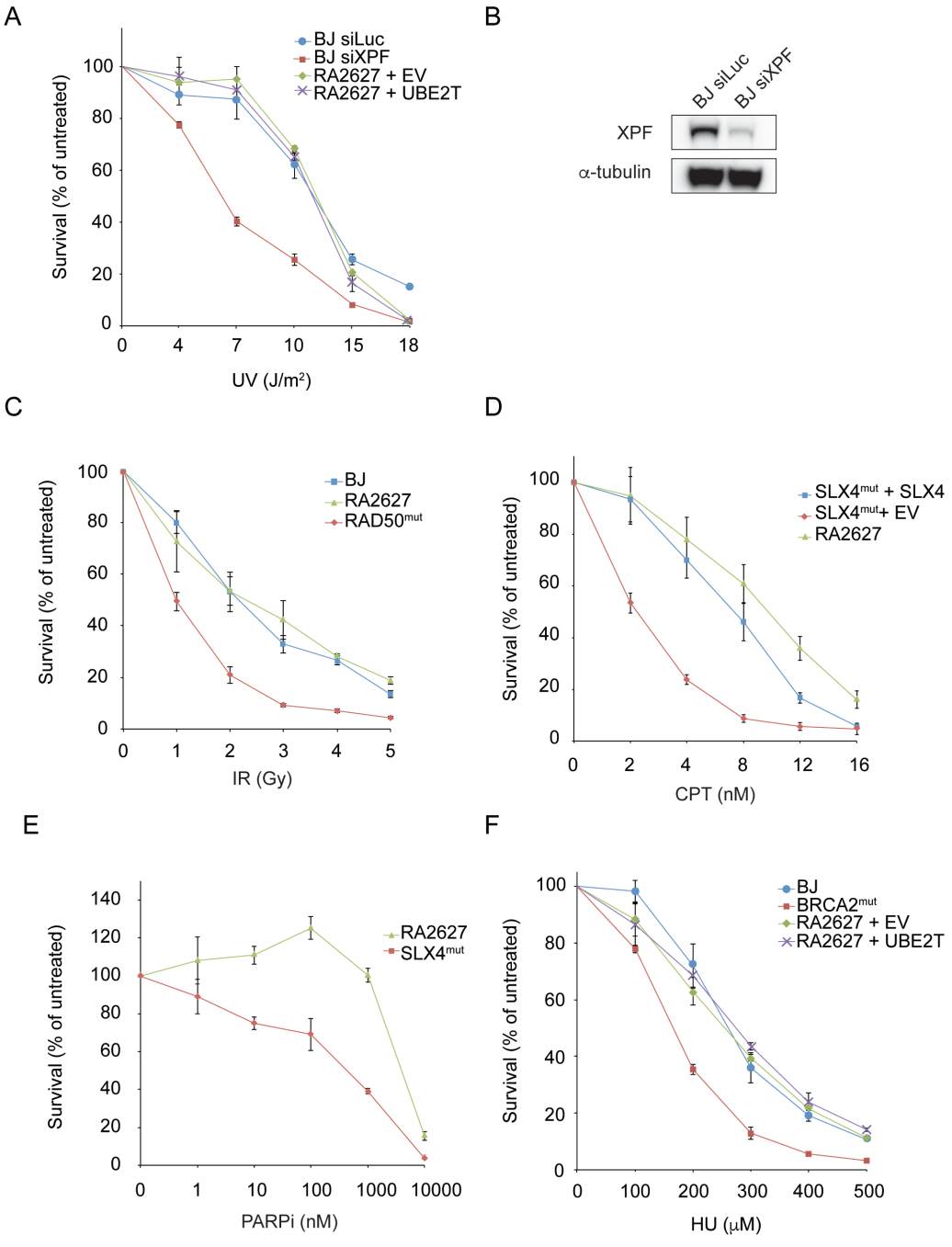

Figure 2.9 UBE2T/FANCT deficient RA2627 cells expressing UBE2T S5D phosphomimetic are defective for FANCD2 and FANCI monoubiquitination.

(A) Western blot of HA-FLAG-tagged UBE2T expression. RA2627 *UBE2T/FANCT* deficient fibroblasts expressing wild type (WT) UBE2T, empty vector control (EV), and UBE2T mutants Q2E and S5D. (B) Western blot analysis of FANCD2 and FANCI monoubiquitination in UBE2T complemented cells following 24h treatment with 1 μM MMC. (C) FANCD2 foci formation in RA2627 cells expressing wild type and mutant UBE2T after 24h treatment with 1 μM MMC. (D) Quantification of FANCD2 foci formation visualized in C. (E) MMC cell survival assay of RA2627 hTERT cells expressing WT and mutant UBE2T. (F) Western blot of HA-FLAG-tagged S5A UBE2T expression in RA2627 cells used in G-H. (G) Quantification of FANCD2 foci formation of UBE2T S5A mutant compared to EV and WT expressing RA2627 fibroblasts. (H) MMC cell survival assay of UBE2T S5A mutant compared to WT and EV expressing RA2627 fibroblast.

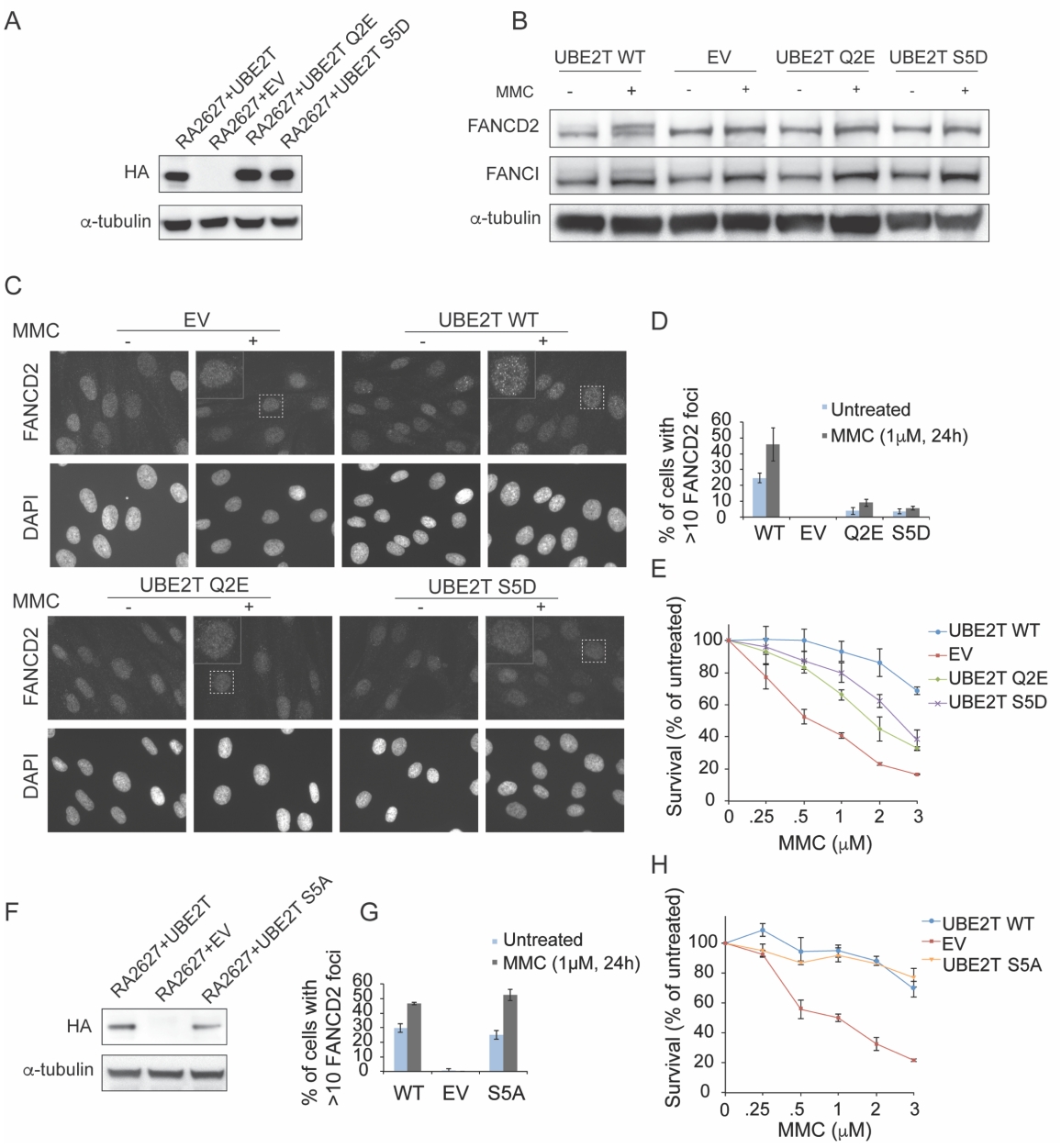

described by Hira *et al*. likely disrupts both E1 and E2 interaction by substitution of an acidic residue leading to suboptimal activation of the FA pathway.

2.3 Summary and Conclusion

In this study, we have identified a Fanconi anemia subtype resulting from deficiency of UBE2T. Analysis of RNA-seq data was critical in identifying UBE2T deficiency stressing that multipronged diagnostic approaches are often necessary in a genetically heterogeneous disease like FA.

We have identified compound heterozygous mutations in *UBE2T*, a large genomic deletion in the paternally derived allele and a large duplication in the maternally derived allele. Both of the mutations appear to be driven by *Alu*-mediated non-allelic homologous recombination (NAHR). NAHR is a prevalent mechanism in genetic disorders arising from copy number defects due to recurrent intrachromosomal recombination events (Deininger, 2011). Recently, sequencing of *FANCA* deletion variants identified that breakpoints preferentially lie within *Alu* elements and has revealed NAHR as a major mechanism of deletion in *FANCA* (Flynn et al., 2014).

The subject presented at birth with classic FA features including developmental defects and increased chromosomal breakage. The subject has not yet developed bone marrow failure at the age of 16. Blood counts are likely preserved due to the somatic mosaicism of the hematopoietic compartment.

Restoration of UBE2T expression is detected in the individual's lymphoblast cells and we have observed increasing rescue of chromosomal breakage in peripheral blood since birth. The subject's bone marrow remains stable but hypocellular for age (30-40%) and it is unclear whether mosaicism will continue to improve the bone marrow cellularity.

The paternally derived deletion mutation is expected to not produce protein due to deletion of the majority of the coding region and start codon, while the maternally derived duplication results in very low levels of the c.-64_468dup *UBE2T* transcript. This transcript may theoretically produce a UBE2T p.A157Cfs*7 protein, but it is clearly insufficient to fully support FA pathway function as evident by the phenotype of the subject and the cellular defects. The subject's fibroblasts are as sensitive as FA-A patient cells by cell survival assay and no monoubiquitination of FANCD2 or FANCI is detected. However, breakage levels are not as elevated as the FA-A fibroblasts leaving the possibility that residual truncated UBE2T may be present and active at a very low level, affecting the breakage phenotype. An alternative explanation could be that another E2 with low levels of activity may partially substitute in the pathway.

UBE2T has been demonstrated to be the major E2 ubiquitin-conjugating enzyme required for the monoubiquitination of FANCD2 and FANCI (Alpi et al., 2008; Hodson et al., 2014; Longerich et al., 2014; Longerich et al., 2009; Machida

et al., 2006; Sato et al., 2012). Efficient and specific FANCD2 monoubiquitination *in vitro* by UBE2T/FANCL requires the presence of FANCI and DNA (Longerich et al., 2014; Sato et al., 2012). *In vitro* studies have demonstrated that a second E2, UBE2W, can also ubiquitinate FANCD2 (Alpi et al., 2008; Zhang et al., 2011). In recent work, the *in vitro* monoubiquitination of FAND2 by UBE2W is demonstrated to be nonspecific, does not require interaction of ID2 complex, and is not stimulated by DNA (Longerich et al., 2014). Additionally, *ΔUBE2W* chicken DT40 cells do not display sensitivity to MMC and display normal levels of MMC induced monoubiquitination of FANCD2 (Longerich et al., 2014).

The RA2627 patient cells do not have any detectable UBE2T by western blot and transcript levels are extremely low making them ideal for studying cellular defects of UBE2T deficiency. Previously, it was reported that UBE2T deficient DT40 cells are sensitivity to UV and HU (Kelsall et al., 2012). In RA2627 cells, UBE2T deficiency does not result in cellular sensitivity to UV and the patient does not report sensitivity to sun exposure. We also demonstrate that UBE2T is not required for cellular resistance to other types of DNA damage produced by IR, CPT, PARP inhibitor, or HU. These results demonstrate the primary role of UBE2T is in ICL repair and not in response to other types of DNA damage by these agents.

The Olsen laboratory determined the *S. pombe* Uba1-Ubc15 E1-E2 complex structure and observed that negative charge or phosphorylation of N-

terminus residues of Ub E2s inhibits their function *in vitro* by interrupting the E1-E2 interaction (Lv et al., 2017). The UBE2T and FANCL RING domain structure also indicates that disruption in this region of UBE2T may also impact the E2-E3 interaction (Hodson et al., 2014; Lv et al., 2017). Expression of phosphomimetic S5D and Q2E UBE2T in RA2627 cells mildly ameliorates UBE2T deficiency but still results in reduced FA pathway activation and ICL sensitivity. UBE2T Ser5 may be a regulatory site that disrupts both E1-E2 and E2-E3 interaction; however, pSer5 was not detected *in vivo*. Nonetheless, the deleteriousness of the patient Q2E substitution, that is the outcome of a point mutation, likely results from the disruption of both the E1-E2 and E2-E3 interactions resulting in inadequate FA pathway activation.

Our identification of biallelic *UBE2T* mutations and UBE2T deficiency in an individual with FA corroborates that UBE2T is the primary E2 of the FA pathway required for the activation of ID2 complex by monoubiquitination of FANCD2 and FANCI and repair of DNA interstrand crosslinks. Deficiency of UBE2T causes complementation group Fanconi anemia-T disease and future evaluation of FA patients with unknown gene mutations should include complementation studies of *UBE2T.*

Chapter 3: Differential roles of the BRCA2 DNA binding domain in replication fork protection in response to hydroxyurea and DNA interstrand crosslink damage

3.1 Introduction

FANCD1/BRCA2 is an essential gene required for organismal development and cellular survival. Single allele mutations in *BRCA2* predispose to breast and ovarian cancer and biallelic mutations results in a subtype of Fanconi anemia, FA-D1 (Howlett et al., 2002). FA is a heterogeneous disease, but even within the disease spectrum, *FANCD1* patients are phenotypically distinct. A higher proportion of FA-D1 patients have developmental abnormalities and the probability of presenting with malignancy is 97% by the age of 5 (Alter et al., 2007). FA-D1 patients are rare, making up only 2% of Fanconi anemia cases (Wang and Smogorzewska, 2015). Here we identify individuals with atypical FA-D1 presentation with mutations that lie within the BRCA2 DNA biding domain (DBD). The identification of these FA-D1 individuals suggests that certain mutations of *BRCA2/FANCD1* may present differently than those previously described (Alter et al., 2007; Myers et al., 2012; Wagner et al., 2004). It provides a unique opportunity to uncover the BRCA2 function that is specific to this domain.

Functional analysis of BRCA2 has historically focused on canonical homologous recombination (HR) and the requirement for BRCA2 in ICL repair has been attributed to the importance of HR repair of DSBs generated during ICL processing. As described in the main introduction of this thesis, the role of BRCA2 has been expanded to the protection of stalled replication forks (Quinet et al., 2017). Analysis of replication fork intermediates by EM corroborates that reversed replication forks are a structure that requires BRCA2-RAD51 protection to prevent

Figure 3.1 BRCA2 mutations identified in a sibling pair with atypical Fanconi anemia

Family pedigree showing a sibling pair with Fanconi anemia (red circles) who are compound heterozygous for BRCA2 c.2330dupA (maternal inheritance) and c.8524C>T (paternal inheritance) mutations. Family history of breast cancer (purple), skin cancer (grey), and colon cancer (green). (B) Chromatograms of Sanger sequencing confirming *BRCA2* c.2330dupA and c.8524C>T mutations identified by whole exome sequencing (WES).

A

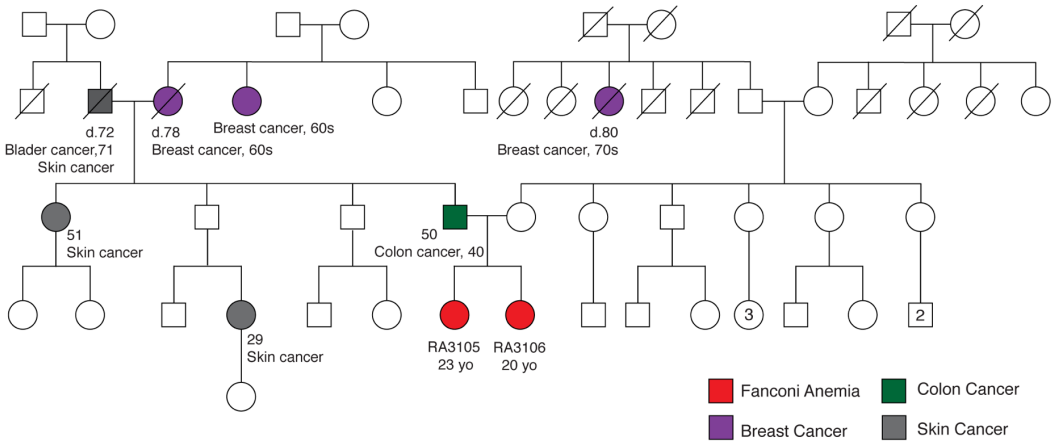

B

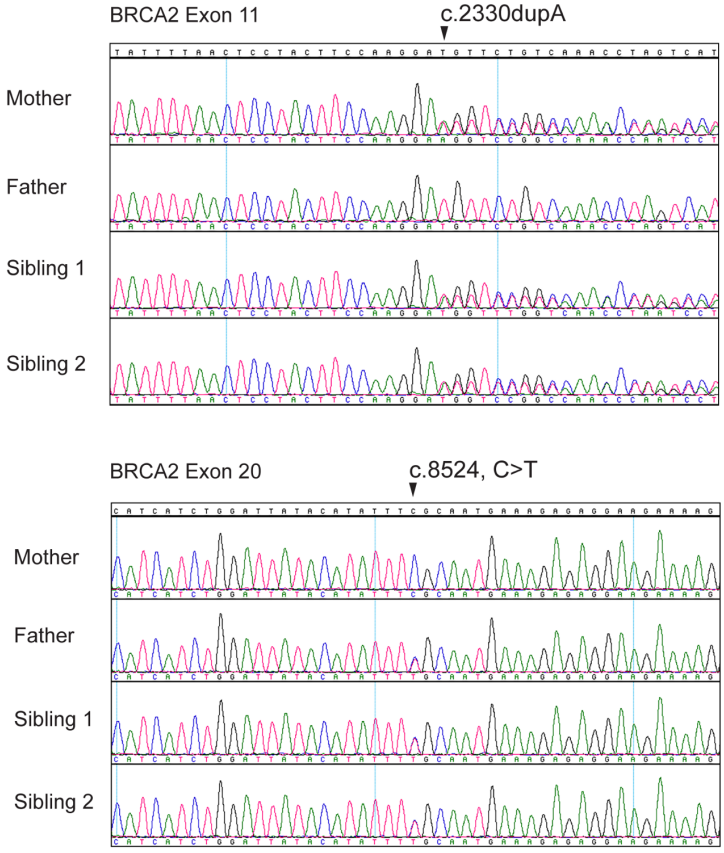

nucleolytic degradation (Lemacon et al., 2017; Mijic et al., 2017). Mitomycin C (MMC) treatment is reported to increase reversed replication fork intermediates but the physiological relevance of fork reversal in ICL repair has not been investigated (Zellweger et al., 2015). RAD51 is recruited to replication forks stalled at ICLs prior to DSB production and has been shown to have a role in protecting ICLs against extensive resection by DNA2 and WRN (Long et al., 2011; Wang et al., 2015). Here, the requirement for BRCA2 to protect against hyper-resection of ICLs, separate from its role in HR, is investigated. These studies reveal that replication fork protection at hydroxyurea-stalled forks and ICLs both require BRCA2 but that they are distinct processes.

3.2 Results

3.2.1 Atypical presentation of Fanconi anemia in individuals with biallelic *FANCD1/BRCA*2 mutations

Two female siblings with unknown causative gene mutations displaying a multitude of congenital abnormalities and mildly elevated levels of chromosomal breakage were entered into the International Fanconi Anemia Registry (IFAR). The first sibling, at three years of age, was diagnosed with probable FA based on congenital abnormalities. A DEB test showing elevated levels of chromosomal breakage above normal but lower than typically seen in FA suggested the possibility of somatic mosaicism. The second sibling was diagnosed at birth with similar findings. There is no reported family history of FA, but there are some cases

Figure 3.2 Schematic of BRCA2 structure showing location of patient DNA binding domain mutations.

(A) Schematic of BRCA2 domain structure and key interacting proteins. (B) BRCA2 structure of the DBD illustrating the location of the patient p.del2830-33 and p.R2842C mutations at the base of the Tower domain and OB2. Structure adapted from Yang *et al*., 2005. (C) Alignment of the DBD peptide sequence in the region of the patient *BRCA2* mutations. The alignment shows that this sequence is evolutionary conserved across many species. In green are the aa residues modified by the patient mutations, p.del2830-33 and p.R2842C are highlighted. Purple arrows indicate aa residues that contact DNA (Yang et al., 2005).

A

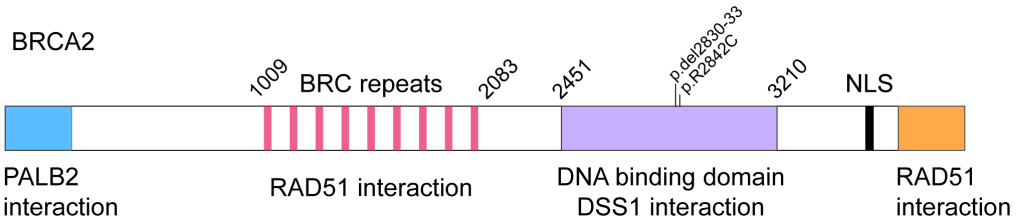

B

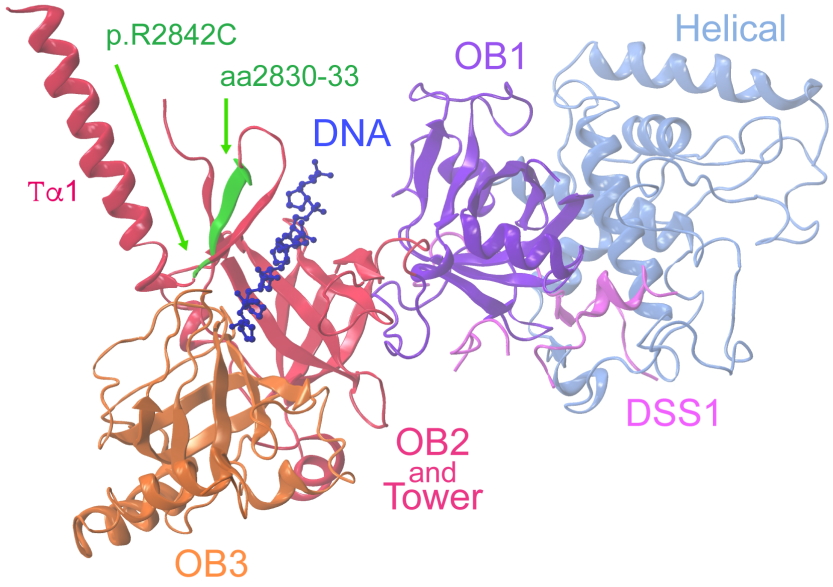

C

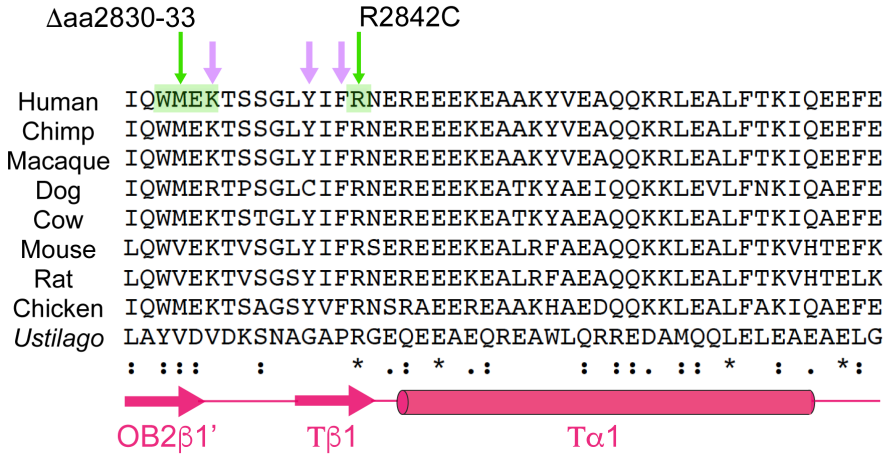

of breast cancer that were all diagnosed later in life (above 60 years of age) (Figure 3.1A).

Analysis of whole exome sequencing (WES) of patient LCLs was performed and the data was filtered for variants that were shared between the siblings with an allele frequency less than 1% in the 1000 genomes database (Genomes Project et al., 2010). Biallelic *FANCD1/BRCA2* mutations, in the now young adult sibling pair, were identified and no other FA gene mutations were observed. These results were surprising since neither sibling displayed the typical clinical findings of the *FANCD1/BRCA2* complementation group with no history of malignancy or bone marrow failure at the ages of 20 and 23. An updated family history was notable for early onset colorectal cancer of the father at the age of 40 and some skin cancer diagnosis in the family (Figure 3.1A). The role of *BRCA2* in colorectal cancer (CRC) susceptibility is controversial, but there is some evidence that mutations in *BRCA2* may account for some familial CRCs (Degrolard-Courcet et al., 2014a; Garre et al., 2015; Phelan et al., 2014).

Sanger sequencing confirmed compound heterozygous *BRCA2* mutations. A frameshift c.2330dupA mutation of exon 11 (maternal origin) results in premature truncation of BRCA2 (p.Asp777Glu Fs*11) and has previously been described in HBOC (Figure 3.1B). A second mutation, c.8524C>T, a missense variant of exon 20 (paternal origin) results in an p.Arg2842Cys residue change in the highly

conserved DNA binding domain (DBD) of BRCA2 and has previously been identified as a variant of unknown significance (VUS) in HBOC (Figure 3.1B and Figure 3.2). At the protein level, the missense mutation results in the p.Arg2842Cys change at a highly conserved residue at the base of the BRCA2 Tower domain of the DBD (Figure 3.2.B-C). Sequencing of peripheral blood and lymphocytes demonstrates the presence of both mutations and no evidence of somatic mosaicism. With the recent release of the Genome Aggregation Database (gnomAD) allele frequencies for c.2330dupA and c.8524C>T are available at 4.068e-6 and 1.084e-5 respectively. A combined annotation dependent depletion (CADD) score of 35 is reported for this variant (Kircher et al., 2014). Given the conservation of the affected amino acid (aa) residue, rare allele frequency, and predicted deleteriousness by prediction tools, we hypothesized that the *BRCA2* VUS c.8524C>T is pathogenic and contributing to diseases in this family.

One other adult individual with biallelic *BRCA2* mutations is cited in the literature (Howlett et al., 2002). This individual is homozygous for c.IVS19-1G>A mutation that impacts the splice acceptor site for exon 20. cDNA analysis demonstrated the use of an alternate spice acceptor that results in the loss of 12 bp of exon 20 and translates into p.del2830-2833 (Howlett et al., 2002). Amino acid residues 2830-2833 are located at the transition of OB2 and the base of the Tower domain (Figure 3.2.B-C). This individual at the age of 30 had history of thumb malformation, but no history of bone marrow failure or malignancy. The

patient is deceased due to cause unrelated to disease. Similar to the sibling pair identified in the IFAR, the reported chromosomal breakage was modest (Howlett et al., 2002).

We pursued characterization of patient-derived cells to determine how these DBD mutations affect the function of BRCA2. We hypothesized that the defects conferred by these BRCA2 DBD mutations leads to characteristic FA developmental defects, but not early childhood bone marrow failure and malignancies typically seen in other *FANCD1* cases. The region of the BRCA2 DBD mutated here has been proposed to bind at ssDNA-dsDNA junctions, but its role and the consequences of mutations here are unknown. In light of the HR independent role of the BRCA2 binding partner RAD51/FANCR in replication fork protection at ICLs, we hypothesized that these mutations may also disrupt replication fork protection where recognition of ssDNA-dsDNA junctions may be important.

3.2.2 Phenotype of *FANCD1/BRCA*2 DNA binding domain patient cell lines

Lymphoblastoid cell lines (LCLs) (RA3105 and RA3106) were derived from the sibling pair with compound heterozygous *BRCA2* mutations, c.2330dupA and c.8524C>T. FA pathway activation, monitored by FANCI ubiquitination, was normal in patient-derived LCLs (Figure 3.3A). Analysis of BRCA2 expression by western blot demonstrated a full length (~390 kDa) band, the presumed product of the c.8524C>T allele, for both patient cell lines (Figure3.3B). DEB breakage

Figure 3.3 Characterization of BRCA2 patient lymphoblast cell lines from a sibling pair with atypical Fanconi anemia.

(A) Immunoblot analysis for FANCI ubiqutination following treatment with 1μM MMC for 24h of RA2985 (WT), RA2939 (FANCA), and patient RA3105 and RA3106 LCLs. (B) Immunoblot showing BRCA2 levels in RA2985 (WT) control, RA2525 (FANCD1) and patient RA3105 and RA3106 LCLs. (C) Quantification of chromosome breaks following DEB treatment of RA2985 (WT), RA2939 (FANCA), and patient RA3105 and RA3106 LCLs. (D) Metaphase for RA2985 and RA3105 following DEB treatment. (E-F) Cell survival assays of patient derived lymphoblast cell line (LCLs) RA3105, RA2939 (FANCA), RA2985 (WT), and RA2525 (FANCD1) after mitomycin C (MMC), diepoxybutane (DEB), PARP inhibitor olaparib (PARPi), and camptothecin (CPT) treatment. Survival assays were performed in triplicate. Cells were treated with increasing concentrations of genotoxic agents and counted after 7-10 days in culture. Relative cell survival was normalized to untreated controls to give percent survival. Error bars indicate s.d.

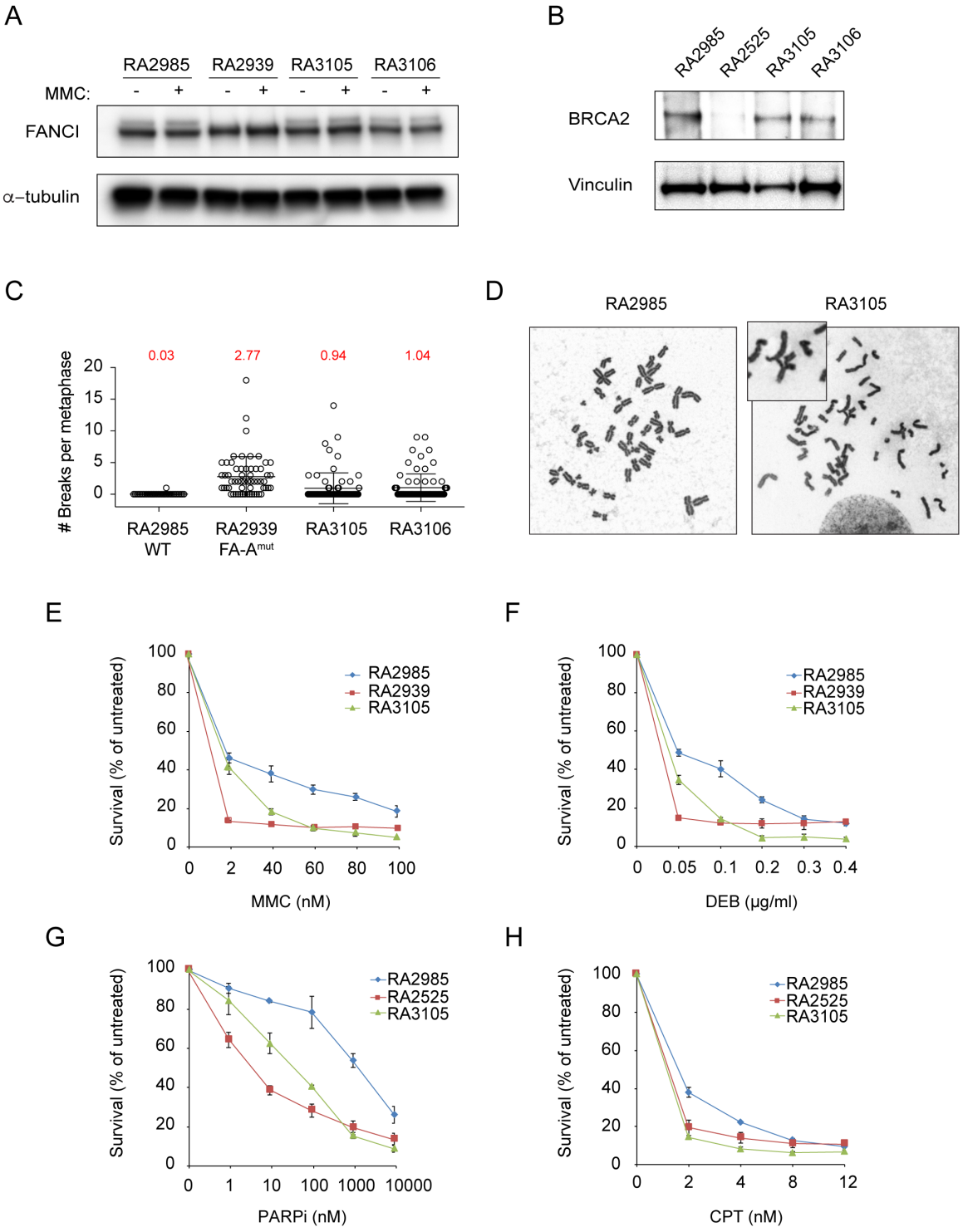

analysis confirmed previous clinical data that breakage is elevated, but not to levels of typical *FANCA* LCLs (RA2939) (Figure 3.3C-D). RA3105 LCLs displayed hypersensitivity to crosslinking agents MMC and DEB, but to a lesser degree than RA2939 *FANCA* LCLs (Figure 3.3E-F). RA3105 cells were also hypersensitive to the replication stress inducing agents including olaparib, a PARP inhibitor (PARPi), and topoisomerase I inhibitor camptothecin (CPT) (Figure 3.3G-H).

Patient derived fibroblasts (HSC62) from the individual with homozygous c.IVS19-1G>A mutations were available (Howlett et al., 2002). Analysis of HSC62 cells revealed more moderate chromosomal breakage to DEB and MMC and cellular hypersensitivity to crosslinking agents, DEB, MMC, and cisplatin (Figure 3.4A-E). Interestingly, the cells were not hypersensitive to ionizing radiation (IR), but were sensitive to replication stress induced by CPT and PARPi (Figure 3.4F-H). In contrast, the cells were not sensitive to replication stress produced by the agents aphidicolin and hydroxyurea (HU).

To determine the impact of DBD disruption on the ability of c.IVS19-1G>A *BRCA2* to load RAD51 onto ssDNA following DNA damage, we analyzed RAD51 foci formation after IR and MMC in HSC62 cells. Levels of RAD51 foci were reduced after IR and MMC treatment (Figure 3.5B-C). The RAD51 foci were quantitatively fewer and qualitatively smaller (Figure 3.5A). Given the normal

Figure 3.4 Cellular sensitivity of HSC62 BRCA2 c.IVS19-1G>A patient fibroblast cell line.

(A-B) Quantification of chromosome breaks following DEB and MMC treatment of BJ wild type fibroblasts, *FANCA* patient fibroblasts (FA-A^{mut}), and HSC62 fibroblasts. (C-J) Cell survival of HSC62 fibroblasts compared to BJ WT fibroblast, *FANCA* patient fibroblast (FA-A^{mut}), *FANCA* complemented patient cells expressing wild type *FANCA* (FA-A+A) or empty vector (FA-A+EV), or FA *BRCA2* patient fibroblast (*BRCA2*^{mut}). Cell survival assays were performed in triplicate. Cells were treated with increasing concentrations of indicated agent. Cell survival was determined by counting cells after 7-9 days in culture. Relative cell survival was normalized to untreated controls to give the percent survival. Error bars indicate s.d.

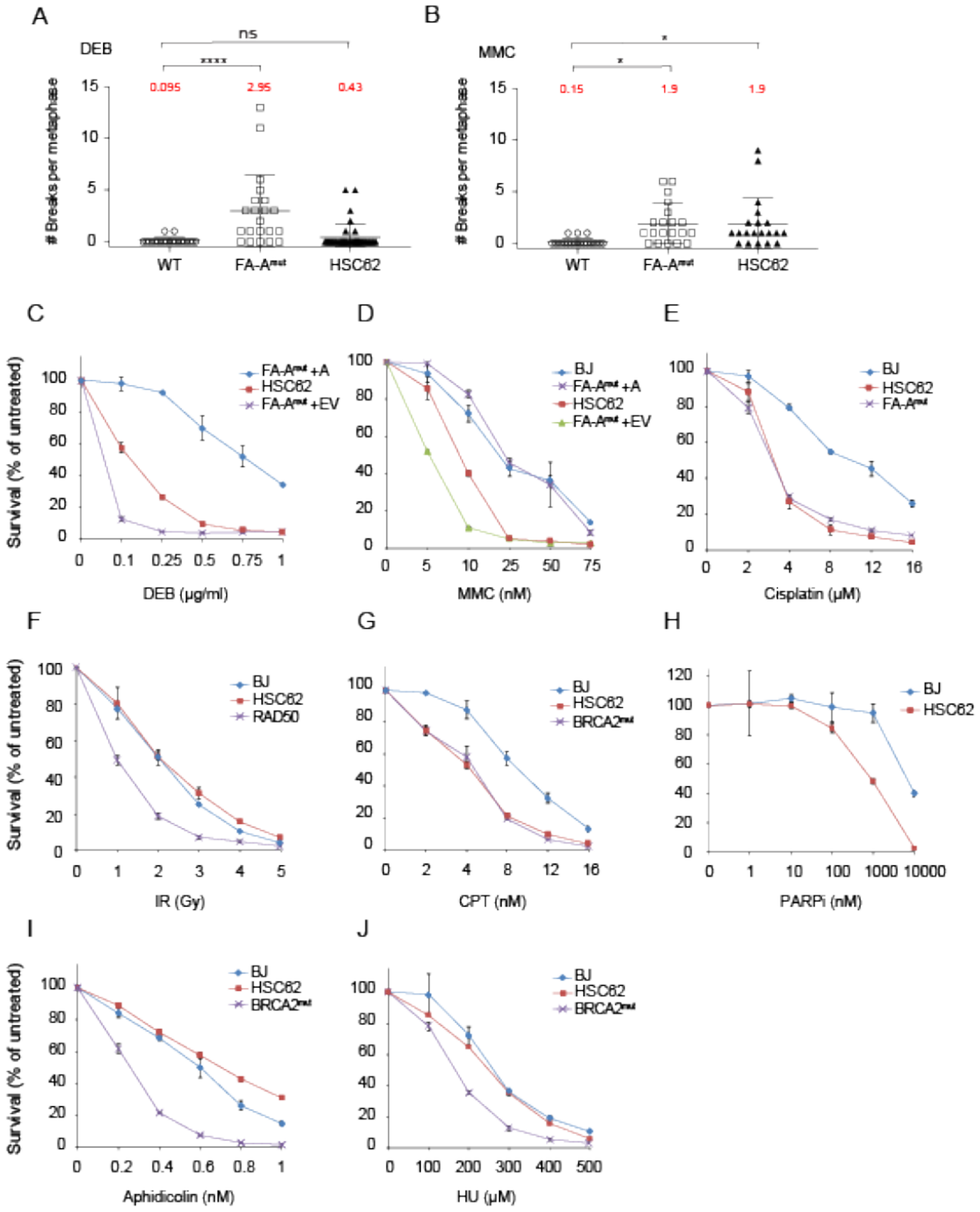

Figure 3.5 Characterization of HSC62 BRCA2 c.IVS19-1G>A fibroblast cell line from an adult patient with atypical Fanconi anemia.

(A) Immunofluorescence images of RAD51 foci, 8h following 12 Gy ionizing radiation (IR) of BJ WT fibroblast and patient derived HSC62 fibroblast, detected with anti-RAD51 antibody. Third row images are individual cells enlarged to better reveal differences in RAD51 foci size. (B) Quantification of RAD51 foci 1h, 8h, and 24h following 12 Gy ionizing radiation (IR) of BJ WT fibroblast and HSC62 fibroblast. Error bars indicate s.d. of two independent experiments (≥200 cells per experiment). (C) Quantification of RAD51 foci 8h, 24h, and 48h following 1h treatment with 3 μM MMC of BJ WT fibroblast and HSC62 fibroblast. (D) Sister chromatid exchange (SCE) assay in BJ WT fibroblast and HSC62 fibroblast following treatment with MMC (0.1 μg/ml or 0.2 μg/ml). (E) SCE assay in BJ WT fibroblast and HSC62 fibroblast following depletion of BLM. (F) Representative images of SCEs in BJ WT fibroblast and HSC62 fibroblast metaphases. (G) qRT-PCR of *BLM* expression levels in cells described in E. Error bars indicate s.d.

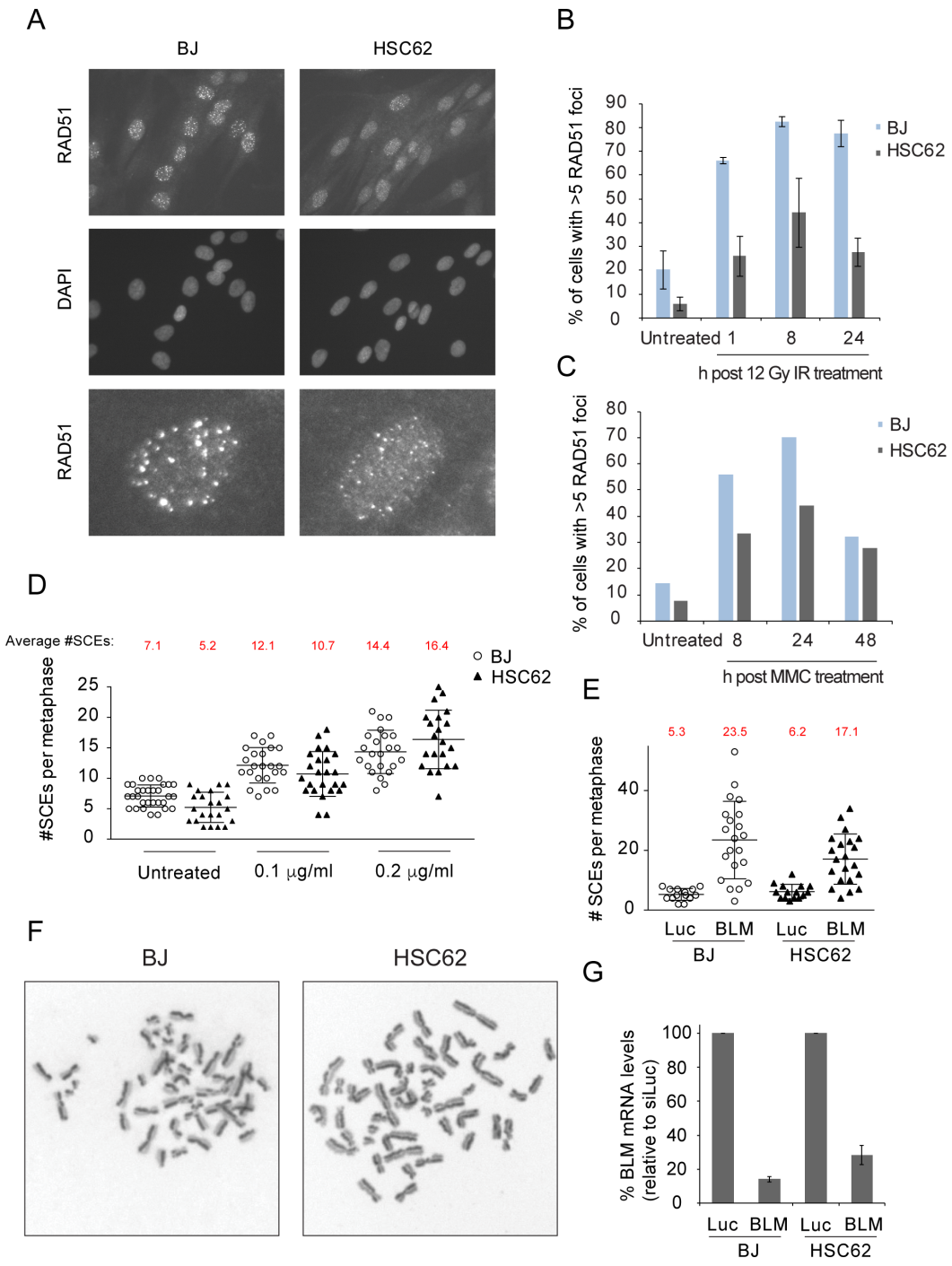

resistance to IR, sister chromatid exchange (SCEs) levels were analyzed as a readout of HR (Sonoda et al., 1999). SCEs were induced by increasing concentrations of MMC or depletion of the Bloom helicase (BLM) and no significant difference in SCE levels was observed between BJ wild type fibroblast and HSC62 cells (Figure 3.5D-F). These observations suggest that the DNA binding domain defect in HSC62 cells, while moderately decreasing RAD51 foci formation, does not result in defective HR as observed by normal resistance to IR and SCE levels in these cells. Interestingly, there is a greater impact on replication fork stress induced by ICL generating agents as determined by cellular sensitivity.

3.2.3 CRISPR/Cas9 mediated correction of the *BRCA2* c.IVS19-1G>A mutation rescues cellular defects of patient HSC62 fibroblasts

We complemented the patient cell line to demonstrate that the c.IVS19-1G>A mutations cause the defects we observe in the HSC62 cell line, and so that future analysis could be performed in isogenic cell lines. The size of *BRCA2* cDNA hinders efficient complementation by overexpression, so the homozygous c.IVS19-1G>A mutations were corrected to wild type at the endogenous locus using CRISPR/Cas9 gene targeting. Both heterozygous and homozygous clones were recovered (HSC62$^{WT/MUT}$ or HSC62$^{WT/WT}$) (Figure 3.6A). cDNA analysis demonstrated that restoration of the splice acceptor base (A>G) in HSC62$^{WT/MUT}$ or HSC62$^{WT/WT}$ clones restored the cDNA exon 19 and exon 20 junction (Figure 3.6C). Both HSC62$^{WT/MUT}$ and HSC62$^{WT/WT}$ clones rescued RAD51 foci formation

Figure 3.6 Complementation of HSC62 BRCA2 c.IVS19-1G>A DNA binding domain patient fibroblast cell line at the endogenous locus by CRISPR/Cas9 mediated gene targeting.

(A) Chromatograms of PCR amplified gDNA of CRISPR/Cas9 targeted HSC62 fibroblasts. Gene editing reverted the c.IVS19-1G>A mutation either to homozygous WT ($HSC62^{WT}$) or heterozygous WT ($HSC62^{mut/WT}$) at the endogenous locus in HSC62 patient cells. The silent mutation that was incorporated to destroy the CRISPR PAM sequence is indicated. (B) Immunoblot showing BRCA2 levels in CRISPR/CAS9 corrected patient cell line $HSC62^{WT}$, uncorrected HSC62 cells ($HSC62^{mut}$), and RA2630 (*FANCR*) patient fibroblasts. (C) cDNA analysis of HSC62 clones with either homozygous or heterozygous correction of the c.IVS19-1G>A mutation demonstrating rescue of the 12bp deletion of exon 20 that results because of alternate splicing.

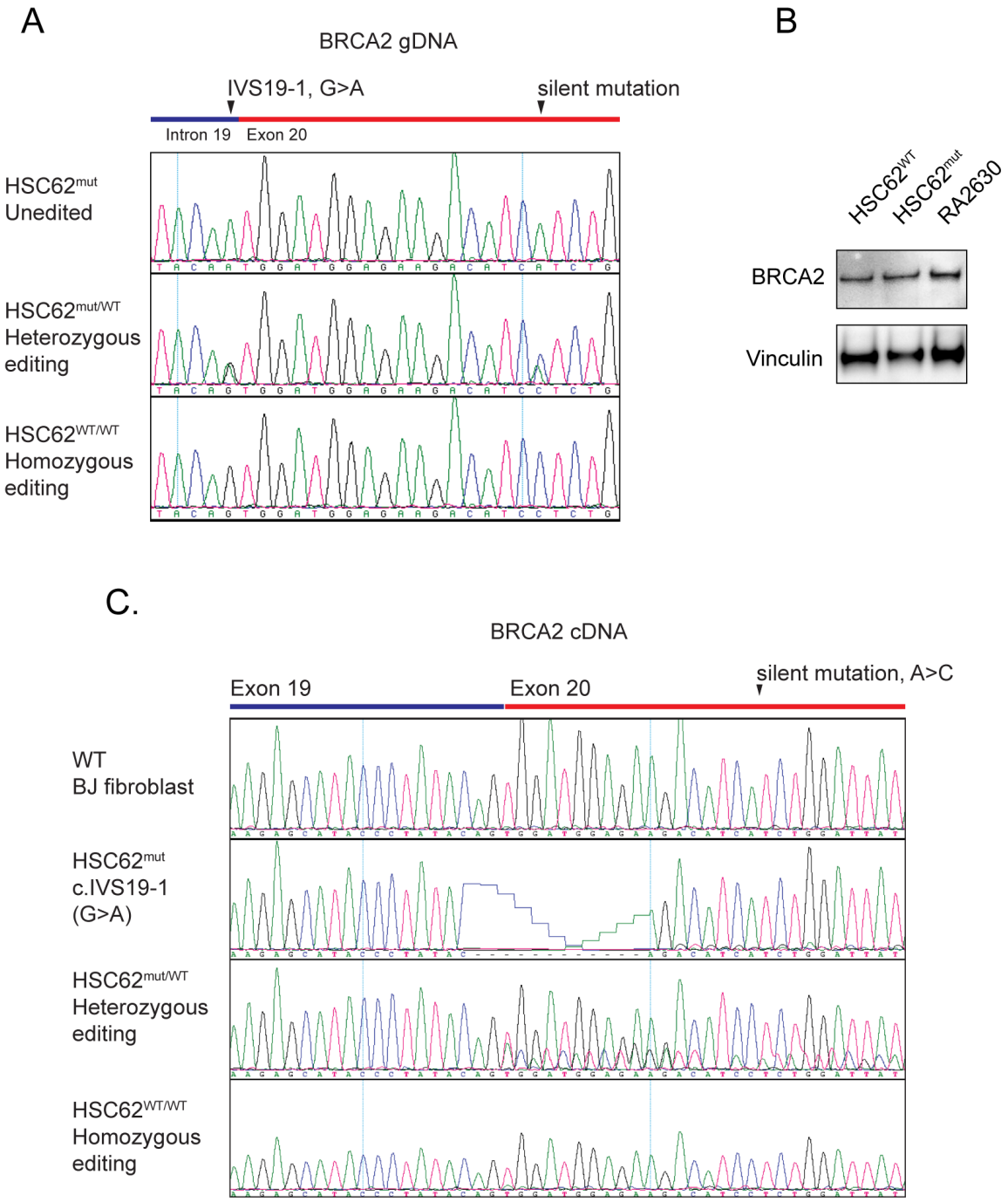

defects after IR and MMC, and also rescued hypersensitivity to replication stress inducing agents MMC, CPT, and PARPi (Figure 3.7A-D and Figure 3.8A-D).

3.2.4 Defective ICL repair in HSC62 cells results in increased RPA activation that is dependent on DNA2 and WRN

Our lab has previously described a *FANCR/RAD51* p.T131P patient-derived cell line that is proficient for HR but defective in ICL repair. One characteristic of this cell lines is hyperactivation of RPA upon MMC treatment (Wang et al., 2015). Given that BRCA2 and RAD51 interaction is required for their canonical function in HR and for the non-canonical function in replication fork protection at HU-stalled forks, we hypothesized that BRCA2 also functions with RAD51 in preventing increased ssDNA generation at ICLs (Schlacher et al., 2011; Wang et al., 2015). We observed an increase in RPA foci formation and phosphorylation in HSC62^{MUT} cells compared to wild type fibroblast upon MMC treatment (Figure 3.9A-B). Similar to *FANCR/RAD51* p.T131P expressing patient cells, the increased RPA foci formation in HSC62 cells was also dependent on DNA2 and WRN activity, but not MRE11, EXO1, CtIP, or BLM (Figure 3.9C). These results support an ICL repair model that requires both BRCA2 and RAD51 activity to protect against aberrant processing by DNA2 and WRN, but not the other effectors of DSB end resection such as MRE11, EXO1, or CtIP (Wang et al., 2015).

Figure 3.7 Defects in RAD51 foci formation in HSC62 BRCA2 patient fibroblasts are rescued by gene correction.

(A) Quantification of RAD51 foci 8h after 12 Gy ionizing radiation (IR) of BJ WT fibroblast, wild type HSC62 ($HSC62^{WT}$) clones 1-3, and HSC62 uncorrected patient cell line ($HSC62^{mut}$). (B) Quantification of RAD51 foci 24h following 1h treatment with 3 uM MMC. Error bars indicate s.d. of three independent experiments (≥200 cells per experiment). Representative images of RAD51 foci, 8h post IR (C) and 24h post MMC (D) detected by immunofluorescence with anti-RAD51antibody.

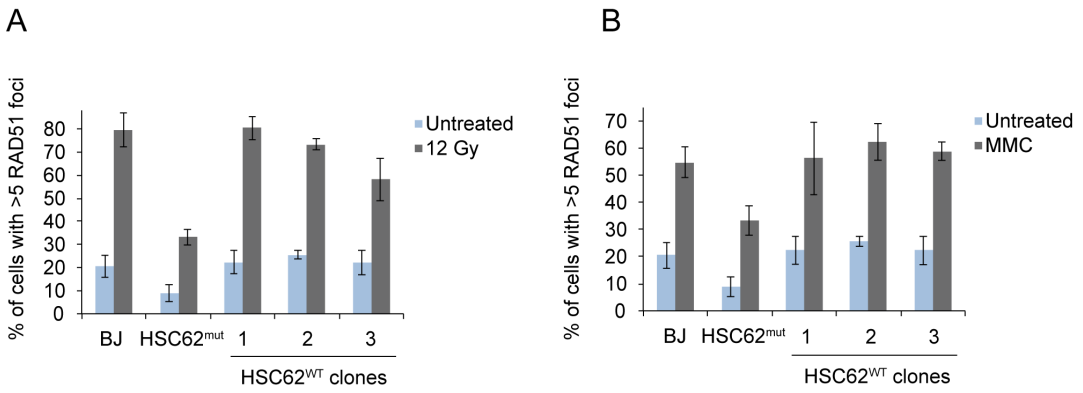

C.

8h post 12Gy IR

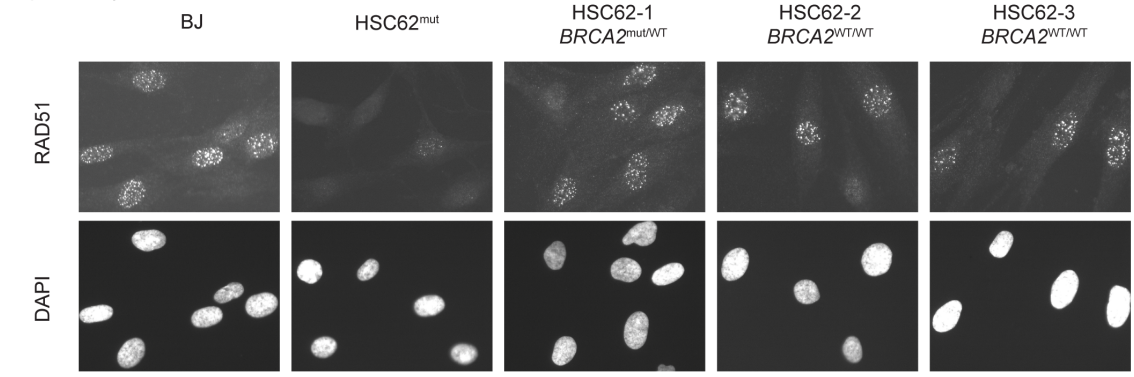

D.

24h post MMC

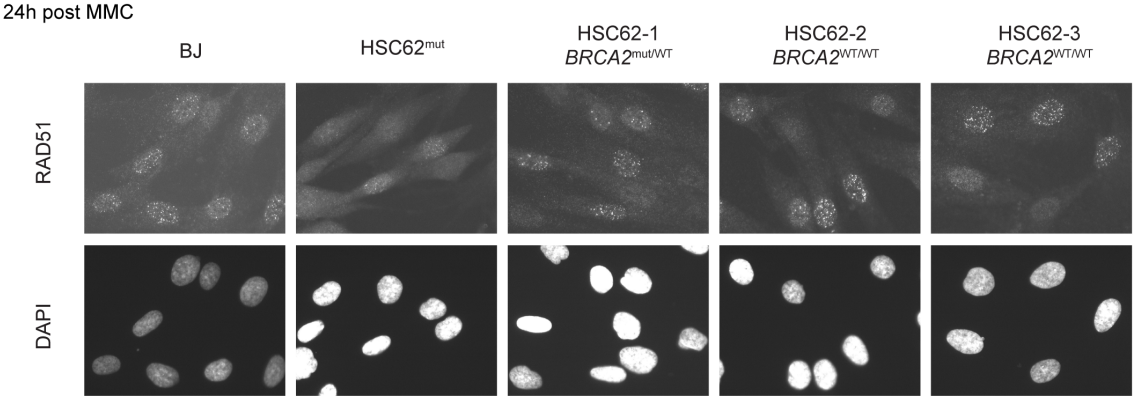

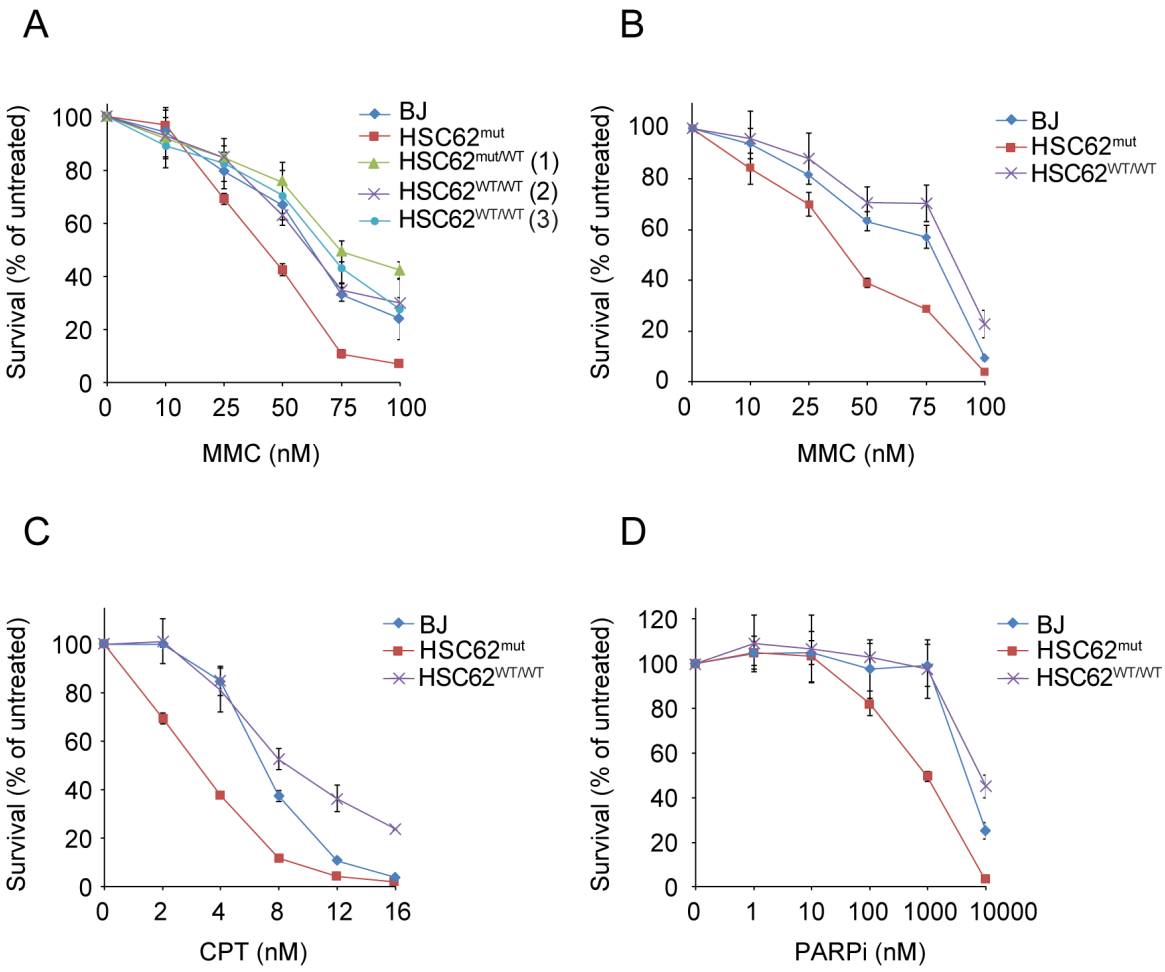

Figure 3.8 Rescue of cellular sensitivity of HSC62 BRCA2 patient fibroblasts to genotoxic agents by gene correction.

(A-D) Cell survival of HSC62 uncorrected patient cell line ($HSC62^{mut}$) compared to BJ WT fibroblast and wild type HSC62 ($HSC62^{WT}$) clones 1-3. Cell survival assays were performed in triplicate. Cells were treated with increasing concentrations of indicated agent. Cell survival was determined by counting cells after 7-9 days in culture. Relative cell survival was normalized to untreated controls to give percent survival. Error bars indicate s.d.

3.2.5 Generation of isogenic *BRCA2* DNA binding domain mutations in human fibroblasts

The lack of patient derived fibroblasts from the sibling pair with compound heterozygous *BRCA2* mutations, c.2330dupA and c.8524C>T, precluded the direct comparison of the DNA binding domain mutations in similar cell types. In order to directly compare the defects conferred by the *BRCA2* DBD mutations c.8524C>T (p.R2842C) and c.IVS19-1G>A (p.del2830-2833), we generated isogenic cell lines by introducing the mutations into wild type BJ fibroblasts with CRISPR/Cas9 gene editing (Figure 3.10). To examine the specific impact of the DBD mutations, cells homozygous for the mutations were selected to be used in further analysis. Knock in of the *BRCA2* c.IVS19-1G>A mutation in BJ fibroblasts confers the same splicing defect, loss of the first 12bp of exon 20 , observed in HSC62 cells (Figure 3.10B). Western blot analysis of BRCA2 levels demonstrates ~390 kDa bands for all mutants except for *BRCA2* clones harboring frameshift mutations in exon 20 (Figure 3.10E). The *BRCA2* frameshift mutant is homozygous c.8531dupA with a predicted p.R2845K FS*22 truncation ($BRCA2^{Trun.}$).

Functional analysis of isogenic DBD mutants demonstrated defects in RAD51 foci formation following IR and MMC (Figure 3.11 and Figure 3.12). The c.IVS19-1G>A mutation has a more deleterious impact on RAD51 foci formation, resulting in reduction of cells with RAD51 foci and reduced foci size. The c.8524C>T mutants do not show a significant reduction in the number of cells with

Figure 3.9 Depletion of DNA2 and WRN in HSC62 patient cells suppresses increased RPA activation and foci formation induced by MMC.

(A) Images of RPA foci, 24h post 1h treatment with 3 μM MMC, detected by immunofluorescence with anti-RPA32 antibody. (B) Quantification of RPA foci 24h following 1h treatment with 3 μM MMC of BJ WT fibroblast, wild type HSC62 clones ($HSC62^{WT}$), and HSC62 uncorrected patient cell line ($HSC62^{mut}$). (C) Quantification of RPA foci 24h following 1h treatment with 3 μM MMC in $HSC62^{mut}$ cells depleted of DNA2, MRE11, EXO1, CtIP, WRN, or BLM by siRNA compared to luciferase control (Luc). Error bars indicate s.d. of four independent experiments. (D) qRT-PCR of *DNA2, EXO1, WRN, and BLM* expression levels of cells in C. Error bars are s.d. (E) Immunoblot analysis of MRE11 and CtIP siRNA depletion for cells utilized in C.

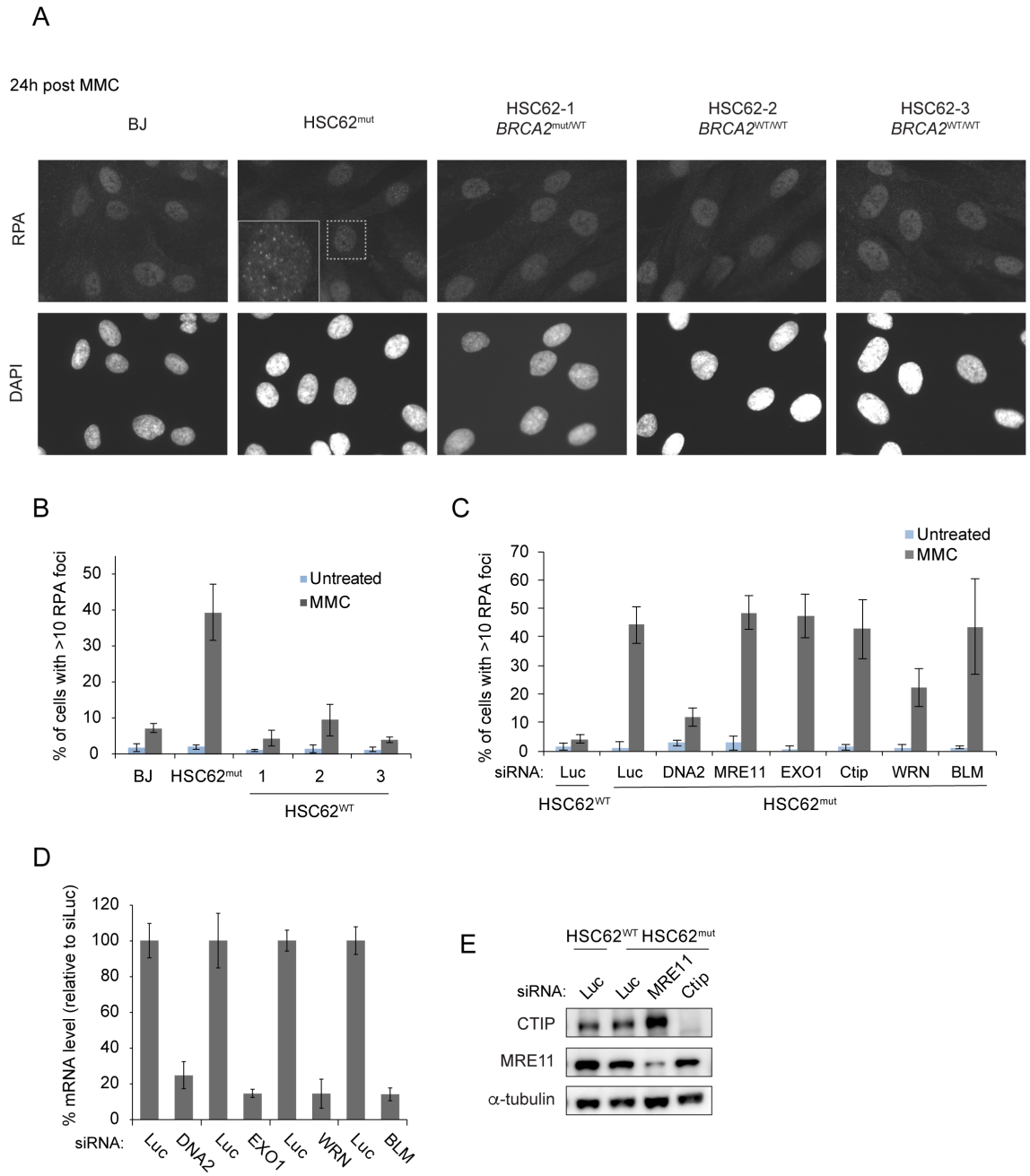

RAD51 foci; however, the foci are much smaller in size (Figure 3.11B and Figure 3.12B). By comparison the BRCA2$^{Trun.}$ mutant has complete loss of observable RAD51 foci formation. Analysis of cellular sensitivity of the DBD mutants revealed trends that correlated with the RAD51 foci data, demonstrating the c.IVS19-1G>A mutation to be more deleterious to BRCA2 function than the c.8524C>T mutation. Both mutations sensitize cells to MMC with some clonal variation for the c.IVS19-1G>A mutation, but overall the same trends are observed (Figure 3.13A-B). Both the c.8524C>T and c.IVS19-1G>A mutants are sensitive to replication stress inducing drugs PARPi and CPT compared to WT cells, but not aphidicolin as seen in the patient HSC62 fibroblast (Figure 3.4 and Figure 3.13C-E). Increased RPA foci following MMC was also observed for c.8524C>T and c.IVS19-1G>A mutants, with a greater increase in RPA foci seen in the c.IVS19-1G>A mutants (Figure 3.14).

The c.IVS19-1G>A mutation confers a splicing defect in which the consequence is the loss of the first four aa of exon 20 in a very conserved region of the DBD, at the OB2 and base of the Tower domain (Figure 3.2). How the loss of these four aa impact protein folding of this region is unknown; however, the greater defects in RAD51 recruitment, cellular viability to genotoxic agents, and increased generation of ssDNA at ICL lesions as measured by RPA foci suggest that this mutation is much more disruptive to BRCA2 activity than the c.8524C>T mutation. In this region, proximal to both the c.8524C>T and c.IVS19-1G>A

mutants, are three aa residues that have been identified for their direct interaction with DNA, K2833, Y2839, and F2841 (Yang et al., 2005). Using CRISPR/Cas9 in BJ wild type fibroblasts, we generated a DBD mutant (BRCA2^{DBDx3A}) by mutating these three codons to alanine (Figure 3.15A). We hypothesized that the DBDx3A mutations would be less disruptive to BRCA2 structure and function than the c.IVS19-1G>A mutation, but would still interfere with proper DNA binding in this region. *BRCA2*^{DBDx3A} cells were hypersensitive to MMC but not to the extent of *BRCA2*$^{IVS19\text{-}1G>A}$. RAD51 foci formation levels were nearly equivalent to WT cells following IR, but foci, similar to *BRCA2*$^{8524C>T}$ clones, were greatly reduced in size (Figure 3.15C-D). A marked increase in RPA foci following MMC was seen in the *BRCA2*^{DBDx3A} cells, but less than *BRCA2*$^{IVS19\text{-}1G>A}$ (Figure 3.15E). These data are consistent with the defects in *BRCA2* c.8524C>T and c.IVS19-1G>A cells being due to diminution of BRCA2 DNA binding ability; however, the greater defects conferred by the c.IVS19-1G>A mutation may be an outcome of a more distorting effect on BRCA2 structure that effects other domains.

Figure 3.10 Generation of isogenic BRCA2 DNA binding domain mutants by CRISPR/Cas9 mediated gene targeting in human fibroblasts.

(A) Chromatograms of *BRCA2* BJ fibroblast clones generated by CRISPR/Cas9 targeting. *BRCA2* exon 20 DNA binding domain mutations c.8524C>T and c.IVS19-1G>A were generated by targeting CRISPR/Cas9 in the vicinity of the desired mutation and supplying a 100bp ssDNA donor containing the mutation. Sanger sequencing of PCR amplified genomic DNA demonstrated homozygous knock-in for both mutations. (B) cDNA analysis of homozygous c.IVS19-1,G>A BJ fibroblast clones demonstrated that the splice site mutation, as seen in the patient HSC62 fibroblasts, results in the usage of an alternative splice site donor resulting in a 12bp deletion at the start of *BRCA2* exon 20. (C) A frameshift exon 20 BRCA2 mutant was generated by a homozygous single base pair insertion (c.8531dupA) during CRISPR/Cas9 targeting. This presumed truncation mutant is annotated as $BRCA2^{Trun}$. (D) cDNA sequencing of c.8524C>T BJ fibroblasts demonstrating the missense mutation and silent mutation introduced by CRISPR/Cas9 targeting. (E) Immunoblot showing BRCA2 levels in bulk BJ WT fibroblasts, $BRCA2^{WT}$ fibroblast clone, c.IVS19-1G>A BJ clones 1-3, c.8524C>T BJ clones 1-2, and $BRCA2^{Trun.}$ clones 1-2.

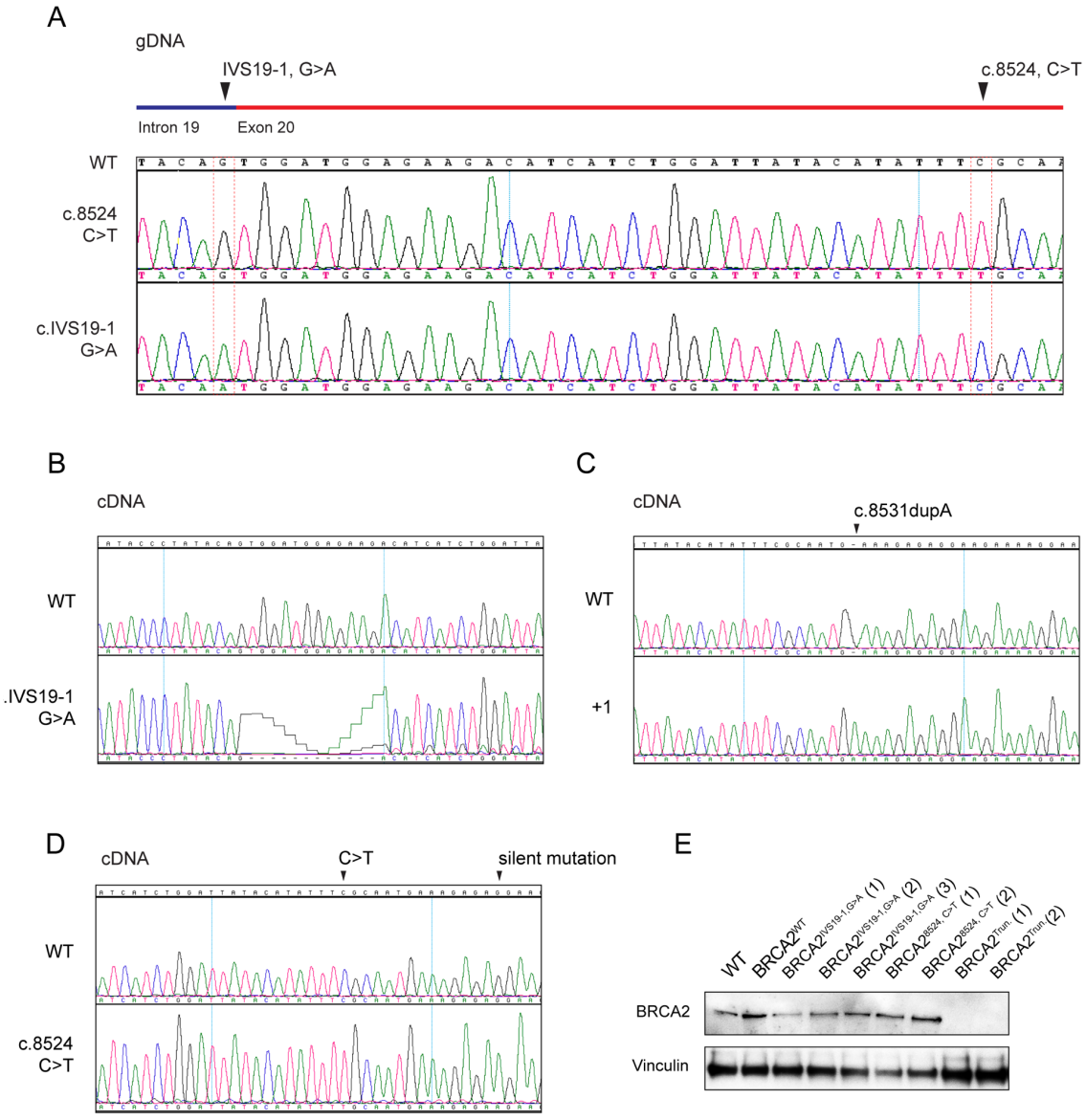

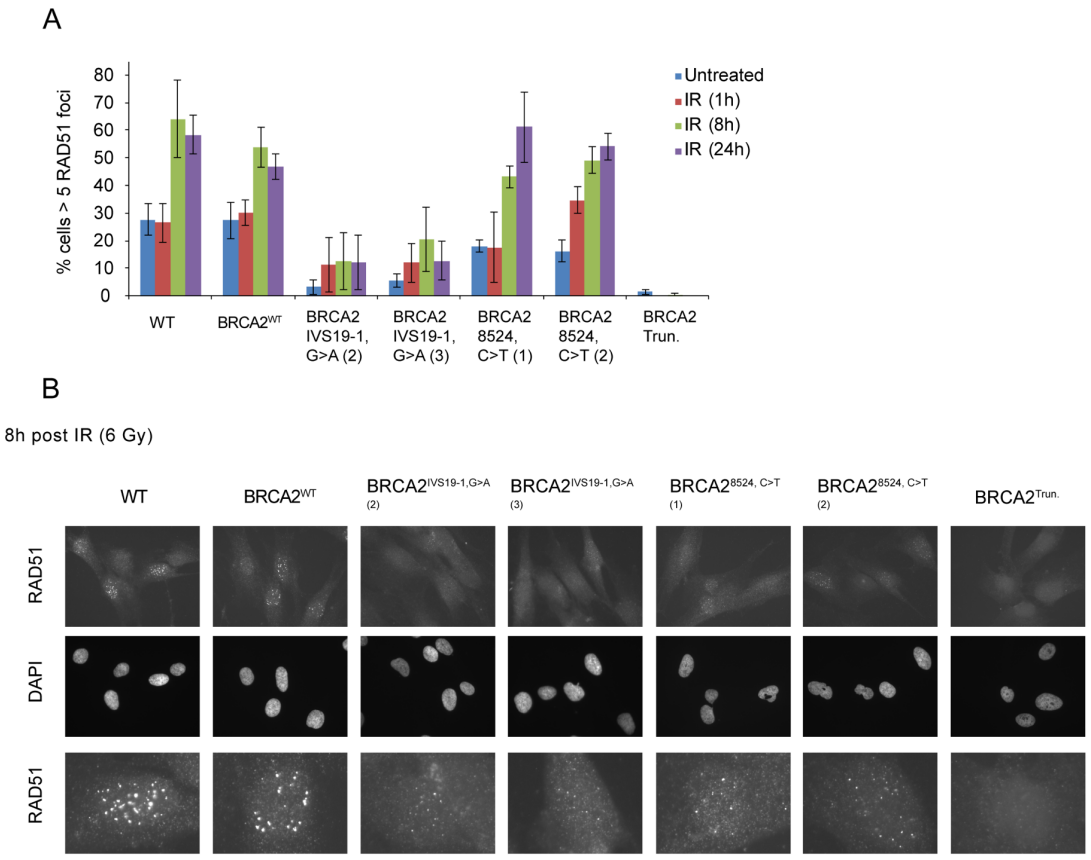

Figure 3.11 RAD51 foci formation in BRCA2 DNA binding domain mutants following ionizing radiation.

(A) Quantification of RAD51 foci 1h, 8h and 24h following 6 Gy ionizing radiation (IR) of BJ WT fibroblasts, BJ WT fibroblast clone ($BRCA2^{WT}$), c.IVS19-1G>A BJ clones 2-3, c.8524C>T BJ clones 1-2, and a *BRCA2* homozygous truncation mutant, c.8531dupA ($BRCA2^{Trun}$). Error bars indicate s.d. of three independent experiments (≥200 cells per experiment). (B) Representative images of RAD51 foci, 8h post 6 Gy IR, detected by immunofluorescence with anti-RAD51 antibody. Third row images are individual cells enlarged to better reveal differences in RAD51 foci size.

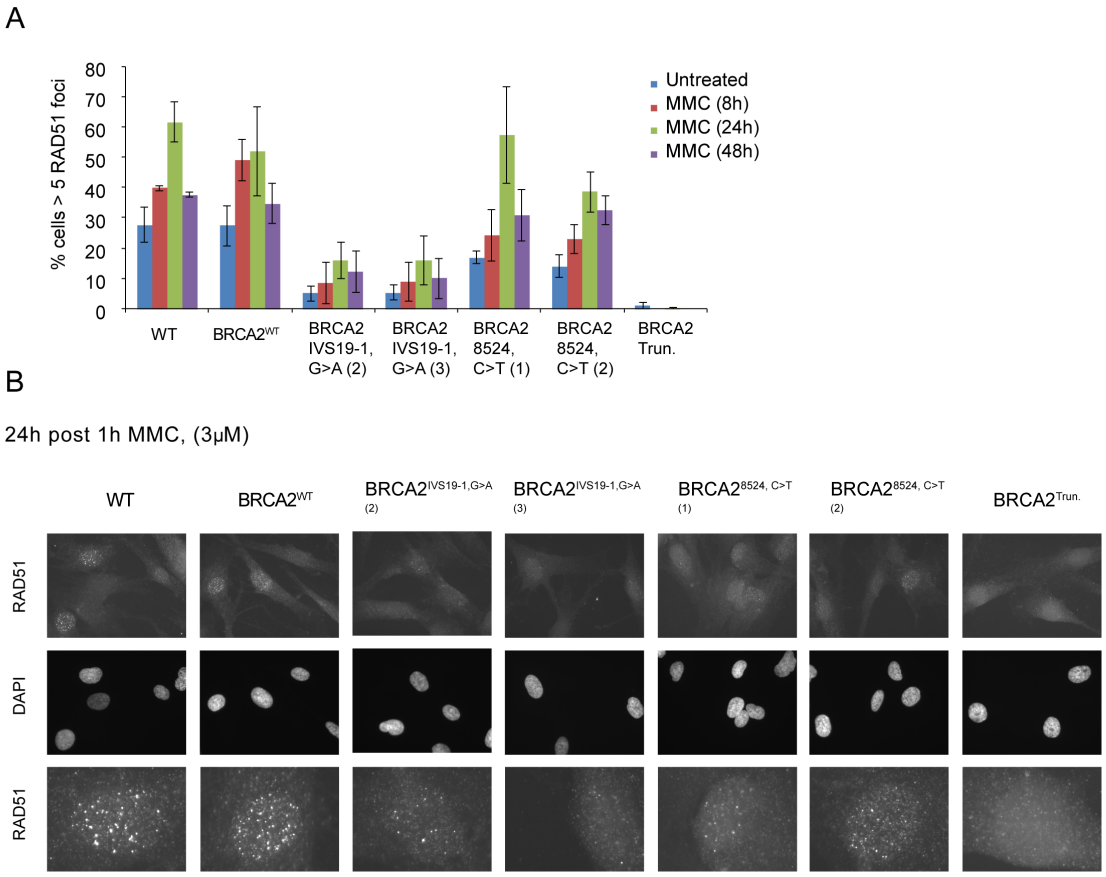

Figure 3.12 RAD51 foci formation in BRCA2 DNA binding domain mutants following mitomycin C.

(A) Quantification of RAD51 foci 8h, 24h and 48h following 1h treatment with 3 μM MMC of BJ WT fibroblasts, BJ WT fibroblast clone ($BRCA2^{WT}$), c.IVS19-1G>A BJ clones 2-3, c.8524C>T BJ clones 1-2, and a BRCA2 truncation mutant, c.8531dupA (*$BRCA2^{Trun}$*). Error bars indicate s.d. of three independent experiments (≥200 cells per experiment). (B) Representative images of RAD51 foci, 24h post 1h treatment with 3 μM MMC, detected by immunofluorescence with anti-RAD51antibody. Third row images are individual cells enlarged to better reveal differences in RAD51 foci size.

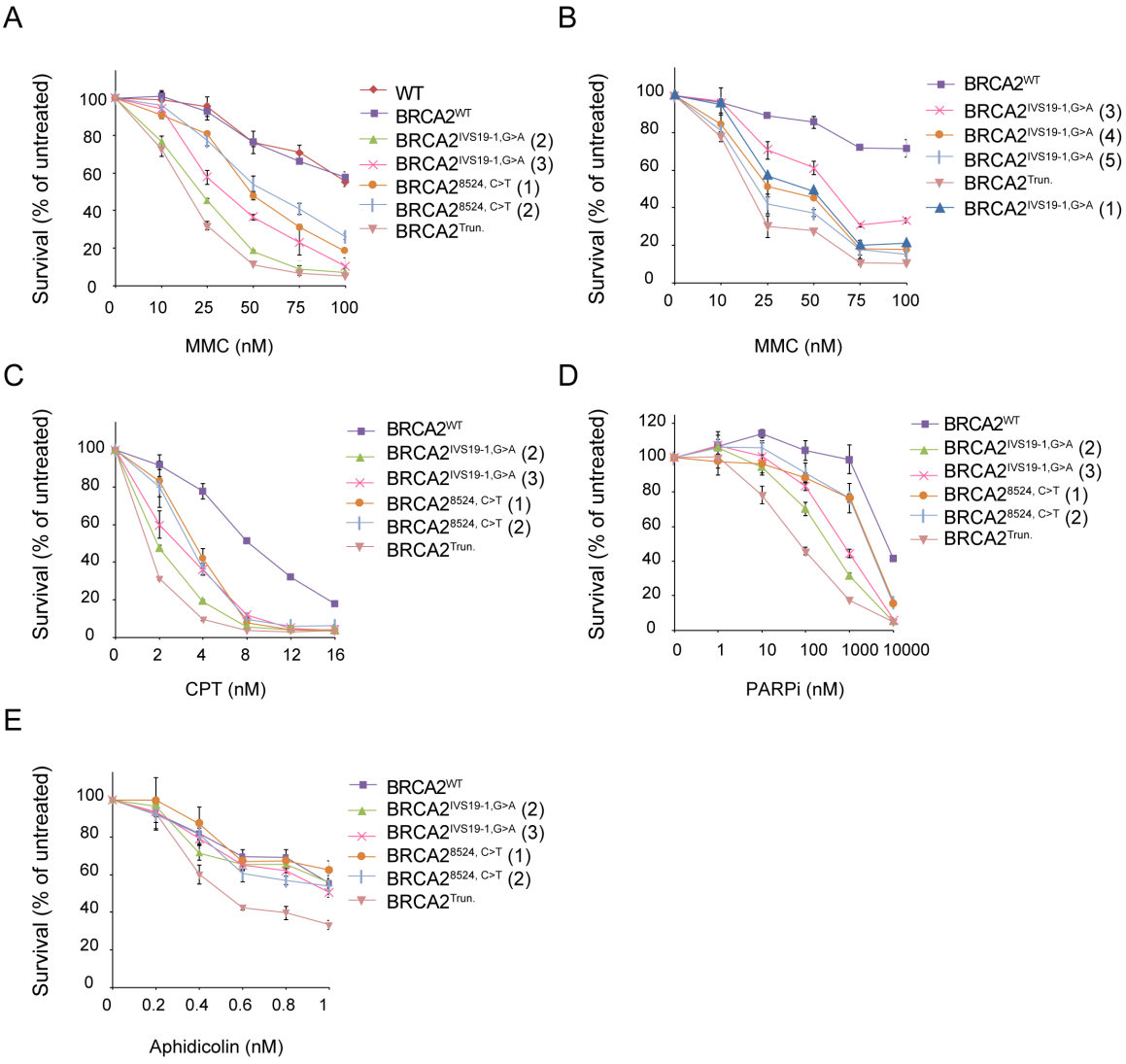

Figure 3.13 Cellular sensitivity of isogenic BRCA2 DNA binding domain mutants.

(A-E) Cell survival of BJ WT fibroblasts, BJ WT fibroblast clone ($BRCA2^{WT}$), c.IVS19-1G>A BJ clones, c.8524C>T BJ clones, and exon 20 *BRCA2* frameshift mutant ($BRCA2^{Trun.}$). Cell survival assays were performed in triplicate. Cells were treated with increasing concentrations of indicated agent. Cell survival was determined by counting cells after 7-9 days in culture. Relative cell survival was normalized to untreated controls to give the percent survival. Error bars indicate s.d.

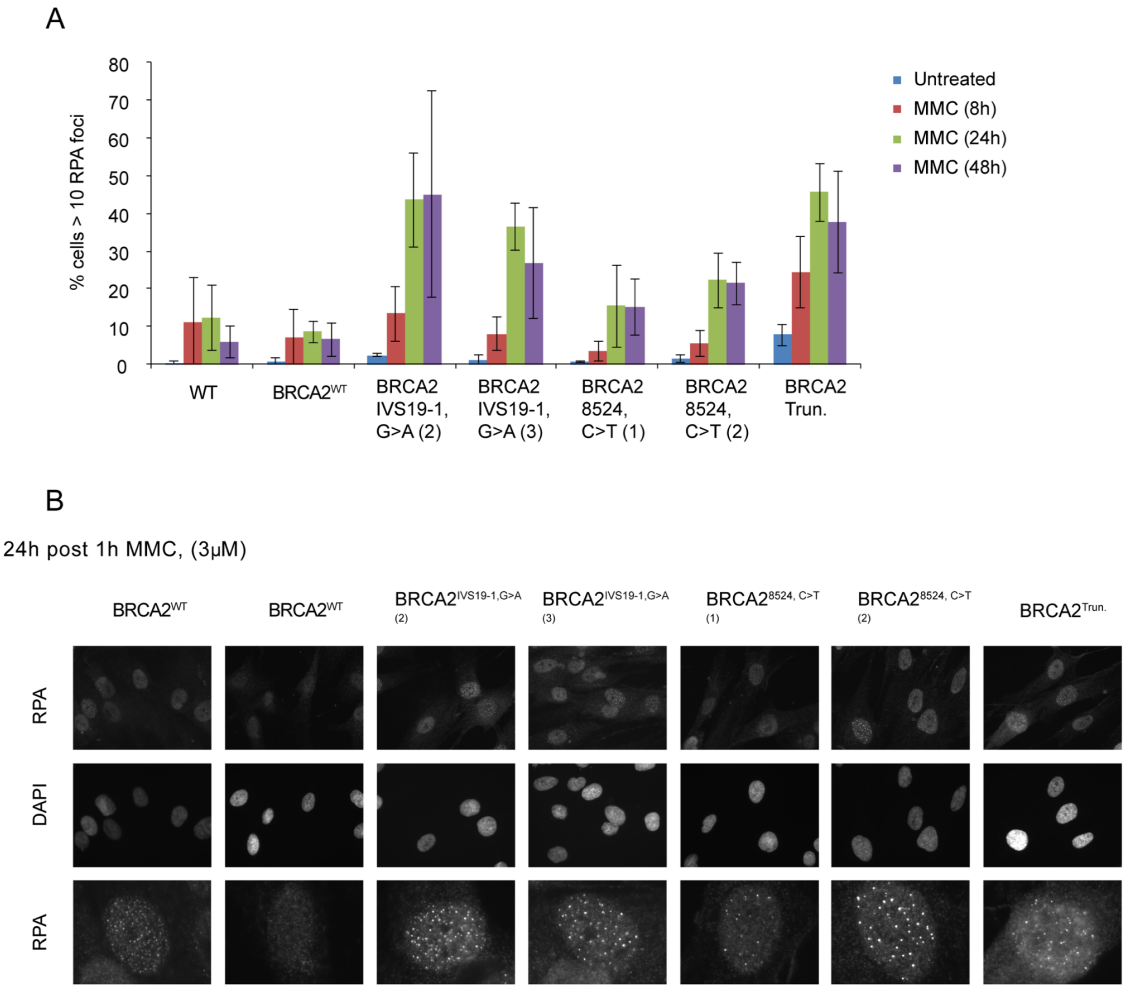

Figure 3.14 BRCA2 DNA binding domain mutants have increased RPA foci formation following mitomycin C.

(A) Quantification of RPA foci 8h, 24h and 48h following 1h treatment with 3 μM MMC of BJ WT fibroblasts, BJ WT fibroblast ($BRCA2^{WT}$), c.IVS19-1G>A BJ clones 2-3, c.8524C>T BJ clones 1-2, and a BJ *BRCA2* truncation mutant ($BRCA2^{Trun.}$). Error bars indicate s.d. of three independent experiments (≥200 cells per experiment). (B) Representative images of RPA foci, 24h post 1h treatment with 3 uM MMC, detected by immunofluorescence with anti-RPA32 antibody. Third row images are individual cells enlarged to better reveal RPA foci.

Figure 3.15 CRISPR/Cas9 mediated gene targeting to mutagenize key DNA interacting residues of the BRCA2 DNA binding domain.

(A) Chromatogram of *BRCA2* CRISPR/Cas9 generated DNA binding domain triple mutant (DBDx3A). Three codons of exon 20, previously identified to interact with DNA (2833K, 2839Y, and 2841F), were mutagenized to produce alanine when translated. $BRCA2^{DBDx3A}$ was generated by targeting CRISPR/Cas9 in the vicinity of the desired mutations and supplying a 100bp ssDNA donor containing the three codon mutations. Sanger sequencing of PCR amplified genomic DNA demonstrates homozygous knock-in of the three alternate codons. (B) Cell survival of $BRCA2^{WT}$, $BRCA2^{IVS19\text{-}1G>A}$, *and* $BRCA2^{DBDx3A}$ BJ fibroblast cell lines. Survival assay was performed in triplicate and treated with increasing concentrations of MMC. Cell survival was determined by counting cells after 8 days in culture. Relative cell survival was normalized to untreated controls for the percent survival. Error bars indicate s.d. (C) Quantification of RAD51 foci 8h after 6 Gy ionizing radiation (IR) of $BRCA2^{WT}$, $BRCA2^{IVS19\text{-}1G>A}$, *and* $BRCA2^{DBDx3A}$ BJ fibroblast cell lines. Error bars indicate s.d of three independent experiments. (D) Representative images of RAD51 foci, 8h post 6 Gy IR, detected by immunofluorescence with anti-RAD51antibody. Third row images are individual cells enlarged to better reveal differences in RAD51 foci size. (E) Quantification of RPA foci, 24h post 1h treatment with 3 μM MMC, of $BRCA2^{WT}$, $BRCA2^{IVS19\text{-}1G>A}$, and $BRCA2^{DBDx3A}$ BJ fibroblast cell lines. Error bars indicate s.d of three independent experiments.

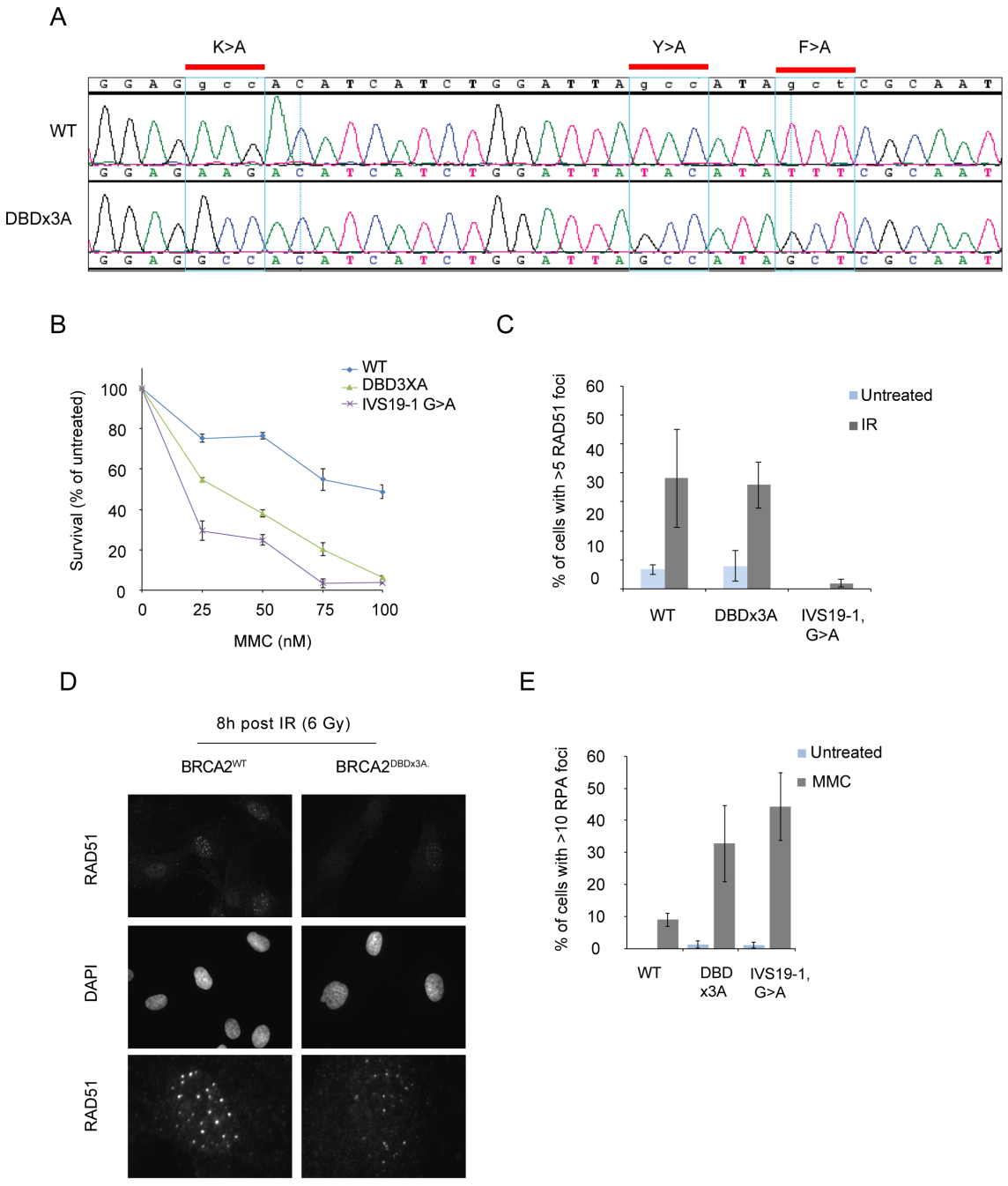

3.2.6 Determination of homologous recombination efficiency in DNA binding domain mutants

The patients harboring the c.8524C>T and c.IVS19-1G>A mutations have an unusually mild clinical presentation for patients in the *FANCD1/BRCA2* complementation group. The embryonal tumors of this complementation group are not a prominent feature in the majority of other FA subtypes, suggesting these tumors may be the result of HR deficiency outside of the FA pathway during development. HR mediated double strand break repair is necessary for resolution of ICLs, but there is debate about the role of the *BRCA2* DBD and its importance for HR (Saeki et al., 2006; Schlacher et al., 2011; Siaud et al., 2011). To analyze HR activity, DBD mutations as well as an exon 27 p.S3291A mutation, previously reported to have no effect on HR, were generated in HEK293T cells (Figure 3.16). Western blot analysis of BRCA2 indicated full length BRCA2 with the exception of a $BRCA2^{Trun.}$ (c.8531dupA) used as a control (Figure 3.16B). Cellular sensitivity to MMC was assessed in the *BRCA2* HEK293T clones demonstrating increasing levels of sensitivity (p.S3291A < c.8524C>T < c.IVS19-1G>A) (Figure 3.16C).

To determine the HR proficiency of $BRCA2^{IVS19\text{-}1G>A}$ and $BRCA2^{8524C>T}$ cells, we utilized an assay that takes advantage of the targeted DSBs generated by CRISPR/Cas9. A CRISPR/Cas9 vector expressing a sgRNA targeting the LMNA locus was transfected along with a *LMNA* homology donor template containing a N-terminus mClover fluorescent protein tag (Figure 3.17A) (Arnoult et al., 2017; Pinder et al., 2015). Cells that undergo HR can utilize the HR donor

template which results in expression of fluorescently tagged LMNA that can be assessed by flow cytometry analysis. Compared to wild type, HR in all *BRCA2* clones was moderately decreased by their mutations (Figure 3.17D). The previously described separation of function mutation, p.S3291A, moderately impacts HR efficiency. This demonstrates that Ser3291 is important for BRCA2 C-terminal domain activity during HR and not just exclusively at stalled replication forks (Kim et al., 2014; Schlacher et al., 2011). The DBD *BRCA2*$^{IVS19\text{-}1G>A}$ and *BRCA2*$^{8524C>T}$ cells showed similar decreases in HR levels to approximately half that of wild type cells, but they retained more HR activity than cells depleted of *RAD51* and *BRCA2* or *BRCA2*^{Trun} cells. Two of the c.IVS19-1G>A mutants appear to express lower BRCA2 levels (Figure 3.16B), suggesting these may be hemizygous clones, but this did not further impair HR levels as compared to similar levels in a third homozygous clone.

3.2.7 The BRCA2 DNA binding domain is required for replication fork protection at HU-stalled forks and ICLs to prevent resection by DNA2

We previously demonstrated, in the patient HSC62 cell line (c.IVS19-1G>A), that increased RPA foci formation observed following MMC treatment is the result of DNA2 and WRN activity. In BJ fibroblast BRCA2 DBD mutants, we also observed increased RPA foci after MMC treatment (Figure 3.14 and Figure 3.18). The increased RPA foci formation and phosphorylation of RPA in *BRCA2*$^{8524C>T}$, *BRCA2*$^{IVS19\text{-}1G>A}$, and *BRCA2*^{DBD3xA} cells were all reduced by DNA2 and WRN depletion (Figure 3.18). The rescue of RPA activation was less striking

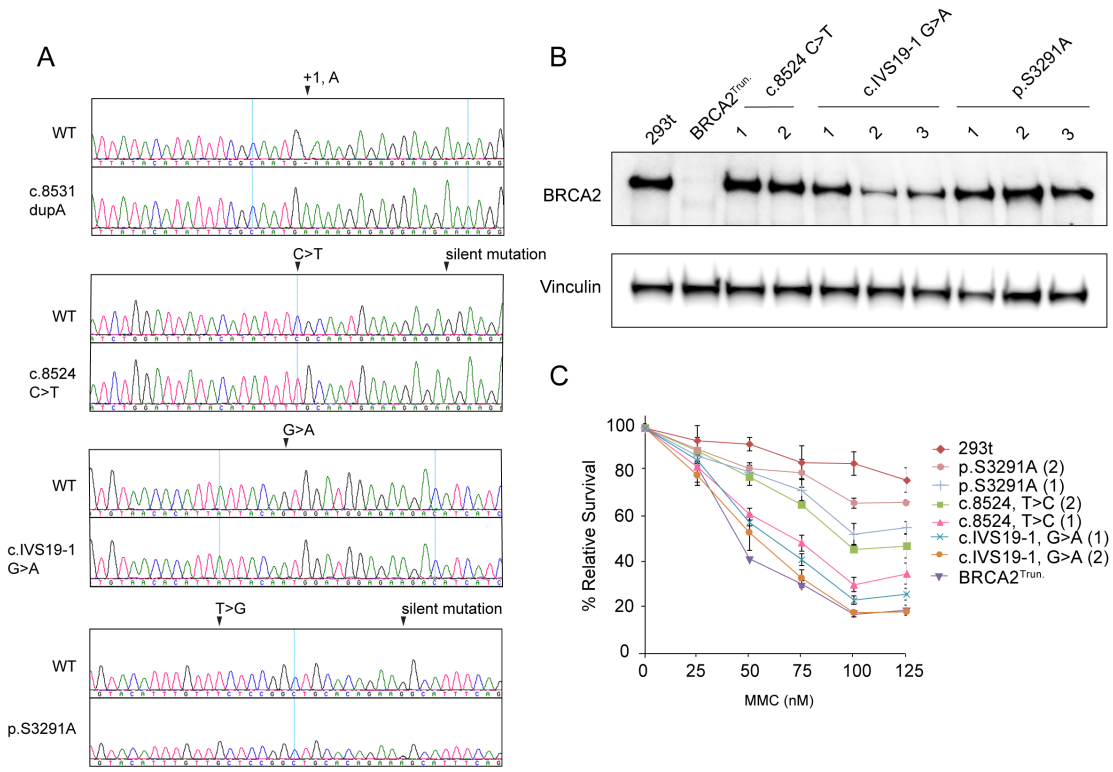

Figure 3.16 HEK293T BRCA2 DNA binding domain and Exon 27 p.S3291A clones generated by CRISPR/Cas9 gene editing.

(A) Chromatograms of *BRCA2* CRISPR/Cas9 generated HEK293T clones aligned to WT. A frameshift Exon 20 BRCA2 mutant ($BRCA2^{Trun.}$) was generated by homozygous single base pair insertion as a result of CRISPR/Cas9 targeting. *BRCA2* exon 20 mutations, c.8524C>T and c.IVS19-1G>A, and Exon 27 p.S3291A clones were generated by targeting the respective BRCA2 exon with CRISPR/Cas9 and a 100bp ssDNA template donor. Where applicable, silent mutations are indicated. (B) Immunoblot showing BRCA2 levels in WT HEK293T cells and *BRCA2* mutant HEK293T clones: c.8531dupA ($BRCA2^{Trun}$), c.8524C>T (clones 1-2), c.IVS19-1G>A (clones 1-3), and p.S3291A (clones 1-3). (C) Cell survival of WT cells and *BRCA2* clones performed in triplicate and treated with increasing concentrations of MMC. Cell survival was determined by counting cells after 6 days in culture. Relative cell survival was normalized to untreated controls for the percent survival. Error bars indicate s.d.

Figure 3.17 Homologous recombination efficiency of BRCA2 DNA binding domain mutants.

(A) Schematic of mClover LMNA homologous recombination CRISPR/Cas9 reporter assay. A plasmid expressing Cas9 and a sgRNA targeting the LMNA 5' UTR was co-transfected with a donor template plasmid containing mClover flanked by LMNA homology. Repair at the LMNA locus by HR using the donor template results in mClover tagging of the N-terminus of LMNA. mClover green cells were quantified by flow cytometry analysis. (B) Immunoblot of RAD51 knockdown for HEK293T cells used in D. (C) qRT-PCR of *BRCA2* expression levels of cells utilized in D. Error bars are s.d. (D) Levels of mClover positive cells were normalized to WT HEK293T (siLuc). Error bars indicate s.d. of three independent experiments performed in triplicate.

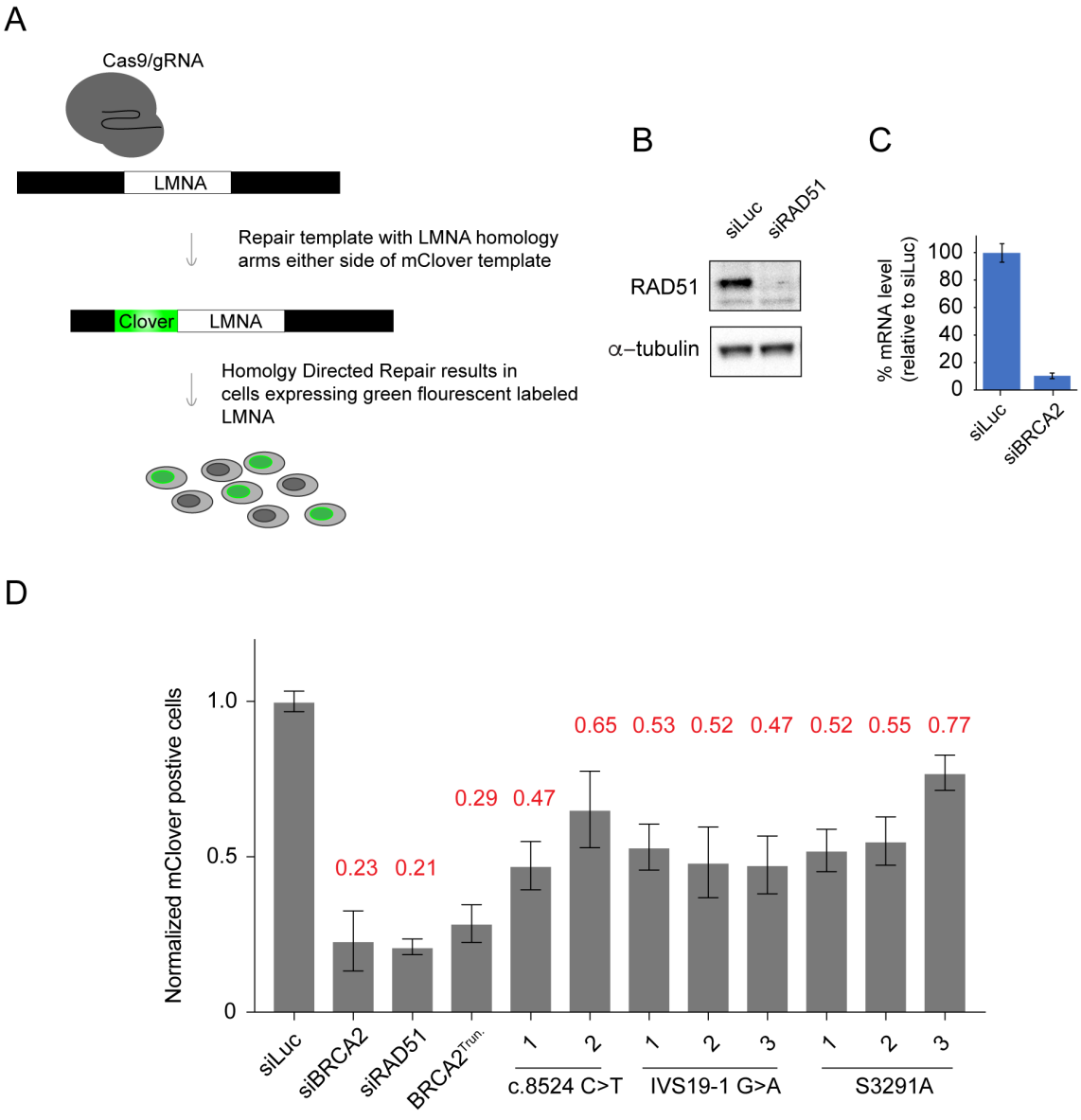

in the *BRCA2*$^{IVS19\text{-}1G>A}$ cells, suggesting that for this more deleterious mutation there may be other sources of ssDNA besides DNA2 and WRN at ICLs. These data are consistent with the requirement for BRCA2 function at replication forks encountering ICLs to prevent over resection by DNA2 and WRN.

To determine the requirement for the BRCA2 DBD in replication fork protection after HU, *BRCA2*$^{8524C>T}$ *and BRCA2*$^{IVS19\text{-}1G>A}$ cells were examined using DNA fiber analysis. Replication fork protection by BRCA2 has largely been attributed to the C-terminal RAD51 interacting domain by analysis of the p.S3291A *BRCA2* mutation. S3291 is a CDK phosphorylation site that when phosphorylated prohibits RAD51 binding. The C-terminal RAD51 interacting domain is thought to stabilize RAD51 nucleofilaments in a cell cycle controlled manner (Ayoub et al., 2009; Schlacher et al., 2011). Our data, and another recently published study suggests that this mutant moderately impacts HR proficiency; nonetheless, it does abrogate replication fork protection at HU-stalled replication forks (Feng and Jasin, 2017).

Analysis of BRCA2$^{Trun.}$, *BRCA2*$^{8524C>T}$, and *BRCA2*$^{IVS19\text{-}1G>A}$ cells demonstrated defects in replication fork protection of HU-stalled forks as measured by the degradation of nascent DNA tracks labeled with nucleotide analogs, IdU and CldU (Figure 3.19). As previously reported, nascent strand degradation in the absence of BRCA2 was rescued by the MRE11 inhibitor mirin and MRE11 depletion (Figure 3.19 and Figure 3.20A). These data demonstrate that the

Figure 3.18 Depletion of DNA2 and WRN suppresses increased RPA activation and foci formation induced by MMC in BRCA2 DNA binding domain mutants.

(A-B) Immunoblot analysis of RPA phosphorylation 24h post 1h treatment with 3 μM MMC. *BRCA2*^{WT}, *BRCA2*$^{c.8524C>T}$, *BRCA2*$^{c.IVS19-1G>A}$, and *BRCA2*^{DBDx3A} BJ fibroblast cells were transfected with siRNA control luciferase (Luc) or siRNAs targeting DNA2 or WRN. (C-D) Quantification of RPA foci 24h following 1h treatment with 3 μM MMC in cells depleted of DNA2 or WRN by siRNA. Error bars indicate s.d of two independent experiments. (E-G) qRT-PCR of *DNA2* and *WRN* expression levels of cells utilized in A-D. Error bars indicate s.d.

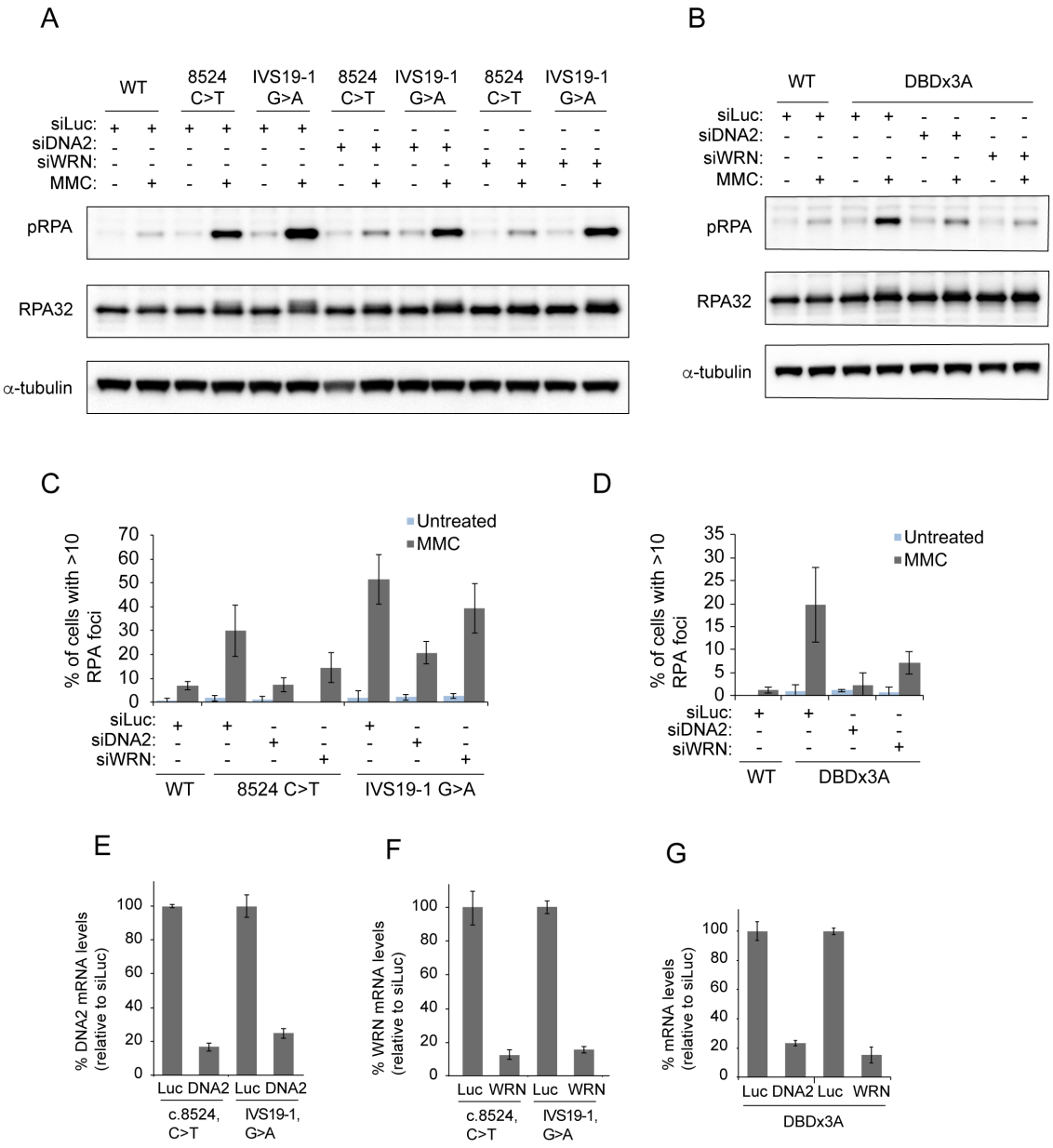

BRCA2$^{Trun.}$, *BRCA2*$^{8524C>T}$, and *BRCA2*$^{IVS19-1G>A}$ cells are all similarly defective for replication fork protection and that the DBD is required for protection of replication forks from MRE11 processing in contrast to a previous report (Schlacher et al., 2011).

At ICLs, DNA2 is involved in aberrant processing in the absence of replication fork protection by RAD51 and BRCA2, as shown here (Wang et al., 2015). To determine if processing of replication forks by DNA2 is distinct to ICLs, DNA2 was depleted in *BRCA2* mutants, and cells were analyzed for nascent strand degradation following HU (Figure 3.20A). Depletion of DNA2 rescues resection in all of the BRCA2 mutants including *BRCA2*$^{Trun.}$, *BRCA2*$^{8524C>T}$, *BRCA2*$^{IVS19-1G>A}$, and *BRCA2*^{S3291A}. These data demonstrate that both the DBD and C-terminal domain of BRCA2 are required for proper replication fork protection at HU-stalled forks, and that both domains are required to protect against degradation by MRE11 and DNA2.

All of the BRCA2 mutants showed similar levels of nascent strand resection as measured by DNA fibers, but levels of chromosomal breakage differed (Figure 3.20B). In parallel to our DNA fiber experiments, metaphases were analyzed after 5 hours of 6 mM HU and release into colcemid. *BRCA2*$^{Trun.}$ cells showed a large increase in genomic instability upon stalling with HU in comparison to WT and the other *BRCA2* mutants. *BRCA2*$^{8524C>T}$ and *BRCA2*^{S3291A} cells did not show an

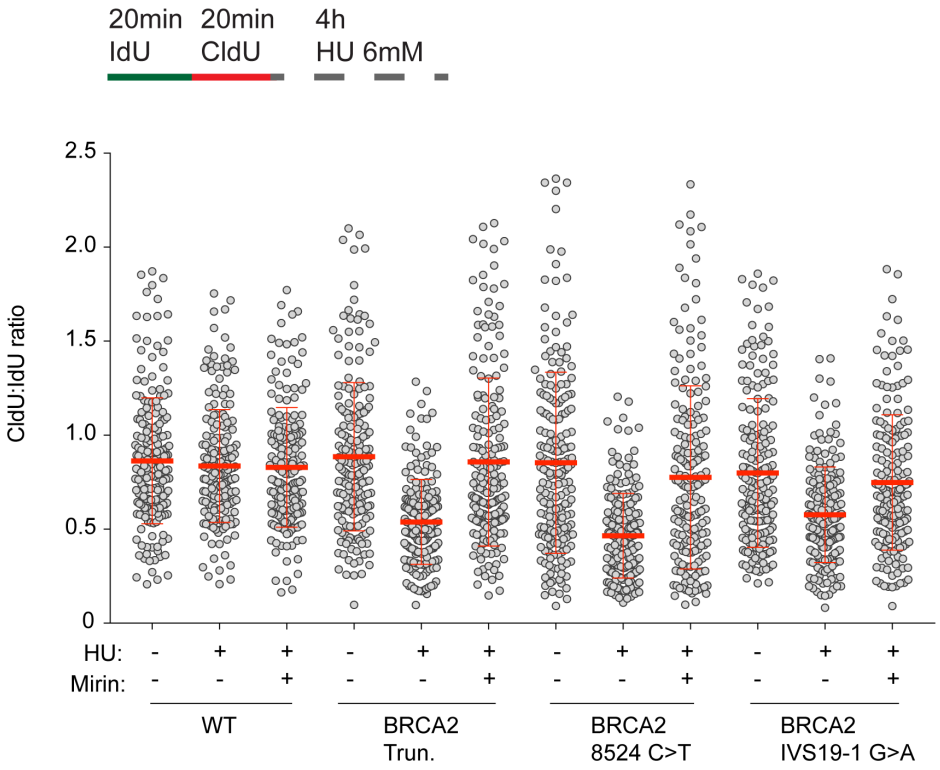

Figure 3.19 BRCA2 DNA binding domain mutants are defective in replication fork protection at hydroxyurea-stalled forks.

Isogenic BJ fibroblast *BRCA2* mutants, *BRCA2*$^{Trun.}$, *BRCA2*$^{8524C>T}$ and *BRCA2*$^{IVS19\text{-}1,G>A}$, were analyzed for replication fork resection. Cells were labeled with DNA analogs, IdU for 20 minutes and then CldU for 20 minutes. Cells were then incubated in 6 mM hydroxyurea (HU) with and without MRE11 inhibitor mirin (50 uM) for 4h before being harvested. DNA fibers were prepared and visualized by immunofluorescence detection of IdU and CldU and measured. Error bars indicate s.d.

Figure 3.20 DNA2 promotes nascent strand degradation at hydroxyurea-stalled replication forks.

(A) Isogenic BJ fibroblast *BRCA2* mutants, *BRCA2*$^{Trun.}$, *BRCA2*$^{8524C>T}$, *BRCA2*$^{IVS19\text{-}1G>A}$, and *BRCA2*^{S3291A}, were transfected with siRNA control luciferase (Luc) or siRNAs targeting DNA2 or MRE11. Cells were labeled with DNA analogs, IdU for 20 minutes and then CldU for 20 minutes. Cells were then incubated in 6 mM hydroxyurea (HU) for 4h before being harvested. Error bars indicate s.d. (B) Quantification of chromosome breaks following 5h of 6 mM HU and released into colcemid. (C) Immunoblot analysis of MRE11 depletion for cells utilized in A. (D) qRT-PCR of *DNA2* expression levels of cells utilized in C. Error bars indicate s.d.

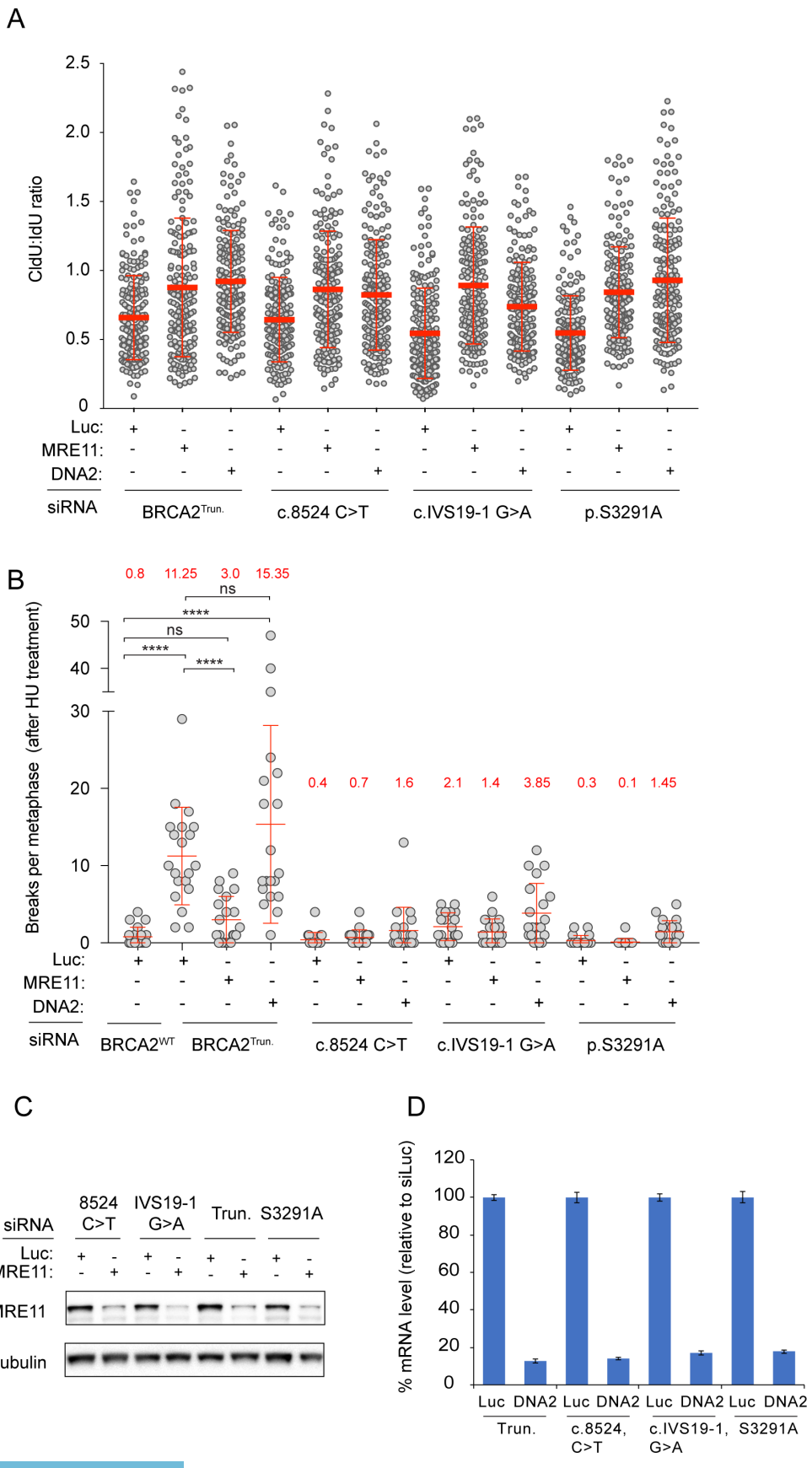

elevation in breakage and *BRCA2*$^{IVS19\text{-}1G>A}$ cells had a mild increase. The elevated chromosomal breakage in *BRCA2*$^{Trun.}$ cells was reduced by MRE11 depletion, but was exacerbated by DNA2 depletion. DNA2 depletion results in a mild increase in breakage for all mutants but none to the extent of *BRCA2*$^{Trun.}$ Previous studies have reported elevated breakage resulting from replication fork degradation in p.S3291A expressing cells and BRCA2 deficient cells (Mijic et al., 2017; Schlacher et al., 2011). However, our data demonstrate that different levels of BRCA2 function have different consequences at HU-stalled forks. These data demonstrate that replication fork resection at HU-stalled forks does not correlate with chromosomal breakage. Neither *BRCA2*$^{8524C>T}$ or *BRCA2*^{S3291A} cells have a significant increase in breakage after HU, despite having levels of fork degradation similar to *BRCA2*$^{Trun.}$ How this breakage results in *BRCA2* depleted or LOF cells needs to be investigated further, but like nascent DNA degradation, it is in part dependent on MRE11.

3.2.8 Depletion of SLX4 or MUS81 does not rescue MMC induced RPA foci in *BRCA2* DBD mutants

SLX4 is a nuclease scaffold protein that complexes with XPF, MUS81, and SLX1, all nucleases that have been implicated in ICL repair (Dendouga et al., 2005; McPherson et al., 2004; Niedernhofer et al., 2004). The unhooking of ICLs is dependent on the SLX4-XPF interaction and deficiency of either protein results in FANCP or FANCO FA complementation group, respectively (Bogliolo et al., 2013; Kim et al., 2011). Furthermore, replication fork collapse has been reported

to be due to MUS81 nuclease activity and depletion of MUS81 has shown to rescue DSBs produced during replication stress. To determine if preventing ICL unhooking or nuclease mediated fork collapse would rescue RPA foci formation in *BRCA2* DBD mutants following MMC, SLX4 and MUS81 were depleted. Depletion of either SLX4 or MUS81 did not rescue RPA hyperactivation in the *BRCA2*$^{8524C>T}$, *BRCA2*$^{IVS19-1G>A}$, and *BRCA2*^{DBDx3A} cells (Figure 3.21A-B). SLX4 depletion further increased RPA activation and foci formation. It was also observed that MMC treatment of *SLX4* patient cells on their own have increased RPA foci formation, presumably due to inappropriate processing of MMC induced ICLs (Figure 3.28A). Depletion of SLX4 exacerbates the RPA phenotype in BRCA2 mutant cells, suggesting that further defects in ICL repair result in the absence of SLX4. This could be due to loss of activity of any of the SLX4-associated nucleases.

3.2.9 Replication fork remodeling by SNF2 family translocases, SMARCAL1, ZRANB3, and HLTF, is not required for ICL repair

Replication fork reversal has been observed as a response to replication stress induced by a number of different classes of genotoxic agents including MMC (Zellweger et al., 2015). SMARCAL1, ZRANB3, and HLTF are ATPase dependent DNA translocases of the SNF2 family of chromatin remodelers that have recently been shown to promote replication fork reversal *in vivo*. Depletion of any of the three rescues nascent strand resection at HU stalled forks in *BRCA2* deficient cells (Mijic et al., 2017; Taglialatela et al., 2017).

Figure 3.21 Depletion of SLX4 or MUS81 does not rescue increased RPA activation and foci formation in BRCA2 DNA binding domain mutants.

(A) Immunoblot analysis of RPA phosphorylation 24h post 1h treatment with 3 μM MMC. *BRCA2*^{WT}, *BRCA2*$^{c.8524C>T}$, *BRCA2*^{DBDx3A}, and *BRCA2*$^{c.IVS19-1G>A}$. BJ fibroblast cells were transfected with control siRNA (Luc) or siRNAs targeting SLX4 or MUS81. (B) Quantification of RPA foci 24h following 1h treatment with 3 uM MMC in cells depleted of SLX4 or MUS81 by siRNA. Error bars indicate s.d of two independent experiments. (C) Immunoblot analysis of MUS81 depletion for cells utilized in A-B. (D) qRT-PCR of *SLX4* expression levels of cells utilized in A-B. Error bars indicate s.d.

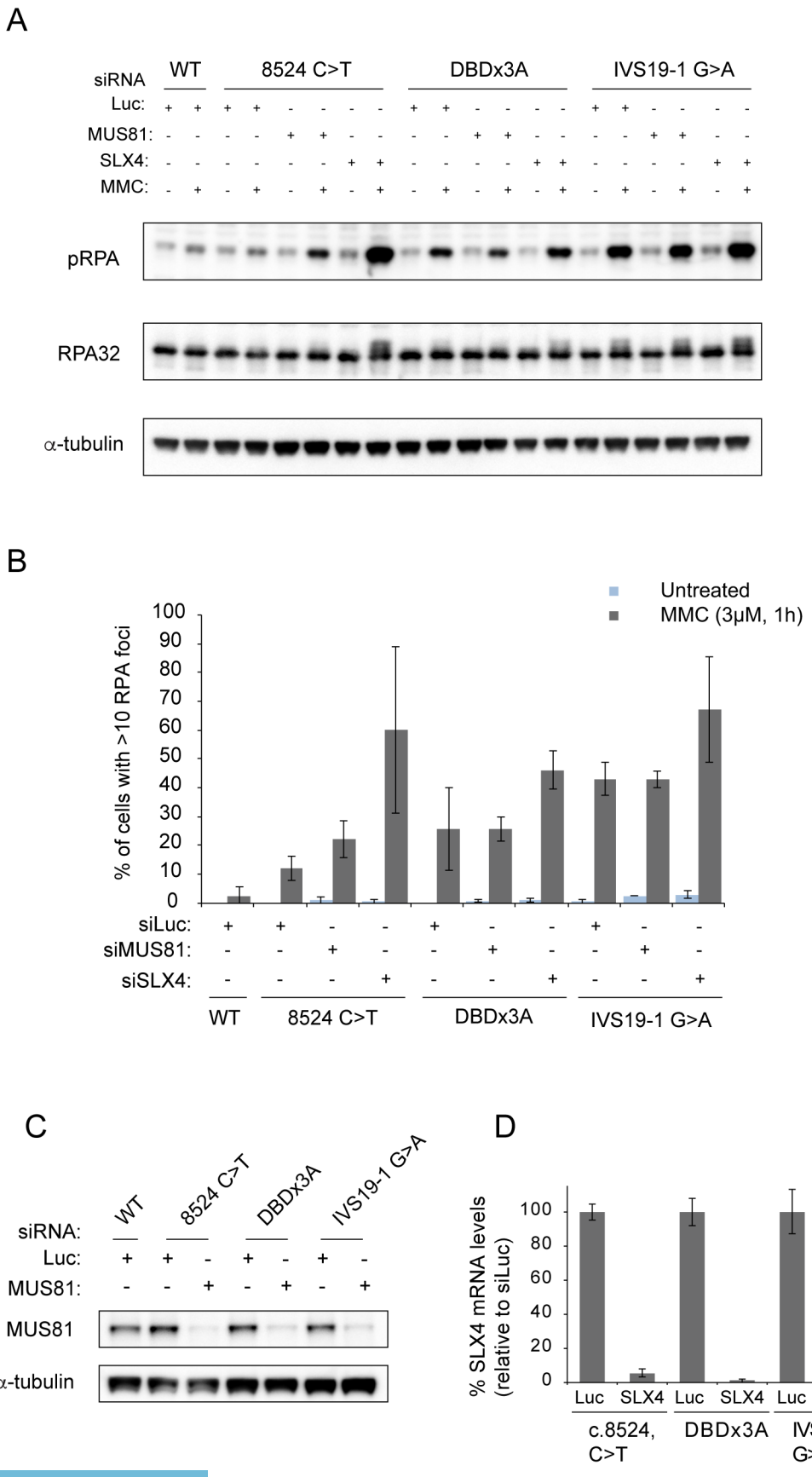

To determine if replication fork reversal is important for the repair of ICLs, wild type cells were depleted of SMARCAL1 or ZRANB3 and tested for sensitization to MMC. Cells depleted of either translocase are not sensitive to MMC (Figure 3.22A). In *BRCA2*$^{8524C>T}$ *and BRCA2*$^{IVS19-1G>A}$ cells depleted of SMARCAL1 or ZRANB3 nascent strand degradation is rescued at HU stalled forks (Figure 3.23A). Depletion of either translocase did not rescue cellular hypersensitivity to MMC or CPT in *BRCA2*$^{IVS19-1G>A}$ cells (Figure 3.23B-C). Depletion of SMARCAL1, ZRANB3, or HLTF also did not rescue increased RPA activation and foci formation after MMC (Figure 3.24 and Figure 3.25). These data suggest that replication fork reversal is not an important intermediate step in ICL repair and that reversed forks observed in MMC treated cells may be part of a more general cellular response to replication stress to prevent genomic instability during replication but not specifically at the ICL.

3.2.10 Depletion of RADX partially rescues defects of ICL repair in BRCA2 DNA binding domain mutants

RADX depletion has been shown to rescue nascent strand degradation at HU-stalled replication forks in BRCA2 deficient cells. RADX depletion restores fork protection without restoring HR, placing the RADX modulation of RAD51 specifically at replication forks. (Dungrawala et al., 2017). We hypothesized that if BRCA2 is involved in the early steps of fork protection at ICLs then RADX depletion would rescue increased ssDNA and RPA foci resulting from MMC treatment (Wang et al., 2015). Consistent with previously reported data, depletion of RADX did

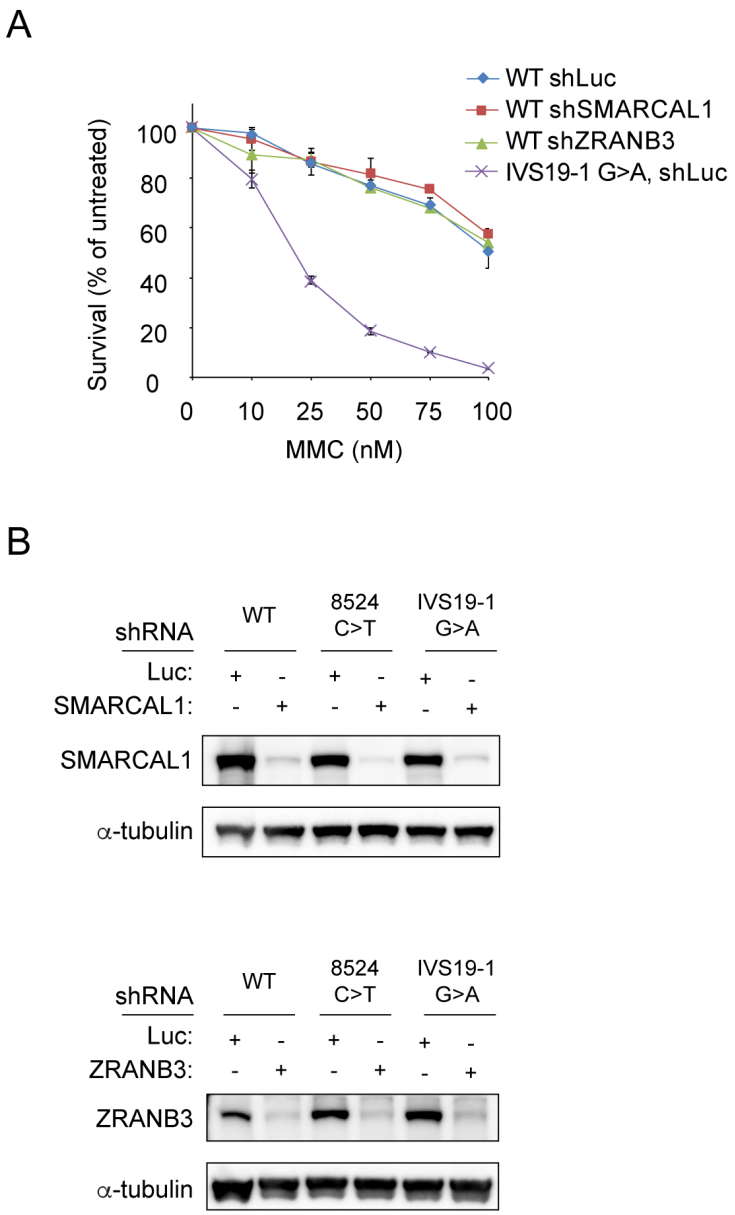

Figure 3.22 SMARCAL1 and ZRANB3 translocases do not have a major role in cellular resistance to DNA interstrand crosslinks.

(A) MMC cell survival of BJ *BRCA2*^{WT} fibroblasts depleted of SMARCAL1 or ZRANB3 by shRNA or transduced with shRNA luciferase control (shLuc). Cell survival assays were performed in triplicate and treated with increasing concentrations of the indicated agent. Cell survival was determined by counting cells after 7-9 days in culture. Relative cell survival was normalized to untreated controls to give percent survival. Error bars indicate s.d. (B-C) Immunoblot analysis of shRNA depletion of SMARCAL1 and ZRANB3.

Figure 3.23 Depletion of SMARCAL1 and ZRANB3 translocases rescues nascent strand degradation at HU-stalled replication forks but does not promote cellular resistance to MMC or CPT in BRCA2 DBD mutants.

(A) BJ fibroblast *BRCA2* mutants *BRCA2*$^{8524C>T}$ and *BRCA2*$^{IVS19\text{-}1G>A}$, were analyzed for replication fork resection when depleted of either SMARCAL1 or ZRANB3 by shRNA or transduced with control shRNA (shLuc). Cells were labeled with DNA analogs, IdU for 20 minutes and then CldU for 20 minutes. Cells were then incubated in 6 mM hydroxyurea (HU) for 4h before being harvested. DNA fibers were prepared and visualized by immunofluorescence detection of IdU and CldU and measured. Error bars indicate s.d. (B-C) MMC and CPT cell survival assay of BJ *BRCA2*$^{c.IVS19\text{-}1G>A}$ depleted of either SMARCAL1 or ZRANB3 by shRNA or transduced with shRNA luciferase control (shLuc). Cell survival assays were performed in triplicate. Cells were treated with increasing concentrations of indicated agent. Cell survival was determined by counting cells after 7-9 days in culture. Relative cell survival was normalized to untreated controls to give percent survival. Error bars indicate s.d.

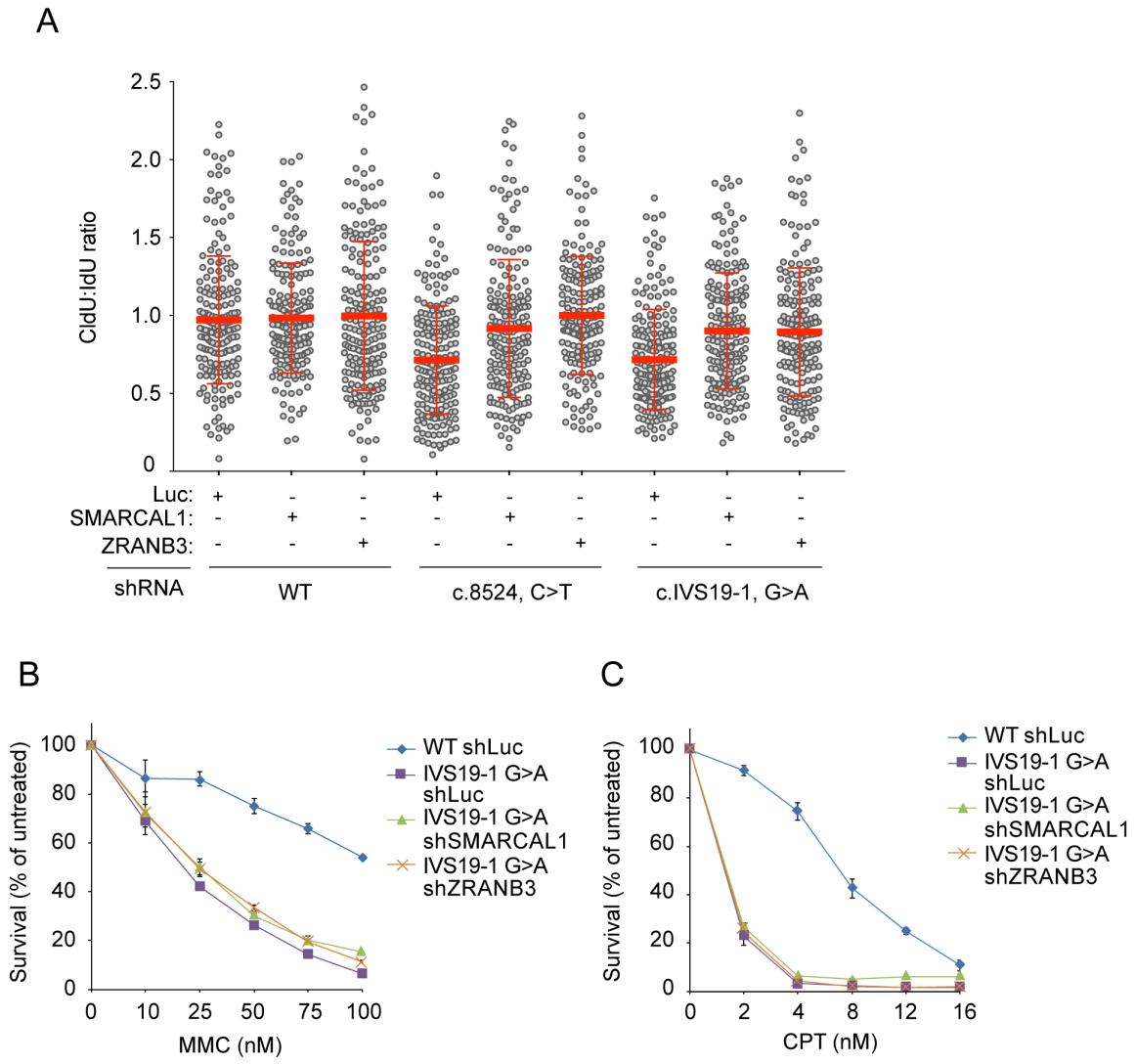

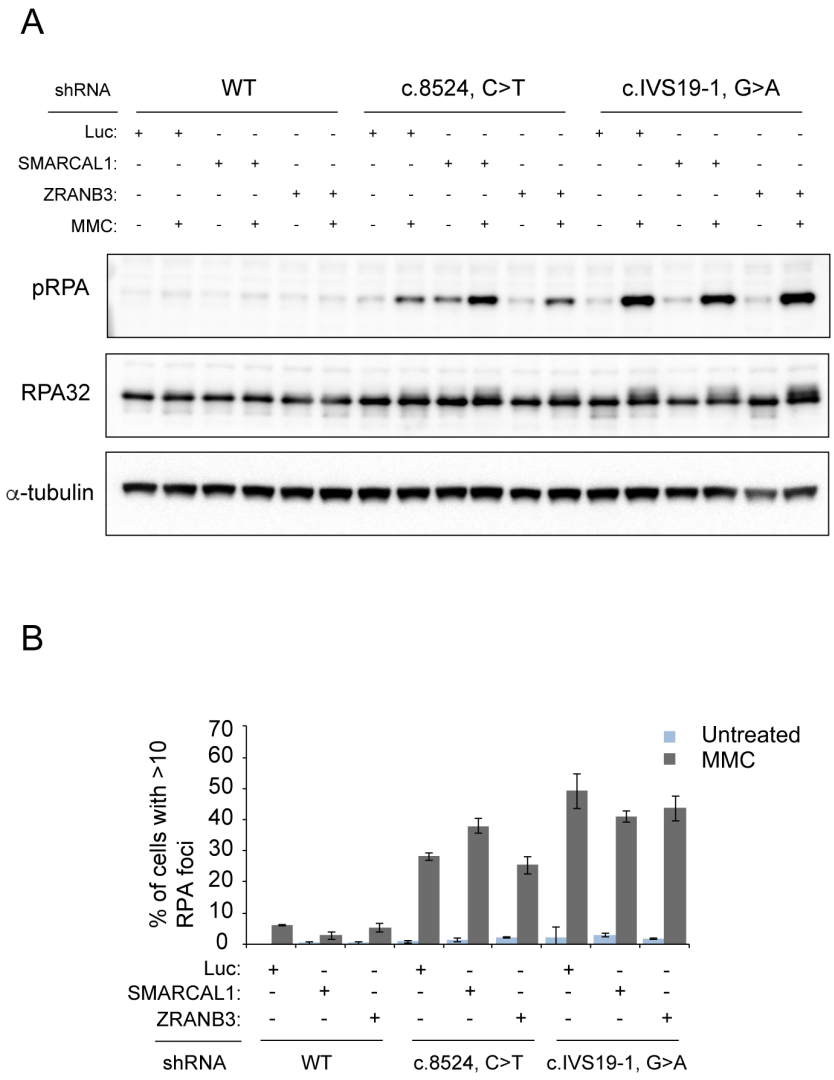

Figure 3.24 Depletion of SMARCAL1 or ZRANB2 translocases does not rescue increased RPA activation and foci formation induced by MMC in BRCA2 DNA binding domain mutants.

(A) Immunoblot analysis of RPA phosphorylation 24h post 1h treatment with 3 uM MMC. *BRCA2*$^{c.8524C>T}$ *and BRCA2*$^{c.IVS19-1G>A}$ BJ fibroblast cells were depleted of either SMARCAL1 or ZRANB3 by shRNA or transduced with shRNA control (Luc) (B) Quantification of RPA foci 24h following 1h treatment with 3 uM MMC in cells depleted of SMARCAL1 or ZRANB3. Error bars indicate s.d of two independent experiments.

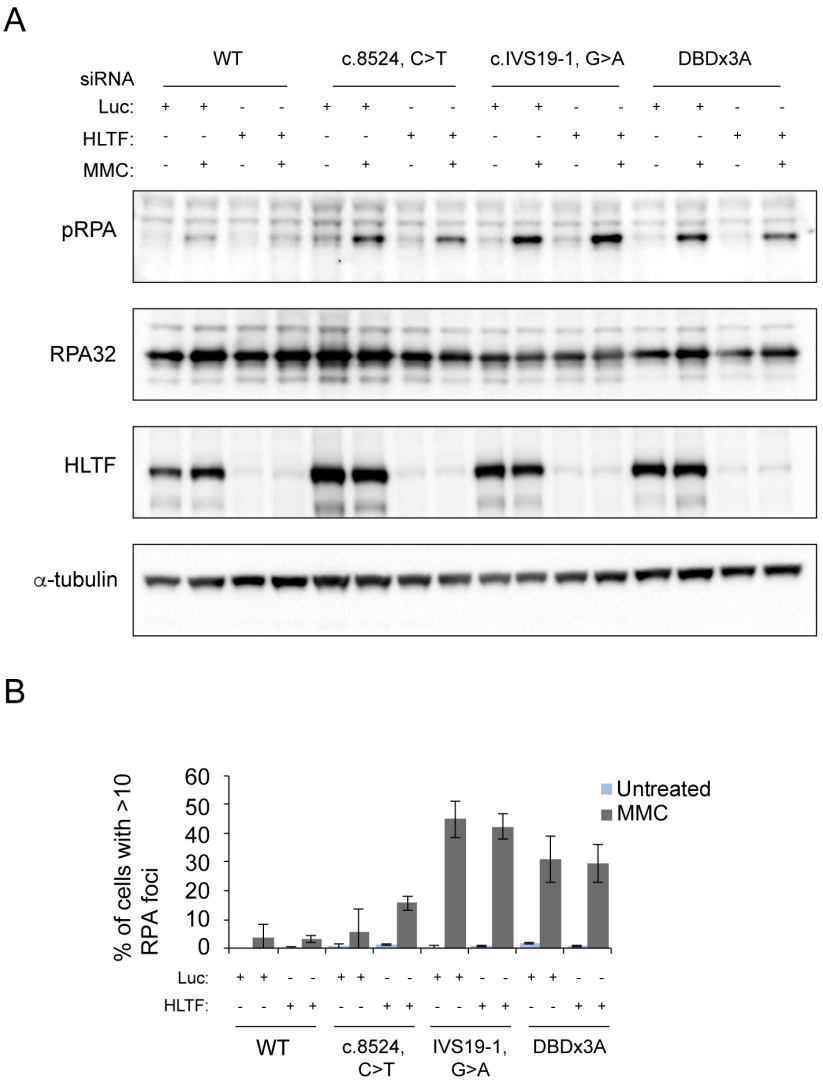

Figure 3.25 Depletion of HLTF translocase does not rescue increased RPA activation and foci formation in BRCA2 DNA binding domain mutants.

A) Immunoblot analysis of RPA phosphorylation 24h post 1h treatment with 3 uM MMC. *BRCA2*^{WT}, *BRCA2*$^{c.8524C>T}$, *BRCA2*^{DBDx3A}, and *BRCA2*$^{c.IVS19\text{-}1G>A}$ BJ fibroblast cells were transfected with siRNA control (Luc) or siRNAs targeting *HLTF*. (B) Quantification of RPA foci 24h following 1h treatment with 3 uM MMC in cells depleted of HLTF. Error bars indicate s.d of two independent experiments.

not rescue HR levels in *BRCA2* mutant cell lines (Figure 3.26C-D) (Dungrawala et al., 2017). However, as expected, RADX depletion rescued nascent strand degradation of HU-stalled replication forks in *BRCA2*$^{8524C>T}$ and *BRCA2*$^{IVS19-1G>A}$ cells (Figure 3.27A).

RADX depletion in *BRCA2*$^{8524C>T}$ and *BRCA2*$^{IVS19-1G>A}$ cells partially ameliorated the increased RPA foci formation following MMC (Figure 3.27B). RADX depletion also makes *BRCA2* mutant cells more resistant to MMC (Figure 3.27C-D). These data taken together support a role for both BRCA2 and RAD51 at the early steps of ICL repair independent of HR (Figure 3.27F). It is possible that in the absence of RADX antagonism that BRCA2 defective cells have improved BRCA2-RAD51 protection at ICLs from DNA2-WRN. However, we also observe that RADX depletion sensitizes WT cells to MMC (Figure 3.27C). RADX activity may also be required for the response to MMC induced ICLs. Further investigation is needed to determine how RADX promotes proper ICL repair and if this is mediated through RAD51 modulation. However, the partial rescue effect of RADX depletion on MMC sensitivity in *BRCA2* mutants also indicates that RADX activity is deleterious for ICL repair in the setting of defective BRCA2 function.

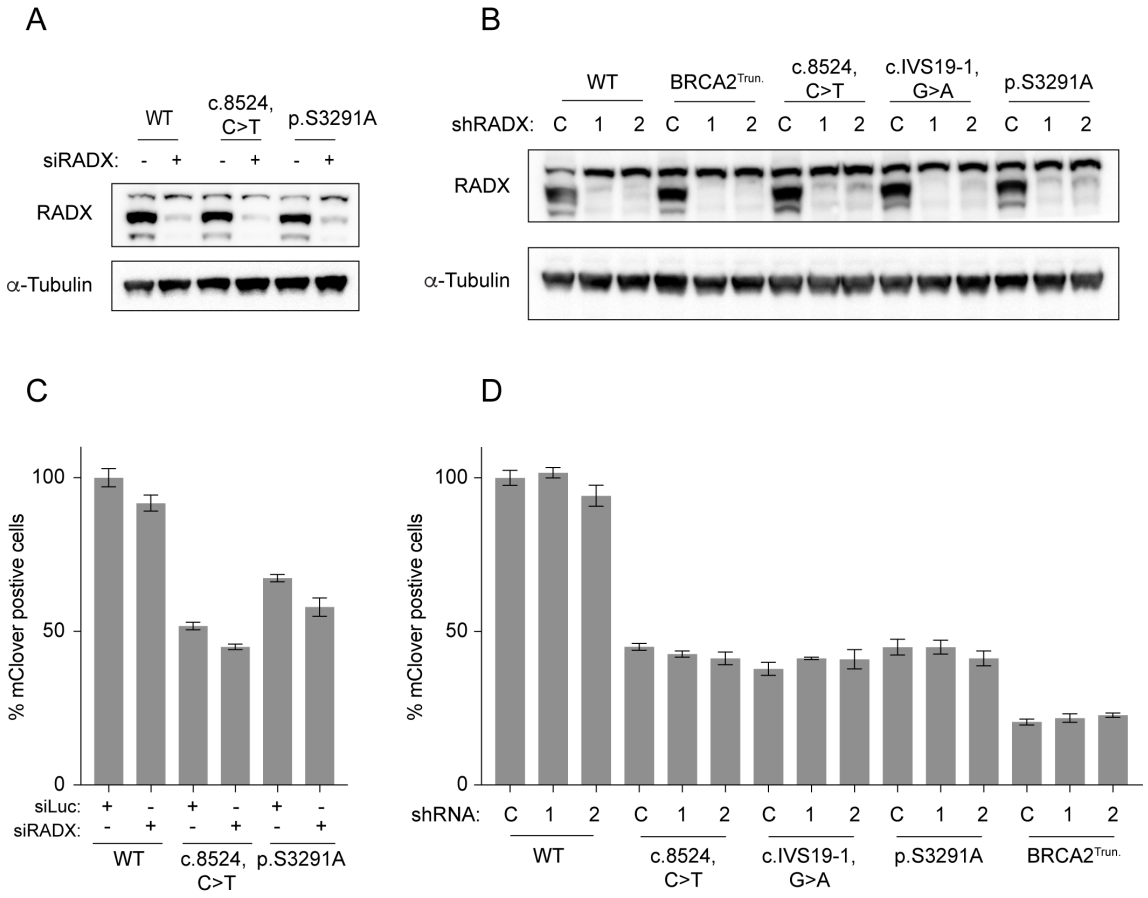

Figure 3.26 Deficiency of RADX does not impact homologous recombination efficiency in BRCA2 DNA binding domain mutants.

(A) Immunoblot analysis of RADX depletion by siRNA for cells utilized in C. (B) Immunoblot analysis of RADX depletion by two shRNAs for cells utilized in D. (C) Comparison of levels of mClover positive cells of HEK293T *BRCA2* mutants transfected with siRNAs targeting RADX or control (Luc). (D) Comparison of levels of mClover positive cells of HEK293T *BRCA2* mutants (c.8524C>T, c.IVS19-1G>A, p.S3291A, BRCA2$^{Trun.}$) transduced with shRNAs targeting RADX (1 or 2) or shRNA control (C). Error bars indicate s.d. of experiments performed in triplicate.

Figure 3.27 Depletion of RADX partially rescues ICL repair defects in BRCA2 DNA binding domain mutants.

(A) BJ fibroblast with *BRCA2* mutations, *BRCA2*$^{8524C>T}$ and *BRCA2*$^{IVS19\text{-}1G>A}$, were analyzed for replication fork resection when depleted of RADX by shRNA or transduced with shRNA control (shCONT.). Cells were labeled with DNA analogs, IdU for 20 minutes and then CldU for 20 minutes. Cells were then incubated in 6 mM hydroxyurea (HU) for 4h before being harvested. DNA fibers were prepared and visualized by immunofluorescence detection of IdU and CldU and measured. Error bars indicate s.d. (B) Quantification of RPA foci 24h following 1h treatment with 3 μM MMC in cells depleted of RADX by shRNA. Error bars indicate s.d. of two independent experiments. (C-D) Cell survival of BJ BRCA2^{WT}, BRCA2$^{c.IVS19\text{-}1G>A}$, and BRCA2$^{c.8524C>T}$ fibroblasts depleted of RADX by shRNA or transduced with control shRNA (shCONT.). Cell survival assays were performed in triplicate and cells were treated with increasing concentrations of MMC. Cell survival was determined by counting cells after 8 days in culture. Relative cell survival was normalized to untreated controls to give percent survival. Error bars indicate s.d. (E) qRT-PCR of *RADX* expression levels of cells utilized in A-C. Error bars indicate s.d. (F) Schematic of proposed model of how RADX depletion partially ameliorates the increased RPA foci formation in *BRCA2* deficient cells.

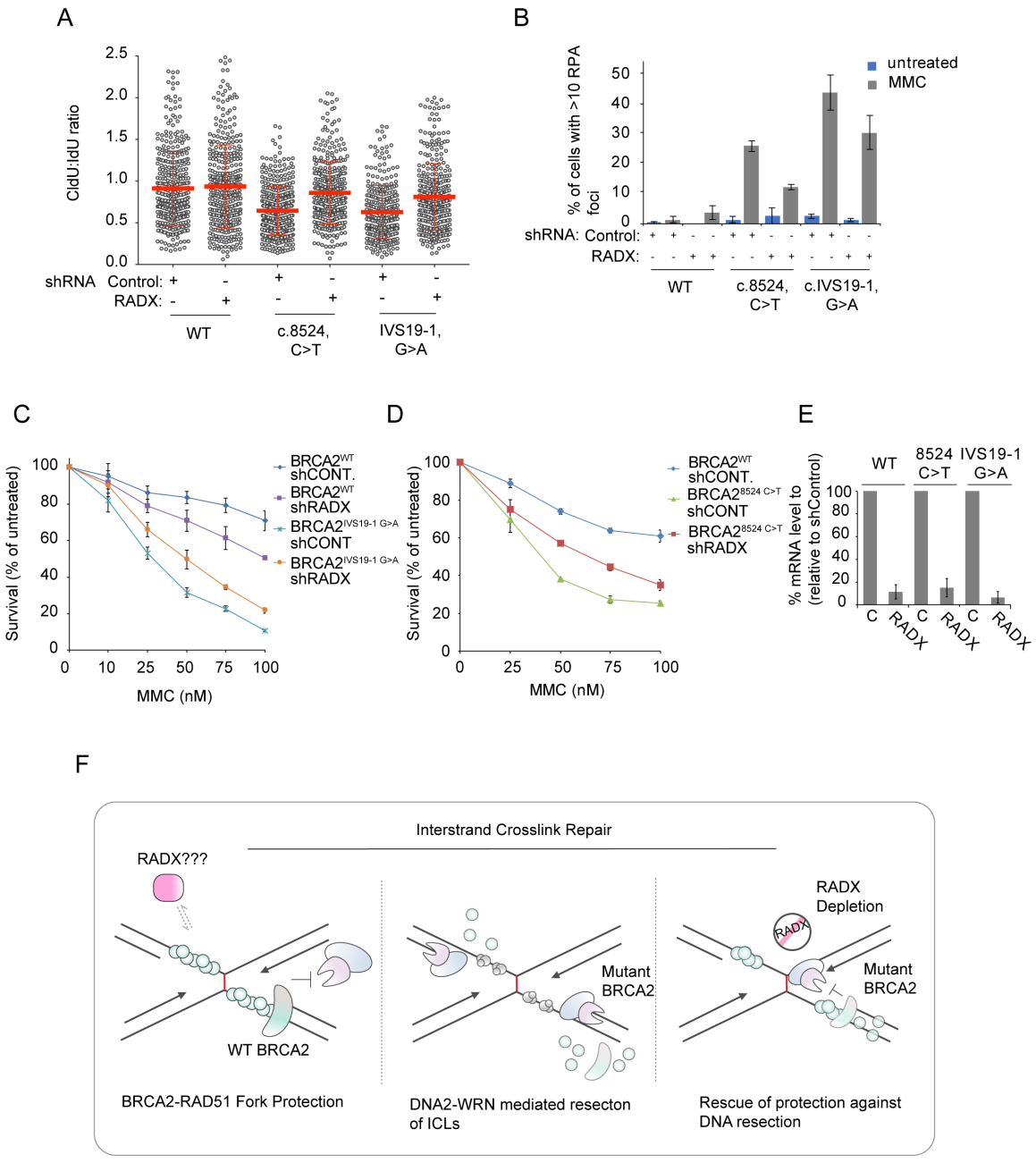

3.2.11 ICLs are a substrate of nucleolytic processing in the absence of a functioning FA pathway

Having demonstrated that BRCA2 and RAD51 share a role in protecting ICLs from over resection by DNA2 and WRN, we investigated whether other FA proteins are required for protection against DNA hyper-resection at ICLs. Analysis of a panel of FA patient derived cells *FANCA*, *FANCL*, *FANCD2*, *FANCI*, *FANCJ*, and *FANCP/SLX4* demonstrated increased RPA foci formation following MMC treatment for all complementation groups (Figure 3.28A). To determine if the source of RPA was the same as in BRCA2 and RAD51 mutant cells, DNA2 and WRN were depleted in a complemented pair of *FANCA* patient-derived cells (Figure 3.28B). Interestingly, the dependence on DNA2 was the same, but the helicase dependency is different, as WRN did not rescue RPA levels but BLM depletion did (Figure 3.28B-C). These data demonstrate a dependence on the FA core complex to prevent resection of ICLs by DNA2 and BLM. However, whether the source of RPA is the same in each of these FA patient cell lines needs further investigation because these factors have different roles in the repair of ICLs.

Figure 3.28 Deficiency of Fanconi anemia proteins results in hyper-phosphorylation and foci formation of RPA after MMC.

(A) Quantification of RPA foci 8h, 24h and 48h following 1h treatment with 3 μM MMC of FA patient derived fibroblasts compared to BJ wild type fibroblasts. Patient cells lines from FA complementation group *FANCR/RAD51* (FA-R^{mut}), *FANCA* (FA-A^{mut}), *FANCL* (FA-L^{mut}), *FANCD2* (FA-$D2^{mut}$), *FANCI* (FA-I^{mut}), *FANCJ/BRIP* (FA-J^{mut}), and *FANCP/SLX4* (FA-P^{mut}). *FANCA* patient complemented cell lines were generated by transducing WT *FANCA* cDNA (FA-A) or empty vector control (EV). Error bars indicate s.d. of two independent experiments. (B) *FANCA* patient cells expressing WT *FANCA* (FA-A+A) or empty vector (FA-A+EV) were transfected with siRNA control luciferase (Luc) or siRNAs targeting DNA2 and WRN. Quantification of RPA foci 24h following 1h treatment with 3 μM MMC. Error bars indicate s.d. of two independent experiments. (C) qRT-PCR of *DNA2* and *WRN* expression levels of *FANCA* cells utilized in B. Error bars indicate s.d. (D) FA-A+EV were transfected with siRNA Luc or siRNAs targeting DNA2 and BLM. Quantification of RPA foci 24h following 1h treatment with 3 μM MMC. Error bars indicate s.d. of two independent experiments. (E) qRT-PCR of *DNA2* and *BLM* expression levels of *FANCA* cells utilized in D. Error bars indicate s.d. Experiment shown in (A) performed by Athena Huang and Experiment shown in (D) performed by Anderson Wang.

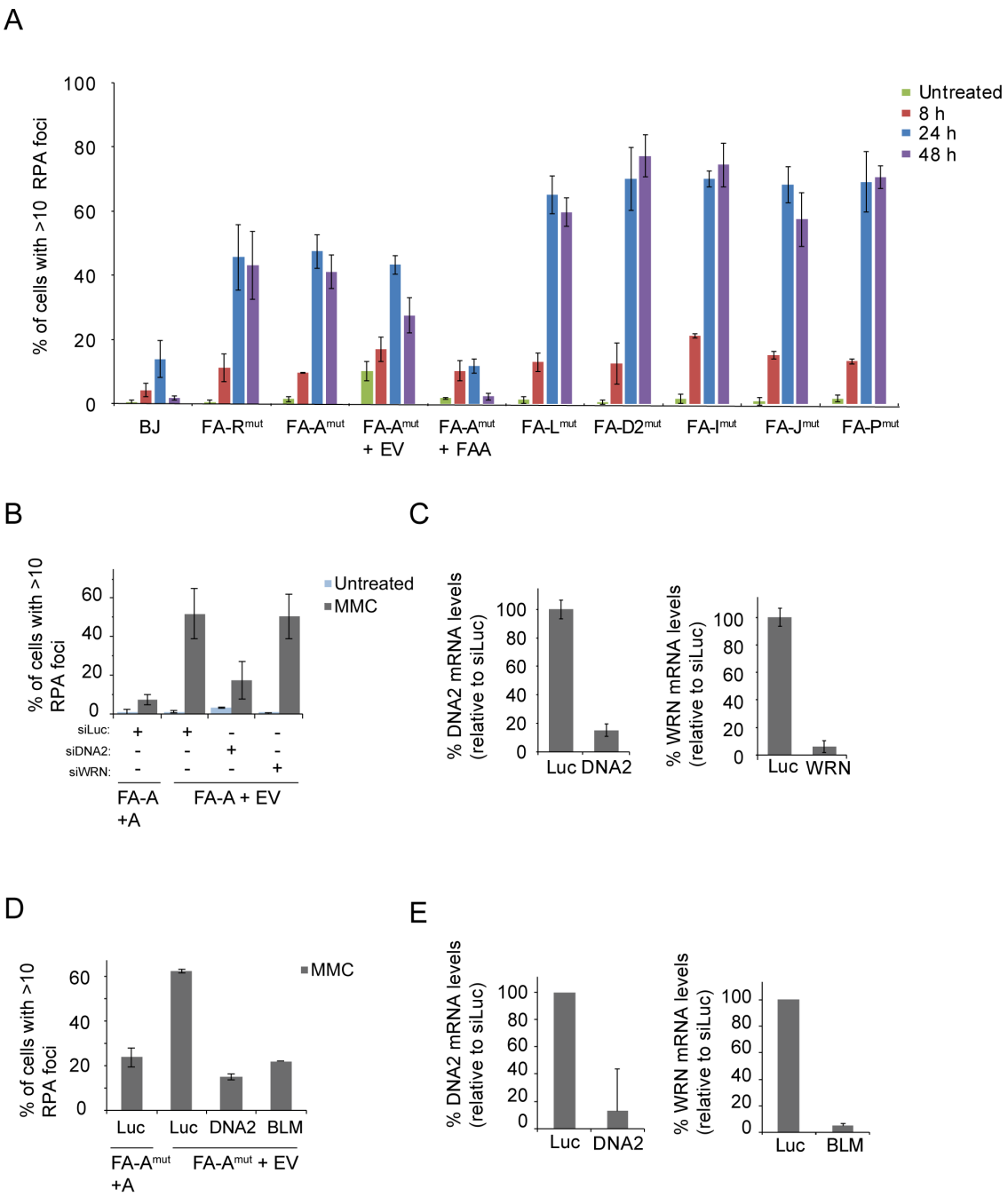

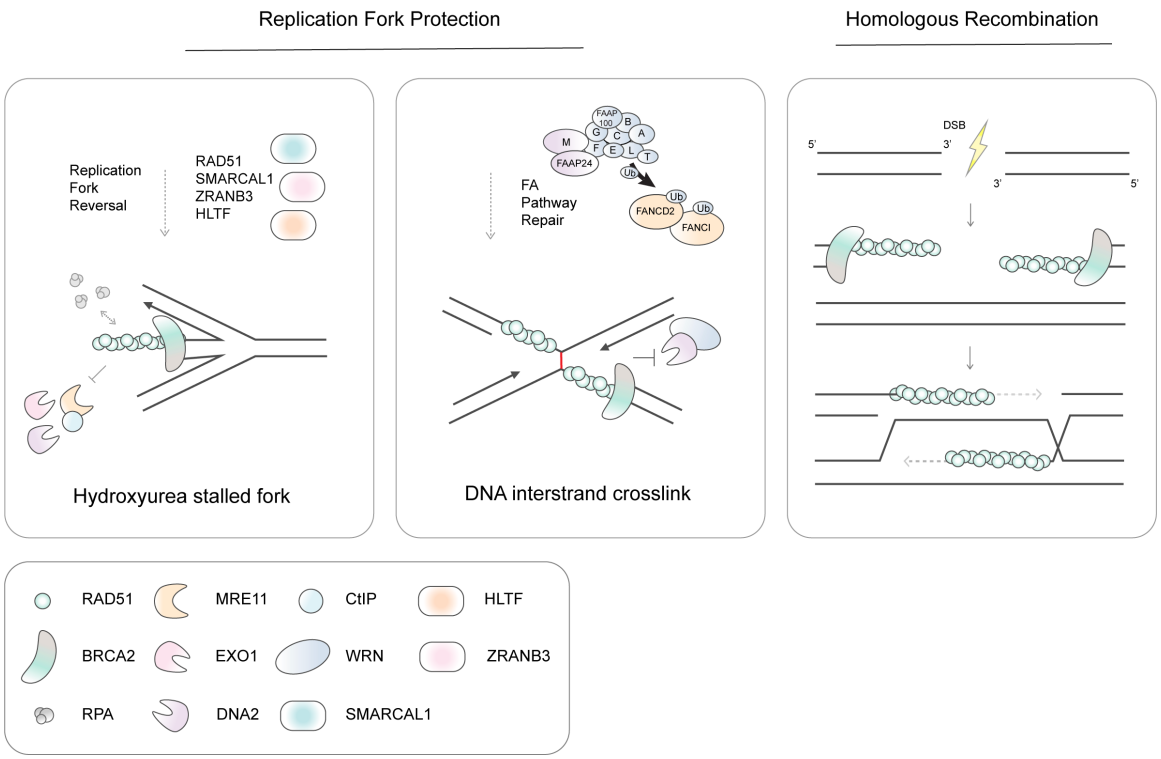

Figure 3.29 The role of BRCA2 in homologous recombination and replication fork protection requires the DNA binding domain.

Schematic representing the different roles of BRCA2 in replication fork protection and homologous recombination. BRCA2 has a role in two distinct types of replication fork protection. At HU stalled forks, BRCA2 and RAD51 protect DNA from degradation by nucleases that include, MRE11, CtIP, EXO1, and DNA2. Replication fork reversal is dependent on RAD51 and the SNF2 translocases, SMARCAL1, ZRANB3, and HLTF. At ICLs, BRCA2 and RAD51protect against resection by DNA2-WRN. This process does not involve replication fork reversal. During homologous recombination repair of DSBs, BRCA2 assembles RAD51 nucleofilaments onto ssDNA overhangs, which is important for the RAD51 mediated homology search of the sister chromatid for use as a repair template.

3.3 Summary and Conclusions

We have identified a family with an unusual clinical presentation of biallelic *BRCA2* mutations. Unlike other *FANCD1/BRCA2* patients, the sibling pair displays a relatively mild phenotype, even as adults, which is characterized by marked developmental abnormalities, but no bone marrow failure or cancer. The *BRCA2* mutations consist of a LOF frameshift mutation of exon 11 in *trans* to a missense mutation c.8524C>T/p.R2842C of the BRCA2 DBD. An additional *FANCD1/BRCA2* adult presenting with mild disease was identified in the literature and is homozygous for the splice site mutation, c.IVS19-1G>A, that translates into the loss of the first four aa of exon 20 of the BRCA2 DBD (Howlett et al., 2002).

Analysis of LCLs from the sibling pair (RA3105/RA3106) show cellular sensitivity to ICL generating agents and a mild elevation in chromosomal breakage to DEB. Comprehensive analysis of HSC62 fibroblasts (c.IVS19-1G>A) reveals sensitivity to ICL generating agents, but not IR. Lack of IR sensitivity and normal SCEs levels suggest that HR is largely intact in these fibroblasts. Using CRISPR/Cas9 gene editing, the c.IVS19-1G>A splice site mutation was corrected to WT in HSC62 fibroblasts, and the observed cellular defects were rescued demonstrating that the c.IVS19-1G>A base substitution is responsible for the cellular defects.

To compare the phenotypes of both DBD mutations in isogenic cell lines, c.8524C>T and c.IVS19-1G>A, were generated in human fibroblasts using

CRISPR/Cas9 targeting of the endogenous *BRCA2* locus. Side-by-side comparison of the mutations demonstrated that the *BRCA2* c.IVS19-1G>A mutation has a more pronounced phenotype than c.8524C>T. *BRCA2*$^{IVS19\text{-}1G>A}$ and *BRCA2*$^{8524C>T}$ cells both have defects in RAD51 foci formation, cellular sensitivity to MMC, and elicit increased RPA activation and foci formation after MMC. Furthermore, to evaluate these mutations for HR proficiency, BRCA2 DBD mutants were generated in HEK293T cells and analyzed using a mClover LMNA homologous recombination CRISPR/Cas9 reporter assay (Arnoult et al., 2017; Pinder et al., 2015). Interestingly, the DBD mutants showed a similar moderate reduction in HR despite the greater defect in MMC sensitivity in the c.IVS19-1G>A clones than the c.8524C>T clones. The previously described separation of function mutant, p.S3291A, showed a moderate reduction in HR, which demonstrated that p.S3291A, like our BRCA2 mutations, decreases HR function in contrast to a previous report (Schlacher et al., 2011). These results demonstrate that the c.8524C>T mutation, identified previously as a VUS, is pathogenic and deleterious to BRCA2 function.

HSC62 cells show markedly increased RPA foci formation that is dependent on DNA2 and WRN after MMC treatment. Previously, DNA2-WRN dependent resection at ICLs was reported in the *RAD51/FANCR* p.T131P patient cell line. In the *RAD51/FANCR* p.T131P patient cell line, the mutant protein makes up 20% of cellular RAD51 and has a dominant negative effect on RAD51 function. The minor

amount of mutant protein does not impact HR, but disrupts RAD51 function at ICLs revealing an HR-independent role for RAD51 in ICL repair (Wang et al., 2015). These results suggest that like the well described interdependence of BRCA2 and RAD51 in HR and the protection of HU-stalled forks, BRCA2 and RAD51 function together to prevent resection at ICLs.

Like HSC62 fibroblasts, isogenic BRCA2 DBD mutants have elevated RPA activation and foci formation after MMC that is DNA2-WRN dependent. The greater increase in RPA activation and foci formation resulting from the c.IVS19-1G>A mutation is not fully rescued. However, there is a marked reduction in pRPA and RPA foci in c.8524C>T cells and in another DBD mutant, DBDx3A. The DBDx3A mutant has 3 aa substitutions at residues that interact with DNA (K2833A, Y2839A, and F2841A) (Yang et al., 2005). We hypothesize that the alanine substitutions of these residues disrupt DNA binding, but are minimally disruptive to the BRCA2 structure. The DBDx3A mutant cells have a slightly milder phenotype than c.IVS19-1G>A cells by MMC cellular sensitivity and RPA activation and RPA foci formation. The c.IVS19-1G>A splice site mutation results in the deletion of four aa, which may distort the BRCA2 structure and further impair BRCA2 function. This likely results in more ssDNA from sources other than DNA2-WRN activity.

Our analysis of *BRCA2* DBD mutants demonstrates that the function of the DBD is required for replication fork protection of HU-stalled forks from MRE11 and

DNA2. While the role of MRE11 in nascent strand degradation of BRCA2 deficient cells has been widely shown, there is conflicting data about resection mediated by DNA2 (Lemacon et al., 2017; Ray Chaudhuri et al., 2016). However, a role for DNA2 with WRN has been described in a mechanism of replication fork restart, and it has also been reported that DNA2 degrades nascent DNA at stalled forks in the setting of RECQ1, BOD1L, or Abro1 deficiency (Higgs et al., 2015; Thangavel et al., 2015; Xu et al., 2017).

Previously, it was reported in Brca2 deficient hamster V-C8 cells, complemented with a *BRCA2* bacterial artificial chromosome (BAC) construct missing the entire DBD (p.Δ2451-3210), that the DBD was dispensable for replication fork protection at HU-stalled forks (Schlacher et al., 2011). Our analysis of BRCA2 DBD mutants demonstrate that the replication fork protection role of BRCA2 at HU-stalled replication forks is not distinct to the C-terminal domain and that fork protection likely requires the DBD to bind DNA at the replication fork. Biochemical analysis of BRCA2 mutants will need to be carried out to determine how these mutations impact binding at replication fork structures. The location of the mutations at the transition of the OB2 and base of the Tower domain suggests that they may interfere with ssDNA-dsDNA binding. The Tower domain contains a 3HB domain at the apex that binds dsDNA, so interruption of this region may preclude binding at replication fork ssDNA-dsDNA junctions where BRCA2 binding may be especially important for replication fork protection (Yang et al., 2002).

Genomic instability resulting from the absence of proper replication fork protection has largely been studied by depletion of BRCA2 by RNAi (Lemacon et al., 2017; Mijic et al., 2017; Taglialatela et al., 2017). Here we show that a significant increase in chromosomal breakage after HU does not correlate with replication fork resection. For some of the BRCA2 mutants (c.8524C>T and p.S3291A) described in this study replication fork protection at HU-stalled forks is defective, but there is no significant increase in chromosomal breakage after HU. Our results showing increased breakage in cells expressing a BRCA2 LOF truncation, are consistent with many previous reports that BRCA2 knockdown results in increased chromosomal breakage that is rescued by MRE11 depletion/inhibition (Lemacon et al., 2017; Mijic et al., 2017; Schlacher et al., 2011; Taglialatela et al., 2017). All of the BRCA2 mutants in our analysis that undergo MRE11 dependent fork resection at HU-stalled replication forks do not have elevated breakage. The consequences of nascent strand degradation requires further investigation in the background of hypomorphic fork protection mutants such as, c.8524C>T and p.S3291A, instead of BRCA2 knockdown by RNAi. These results demonstrate the importance of using *BRCA2* mutants that permit distinguishing between different BRCA2 functions as opposed to RNAi depletion that removes all function.

We show that DNA2 depletion in BRCA2 mutant cells also rescues resection at HU-stalled replication forks. Interestingly, at the same time we observe

that DNA2 depletion exacerbates chromosomal breakage to HU. This observation suggests that in the setting of BRCA2 deficiency DNA2 depletion is deleterious, which may be due to its role in replication-coupled repair or modulation of reversed forks (Hu et al., 2012; Karanja et al., 2012; Thangavel et al., 2015). Recent reports have also implicated EXO1 and CtIP as degrading HU-stalled forks in the absence of BRCA2 (Lemacon et al., 2017). It would be interesting to know what the consequences of EXO1 and CtIP depletion are on chromosomal breakage to HU given the different effects of MRE11 and DNA2 depletion on the breakage levels. Taken together, resection of the regressed fork in the absence of BRCA2 is now reported to involve all of the DSB end-resection nucleases. MRE11 and DNA2 are already reported to be required for replication fork restart (Bryant et al., 2009; Thangavel et al., 2015). However, further investigation is required to determine if all of these factors have a normal function in processing stalled forks or restoring reversed forks under normal genetic conditions. These results are also interesting in that all of the nucleases may be acting at HU-stalled forks in BRCA2 deficient cells, but only DNA2 has activity at the ICL.

Depletion of the replication fork remodelers SMARCAL1, ZRANB3, and HLTF rescues nascent strand degradation at HU-stalled forks in BRCA2 DBD mutants, but does not mitigate cellular sensitivity or increased RPA after MMC. Despite the observation that MMC increases replication fork reversal in cells (Zellweger et al., 2015), our study demonstrates that replication fork reversal is not

a major step in the repair of ICLs and that the processing at HU-stalled forks is different from ICLs. However, RADX depletion does ameliorate the increased RPA foci and cellular sensitivity to MMC independent of HR. RADX specifically modulates RAD51 at replication forks indicating that this rescue is related to BRCA2-RAD51 replication fork protection at the ICL and not downstream processing of DSBs. This is also consistent with the previous identification of RAD51 localization to ICLs prior to DSBs (Long et al., 2011).

FA proteins have previously been shown to be important for protection at HU-stalled replication forks (Schlacher et al., 2012). Analysis of FA patient cell lines of various complementation groups also demonstrates increased ssDNA and RPA foci formation after MMC. In *FANCA* cells, the increase in RPA foci is due to DNA2 and BLM, but not WRN. This suggest that the fork protection of BRCA2-RAD51 is not redundant with the FA core complex, but further investigation would be needed to determine the source of increased ssDNA in the absence of the other FA proteins. DNA2 has previously been reported to interact with FANCD2 and be recruited to ICLs where it is required for repair but is deleterious in the absence of FANCD2 (Karanja et al., 2012; Karanja et al., 2014). BLM has been reported to interact with a number of FA proteins and co-localize with FANCD2 at ICLs (Meetei et al., 2003b; Pichierri et al., 2004; Suhasini and Brosh, 2012). Consistent with BLM depletion rescuing increased ssDNA at the fork in the absence of FANCA, BLM knockout was also recently reported to rescue ICL sensitivity and reduce DNA

damage in FA deficient cells (Moder et al., 2017). It is possible that DNA2, WRN, and BLM are recruited to ICLs to perform normal functions, but in the absence of key FA/BRCA pathway components are left unregulated.

The mutations reported in this study may have more differential impact on BRCA2 function depending on the nature of the DNA lesion. It is clear that the BRCA2 DBD is important for HR and replication fork protection (Figure 3.29). Both BRCA2 mutations, c.8524C>T and c.IVS19-1G>A, have a similar and moderate impact on HR efficiency. However, the impact on BRCA2 function in ICL repair demonstrates the c.IVS19-1G>A mutation to be more deleterious than either the c.8524C>T substitution or DBDx3A mutant. For HR, DSBs generated by targeted nuclease are likely different than DNA substrates encountered by the replication fork due to stalling by HU or ICLs. It is possible that DSB repair by HR may not be as sensitive to defects in BRCA2 ssDNA-dsDNA binding which could be of greater importance at a replication fork.

The identification of *BRCA2* DBD mutations in conjunction with atypical disease presentation gives the opportunity to investigate how defects in the DBD impact BRCA2 function and gives insight into how these defects may give rise to the developmental defects characteristic of FA but not the early childhood malignancies seen in other patients with biallelic *FANCD1/BRCA2* mutations. There is not a clear correlation of disease severity and deleteriousness of the

mutation for the sibling pair with the c.8524 C>T variant and the individual with homozygous c.IVS19-1G>A mutation. Analysis of the mutations in isogenic cell lines in the homozygous state demonstrates the c.IVS19-1G>A to be more deleterious to BRCA2 function than c.8524C>T. However, the sibling pair presents with much more severe congenital abnormalities. It is possible that there are other modifying factors, environmental and/or genetic, that impact the phenotypes of these patients. The dose of hypomorphic BRCA2 during development may also play a role. In the sibling pair the c.8524C>T mutation is in *trans* to a LOF allele instead of two hypomorphic alleles in the case of the individual with c.IVS19-1G>A. Regardless, the disease presentation of these individuals is very atypical for *FANCD1/BRCA2* complementation group and resembles the phenotype of FA-like patients described for *FANCR/RAD51* and *FANCO/RAD51C* complementation groups (Vaz et al., 2010; Wang et al., 2015). The patients have congenital abnormalities typical of FA but no bone marrow failure or malignancy even into adulthood. Due to the moderate impact that these DBD mutations have on HR, we hypothesize that the retention of ~50% of HR function that we observe is sufficient enough for cellular function and to safeguarded against early embryonal tumors in these individuals. However, the sibling pair will have to be monitored for hematopoietic abnormalities, FA related cancers, and HBOC cancers as adults. In the future, diagnosis and classification as FANCD1/BRCA2 complementation group should also be considered for patients appearing with FA-like syndrome.

Chapter 4: Novel bone marrow failure and DNA repair deficiency syndrome

4.1 Introduction

Bone marrow failure (BMF) occurring during childhood is frequently genetic while BMF arising later in life is more often acquired. The most common inherited causes of aplastic anemia are Fanconi anemia (FA), Dyskeratosis congenita (DKC), Diamond Blackfan anemia (DBA), and Shwachman-Diamond syndrome (SDS) (Alter, 2017). DKC is the result of defects in telomere homeostasis and DBA and SDS are a result of defects in ribosome biogenesis. All three disorders are also associated with an increase in hematopoietic malignancies and solid tumors (Alter, 2002; Khincha and Savage, 2013). Diagnostically FA can be distinguished from other BMF syndromes by chromosomal breakage analysis. However, somatic mosaicism can skew breakage results and false positive results can occur in cases of other chromosomal instability syndromes (Oostra et al., 2012). FA is a very heterogeneous disorder and as a consequence of overlapping clinical features with BMF and chromosomal instability syndromes, patients may be misdiagnosed. Our studies have identified an individual enrolled in the IFAR misdiagnosed with FA. The characterization of patient derived cells indicated proficient ICL repair, but a deficiency in response to replication stress, not previously described in a genetic syndrome.

4.2 Results

4.2.1 A patient enrolled in the International Fanconi Anemia Registry identified as non-FA

An individual enrolled in the IFAR without known disease-causing mutations presented at 5 years of age with recurrent pneumonia and was discovered to be

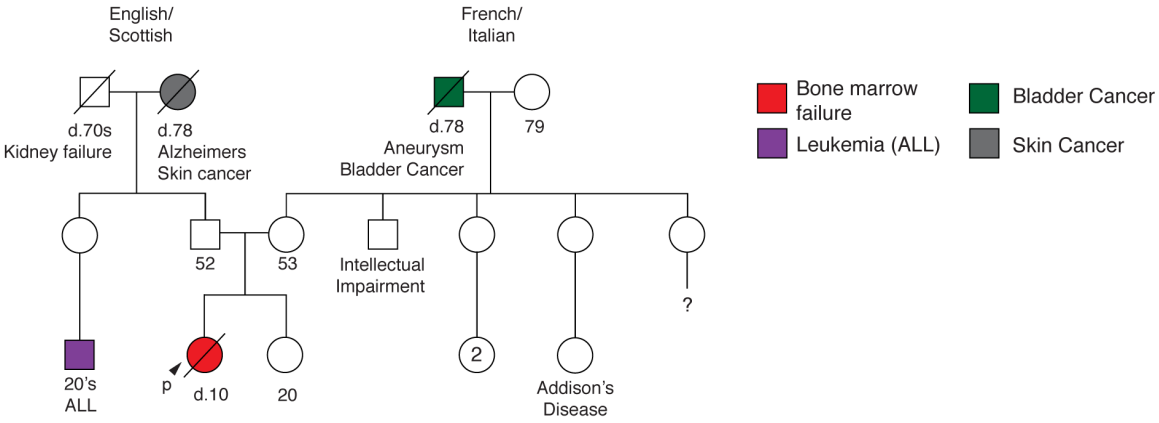

Figure 4.1 Bone marrow failure in a non-Fanconi anemia family enrolled in the IFAR.

Family pedigree showing a child with bone marrow failure diagnosed at 5 years old. The patient had two failed bone marrow transplants and died after complications of the second transplant. Family history is significant for a first cousin that was diagnosed with acute lymphoblastic leukemia (ALL) at 4 years old who was treated, and is currently alive and well. Maternal grandmother had history of skin cancer and paternal grandfather had history of bladder cancer. There was no history of FA.

pancytopenic. On exam, the patient was described as having short stature, small midface, microopathalmia, and café-au-lait spots. Birth history reported a normal full-term pregnancy without complication and a birth weight of 6lbs 4oz (25^{th} percentile). The patient had no history of myelodysplasia or leukemia and bone marrow studies only reported hypocellularity.

Two subsequent DEB-induced chromosomal breakage tests on peripheral blood showed mildly elevated breakage, 0.54 and 0.61 breaks per cell. These values are higher than normal but much lower than expected for a typical FA patient. The patient was presumed to have FA with somatic mosaicism to account for the low chromosomal breakage levels. There was no family history of FA, but a first cousin was diagnosed with leukemia (ALL) at 4 years of age (Figure 4.1). The maternal grandmother had a history of skin cancer and paternal grandfather had history of bladder cancer. The family denied consanguinity.

The patient underwent bone marrow transplant (BMT) at 8 years old with a FA conditioning regimen of fludarabine and cyclophosphamide which ultimately failed. A second transplant with the same donor was performed with the addition of total body irradiation (TBI) to the regimen. The second transplant failed and the patient developed graft versus host disease (GVHD). The patient developed encephalopathy, Parkinsonian features, congestive heart failure, respiratory failure, and died at 10 years of age.

4.2.2 Characterization of patient derived cells reveals no defects in ICL repair

Bone marrow failure can have many etiologies so to better characterize the presumed defect in ICL repair in this family, patient derived fibroblasts were analyzed. Unlike typical FA cells, the patient derived fibroblasts (RA2177) were not sensitive to the crosslinking agents MMC or cisplatin and did not show increased chromosomal aberrations upon treatment with DEB (Figure 4.2A-C). Clinical breakage analysis showed a mild increase in breakage to DEB, but our analysis of chromosomal breakage in LCLs from the proband (RA2143) and family (father, mother, and healthy sibling) does not show an increase above normal cells (Figure 4.2D-E). The patient cells do not show the hallmark LCL sensitivity and chromosomal breakage of FA. The lack of ICL repair deficits in the patient derived fibroblasts indicates that the patient does not have FA.

To investigate whether the patient's disease may be due to defects in DNA repair of other pathways, the cells were tested for hypersensitivity to other DNA damaging agents. Patient cells did not show increased sensitivity to IR (Figure 4.3A) suggesting no defect in the NHEJ pathway of DSB repair. Additionally, the patient cells did not show a significant increase or decrease in SCEs compared to BJ wild type fibroblasts suggesting no defect in HR or deficiency of BLM helicase (Figure 4.3B). The patient RA2177 fibroblasts were sensitive to a number of replication stress inducing agents including CPT, olaparib (PARPi), HU, and aphidicolin (Figure 4.4C-F). These data demonstrate that the patient's disease may result from defects in the cellular response to replication stress. Defects in HR

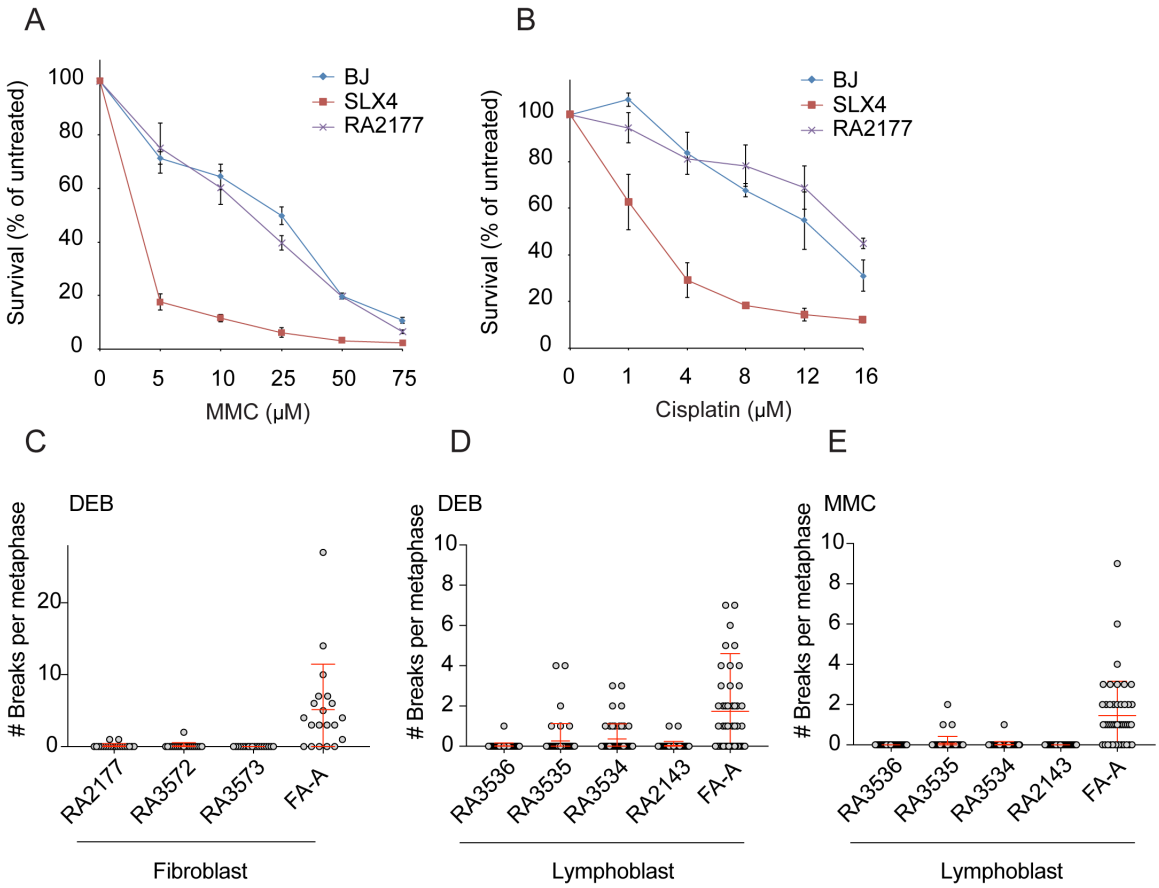

Figure 4.2 RA2177 fibroblasts do not display features of ICL repair defects.

(A-B) MMC and DEB treated cell survival assays of RA2177 patient fibroblasts, WT BJ fibroblasts, and *SLX4* patient fibroblasts (SLX4^{mut}). (C) Quantification of chromosomal breaks in metaphases of DEB treated RA2177, parental (RA3572, RA3573), and *FANCA* deficient (FA-A) fibroblasts. (D-E) Quantification of chromosomal breaks in metaphases of DEB treated LCLs from the proband (RA2143), parents (RA3534, RA3535), and *FANCA* deficient (FA-A) cells. Error bars indicate s.d.

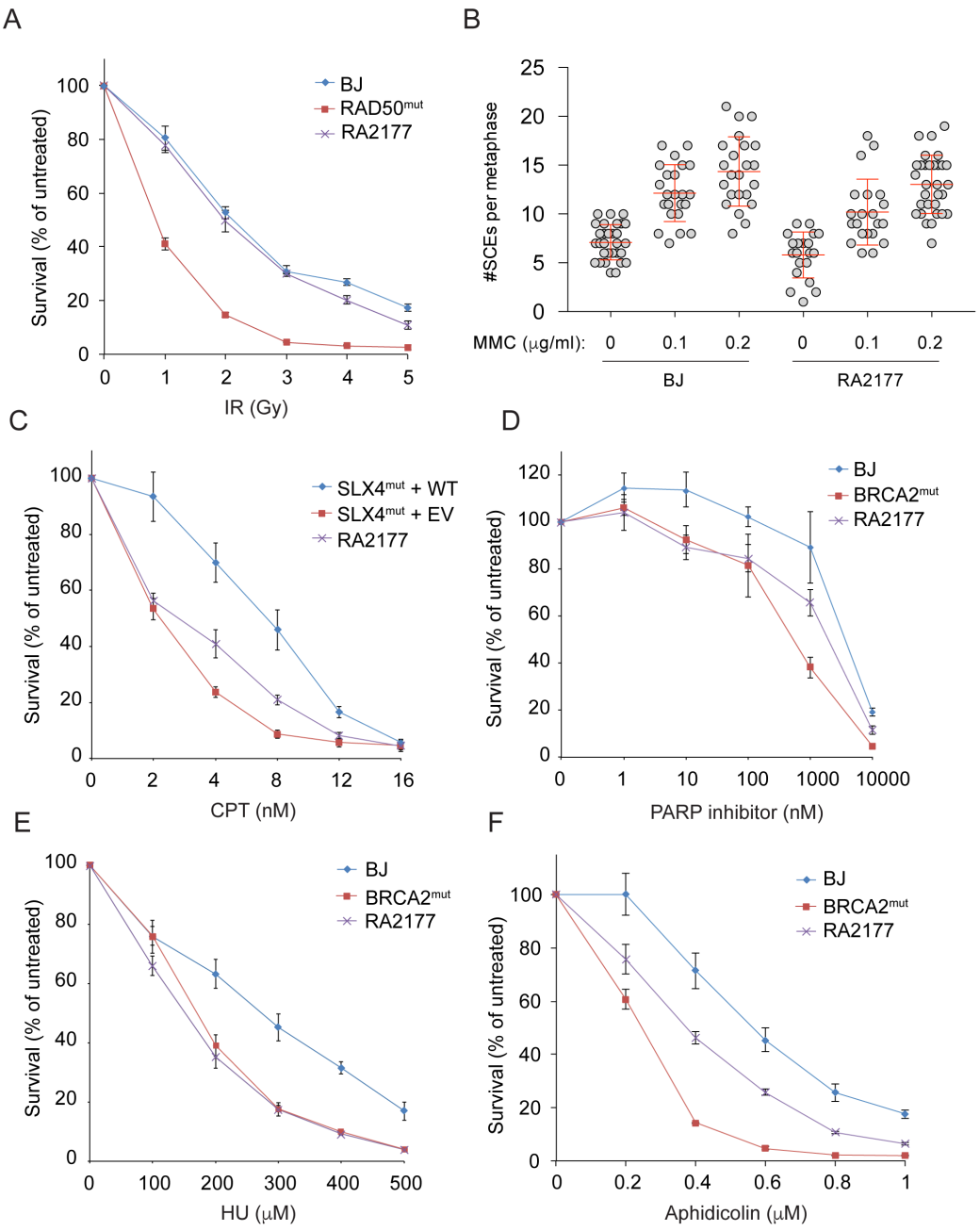

Figure 4.3 RA2177 fibroblasts are hypersensitive to replication stress inducing agents

(A) Cell survival of RA2177 cells after IR compared to *RAD50* patient fibroblasts ($RAD50^{mut}$). (B) SCE assay in BJ WT fibroblasts and RA2177 fibroblasts following treatment with MMC (0.1 μg/ml or 0.2 μg/ml). (C-F) Cell survival of RA2177 cells after CPT, olaparib (PARPi), HU, and aphidicolin treatment. $SLX4^{mut}$ and $BRCA2^{mut}$ are FA patient control cell lines. Error bars indicate s.d.

can also result in sensitivity to these agents, but HR is also required in the later steps of ICL repair and similar cellular sensitivity would then be expected for ICL generating agents which was not observed (Figure 4.2A-B).

Fibroblasts derived from the proband's parents were obtained to evaluate for similar defects. The parental fibroblasts (RA3572 and RA3573) behaved as wild type and were not sensitive to replication stress inducing agents (Figure 4.4A-D). The fibroblasts were tested for chromosomal breakage following treatment with HU and aphidicolin. The patient RA2177 cells displayed a significant increase in chromosomal breakage compared to BJ wild type fibroblasts and parental fibroblasts (Figure 4.4E-F). Analysis of LCLs derived from the proband also demonstrated sensitivity to HU and CPT suggesting no somatic mosaicism of the blood (Figure 4.5A-B).

4.2.3 Analysis of DNA replication in RA2177 cells reveals abnormalities only under conditions of replication stress

Given the hypersensitivity of RA2177 cells to replication stress inducing agents, we wanted to investigate the replication dynamics in these cell on the single molecule level. To visualize *in situ* replication dynamics, DNA combing of patient and parental cells grown in the presence of replication stress inducing agents (hydroxyurea or aphidicolin) was performed (Figure 4.6). For DNA combing analysis, DNA was labeled in replicating cells with the nucleotide analogs IdU and CldU and then immunostained for visualization. RA2177 cells have replication

speeds that are similar to those of parental cell lines, RA3572 and RA3573, under unperturbed conditions (Figure 4.6B). RA2177 cells have slowed replication compared to parental cell lines under conditions of replication stress induced by low dose HU or aphidicolin (Figure 4.6C-D). To test the ability of RA2177 cells to resume replication following replication fork stalling, cells were treated with high dose HU (2 uM) to stall progressing forks. HU was then washed out and resumption of replication was monitored by incorporation of CldU. RA2177 cells did not have increased levels of fork stalling as measured by analysis of IdU and CldU labeled DNA fibers (Figure 4.7A-C). However, in RA2177 cells, CldU:IdU ratios were lower, indicating that CldU tracks after HU were shorter. It is possible that in RA2177 cells the replication forks are able to recover from replication stalling but the recovery or the ensuing replication may be slower (Figure 4.7D). These data demonstrate that unperturbed replication is normal in RA2177 cells but under conditions of replication stress it is defective

4.2.4 Genetic analysis and evaluation of candidate disease-causing genes

The analysis of the patient-derived cell lines links a defect in cellular response to replication stress to the patient's disease. Previously described diseases, including Fanconi anemia and Dyskeratosis congenita, link genome instability and bone marrow failure like in this patient. Both fibroblasts and LCLs were equally susceptible to replication stress demonstrating the genetic cause to likely be germline and not somatic. WES was analyzed for gene candidates from the family trio. WES data revealed no mutations in known FA genes or genes

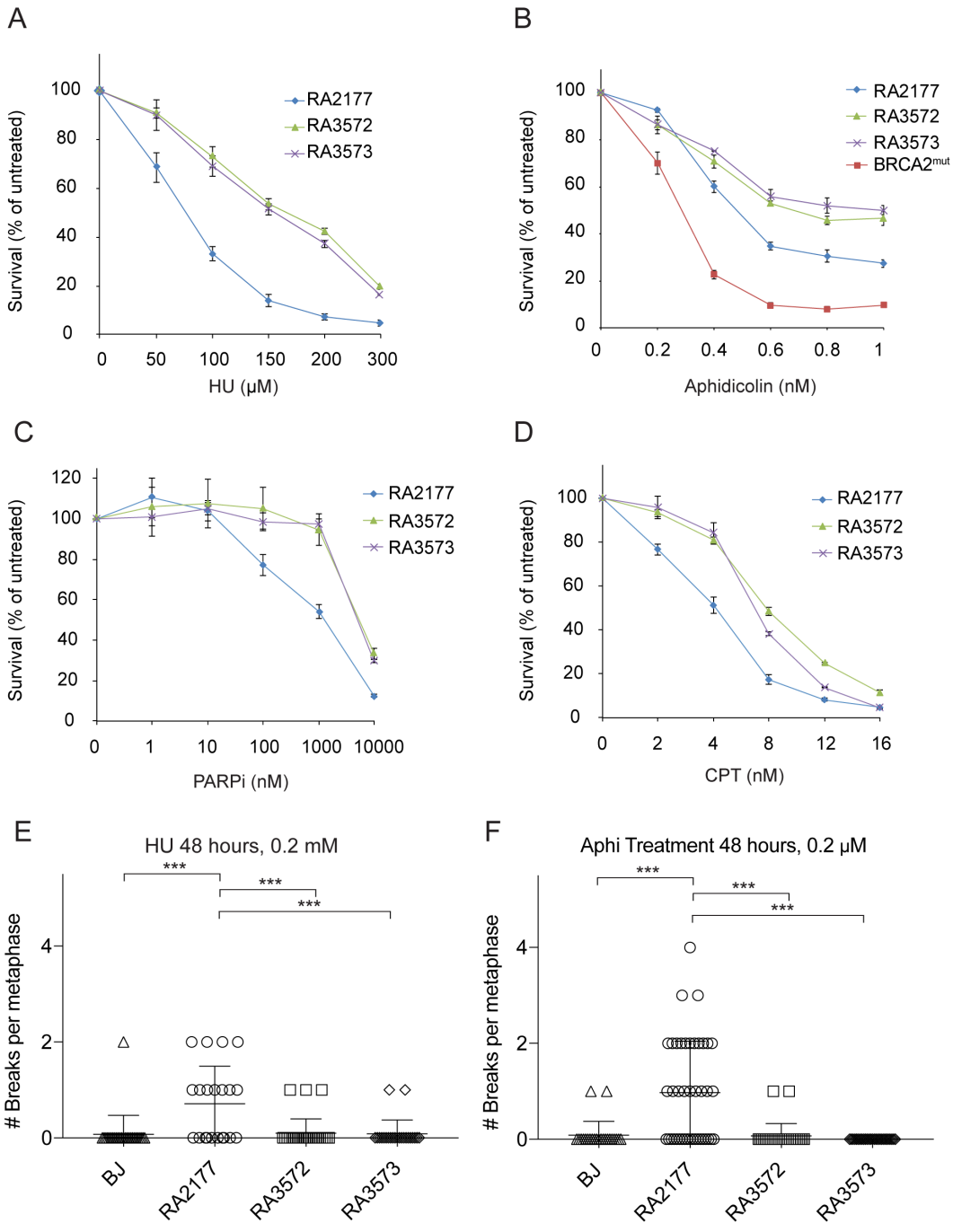

Figure 4.4 Parental fibroblasts behave as wild type.

(A-D) Cell survival of RA2177 fibroblasts and parental fibroblasts, RA3572 and RA3573, after HU, aphidicolin, olaparib (PARPi), and CPT treatment. (E-F) Quantification of chromosomal breaks in metaphases of HU and aphidicolin treated BJ, RA2177 (proband), RA3572 (paternal), and RA3573 (maternal) fibroblasts. Error bars indicate s.d.

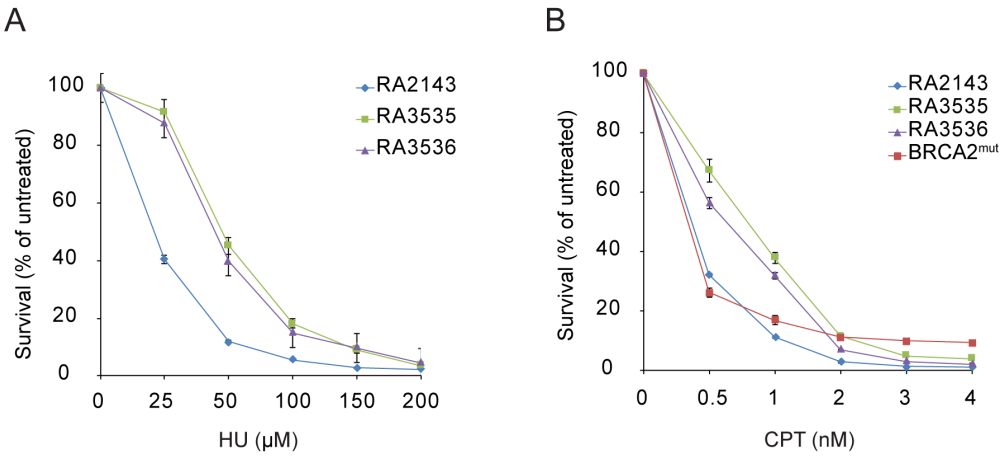

Figure 4.5 RA2143 patient LCLs display hypersensitivity to replication stress.

(A-B) Cell survival of RA2143 patient derived LCLs and parental LCLs (RA3535 and RA3536) after HU and CPT treatment. Error bars indicate s.d. Assays performed by Sonia Singh.

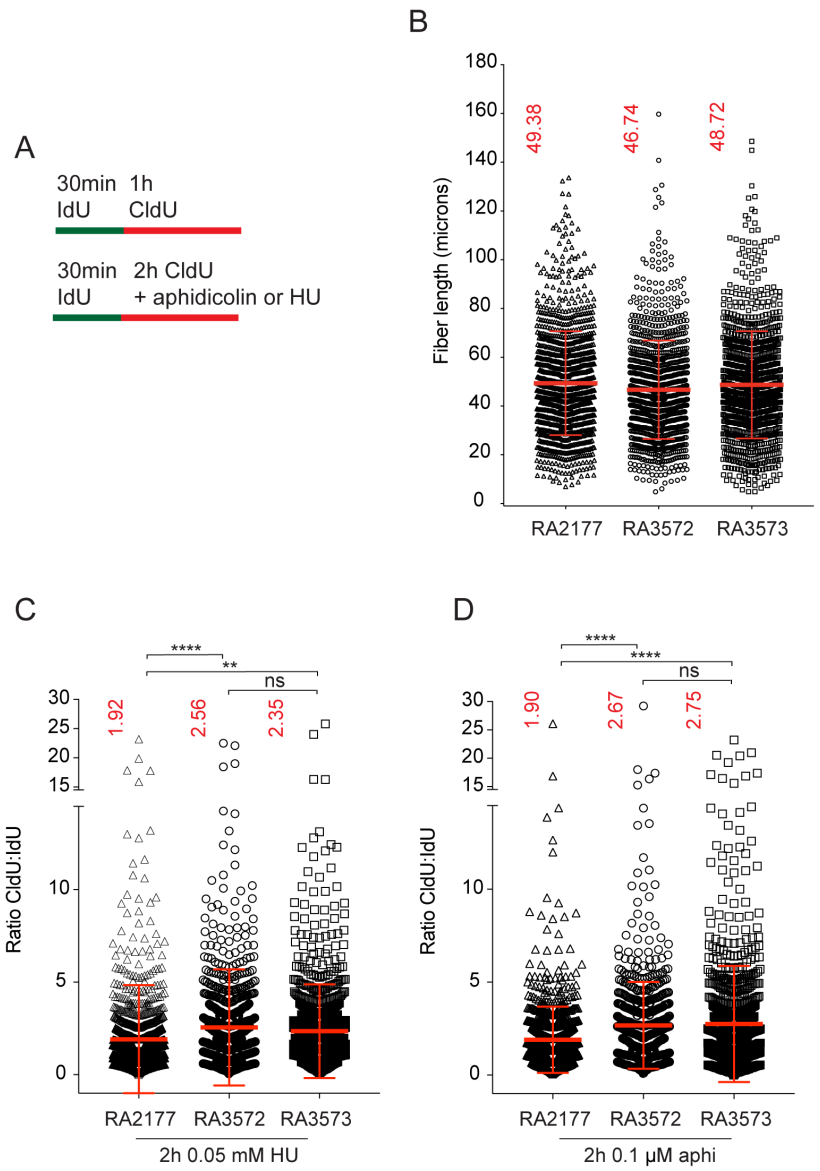

Figure 4.6 Assessment of replication fork progression in RA2177 cells under conditions of replication stress.

(A) Schematic of experimental conditions. Cells were labeled with nucleotide analogs Idu and CldU and DNA fibers were immunostained and visualized. (B) Average DNA fiber lengths in RA2177 patient cells and wild type parental cell lines RA3572 and RA3573. Total DNA track length was measured after 30min of IdU and 1h of CldU treatment. (C-D) Ratio of CldU:IdU DNA track lengths. Cells were labeled with IdU for 30 mins and subsequently with CldU for 2h with HU or aphidicolin. Error bars indicate s.d.

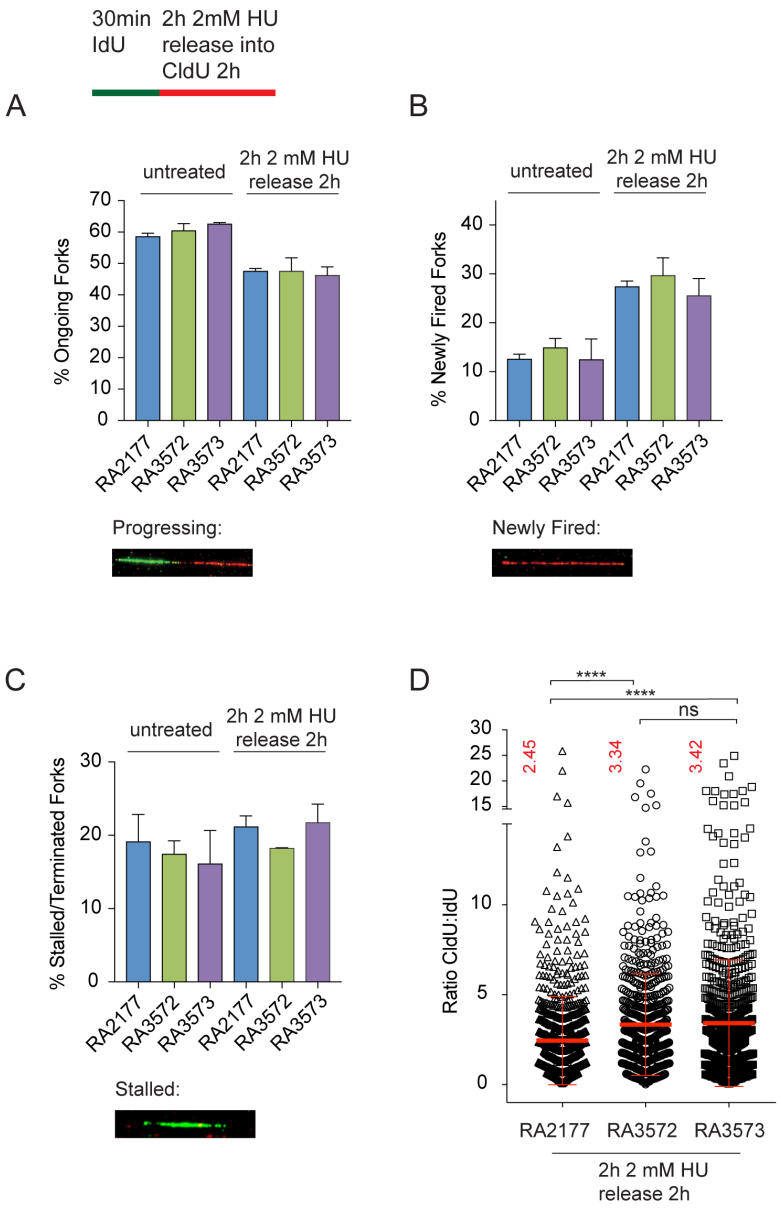

Figure 4.7 Assessment of replication fork dynamics in RA2177 patient cells.

(A) Cells were labeled with IdU for 30 mins and subsequently treated with 2 mM HU to stall replication forks for 2 hours. Cells were washed and released into CldU for 2 hours. Quantification of ongoing replication forks, characterized as having both IdU and CldU label, as a percent of all DNA species. (B) Quantification of newly fired replication forks, characterized as CldU only. (C) Quantification of stalled or terminated replication forks, characterized as IdU only. (D) Ratio of CldU:IdU DNA track lengths. Error bars indicate s.d.

mutated in known DNA repair disorders. Variants were filtered for an allele frequency of 0.01 or less in the 1000 Genome database. Possible modes of inheritance that were prioritized were autosomal recessive and *de novo*. The family reported non-consanguinity.

No LOF *de novo* mutations were identified. One coding *de novo* missense mutation of sedoheptulokinase (*SHPK*) was identified; however, a second mutation was not identified and homozygous LOF has previously been described in isolated Sedoheptulokinase deficiency and infantile nephropathic cyctinosis that includes a 53kb deletion encompassing *SHPK* (Wamelink et al., 2015). No LOF or missense homozygous coding variants of rare allele frequency in genes that could be linked to the phenotype were identified. Compound heterozygous mutations, p.R206H and p.A466T, in *PFAS* were identified having an allele frequency less than or equal to 0.01 in 1000 Genome database (0.01 and 0.002, respectively) and CADD scores of 25.4 and 31. Each parent is a carrier of one allele and the healthy sibling only carries one variant (Figure 4.8A). We decided to pursue this as a candidate gene as PFAS is important for the 4th step of *de novo* purine synthesis. Purines are necessary for cellular processes such as DNA replication, transcription, and energy metabolism. Disorders of nucleotide metabolism have previously been described and have a heterogeneous clinical spectrum that includes immunodeficiency and anemia (Ng et al., 2015; Ng et al., 2010; Rainger et al., 2012; Roach et al., 2010; Stone et al., 1992).

Depletion of *PFAS* in BJ WT fibroblasts results in cellular sensitivity to HU and CPT similar to RA2177 fibroblasts (Figure 4.8C-E). Complementation of patient RA2177 fibroblasts by expression of wild type *PFAS* was complicated by toxicity and increased hypersensitivity resulting from overexpression of the protein (Figure 4.8B). To test *PFAS* variants for pathogenicity, CRISPR/Cas9 gene editing was used to knock in the p.A466T mutation at the endogenous locus in the maternal cell line RA3573, so that the protein is expressed at levels regulated by the cell (Figure 4.8E). Homozygous p.A466T RA3573 cells were tested for hypersensitivity to HU and the homozygous mutation did not produce the cellular hypersensitivity seen in the proband's RA2177 cell line (Figure 4.8F). These data demonstrate that the *PFAS* variants are not responsible for the defect in this patient's cells and are unlikely to have caused her disease.

Whole genome sequencing (WGS) on DNA derived from primary fibroblasts obtained from the mother, father, and proband was performed. Thus far, no additional gene candidates were identified using a 0.001 allele frequency cut off for coding variants in the Exome Aggregation Consortium (ExAC) with CADD scores greater than the mutational significance cutoff (MSC) (Itan et al., 2016). Further analysis of WGS will permit a more comprehensive investigation of copy number and non-coding variants that may be disease-causing.

Figure 4.8 *PFAS* variants do not cause the cellular defects to replication stress in RA2177 patient cells

(A) Chromatograms of Sanger sequencing of *PFAS* variants identified in this family, exon 6 p.R206H and exon 12 p.A466T. (B) CPT treated cell survival assays of patient RA2177 cells expressing empty vector (EV) control and HA tagged WT PFAS compared to WT BJ fibroblasts. (C-D) HU and CPT treated cell survival assays of WT BJ fibroblasts with *PFAS* targeting shRNAs (1 and 2) and shRNA control (shCONT.) compared to RA2177 cells. (E) Validation of shRNA knockdown of *PFAS* in BJ WT cells by RTqPCR. (F) Chromatograms of Sanger sequencing of CRISPR/Cas9 edited RA3573 fibroblasts (maternal cell line) containing the exon 12 p.A466T mutation. (G) Cell survival assay of RA3573 clone homozygous for exon 12 p.A466T mutation compared to RA2177 cells. Error bars indicate s.d.

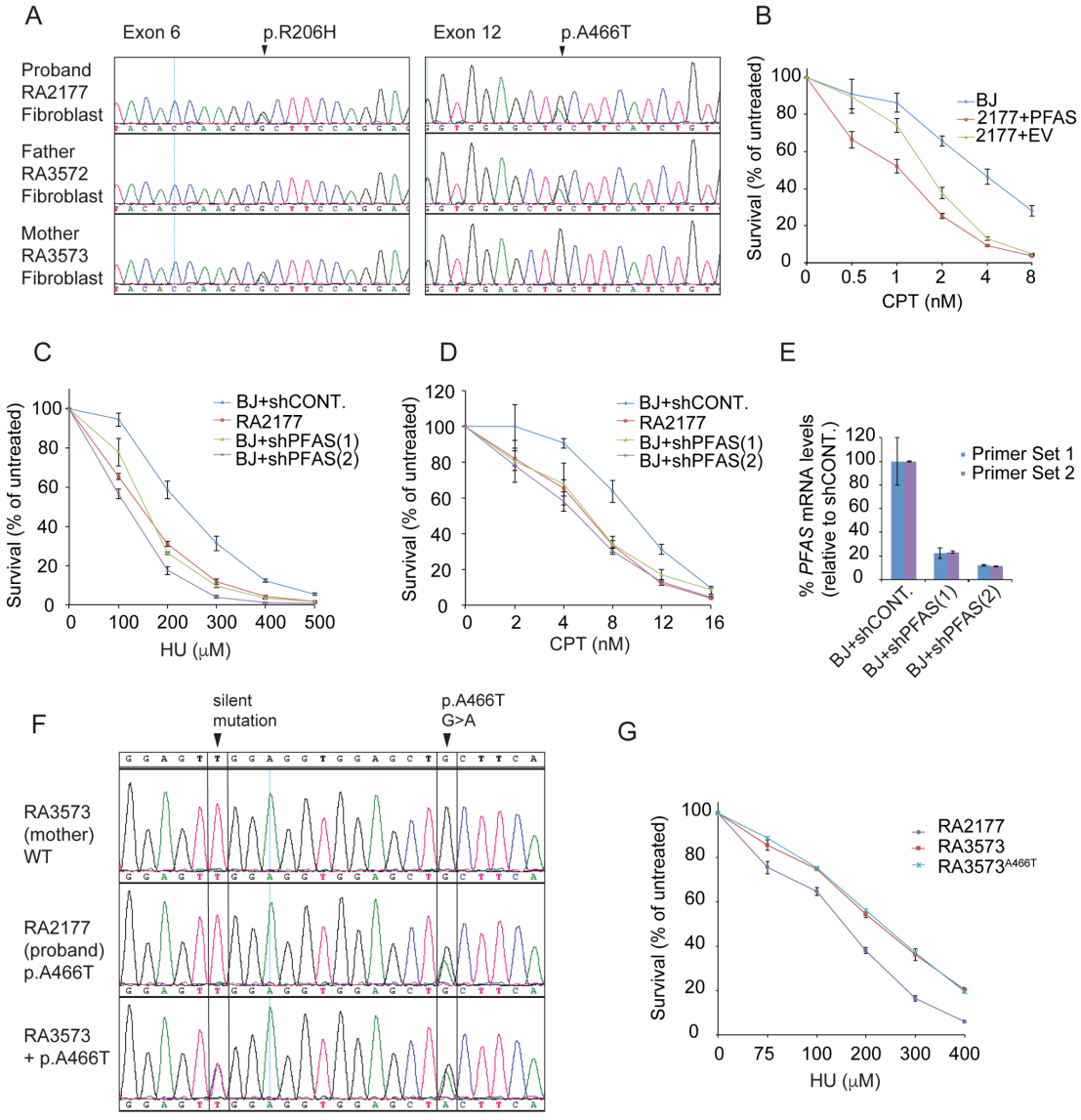

4.3 Summary and Conclusions

Here we describe an individual with proficient ICL repair but defects in cellular response to replication stress. The patient's clinical picture had many overlapping features of FA including developmental abnormalities and BMF in childhood. DEB chromosomal breakage testing is the gold standard for FA diagnosis, but in some instances a mild increase in breakage can be observed due to another chromosomal instability syndrome (Oostra et al., 2012). Another explanation for lower breakage levels in the blood in FA is somatic mosaicism, which was the conclusion for this individual at the time of diagnosis. Examination of patient derived cells, LCLs and fibroblasts, demonstrates no defects in ICL repair. Fibroblasts from FA patients with somatic mosaicism display the typical hallmarks of ICL deficiency, so this individual does not have FA. The failure of bone marrow transplant in this individual may have been in part due to modified conditioning protocol typically used for FA patients.

Patient-derived fibroblasts, RA2177, are hypersensitive to PARP inhibitor, CPT, aphidicolin, and HU and display elevated chromosomal breaks following HU or aphidicolin, suggesting a defect in resolving replication stress. Replication stress, if not resolved, can cause replication fork collapse and DNA double strand breaks that are repaired by homologous recombination (HR) mediated double strand break repair (Lundin et al., 2002). RA2177 cells do not display hypersensitivity to double strand breaks induced by ionizing radiation (IR) and have normal levels of homologous recombination as measured by sister chromatid

exchange levels (SCE) suggesting proficient HR and double strand break repair (Sonoda et al., 1999). This is also consistent with proficient ICL repair that requires HR mediated DSB repair. Single molecule analysis of replication forks demonstrates that the RA2177 cells replicate at normal speeds when not perturbed, but are significantly slower during conditions of replication stress and recover from replication fork stalling more slowly than parental control cell lines.

These studies help us to better understand what cellular processes may be defective in this individual and suggest that defects in the cellular response to replication stress may underlie disease in this individual. In cases where breakage analysis of peripheral blood is inconclusive and disease-causing mutations are not known, analysis of fibroblasts should be performed to support a FA diagnosis. In this case, a diagnosis of FA had implications for treatment and impacted the choice of the bone marrow transplant regimen. Fludarabine is a purine analog, that like HU, inhibits DNA synthesis by causing a shortage of nucleotides (Montillo et al., 2006). Whether RA2177 cells are hypersensitive to fludarabine still needs to be investigated, but given the similar mechanism of action to HU it seems likely. The patient cells are sensitive to replication stress so the use of this drug as a conditioning regimen may have contributed to the patients decline and multi organ failure.

The investigation into the genetic cause of disease in this individual is ongoing. Analysis of WES yielded candidate disease-causing variants, compound

heterozygous missense mutations in *PFAS,* but after thorough investigation we conclude that the variants identified are not disease causing. WGS was performed on the family trio using fibroblast DNA to compare to our WES results, done on LCLs, in the event of somatic mosaicism and for better mutation detection (Belkadi et al., 2015). The more recently published Exome Aggregation Consortium (ExAC) and Genome Aggregation Database (gnomAD) are much larger gene variant databases that permit filtering patient sequencing data at a lower allele frequency without possibly removing rare variants (Lek et al., 2016). The WGS was analyzed using a MAF cutoff of 0.001 in ExAC to be consistent with rare disease incidence of pediatric bone marrow failure and FA (Young et al., 2008). No new gene candidates with biallelic coding variants were identified. Analysis of WGS will have to be expanded to copy number variants and non-coding regions of the genome. Identification of disease-causing variants in a single patient can be challenging, but here we have an ideal system in which a cellular phenotype has been identified and complementation can be used to rescue defects conferred by the defective gene. In this individual, the characterization of patient cells gives insight into potential gene candidates that can be explored further. In similar cases, concomitant cellular characterization, even in the absence of knowing the genetic origin of the disease, may improve disease management.

Chapter 5: Discussion

5.1 Investigating the genetic cause of disease in individuals not assigned to a Fanconi anemia complementation group

The International Fanconi Anemia Registry (IFAR) at the Rockefeller University has been enrolling patients since 1982 when it was established by Dr. Arleen Auerbach. The IFAR has numerous FA patient-derived cell lines and DNA samples archived, which presents the opportunity to investigate those patients enrolled in the registry without a designated FA complementation group. The studies described in this thesis evolved from the hypothesis that the patients without gene classifications may represent undiscovered FA complementation groups and thus, provide the opportunity to study new genes important for DNA interstrand crosslink (ICL) repair.

A key advantage of our study was the ability to search for the genetic cause of disease in several unclassified patients while simultaneously characterizing their patient-derived cell lines. The characterization of patient-derived cells from the families of interest, allowed for the patients to be classified into different subgroups. We were able to exclude some patients from further study, because, although they appeared to have FA, no DNA repair deficits were identified in their cell lines. Our understanding of the FA pathway was applied to further delineate the patients. A key step in the FA pathway is the activation of FANCI and FANCD2 by monoubiquitination, which requires an intact FA core complex, composed of 8 FA proteins and associated factors. Some of the cell lines we studied were defective for monoubiquitination of FANCI and FANCD2, so our genetic analysis could be

focused to core complex proteins and associated factors. With regards to this group, we identified the subject of the new FANCT complementation group as well as an individual of the already established FANCE complementation group.

Other individuals had normal activation of the FA pathway, but defective ICL repair. From this subgroup, the sibling pair with atypical presentation of biallelic *FANCD1/BRCA2* mutations was identified. We also followed a bone marrow failure (BMF) patient, whose analysis revealed no defects in ICL repair, but rather demonstrated defects in another DNA damage pathway that could underlie their disease. Collectively, in these studies we discovered a surprisingly wide spectrum of cellular phenotypes that provided insight for our genetic analysis. These studies resulted in the identification of a new FA complementation group, surprising separation of function mutations in an already known FA gene, and exclusion of some patients from FA.

Whole exome sequencing (WES) was performed on patient and parental DNA where available. We found that for some cases, the identification of candidate disease-causing mutations was more straightforward as rare coding mutations were identified in genes that could be linked to the phenotype and further validated. However, there are still significant challenges in identifying patient disease-causing mutations by Next-generation sequencing (NGS) because of the limitations in detecting structural and copy number variants (Boycott and Ardigo,

2018). For instance, WES analysis was not sufficient alone to ascertain the *UBE2T* patient mutations because the large paternal indel was not detected and the LCLs were mosaic for the maternal indel. We identified low UBE2T transcript levels in patient fibroblasts by RNAseq, which was supported by the absence of UBE2T protein by immunoblot. We utilized Sanger sequencing of the UBE2T locus to identify the mutations, which was aided by SNPs detected in the UBE2T locus by WES. Therefore, even though NGS has increased the pace at which rare genetic diseases can be identified and enables single patient studies, our study highlights some of the limitations of its application (Boycott et al., 2017; Casanova et al., 2014). We have demonstrated here that a multifaceted approach may be required to identify disease-causing mutations that are structural or copy number variants (CNV), or reside outside coding regions (Boycott et al., 2017; Casanova et al., 2014). Although WGS offers broader coverage of the genome and better SNP detection in coding regions, CNV and structural variant identification still remains unreliable (Boycott and Ardigo, 2018; Casanova et al., 2014). Non-coding variants identified in WGS are more problematic to interpret given their vast numbers and the difficulty in predicting their functional consequences. Moreover, current variant databases have much lower genome coverage than exome for precisely determining non-coding variant allele frequency (Lek et al., 2016).

In the case of the individual described in Chapter 4, with BMF of unknown genetic origin and cellular defects in responding to DNA replication stress, we will

have to expand our analysis of the WGS and employ other strategies to determine the genetic basis of their disease. With the development of new informatics tools, more information and annotations of non-coding genetic variants may be available to streamline WGS analysis. In the meantime, the clinical knowledge and cellular observations in this case can be applied to analyze the non-coding variants of potential candidate genes. We can consider various possibilities including the likelihood that the disease presentation and cellular phenotypes described may be the result of a novel disorder or alternatively, an atypical clinical presentation of a known disease. Our investigation going forward should include screening intronic regions of genes implicated in disorders with overlapping features.

Our knowledge of proteins at the replication fork during normal replication and conditions of stress are expanding. We can apply this data to identifying additional gene candidates. cDNA screening is another possible technique that we can employ to identify deficient genes. Patient cells can be transduced with a cDNA library and their pronounced cellular sensitivity to replication stress can be exploited in a competition screen to enrich for and identify the complementing cDNA (Buck et al., 2006). While the genetic cause of disease remains elusive in this individual, the cellular characterization provides information about potential pathways and genes that may be of interest for future investigation.

Identifying the genetic etiology of rare diseases is important for improving the understanding of the mechanism of DNA repair and how lack of repair results in abnormal function. It also aids in the classification of other affected individuals and leads to improved patient care. For example, our identification of the *FANCT* complementation group will permit the classification of FA patients to this complementation group in the future. Our analysis also demonstrates that complex copy number variants may occur at this locus and that besides sequencing, *UBE2T/FANCT* complementation may be necessary for classification. The clinical presentation of the *FANCT* patient identified in our study differed from two patients published in another parallel study (Hira et al., 2015; Rickman et al., 2015). Due to somatic mosaicism of the blood our patient was likely protected from bone marrow failure, but Hira *et al*. reported a case of bone marrow failure and AML in two *FANCT* individuals. Taken together, these cases give a clinical picture for the *FANCT* complementation group, and suggest that *FANCT* patients will likely present with typical FA and are susceptible to bone marrow failure.

The identification and analysis of the individuals with biallelic *FANCD1/BRCA2* mutations and their atypical presentation expands the phenotypic spectrum for this complementation group. These *FANCD1/BRCA2* patients have phenotypes that are akin to the FA-like complementation groups *FANCR/RAD51* and *FANCO/RAD51C* (Jacquinet et al., 2018; Vaz et al., 2010; Wang et al., 2015). Our findings highlight that in the future, patients with FA-like

disease features should also be screened for *BRCA2* mutations. The *FANCD1* complementation group also has implications for HBOC in carriers, so earlier molecular designation for these individuals is advantageous for preventative screening in the family.

5.2 *BRCA2* DNA binding domain mutations and implications for cancer

The analysis of individuals with atypical disease presentation of the *FANCD1/BRCA2* complementation group determined that their disease is due to mutations in the highly conserved *BRCA2* DBD. Interestingly, these patients presented with developmental defects seen in FA, but have no history of BMF or malignancy into adulthood (Alter, 2014; Howlett et al., 2002). We functionally analyzed their *BRCA2* DBD mutations, c.8524C>T, and c.IVS19-1G>A, to determine if the atypical patient phenotypes were a consequence of disturbing a specific function of BRCA2. In our studies, we observed that both mutations reduced HR efficiency by about half and that replication fork protection was defective at HU-stalled forks and ICLs.

Previously reported analysis of cDNA from HSC62 patient-derived cells, homozygous for the c.IVS19-1G>A mutation, revealed the mutation to cause aberrant splicing that results in a 4 aa deletion of exon 20 (Howlett et al., 2002). HSC62 cells were also reported to have moderately elevated chromosomal breakage, and taken together c.IVS19-1G>A was presumed pathogenic (Alter et al., 2007; Howlett et al., 2002). Our analysis, also confirmed these findings. By

complementing the homozygous c.IVS19-1G>A patient fibroblasts by CRISPR/Cas9 mediated genome editing, we have demonstrated that this mutation is indeed the cause of cellular defects and disease in this individual, proving this variant to be pathogenic. Recently c.IVS19-1G>A has also been reported to segregate with familial breast cancer (Santos et al., 2014).

The c.8524C>T mutation has previously been described as a variant of unknown significance (VUS) in HBOC. Many pathogenic LOF mutations of BRCA2 have previously been described that result in early termination of the protein. However, in BRCA HBOC genetic testing, approximately 1,600 unique VUS have been discovered and they account for 2-10% of all variants identified during testing (Guidugli et al., 2014). The clinical significance of these rare missense mutations is unclear and often, familial information is limited, so variant segregation cannot be determined. Evaluation of many BRCA2 VUS relies on multifactorial probability models to estimate if a variant is pathogenic (Guidugli et al., 2014). *In vitro* analysis of BRCA2 VUS function is an alternative approach to determine potential pathogenicity. Functional assays have traditionally assessed HR through reporter assays by measuring HR mediated repair of DSBs in reporter constructs (Moynahan et al., 2001). Several studies have utilized the V-C8 *Brca2* deficient hamster cell line or mouse embryonic stem cells to assess HR of BRCA2 VUS by the DR-GFP assay (Farrugia et al., 2008; Guidugli et al., 2014; Guidugli et al., 2013; Wu et al., 2005). Additional studies have used other functional readouts of

BRCA2 VUS including ssDNA binding assays, nuclear localization, centrosome amplification, and MMC or PARP inhibitor cell survival (Guidugli et al., 2014).

A large number of *BRCA2* DBD mutants, including c.8524C>T, were analyzed for HR proficiency in V-C8 cells using the DR-GFP assay. The pathogenicity of the VUS were predicted by comparing their HR efficiency to that of known pathogenic and benign variants in this study (Guidugli et al., 2013). Some VUS can be easily classified if HR is dramatically reduced; however, a number of VUS including c.8524C>T showed intermediate phenotypes in this evaluation, making it difficult to interpret their role in HBOC (Guidugli et al., 2013; Shimelis et al., 2017).

One caveat of these studies is that they only consider the HR function of BRCA2 for pathogenic classification. The contribution of other BRCA2 functions, including replication fork protection, to cellular function and tumorigenesis requires further investigation. In our system, the c.8524C>T mutant did have a moderate impact on HR, but we also demonstrate additional deficiency in replication fork protection. The consequences of loss of replication fork protection in c.8524C>T cells is still unclear given the observation that this mutant does not show a significant increase in chromosomal breakage after replication fork stalling by HU. Predicting VUS pathogenicity only in the context of HR efficiency does not give a complete picture for all of the functions of BRCA2. It is important to further

understand the full spectrum of BRCA2 functions and how each might contribute to genomic instability and tumorigenesis. This determination is essential to gain a better understanding of how HBOC cancers arise and to make more confident predictions about the outcome of patient mutations.

The individual with homozygous c.IVS19-1G>A mutations is deceased due to causes unrelated to FA, but they were not reported to have acquired malignancy to the age of 30. We note that the *FANCD1/BRCA2* sibling pair will have to be screened for FA related cancers and HBOC. These patients seem to have been protected from early embryonal cancers, which we hypothesize to be due to sufficient HR activity of the hypomorphic BRCA2 alleles expressed in their cells. However, it is unclear whether these patients will be predisposed to squamous cell carcinoma (SCC) because the majority of FANCD1 patients develop early childhood malignancy long before SCCs are diagnosed in FA. SCCs in FA are generally diagnosed in adulthood with a median age of 30, therefore the patients should be screened regularly for these malignancies because of their cellular defects in ICL repair (Kutler et al., 2016). HBOC cancer risk may be especially high for these individuals in adulthood because they have biallelic *BRCA2* mutations, one of which (c.2330dupA) is already reported to predispose to HBOC. There is insufficient evidence for whether the c.8524C>T variant predisposes to HBOC in this family, but it is deleterious in terms of BRCA2 function, and causes FA in the context of biallelic mutations. The father is a carrier of the c.8524C>T mutation and

developed early onset colorectal cancer, which may have been related to his carrier status (Degrolard-Courcet et al., 2014b; Garre et al., 2015; Phelan et al., 2014). However, the father's tumor was not assessed to determine *BRCA2* status.

5.3 Defective replication fork protection at ICLs and HU-stalled forks

We have examined the requirement of the BRCA2 DBD for replication fork protection in the context of HU- and ICL-stalled replication forks. By studying the BRCA2 DBD mutant cell lines, we determined some differences in how cells respond to replication forks stalled by HU versus at ICLs. In this analysis, it was determined that replication fork protection of HU stalled forks is as much dependent on the BRCA2 DBD as the C-terminal RAD51 interacting domain. Similar to previously published studies, the nascent strand degradation at HU stalled replication forks in our *BRCA2* DBD mutant cells is rescued by inhibition of nucleases or by inhibiting replication fork reversal by the depletion of fork remodelers, SMARCAL1, ZRANB3, or HLTF (Lemacon et al., 2017; Mijic et al., 2017; Schlacher et al., 2011; Taglialatela et al., 2017). We found that by comparison, depletion of these fork remodelers does not rescue the increased ssDNA generated at ICLs and their deficiency does not sensitize wild type cells to MMC. These observations, suggest that fork reversal is not an important intermediate in the repair at ICLs.

We note that when interpreting results, we have to keep in mind that cells respond differently to treatment with HU and MMC making some direct

comparisons of DNA fiber analysis after HU and MMC difficult. Here we looked at single molecule DNA fiber analysis of HU stalled replication forks to measure nuclease resection. At the dose of HU used for these investigations, all of the replication forks are prohibited from replicating due to nucleotide depletion in both WT and *BRCA2* mutant cells. Using DNA fibers to study replication fork resection in MMC treated cells has been confounding because MMC does not globally stall all forks even at high concentrations (Kehrli and Sidorova, 2014 and data not shown). This would be consistent with replication forks stalling as a result of collision with an ICL; while other replication forks that do not encounter a DNA lesion, continue replicating. It is also possible, that in a FANCM dependent manner, some replication forks bypass the ICL, and are also able to keep replicating (Huang et al., 2013).

The next steps to investigate processing of ICLs specifically, would be to utilize the ICL generating agent trimethylpsoralen, tagged with digoxigenin (Dig-TMP), that can be detected by immunolabeling of DNA fibers (Huang et al., 2013). We hypothesize that by using this method our analysis could be limited to those replication forks that have encountered ICLs. A similar strategy could also be applied to EM studies if TMP was detected with an appropriate probe. By EM analysis ssDNA can be detected and measured at replication forks based on the differences in the width of the DNA molecules (Vindigni and Lopes, 2017). We predict that with these experimental approaches, the replication fork structures and

genetic requirements of nucleases and helicases for resection at ICLs can be examined in FA/BRCA pathway defective cells.

5.4 Implications of defective replication fork protection

As discussed in detail in the introduction, rescue of replication fork protection in BRCA2 deficient cells has been observed by depleting factors that either promote MRE11 association with the fork or prevent replication fork reversal. As an essential gene, the HR function of BRCA2 has traditionally been viewed as its critical activity for cell viability. Deficiency of PARP1 is reported to prevent degradation of stalled replication forks and genomic instability by preventing MRE11 recruitment (Bryant et al., 2009; Ding et al., 2016; Ray Chaudhuri et al., 2016; Ray Chaudhuri et al., 2012). A recent study reported that PARP1 or PTIP deficiency rescues lethality of *BRCA2* knockout mouse embryonic stem cells (mESC), which was attributed to restoration of fork protection (Ding et al., 2016; Ray Chaudhuri et al., 2016). However, in another system, MCF10 epithelial cells, *PARP1* knockout does protect against nascent strand degradation, but it does not rescue viability of *BRCA2* null cells (Feng and Jasin, 2017). Moreover, cells expressing the *BRCA2* S3291E/A fork protection mutant show defects in fork protection similar to losses incurred by *BRCA2* LOF or depletion, but do not have the marked hypersensitivity or breakage phenotype to DNA damaging agents (Schlacher et al, 2011; Feng and Jasin, 2017). These reported findings, along with our data, converge on the central question of what are the specific consequences of the loss of replication fork protection on viability, cellular function, and genomic

instability. There needs to be further investigation to determine how this function specifically contributes to the process of tumorigenesis and later chemoresistance.

In our analysis, we observed that increased chromosomal breakage after HU-mediated replication fork stalling, does not underlie replication fork resection. Stalled replication forks in BRCA2 c.8524C>T and p.S3291A cells undergo resection by MRE11, but do not have elevated levels of chromosomal breakage as a result. BRCA2 c.IVS19-1G>A mutant cells however, have a mild increase in breakage and cells expressing truncated BRCA2 show a large increase in breakage that is MRE11 dependent. We speculate that it is possible that c.8524C>T and p.S3291A BRCA2 are functionally able to prevent breaks at the stalled replication forks or alternatively, these mutants retain enough HR function to repair breaks that do arise. The majority of BRCA2 replication fork protection studies have been done in the context of BRCA2 knockdown using siRNAs, so the reported chromosomal breakage cannot be attributed to only deficiency of replication fork protection, because the cells would also be deficient for HR. It is already known that DSBs can arise from replication fork collapse as a result of HU treatment. In the context of BRCA2 deficiency or LOF, the absence of replication fork protection may further precipitate fork collapse that cannot be properly repaired due to the concomitant loss of HR function.

Further investigation is needed to fully determine the consequences of the loss of BRCA2 replication fork protection function. It is possible that there is another mutagenic process occurring at replication forks in the context of defective replication fork protection other than chromosomal breakage. The recent study of replication through the *Escherichia coli* Tus/Ter replication fork barrier complex in mouse cells demonstrates that BRCA2 suppresses long tract gene conversions at stalled forks (Willis et al., 2014). How exactly the different functions of BRCA2 converge to prevent gene conversion at replication forks needs further investigation. The BRCA2 mutants that we have identified may be helpful in parsing out whether this function relies on replication fork protection, HR, or both. It will be interesting to investigate whether fork protection mutants have an increase in mutations or gene conversion events at the sites of stalled forks. This would give insight into the outcome of these resection events and would help clarify how different defects in BRCA2 may contribute to genomic instability.

In the context of cancer cells, replication fork protection might play a more significant role for chemoresistance. Alterations in a number of proteins already discussed, restore fork protection (without restoring HR activity) by precluding nuclease recruitment or access to DNA. Analysis of *BRCA2* ovarian cancers, with low PTIP or CHD4 expression had poorer prognosis, which hints at a potential mechanism of restoration of fork protection in these tumors (Guillemette et al., 2015; Ray Chaudhuri et al., 2016). Similarly, low levels of SMARCAL1 also

correlated with poor prognosis in BRCA1 breast cancer (Taglialatela et al., 2017). In BRCA2 ovarian cancers, low EZH2 levels were associated with worse prognosis (Rondinelli et al., 2017). Taken together these studies link restorations of replication fork protection with the development of chemoresistance in BRCA1/2 deficient cancers; however, validation of the mechanism conferring chemoresistance in these cancers warrants further investigation. It would be interesting to know if specific loss of replication fork protection results in increased breakage in cancer cell lines or if this occurs only with BRCA2 LOF. It is possible that BRCA2 replication fork protection might play a more important role in the context of cancers where replication fork reversal may be deregulated and oncogenic stress or chemotherapy agents might be driving increased fork reversal activity (Neelsen et al., 2013)

5.5 Concluding Remarks

This work was pursued under the hypothesis that by studying a subset of patients with unclassified FA we would likely discover novel genes not previously identified in FA. We found that some of the subjects had deficiencies in the FA pathway which resulted in the identification of a new complementation group and interesting separation of function mutations. While other patients had defects in different DNA repair pathways that are imperative to genome maintenance. In studying these individuals' mutations, we have increased our understanding of how these factors operate to maintain genome integrity. Even in the case of an already

discovered FA complementation groups, the study of specific patient mutations provides a unique tool to learn about a protein's functions.

Chapter 6: Materials and Methods

6.1 Experimental Procedures

6.1.1 Study subjects

DNA samples and cell lines were derived from subjects enrolled in the International Fanconi Anemia Registry (IFAR) after obtaining informed written consent. The Institutional Review Board of The Rockefeller University, New York, NY, USA, approved these studies.

6.1.2 Cell lines

Patient-derived fibroblast cell lines (Table 6.1) and BJ foreskin normal control fibroblasts (ATCC) were transformed by expression of HPV16 E6E7 and immortalized with the catalytic subunit of human telomerase (hTERT). Fibroblasts were cultured in Dulbecco Modified Eagle medium (DMEM) supplemented with 15% FBS, 100 units of penicillin per mL, 0.1 mg of streptomycin per mL, non-essential amino acids, and glutamax (Invitrogen). Fibroblasts cell lines were incubated at 37°C, 5% CO_2, and 3% O_2. Lymphoblast cell lines (Table 6.1) were established from patient peripheral blood mononuclear cells by Epstein-Barr Virus (EBV) transformation and grown in Roswell Park Memorial Institute medium (RPMI) with 20% FBS and further supplemented as above. HEK293T (ATCC) cells were cultured in DMEM supplemented with 10% FBS and penicillin/streptomycin and glutamax as indicated above. Lymphoblast and HEK293T cell lines were incubated at 37°C, 5% CO_2, and ambient O_2.

6.1.3 Plasmids and mutagenesis

UBE2T cDNA (Human ORFeome V8.1 Library, GE Healthcare) was recombined into pDONR223 using Gateway system BP reaction (Invitrogen). A Gateway system LR reaction (Invitrogen) was used to recombine the pDONR223 with a pMSCV retroviral vector resulting in a C-terminally HA-FLAG tagged UBE2T. A *PFAS* expressing pMSCV vector was made by cloning PFAS from WT cDNA with attB primers for recombination by BP reaction into the pDONR223. pDONR223-PFAS was recombined with pMSCV by LR reaction. Mutagenesis was performed using QuickChange Multi Site-Directed Mutagenesis Kit (Agilent) see Table 6.2 for primers.

6.1.4 Viral transfection/transduction

cDNAs were delivered by retroviral or lentiviral transduction after packaging in HEK293T cells (TransIT-293 transfection reagent, Mirus). HEK293T cells were plated at $4.5*10^6$ the evening before transfection of DNA and viral packaging vectors. Transfection was performed according to the manufacturer's instructions. The next day after transfection cell media was replaced and two days after transfection viral supernatants were harvested and used to infect target cells in the presence of 4 mg/ml polybrene. Stably expressing cells were selected with the appropriate agent ((puromycin (2 μg/ml), hygromycin (100-200 μg/ml), blasticidin (500 μg/ml), neomycin (600 μg/ml).

6.1.5 RNAi

Cells were transfected with pools of 3 siRNAs against MRE11, DNA2, EXO1, CtIP, WRN, BLM, BRCA2, RAD51, MUS81, XPF, and SLX4. For RADX and HLTF depletion a single previously published siRNA was used (Table 6.3) (Dungrawala et al., 2017; Taglialatela et al., 2017). Cells were transfected using Lipofectamine RNAiMAX (Invitorgen) according to the manufacturer's instructions. For shRNA depletion, virus was packaged in HEK293T cells and used to infect target cells and cells with stable integration were selected. shRNA constructs for SMARCAL1 and ZRANB3 were a gift from Alberto Ciccia (Table 6.4). shRNAs to *RADX* and *PFAS* were purchased from Transomics and used in the pZIP_hCMV_Puro vector or pMSCV-PM-mir30. shRNAs were PCR amplified and cloned into pMSCV-PM-mir30 by digestion with XhoI and MluI and vector ligation. See Table 6.2 for PCR primers for amplification of shRNA from UltramiRs of pZIP_hCMV vector. RNAi knockdown was measured by RT qPCR or western blot.

6.1.6 PCR, reverse transcription, and RT qPCR

PCR reactions were performed using Taq DNA Polymerase (Qiagen), Phusion High-Fidelity PCR Master Mix with GC buffer (Thermo Scientific), and PCR SuperMix High Fidelity (Invitrogen) according to manufacturer's protocols and primers are listed in Table 6.5. Total messenger RNA was extracted using RNeasy plus kit (Qiagen). RNA was reverse transcribed to cDNA using the SuperScript III Reverse Transcriptase (Invitrogen). Platinum SYBR Green SuperMix-UDG (Invitrogen) was used according to manufacturer's protocol to

determine relative transcript levels which were normalized against GAPDH levels. See Table 6.6 for RT qPCR primers.

6.1.7 Gene targeting

To correct the BRCA2 c.IVS19-1G>A mutation in HSC62 fibroblasts, cells were transduced with the pCW-Cas9-Puro (addgene #50661) vector which contains a doxycycline inducible Cas9. Subsequently, HSC62 cells were transduced with plentiGuide-Hygro (derived from addgene #52963) that expresses a single guide RNA (sgRNA) (see Table 6.7 for sgRNA sequence) that targets DNA in proximity to the c.IVS19-1G>A mutation. sgRNAs were designed using the online CRISPR design tool from the Zhang laboratory (crispr.mit.edu). $1*10^6$ cells were electroporated with a 100bp template oligonucleotide (see Table 6.8 for sequence) using Lonza 2b-Nucleofector. Cells were cultured in 500 ng/mL doxycycline for 48 hours to induce Cas9 expression and then incubated in fresh doxycycline free media for another 48 hours before being single cell cloned into 96-well plates. Clones were expanded and screened by sequencing of genomic DNA. For clones HSC62$^{mut/WT}$-1and HSC62$^{WT/WT}$-2, cells were selected in low dose MMC (50 ng/mL) once a week for three weeks before seeding in 96-wells. Clone 3 (HSC62$^{WT/WT}$) was not selected for.

The rest of the gene targeting was performed by electroporation of Cas9/gRNA ribonucleoprotein (RNP) complexes with 100bp oligonucleotide donor templates, with phosphorothioate protected ends. sgRNA was prepared by

combining crRNA (designed using crispr.mit.edu) and universal tracrRNA as per manufactures guidelines (IDT). To form RNP complexes gRNA duplex and Cas9-3NLS (IDT) were combined, incubated at room temperature for 10-15 minutes, and then placed on ice until used. RNP complexes and 10 ug of 100bp donor template oligonucleotide were electroporated into $2*10^5$ fibroblasts or $3.5*10^5$ HEK293T cells using Lonza 4D-Nucleofector. Cells were plated in a 12-well for 48-72 hours to recover before single-cell plating in 96-wells. Clones were expanded and screened by sequencing of genomic DNA. No selection was used.

6.1.8 Chromosomal breakage

Cells were treated with 0.1 μg DEB per mL of media for 48-72 hours or 45-100 nM of MMC for 24 hours. HU and aphidicolin treatments were as indicated. LCLs were arrested with colcemid (0.17 μg/mL) for 20 minutes and fibroblasts for 90 minutes. Cells were harvested and incubated in 0.075 M KCL for 10 minutes before being fixed in methanol and acetic acid (3:1). Cells were dropped onto wet slides and dried at 40°C for at least one hour before staining with Karyomax Giemsa (Invitrogen) for three minutes. Dry slides were then imaged on the Metasystems Metafer slide scanning platform.

6.1.9 Cell survival studies

Fibroblasts were seeded overnight in triplicate and treated the next day with DNA damaging agents at indicated concentrations. Cells were grown for 4-6 days and passaged once at appropriate ratios. Once cells reached near confluence (7-

9 days), cells were counted using Z2 Coulter counter (Beckman Coulter). In the case of cisplatin treatment, drug was removed after 1 hour and cells were washed with PBS and given fresh drug-free media. For aphidicolin treatment, after 48 hours cells were washed with PBS and given fresh drug-free media. For PARPi treatment, cells were given fresh media with olaparib daily. For ionizing radiation cells were treated with the indicated IR dose in Falcon tubes prior to being plated. LCLs were treated at the time of seeding, agitated daily, and counted on the 7th day. HEK293T cells were seeded overnight, treated with MMC, passaged after 3 days, and counted on the 5th day.

6.1.10 Cell cycle

For cell cycle analysis cells were treated with 45 nM MMC for 48 hours. Cells were collected and washed in cold PBS. Cells were resuspended in 300 ul PBS and slowly vortexed while 700 ul of cold 100% ethanol was added dropwise. Cells were stored at -20°C overnight or longer. Fixed cells were washed two times in cold PBS and resuspended in propidium iodine solution with RNase in PBS. Cells were incubated at 37°C for 30 minutes and cell cycle analysis was performed on BD Accuri C6 and analyzed with FlowJo software.

6.1.11 Western blot

Whole cell extracts were prepared by lysing cell pellets in Laemmli sample buffer (Bio-Rad or 4% SDS, 20% glycerol, 125 mM Tris-HCl pH 6.8). Samples were either sonicated or vortexed at highest speed for 30 seconds. Samples were boiled

for 5 minutes. For pRPA and BRCA2 western blots, samples were instead heated at 50°C for 10 minutes. Proteins were separated on 4-12% or 3-8% gradient gels (Invitrogen) by SDS-PAGE. Immunoblotting was performed using the antibodies indicated in Table 6.9.

6.1.12 Immunofluorescence

Cells were seeded on coverslips the day before. For FAND2 foci, cells were treated with 1 μM MMC for 24 hours. For RAD51 foci, cells were irradiated for indicated dose or treated with 3 μM MMC for 1 hour and harvested at indicated times. For RPA foci cells were treated with 3 μM MMC for 1 hour and harvested at indicated times. Cells were washed with PBS twice, fixed in 3.7% formaldehyde for 10 minutes, washed twice with PBS, and permeablized with 0.5% Triton in PBS for 10 mins. Cells were blocked in 5% [v/v] FBS in PBS, and incubated with primary antibodies in blocking buffer for two hours at room temperature or overnight at 4°C (for antibodies see Table 6.9). Cells were washed three times for five minutes with blocking buffer and then incubated with secondary antibody (1:1000) (Alexa Fluor). Cells were washed again three times with blocking buffer, rinsed quickly with water, air dried, and then embedded on glass slides with DAPI Fluoromount-G (SouthernBiotech).

6.1.13 Sister chromatid exchange

For MMC induced SCEs, fibroblasts were cultured for 24 hours in 10 ug/mL BrdU and then treated with 0.1 or 0.2 ug/mL MMC for one hour. Cells were washed

and put into fresh media with 10 ug/mL BrdU for another 24 hours. For cells depleted of BLM, siRNA transfection was performed twice as described. For the second siRNA transfection 10 ug/mL BrdU was added to media and cells were cultured in BrdU for a total of 48 hours before harvest. Cells were collected, fixed, and dropped on glass slides for metaphases as previously described. Slides were dried overnight at 42°C and then stained in 20 ug/mL Hoechst 33342 for 30 minutes. Slides were treated with 254 nM UV light for 3 hours. Slides were incubated at 65°C in 2x SCC for 2 hours, then rinsed in 1x GURR buffer, and stained in 8% Giemsa Karyomax for 3 minutes. Metaphases were scanned and imaged on Metasystems Metafer Slide Scanning Platform.

6.1.14 mClover homologous recombination assay

Cells were plated in a 24-well plate the day before and transfected with 0.25 ug pCMV-Cas9-sgLMNA-BFP and 0.4 ug pDONR-LMNA using TransIT-293 Transfection Reagent (Mirus) according to manufactures instructions (plasmids were a gift from Jan Karlseder)(Arnoult et al., 2017). 24 hours after transfection cell media was replaced. Cells were incubated for another 48 hours and were then harvested and analyzed on BD LSRII to determine the proportion of mClover positive cells and data was analyzed with FlowJo.

6.1.15 DNA molecular combing and DNA fibers

For DNA molecular combing, cells were plated the evening before and labeled with nucleotide analogs and treated with genotoxic agents as indicated.

Cells were harvested and pellets were processed using Genomic Vision Extraction Kit. Briefly, cells were embedded in low melting point agarose. Within the agarose gel matrix, proteins were digested and cell membranes were solubilized. The agarose plugs were melted and digested with beta-agarase. Using the Genomic Vision Molecular Combing System DNA molecules were stretched on coverslips. Coverslips were dried at 65°C for 2-4 hours. Coverslips were denatured in 0.5M NaOH and 1M NaCl solution for 8 minutes at room temperature. Coverslips were then dehydrated 5 minutes each in 70, 90, and 100 percent ethanol and then air dried at room temperature. For immunostaining coverslips were blocked in 5% FBS in PBS [v/v] for 30 minutes at 37°C and then incubated with primary antibodies for one hour at 37°C. Rat anti-BrdU antibody (1:25) was used to detect CldU and mouse anti-BrdU antibody (1:10) was used to detect IdU. Coverslips were washed and then incubated with secondary (Alexa Fluor) anti-rat (594) and anti-mouse (488) at a dilution of 1:100 each for 30 minutes at 37°C. Coverslips were washed and air dried. Dry coverslips were mounted on glass slides using Fluoromount-G (SouthernBiotech).

For DNA fibers, cells were plated and treated/labeled as above. Cells were harvested and cell pellets were washed one time in cold PBS. Cells were resuspended at a concentration of $1*10^6$ cells/mL in cold PBS. On a clean glass coverslip 10 ul droplets of spreading buffer (0.5% SDS, 200mM Tris-HCl pH 7.4, and 50 mM EDTA pH 8) was placed. 2.5 ul of cell suspension was pipetted into

the spreading buffer, stirred, and pipetted up and down three times. Coverslips were incubated horizontally for nine minutes at room temperature before gently being tilted vertically to allow the buffer to run down the slide. Coverslips were dried at room temperature at an angle and then heated at 65°C for 30 minutes. Coverslips were fixed in methanol/acetic acid 3:1 overnight at 4°C. The next day coverslips were washed in PBS three times at room temperature and then incubated in 2.5M HCl for 1 hour. Coverslips were then washed five times for five minutes with PBS and after the final wash they were blocked in 5% FBS in PBS for 30 minutes. For immunostaining, coverslips were incubated with primary antibodies for 2.5 hours at room temperature. Rat anti-BrdU antibody (1:40) was used to detect CldU and mouse anti-BrdU antibody (1:20) was used to detect IdU. Coverslips were washed 5 times with PBS with 0.2% Tween and then blocked for 30 minutes in 5% FBS in PBS. Coverslips were incubated with secondary (Alexa Fluor) anti-rat (594) and anti-mouse (488) at a dilution of 1:300 for 1 hour at room temperature. Coverslips were washed 5 times with with PBS with 0.2% Tween and rinsed with water and air dried. Dry coverslips were mounted on glass slides using Fluoromount-G. DNA tracks were all imaged on the DeltaVision Image Restoration microscope and measured using ImageJ.

6.1.16 aCGH

A custom CGH array was designed as previously described (Chandrasekharappa et al., 2013). NimbleGen Service for CGH was used for manufacturing, hybridization, scanning, and preliminary analysis. DNA from the

proband was compared to reference human male DNA (Promega). Data analysis was performed using NimbleScan and intensity variations were visualized using SignalMap (NimbleGen software).

6.1.17 Whole Exome Sequencing

The libraries for whole exome sequencing (WES) were constructed and sequenced on Illumina HiSeq 2000 or Illumina GA-IIX using 76 bp paired-end reads at the Broad Institute or by using Agilent SureSelect Human All Exon V4 capture kit and 100 bp paired-end sequencing on Illumina HiSeq 2500. Sequence was aligned to human genome build GRCh37 using BWA (Burrows-Wheeler Aligner) (Li and Durbin, 2009). Duplicate reads were marked using Picard [http://picard.sourceforge.net]. Genome Analysis Toolkit (GATK) was used for base quality score recalibration (BQSR), and local realignment around indels (DePristo et al., 2011). Variant discovery was performed in part by variant calling with GATK HaplotypeCaller and then joint genotyping with GATK GenotypeGVCFs. The variant call sets were then refined with Variant Quality Score Recalibration (VQSR) and VQSR scores helped discriminate low quality variants. Variant annotation was performed using SnpEff, VCFtools, and in-house software (NYGC) (Cingolani et al., 2012; Danecek et al., 2011). All WES was analyzed with the NYGC sequence analysis pipeline.

6.1.18 RNA sequencing

Indexed RNA sequencing (RNA-seq) libraries were constructed using TruSeq RNA Sample Prep Kit version 2 (Illumina). Each library was sequenced in pair-end mode using 1 lane of Illumina HiSeq2000 flowcell to generate 2 x 100 bp reads. Raw-reads were aligned to the human genome (hg19) using TopHat with default parameters. Cufflinks with GC and upper quartile normalization was then used to calculate normalized expression levels, Fragments Per Kilobase of transcripts per Million reads (FPKM) (Trapnell et al., 2012).

Table 6.1 List of cell lines

Cell Line		Cell type	Source
BJ	WT	Fibroblast	ATCC
HA239F	RAD50	Fibroblast	(Waltes et al., 2009)
HEK293T	WT	Epithelial kidney	ATCC
HSC62	BRCA2/FANCD2	Fibroblast	Howlett et al., 2002
RA3226	FANCD1/BRCA2	Fibroblast	IFAR, (Kim et al., 2013)
RA2143	BMF patient, unknown	Lymphoblast	IFAR
RA2177	BMF patient, unknown	Fibroblast	IFAR
RA2374	BRIP1/FANCJ	Fibroblast	IFAR
RA2480	FANCI	Fibroblast	IFAR, (Kim et al., 2013)
RA2525	BRCA2/FANCD1	Lymphoblast	IFAR
RA2627	UBE2T/FANCT	Fibroblast	IFAR, (Rickman et al., 2015)
RA2630	RAD51/FANCR	Fibroblast	IFAR, (Wang et al., 2015)
RA2645	FAND2	Fibroblast	IFAR, (Kalb et al., 2007)
RA2939	FANCA	Lymphoblast	IFAR, (Zhou et al., 2012)
RA2985	WT	Lymphoblast	IFAR
RA2987	WT	Lymphoblast	IFAR
RA3045	FANCL	Fibroblast	IFAR
RA3087	FANCA	Fibroblast	IFAR, (Kim et al., 2013)
RA3105	BRCA2/FANCD1	Lymphoblast	IFAR
RA3106	BRCA2/FANCD1	Lymphoblast	IFAR
RA3331	SLX4/FANCP	Fibroblast	IFAR, (Kim et al., 2011)
RA3534	Unaffected sibling control	Lymphoblast	IFAR
RA3535	Unaffected parental control	Lymphoblast	IFAR
RA3536	Unaffected parental control	Lymphoblast	IFAR
RA3572	Unaffected parental control	Fibroblast	IFAR
RA3573	Unaffected parental control	Fibroblast	IFAR

Table 6.2 List of cloning primers

Name	Sequence
Mutagenesis primers	
UBE2T_mutagen_S5DFwd	GCAGCTCTCTCTTCAGACGATCAGC TCTCTGCATGCCAACTTT
UBE2T_mutagen_S5DRev	AAAGTTGGCATGCAGAGAGCTGAT CGTCTGAAGAGAGAGCTGC
UBE2T_mutagen_Q2EFwd	CAGACGTGAAGCTCTCTCCATGCC AACTTTTTTGT
UBE2T_mutagen_Q2ERev	ACAAAAAAGTTGGCATGGAGAGAG CTTCACGTCTG
cDNA Cloning Primers	
attbUBE2TFwd	GGGGACAAGTTTGTACAAAAAAGCA GGCTTAATGCAGAGAGCTTCACGT
attbUBE2T_noSTOP_Rev	GGGGACCACTTTGTACAAGAAAGC TGGGTAACATCAGGATGAAATTTC
attbPFASFwd	GGGGACAAGTTTGTACAAAAAAGCA GGCTTAATGTCCCCAGTCCTTCACT T
attbPFAS_wSTOP_Rev	GGGGACCACTTTGTACAAGAAAGC TGGGTTCAGCAGCTCCCTTCCAGG G
shRNA cloning primers	
5'ultramir_XhoIsite	TTTTCTCGAGAAGGTATATTGCTGT TGACAG
3'ultramir_MluIsite	AAAAACGCGTAAAGTGATTTAATTT ATACCA
shRNA_5mir30Fwd	GCCTGCACATCTTGGAAACA
shRNA_3mir30Rev	GATAATTGCTCCTAAAGTAGCC

Table 6.3 List of siRNAs

siRNAs		
Name	Sequence	Supplier
siLuciferase	CGUACGCGGAAUACUUCGA	Sigma
siRAD51	GGUAGAAUCUAGGUAUGCAtt	Ambion
siRAD51	CAGUGGUAAUCACUAAUCAtt	Ambion
siRAD51	CCAGCUCCUUUAUCAAGCAtt	Ambion
siMRE11	GAUAGACAUUAGUCCGGUUtt	Ambion
siMRE11	CCCGAAAUGUCACUACUAAtt	Ambion
siMRE11	CGACUGCGAGUGGACUAUAtt	Ambion
siCTIP	GUACAAGGUUUACAAGUAAtt	Ambion
siCTIP	GGAUCUGUCUGAUCGAUUUtt	Ambion
siCTIP	GGGUCUGAAGUGAACAAGAtt	Ambion
siEXO1	GCCUGAGAAUAAUAUGUCUtt	Ambion
siEXO1	CUUUUGAACAGAUCGAUGAtt	Ambion
siEXO1	GGCUAGGAAUGUGCAGACAtt	Ambion
siDNA2	CAUCCAAUAUUUUCCCGUAt	Ambion
siDNA2	CCGUACAGGCAGCAAUUAAtt	Ambion
siDNA2	GUAACUUGUUUAUUAGACAtt	Ambion
siBLM	CCCACUACUUUGCAAGUAA	Ambion
siBLM	GGAUGUUCUUAGCACAUCA	Ambion
siBLM	GAUAUCUUCCAAAACGAAA	Ambion
siWRN	GGAGGGUUUCUAUCUUACUtt	Ambion
siWRN	CUGUAGCAAUUGGAGUAAAtt	Ambion
siWRN	CGAUGCUAGUGAUUGCUCUtt	Ambion
siMUS81	UUCUGAAAUACGAAGCGCG	Ambion
siMUS81	AGAGGGUUUGGAGAGGUCAU	Ambion
siMUS81	UUAGGAUUCAGGUGCUCCC	Ambion
siBRCA2	UAAUGGAUCAGUAUCAUUUGGUUC	Invitrogen
siBRCA2	GGAGGACUCCUUAUGUCCAAAUUU	Invitrogen
siBRCA2	GAGCGCAAAUAUAUCUGAAACUUC	Invitrogen
siSLX4	UUUGGAUGAAGAUUUCUGAGAUCUG	Invitrogen
siSLX4	UUCCGUGGCUCCUUCUUGCUGGUGG	Invitrogen
siSLX4	AAGAGUUCCUGGAAAUUCUCGGCCC	Invitrogen
siXPF	UCGAAAUUCACGCAUAUCC	Invitrogen
siXPF	UGUAUAGCAAGCAUGGUAG	Invitrogen
siXPF	AAGUCAACCACAAGUAUCC	Invitrogen
siHLTF	GGAAUAUAAUGUUAACGAUtt	Thermo Fisher Scientific
siRADX	CAUAGAGGCCAGCCGUAUA	Dharmacon

Table 6.4 List of shRNAs

shRNAs	
Name	Selection
pMSCV-shSMARCAL1#53711	GGAACTCATTGCAGTGTTTAA
pMSCV-shZRANB3#D3	CTGGATCAGACATCACACGATT
shRADX #46	ACAGCTTGAACTCTCTCGTATA
shRADX #49	CCACGCTAATCCAGTTGCTGTA
shPFAS #87	CCAGCCGACACTGGTTCTTCAA
shPFAS #88	CCGGGAGTGTCCTGTCAGAAGA

Table 6.5 List of sequencing primers

Sequencing primers	
Name	Sequence
474Fwd	GCGTTGCTGCGTTGTGAGG
479Rev	TTAACTAAGATGAACCAGGACAAG
509Fwd	GTTGTGGGTAAATGGTTGACTCTA
510Fwd	CAGAGAAGCATGCAAGACAGAAAC
538Rev	AGCCACACTGCACTATTCCTG
BRCA2 Exon20_FWD	GTTCAAGTGATTCTCCTGCCT
BRCA2 Exon20_REV	CAATAGGTCCTAGTTCCAGGC
BRCA2 Exon27_FWD	GGAGACTGTGTGTAATATTTGCG
BRCA2 Exon27_REV	GTCGCCTTTGCAAATGCTTAGA
BRCA2 cDNA_313	GCTGTTAAGGCCCAGTTAGATCC
BRCA2 cDNA_311	CCTAATTTCCAACTGGATCTGAGC
PFAS_RA2177_Exon6mut_Fwd	TATACTGGGTGAGGGCCGGCTT
PFAS_RA2177_Exon6mut_Rev	TGGTCTCTCCCAACACCCATG
PFAS_RA2177_Exon12mut_Fwd	CTGTGTTCACGCTGCCTTGCT
PFAS_RA2177_Exon12mut_Rev	CCAAAGTCCAGGTCACTGGTGTT

Table 6.6 List of RT qPCR primers

RTqPCR primers	
Name	Sequence
BLM_Fwd	TTTATCCTGATGCCGACTGG
BLM_Rev	ACCCCAGGAGAAACACAGG
DNA2_Fwd	GCTGTCCTGAGTGAAACTTTTAGG
DNA2_Rev	CCTCATGGAGAACCGTACCA
EXO1_Fwd	CTTTCTCAGTGCTCTAGTAAGGACTCT
EXO1_Rev	TGGAGGTCTGGTCACTTTGA
WRN_Fwd	GATGTTGCCAATAAAAAGCTGA
WRN_Rev	GTTTACCTAAGAGGTGTTTAACCAGAC
UBE2T_Fwd	GATGACCTGCGAGCTCAAATA
UBE2T_Rev	GGATCTGAGGAGGTTCAAATGG
RADX_FWD	AAGTGCCTCAGCATCAGAAA
RADX_REV	TGAGGTACAGCAACTGGATTAG
PFAS_Fwd_2	CATCATGAGCACCCAGGAAT
PFAS_Rev_2	GGCATACTCCTGTGGGAAAG
PFAS_Fwd_3	CCAGCTGGAGCCATCATTTA
PFAS_Rev_3	CAGCACTATTCTCCGGTCTC

Table 6.7 List of sgRNAs

sgRNAs	
Name	Selection
HSC62_g7	TGGATGGAGAAGACATCATC
HSC62_g6	TGTGTAACACATTATTACAG
BRCA2_Ex20g5	CATATTTCGCAATGAAAGAG
BRCA2_Ex27g9	TGTTTCTCCGGCTGCACAGA
PFAS_Exon12g11	GTCTACAGGATTGGAGTcGG

Table 6.8 List of oligonucleotide donor templates for CRISPR/Cas9

CRISPR ssDNA templates	
Name	Sequence
IVS19-1_G	TTGAATGTTATATATGTGACTTTTTTGGTGT GTGTAACACATTATTACAgTGGATGGAGAA GACATCcTCTGGATTATACATATTTCGCAAT GAAAGAGA
IVS19-1_A	TTGAATGTTATATATGTGACTTTTTTGGTGTG TGTAACACATTATTACAaTGGATGGAGAAGAA TCcTCTGGATTATACATATTTCGCAATGAAAGA GA
8524C>T	CATTATTACAGTGGATGGAGAAGACATCATCT GGATTATACATATTTtGCAATGAAAGAGAaGAA GAAAAGGAAGCAGCAAAATATGTGGAGGCCC AACA
DBDx3A	GTGTGTGTAACACATTATTACAGTGGATGGAG gccACATCATCTGGATTAgccATAgctCGCAATGA AAGAGAaGAAGAAAAGGAAGCAGCAAAATATGT
S3291A	GACTGCCTTTACCTCCACCTGTgAGTCCCATT TGTACATTTGTTgCTCCGGCTGCACAGAAaGC ATTTCAGCCACCAAGGAGTTGTGGCACCAAA TACGA
PFAS_WT	GCATGGAAGTTGTAAAGGTTGGAGGTCCCGTC TACAGGATTGGAGTcGGAGGTGGAGCTgCTTCA TCTGTGCAGGTGAGTGGGAATTGCTAAAGGTG CAG
PFAS_A466T	GCATGGAAGTTGTAAAGGTTGGAGGTCCCGTC TACAGGATTGGAGTcGGAGGTGGAGCTaCTTCA TCTGTGCAGGTGAGTGGGAATTGCTAAAGGTGC AG

Table 6.9 List of antibodies

Antibody		IF	Western
α-tubulin	Sigma T9026	NA	1:1000
BRCA2	Millipore Sigma OP95	NA	1:250
CtIP	Bethyl A300-488	NA	1:500
FANCA	Bethyl A301-980A	NA	1:1000
FANCD2	Novus NB100-182	1:1000	1:1000
FANCI	antibody raised in-house, #589	NA	1:1000
HA	Covance MMS-101R	1:5000	1:1000
HLTF	Abcam ab17984	NA	1:1000
MRE11	Gift from John Petrini	NA	1:10000
MUS81	Abcam MTA30 2G10/3	NA	1:1000
pRPA S4/S8	Bethyl A300-245A	NA	
RAD51	Clone SWE47, gift from Steve West	1:1000	1:1000
RPA32	Bethyl A300-244A	1:5000	1:1000
SMARCAL1	Santa Cruz sc-376377	NA	1:1000
UBE2T	Abcam EPR9446	NA	1:1000
Vinculin	Sigma hVIN-1	NA	1:1000
XPF	NeoMarkers MS1381P	NA	1:1000
ZRANB3	Bethyl A303-033A	NA	1:1000
DNA combing and fibers		Fibers	Combing
BRDU	BD Biosciences B44	1:20	1:10
BRDU	EuroBioSciences (BU1/75)	NA	1:20
BRDU	Abcam ab6326 (BU1/75)	1:40	1:20

Chapter 7: References

Ahuja, A.K., K. Jodkowska, F. Teloni, A.H. Bizard, R. Zellweger, R. Herrador, S. Ortega, I.D. Hickson, M. Altmeyer, J. Mendez, and M. Lopes. 2016. A short G1 phase imposes constitutive replication stress and fork remodelling in mouse embryonic stem cells. *Nat Commun*. 7:10660.

Alpi, A.F., P.E. Pace, M.M. Babu, and K.J. Patel. 2008. Mechanistic insight into site-restricted monoubiquitination of FANCD2 by Ube2t, FANCL, and FANCI. *Molecular cell*. 32:767-777.

Alter, B.P. 2002. Bone marrow failure syndromes in children. *Pediatr Clin North Am*. 49:973-988.

Alter, B.P. 2014. Fanconi anemia and the development of leukemia. *Best Pract Res Clin Haematol*. 27:214-221.

Alter, B.P. 2017. Inherited bone marrow failure syndromes: considerations pre- and posttransplant. *Hematology Am Soc Hematol Educ Program*. 2017:88-95.

Alter, B.P., and P.S. Rosenberg. 2013. VACTERL-H Association and Fanconi Anemia. *Mol Syndromol*. 4:87-93.

Alter, B.P., P.S. Rosenberg, and L.C. Brody. 2007. Clinical and molecular features associated with biallelic mutations in FANCD1/BRCA2. *J Med Genet*. 44:1-9.

Ameziane, N., P. May, A. Haitjema, H.J. van de Vrugt, S.E. van Rossum-Fikkert, D. Ristic, G.J. Williams, J. Balk, D. Rockx, H. Li, M.A. Rooimans, A.B. Oostra, E. Velleuer, R. Dietrich, O.B. Bleijerveld, A.F. Maarten Altelaar, H. Meijers-Heijboer, H. Joenje, G. Glusman, J. Roach, L. Hood, D. Galas, C. Wyman, R. Balling, J. den Dunnen, J.P. de Winter, R. Kanaar, R. Gelinas, and J.C. Dorsman. 2015. A novel Fanconi anaemia subtype associated with a dominant-negative mutation in RAD51. *Nat Commun*. 6:8829.

Arnoult, N., A. Correia, J. Ma, A. Merlo, S. Garcia-Gomez, M. Maric, M. Tognetti, C.W. Benner, S.J. Boulton, A. Saghatelian, and J. Karlseder. 2017. Regulation of DNA repair pathway choice in S and G2 phases by the NHEJ inhibitor CYREN. *Nature*. 549:548-552.

Attard, G., C. Parker, R.A. Eeles, F. Schroder, S.A. Tomlins, I. Tannock, C.G. Drake, and J.S. de Bono. 2016. Prostate cancer. *Lancet*. 387:70-82.

Auerbach, A.D. 2009. Fanconi anemia and its diagnosis. *Mutation research*. 668:4-10.

Auerbach, A.D., and S.R. Wolman. 1976. Susceptibility of Fanconi's anaemia fibroblasts to chromosome damage by carcinogens. *Nature*. 261:494-496.

Ayoub, N., E. Rajendra, X. Su, A.D. Jeyasekharan, R. Mahen, and A.R. Venkitaraman. 2009. The carboxyl terminus of Brca2 links the disassembly of Rad51 complexes to mitotic entry. *Curr Biol*. 19:1075-1085.

Bacquin, A., C. Pouvelle, N. Siaud, M. Perderiset, S. Salome-Desnoulez, C. Tellier-Lebegue, B. Lopez, J.B. Charbonnier, and P.L. Kannouche. 2013. The helicase FBH1 is tightly regulated by PCNA via CRL4(Cdt2)-mediated proteolysis in human cells. *Nucleic Acids Res*. 41:6501-6513.

Bagby, G. 2018. Recent advances in understanding hematopoiesis in Fanconi Anemia. *F1000Res*. 7:105.

Bansbach, C.E., R. Betous, C.A. Lovejoy, G.G. Glick, and D. Cortez. 2009. The annealing helicase SMARCAL1 maintains genome integrity at stalled replication forks. *Genes Dev*. 23:2405-2414.

Barber, L.J., S. Sandhu, L. Chen, J. Campbell, I. Kozarewa, K. Fenwick, I. Assiotis, D.N. Rodrigues, J.S. Reis Filho, V. Moreno, J. Mateo, L.R. Molife, J. De Bono, S. Kaye, C.J. Lord, and A. Ashworth. 2013. Secondary mutations in BRCA2 associated with clinical resistance to a PARP inhibitor. *J Pathol*. 229:422-429.

Bass, T.E., J.W. Luzwick, G. Kavanaugh, C. Carroll, H. Dungrawala, G.G. Glick, M.D. Feldkamp, R. Putney, W.J. Chazin, and D. Cortez. 2016. ETAA1 acts at stalled replication forks to maintain genome integrity. *Nat Cell Biol*. 18:1185-1195.

Belkadi, A., A. Bolze, Y. Itan, A. Cobat, Q.B. Vincent, A. Antipenko, L. Shang, B. Boisson, J.L. Casanova, and L. Abel. 2015. Whole-genome sequencing is more powerful than whole-exome sequencing for detecting exome variants. *Proceedings of the National Academy of Sciences of the United States of America*. 112:5473-5478.

Berti, M., A. Ray Chaudhuri, S. Thangavel, S. Gomathinayagam, S. Kenig, M. Vujanovic, F. Odreman, T. Glatter, S. Graziano, R. Mendoza-Maldonado, F. Marino, B. Lucic, V. Biasin, M. Gstaiger, R. Aebersold, J.M. Sidorova, R.J. Monnat, Jr., M. Lopes, and A. Vindigni. 2013. Human RECQ1 promotes restart of replication forks reversed by DNA topoisomerase I inhibition. *Nat Struct Mol Biol*. 20:347-354.

Betous, R., F.B. Couch, A.C. Mason, B.F. Eichman, M. Manosas, and D. Cortez. 2013. Substrate-selective repair and restart of replication forks by DNA translocases. *Cell Rep*. 3:1958-1969.

Betous, R., A.C. Mason, R.P. Rambo, C.E. Bansbach, A. Badu-Nkansah, B.M. Sirbu, B.F. Eichman, and D. Cortez. 2012. SMARCAL1 catalyzes fork regression

and Holliday junction migration to maintain genome stability during DNA replication. *Genes Dev*. 26:151-162.

Blackford, A.N., and S.P. Jackson. 2017. ATM, ATR, and DNA-PK: The Trinity at the Heart of the DNA Damage Response. *Mol Cell*. 66:801-817.

Bogliolo, M., B. Schuster, C. Stoepker, B. Derkunt, Y. Su, A. Raams, J.P. Trujillo, J. Minguillon, M.J. Ramirez, R. Pujol, J.A. Casado, R. Banos, P. Rio, K. Knies, S. Zuniga, J. Benitez, J.A. Bueren, N.G. Jaspers, O.D. Scharer, J.P. de Winter, D. Schindler, and J. Surralles. 2013. Mutations in ERCC4, encoding the DNA-repair endonuclease XPF, cause Fanconi anemia. *American journal of human genetics*. 92:800-806.

Boycott, K.M., and D. Ardigo. 2018. Addressing challenges in the diagnosis and treatment of rare genetic diseases. *Nat Rev Drug Discov*. 17:151-152.

Boycott, K.M., A. Rath, J.X. Chong, T. Hartley, F.S. Alkuraya, G. Baynam, A.J. Brookes, M. Brudno, A. Carracedo, J.T. den Dunnen, S.O.M. Dyke, X. Estivill, J. Goldblatt, C. Gonthier, S.C. Groft, I. Gut, A. Hamosh, P. Hieter, S. Hohn, M.E. Hurles, P. Kaufmann, B.M. Knoppers, J.P. Krischer, M. Macek, Jr., G. Matthijs, A. Olry, S. Parker, J. Paschall, A.A. Philippakis, H.L. Rehm, P.N. Robinson, P.C. Sham, R. Stefanov, D. Taruscio, D. Unni, M.R. Vanstone, F. Zhang, H. Brunner, M.J. Bamshad, and H. Lochmuller. 2017. International Cooperation to Enable the

Diagnosis of All Rare Genetic Diseases. *American journal of human genetics*. 100:695-705.

Bryant, H.E., E. Petermann, N. Schultz, A.S. Jemth, O. Loseva, N. Issaeva, F. Johansson, S. Fernandez, P. McGlynn, and T. Helleday. 2009. PARP is activated at stalled forks to mediate Mre11-dependent replication restart and recombination. *EMBO J*. 28:2601-2615.

Bryant, H.E., N. Schultz, H.D. Thomas, K.M. Parker, D. Flower, E. Lopez, S. Kyle, M. Meuth, N.J. Curtin, and T. Helleday. 2005. Specific killing of BRCA2-deficient tumours with inhibitors of poly(ADP-ribose) polymerase. *Nature*. 434:913-917.

Buck, D., L. Malivert, R. de Chasseval, A. Barraud, M.C. Fondaneche, O. Sanal, A. Plebani, J.L. Stephan, M. Hufnagel, F. le Deist, A. Fischer, A. Durandy, J.P. de Villartay, and P. Revy. 2006. Cernunnos, a novel nonhomologous end-joining factor, is mutated in human immunodeficiency with microcephaly. *Cell*. 124:287-299.

Budzowska, M., T.G. Graham, A. Sobeck, S. Waga, and J.C. Walter. 2015. Regulation of the Rev1-pol zeta complex during bypass of a DNA interstrand cross-link. *The EMBO journal*. 34:1971-1985.

Bunting, S.F., E. Callen, N. Wong, H.T. Chen, F. Polato, A. Gunn, A. Bothmer, N. Feldhahn, O. Fernandez-Capetillo, L. Cao, X. Xu, C.X. Deng, T. Finkel, M. Nussenzweig, J.M. Stark, and A. Nussenzweig. 2010. 53BP1 inhibits homologous recombination in Brca1-deficient cells by blocking resection of DNA breaks. *Cell*. 141:243-254.

Cao, L., X. Xu, S.F. Bunting, J. Liu, R.H. Wang, L.L. Cao, J.J. Wu, T.N. Peng, J. Chen, A. Nussenzweig, C.X. Deng, and T. Finkel. 2009. A selective requirement for 53BP1 in the biological response to genomic instability induced by Brca1 deficiency. *Molecular cell*. 35:534-541.

Casanova, J.L., M.E. Conley, S.J. Seligman, L. Abel, and L.D. Notarangelo. 2014. Guidelines for genetic studies in single patients: lessons from primary immunodeficiencies. *The Journal of experimental medicine*. 211:2137-2149.

Chandrasekharappa, S.C., F.P. Lach, D.C. Kimble, A. Kamat, J.K. Teer, F.X. Donovan, E. Flynn, S.K. Sen, S. Thongthip, E. Sanborn, A. Smogorzewska, A.D. Auerbach, E.A. Ostrander, and N.C.S. Program. 2013. Massively parallel sequencing, aCGH, and RNA-Seq technologies provide a comprehensive molecular diagnosis of Fanconi anemia. *Blood*. 121:e138-148.

Chen, P.L., C.F. Chen, Y. Chen, J. Xiao, Z.D. Sharp, and W.H. Lee. 1998. The BRC repeats in BRCA2 are critical for RAD51 binding and resistance to methyl

methanesulfonate treatment. *Proceedings of the National Academy of Sciences of the United States of America*. 95:5287-5292.

Chu, W.K., M.J. Payne, P. Beli, K. Hanada, C. Choudhary, and I.D. Hickson. 2015. FBH1 influences DNA replication fork stability and homologous recombination through ubiquitylation of RAD51. *Nat Commun*. 6:5931.

Ciccia, A., A.L. Bredemeyer, M.E. Sowa, M.E. Terret, P.V. Jallepalli, J.W. Harper, and S.J. Elledge. 2009. The SIOD disorder protein SMARCAL1 is an RPA-interacting protein involved in replication fork restart. *Genes Dev*. 23:2415-2425.

Ciccia, A., and S.J. Elledge. 2010. The DNA damage response: making it safe to play with knives. *Mol Cell*. 40:179-204.

Ciccia, A., A.V. Nimonkar, Y. Hu, I. Hajdu, Y.J. Achar, L. Izhar, S.A. Petit, B. Adamson, J.C. Yoon, S.C. Kowalczykowski, D.M. Livingston, L. Haracska, and S.J. Elledge. 2012. Polyubiquitinated PCNA recruits the ZRANB3 translocase to maintain genomic integrity after replication stress. *Mol Cell*. 47:396-409.

Cingolani, P., A. Platts, L. Wang le, M. Coon, T. Nguyen, L. Wang, S.J. Land, X. Lu, and D.M. Ruden. 2012. A program for annotating and predicting the effects of single nucleotide polymorphisms, SnpEff: SNPs in the genome of Drosophila melanogaster strain w1118; iso-2; iso-3. *Fly*. 6:80-92.

Collis, S.J., A. Ciccia, A.J. Deans, Z. Horejsi, J.S. Martin, S.L. Maslen, J.M. Skehel, S.J. Elledge, S.C. West, and S.J. Boulton. 2008. FANCM and FAAP24 function in ATR-mediated checkpoint signaling independently of the Fanconi anemia core complex. *Molecular cell*. 32:313-324.

Connor, F., D. Bertwistle, P.J. Mee, G.M. Ross, S. Swift, E. Grigorieva, V.L. Tybulewicz, and A. Ashworth. 1997. Tumorigenesis and a DNA repair defect in mice with a truncating Brca2 mutation. *Nature genetics*. 17:423-430.

Cortez, D. 2015. Preventing replication fork collapse to maintain genome integrity. *DNA Repair (Amst)*. 32:149-157.

Couch, F.B., C.E. Bansbach, R. Driscoll, J.W. Luzwick, G.G. Glick, R. Betous, C.M. Carroll, S.Y. Jung, J. Qin, K.A. Cimprich, and D. Cortez. 2013. ATR phosphorylates SMARCAL1 to prevent replication fork collapse. *Genes Dev*. 27:1610-1623.

Danecek, P., A. Auton, G. Abecasis, C.A. Albers, E. Banks, M.A. DePristo, R.E. Handsaker, G. Lunter, G.T. Marth, S.T. Sherry, G. McVean, R. Durbin, and G. Genomes Project Analysis. 2011. The variant call format and VCFtools. *Bioinformatics*. 27:2156-2158.

Davies, O.R., and L. Pellegrini. 2007. Interaction with the BRCA2 C terminus protects RAD51-DNA filaments from disassembly by BRC repeats. *Nat Struct Mol Biol*. 14:475-483.

Degrolard-Courcet, E., J. Sokolowska, M.M. Padeano, S. Guiu, M. Bronner, C. Chery, F. Coron, C. Lepage, C. Chapusot, C. Loustalot, J.L. Jouve, C. Hatem, E. Ferrant, L. Martin, C. Coutant, A. Baurand, G. Couillault, A. Delignette, S. El Chehadeh, S. Lizard, L. Arnould, P. Fumoleau, P. Callier, F. Mugneret, C. Philippe, T. Frebourg, P. Jonveaux, and L. Faivre. 2014a. Development of primary early-onset colorectal cancers due to biallelic mutations of the FANCD1/BRCA2 gene. *Eur J Hum Genet*. 22.

Degrolard-Courcet, E., J. Sokolowska, M.M. Padeano, S. Guiu, M. Bronner, C. Chery, F. Coron, C. Lepage, C. Chapusot, C. Loustalot, J.L. Jouve, C. Hatem, E. Ferrant, L. Martin, C. Coutant, A. Baurand, G. Couillault, A. Delignette, S. El Chehadeh, S. Lizard, L. Arnould, P. Fumoleau, P. Callier, F. Mugneret, C. Philippe, T. Frebourg, P. Jonveaux, and L. Faivre. 2014b. Development of primary early-onset colorectal cancers due to biallelic mutations of the FANCD1/BRCA2 gene. *Eur J Hum Genet*. 22:979-987.

Deininger, P. 2011. Alu elements: know the SINEs. *Genome biology*. 12:236.

Dendouga, N., H. Gao, D. Moechars, M. Janicot, J. Vialard, and C.H. McGowan. 2005. Disruption of murine Mus81 increases genomic instability and DNA damage sensitivity but does not promote tumorigenesis. *Molecular and cellular biology*. 25:7569-7579.

Deng, C.X., and F. Scott. 2000. Role of the tumor suppressor gene Brca1 in genetic stability and mammary gland tumor formation. *Oncogene*. 19:1059-1064.

DePristo, M.A., E. Banks, R. Poplin, K.V. Garimella, J.R. Maguire, C. Hartl, A.A. Philippakis, G. del Angel, M.A. Rivas, M. Hanna, A. McKenna, T.J. Fennell, A.M. Kernytsky, A.Y. Sivachenko, K. Cibulskis, S.B. Gabriel, D. Altshuler, and M.J. Daly. 2011. A framework for variation discovery and genotyping using next-generation DNA sequencing data. *Nature genetics*. 43:491-498.

Di Virgilio, M., E. Callen, A. Yamane, W. Zhang, M. Jankovic, A.D. Gitlin, N. Feldhahn, W. Resch, T.Y. Oliveira, B.T. Chait, A. Nussenzweig, R. Casellas, D.F. Robbiani, and M.C. Nussenzweig. 2013. Rif1 prevents resection of DNA breaks and promotes immunoglobulin class switching. *Science*. 339:711-715.

Ding, X., A. Ray Chaudhuri, E. Callen, Y. Pang, K. Biswas, K.D. Klarmann, B.K. Martin, S. Burkett, L. Cleveland, S. Stauffer, T. Sullivan, A. Dewan, H. Marks, A.T. Tubbs, N. Wong, E. Buehler, K. Akagi, S.E. Martin, J.R. Keller, A. Nussenzweig,

and S.K. Sharan. 2016. Synthetic viability by BRCA2 and PARP1/ARTD1 deficiencies. *Nat Commun*. 7:12425.

Domchek, S.M., J. Tang, J. Stopfer, D.R. Lilli, N. Hamel, M. Tischkowitz, A.N. Monteiro, T.E. Messick, J. Powers, A. Yonker, F.J. Couch, D.E. Goldgar, H.R. Davidson, K.L. Nathanson, W.D. Foulkes, and R.A. Greenberg. 2013. Biallelic deleterious BRCA1 mutations in a woman with early-onset ovarian cancer. *Cancer Discov*. 3:399-405.

Dungrawala, H., K.P. Bhat, R. Le Meur, W.J. Chazin, X. Ding, S.K. Sharan, S.R. Wessel, A.A. Sathe, R. Zhao, and D. Cortez. 2017. RADX Promotes Genome Stability and Modulates Chemosensitivity by Regulating RAD51 at Replication Forks. *Mol Cell*. 67:374-386 e375.

Dungrawala, H., K.L. Rose, K.P. Bhat, K.N. Mohni, G.G. Glick, F.B. Couch, and D. Cortez. 2015. The Replication Checkpoint Prevents Two Types of Fork Collapse without Regulating Replisome Stability. *Mol Cell*. 59:998-1010.

Edwards, S.L., R. Brough, C.J. Lord, R. Natrajan, R. Vatcheva, D.A. Levine, J. Boyd, J.S. Reis-Filho, and A. Ashworth. 2008. Resistance to therapy caused by intragenic deletion in BRCA2. *Nature*. 451:1111-1115.

Esashi, F., N. Christ, J. Gannon, Y. Liu, T. Hunt, M. Jasin, and S.C. West. 2005. CDK-dependent phosphorylation of BRCA2 as a regulatory mechanism for recombinational repair. *Nature*. 434:598-604.

Escribano-Diaz, C., A. Orthwein, A. Fradet-Turcotte, M. Xing, J.T. Young, J. Tkac, M.A. Cook, A.P. Rosebrock, M. Munro, M.D. Canny, D. Xu, and D. Durocher. 2013. A cell cycle-dependent regulatory circuit composed of 53BP1-RIF1 and BRCA1-CtIP controls DNA repair pathway choice. *Mol Cell*. 49:872-883.

Farrugia, D.J., M.K. Agarwal, V.S. Pankratz, A.M. Deffenbaugh, D. Pruss, C. Frye, L. Wadum, K. Johnson, J. Mentlick, S.V. Tavtigian, D.E. Goldgar, and F.J. Couch. 2008. Functional assays for classification of BRCA2 variants of uncertain significance. *Cancer research*. 68:3523-3531.

Feng, W., and M. Jasin. 2017. BRCA2 suppresses replication stress-induced mitotic and G1 abnormalities through homologous recombination. *Nat Commun*. 8:525.

Flynn, E.K., A. Kamat, F.P. Lach, F.X. Donovan, D.C. Kimble, N. Narisu, E. Sanborn, F. Boulad, S.M. Davies, A.P. Gillio, 3rd, R.E. Harris, M.L. MacMillan, J.E. Wagner, A. Smogorzewska, A.D. Auerbach, E.A. Ostrander, and S.C. Chandrasekharappa. 2014. Comprehensive analysis of pathogenic deletion variants in Fanconi anemia genes. *Human mutation*. 35:1342-1353.

Franchitto, A., L.M. Pirzio, E. Prosperi, O. Sapora, M. Bignami, and P. Pichierri. 2008. Replication fork stalling in WRN-deficient cells is overcome by prompt activation of a MUS81-dependent pathway. *J Cell Biol*. 183:241-252.

Freire, B.L., T.K. Homma, M.F.A. Funari, A.M. Lerario, A.M. Leal, E. Velloso, A.C. Malaquias, and A.A.L. Jorge. 2018. Homozygous loss of function BRCA1 variant causing a Fanconi-anemia-like phenotype, a clinical report and review of previous patients. *Eur J Med Genet*. 61:130-133.

Garaycoechea, J.I., G.P. Crossan, F. Langevin, M. Daly, M.J. Arends, and K.J. Patel. 2012. Genotoxic consequences of endogenous aldehydes on mouse haematopoietic stem cell function. *Nature*. 489:571-575.

Garcia-Higuera, I., T. Taniguchi, S. Ganesan, M.S. Meyn, C. Timmers, J. Hejna, M. Grompe, and A.D. D'Andrea. 2001. Interaction of the Fanconi anemia proteins and BRCA1 in a common pathway. *Mol Cell*. 7:249-262.

Garre, P., L. Martin, J. Sanz, A. Romero, A. Tosar, I. Bando, P. Llovet, P. Diaque, B. Garcia-Paredes, E. Diaz-Rubio, M. de la Hoya, and T. Caldes. 2015. BRCA2 gene: a candidate for clinical testing in familial colorectal cancer type X. *Clin Genet*. 87:582-587.

Genomes Project, C., G.R. Abecasis, D. Altshuler, A. Auton, L.D. Brooks, R.M. Durbin, R.A. Gibbs, M.E. Hurles, and G.A. McVean. 2010. A map of human genome variation from population-scale sequencing. *Nature*. 467:1061-1073.

Gowen, L.C., B.L. Johnson, A.M. Latour, K.K. Sulik, and B.H. Koller. 1996. Brca1 deficiency results in early embryonic lethality characterized by neuroepithelial abnormalities. *Nat Genet*. 12:191-194.

Gravel, S., J.R. Chapman, C. Magill, and S.P. Jackson. 2008. DNA helicases Sgs1 and BLM promote DNA double-strand break resection. *Genes Dev*. 22:2767-2772.

Gregory, J.J., Jr., J.E. Wagner, P.C. Verlander, O. Levran, S.D. Batish, C.R. Eide, A. Steffenhagen, B. Hirsch, and A.D. Auerbach. 2001. Somatic mosaicism in Fanconi anemia: evidence of genotypic reversion in lymphohematopoietic stem cells. *Proceedings of the National Academy of Sciences of the United States of America*. 98:2532-2537.

Guidugli, L., A. Carreira, S.M. Caputo, A. Ehlen, A. Galli, A.N. Monteiro, S.L. Neuhausen, T.V. Hansen, F.J. Couch, M.P. Vreeswijk, and E. consortium. 2014. Functional assays for analysis of variants of uncertain significance in BRCA2. *Human mutation*. 35:151-164.

Guidugli, L., V.S. Pankratz, N. Singh, J. Thompson, C.A. Erding, C. Engel, R. Schmutzler, S. Domchek, K. Nathanson, P. Radice, C. Singer, P.N. Tonin, N.M. Lindor, D.E. Goldgar, and F.J. Couch. 2013. A classification model for BRCA2 DNA binding domain missense variants based on homology-directed repair activity. *Cancer research*. 73:265-275.

Guillemette, S., R.W. Serra, M. Peng, J.A. Hayes, P.A. Konstantinopoulos, M.R. Green, and S.B. Cantor. 2015. Resistance to therapy in BRCA2 mutant cells due to loss of the nucleosome remodeling factor CHD4. *Genes Dev*. 29:489-494.

Haahr, P., S. Hoffmann, M.A. Tollenaere, T. Ho, L.I. Toledo, M. Mann, S. Bekker-Jensen, M. Raschle, and N. Mailand. 2016. Activation of the ATR kinase by the RPA-binding protein ETAA1. *Nat Cell Biol*. 18:1196-1207.

Hakem, R., J.L. de la Pompa, C. Sirard, R. Mo, M. Woo, A. Hakem, A. Wakeham, J. Potter, A. Reitmair, F. Billia, E. Firpo, C.C. Hui, J. Roberts, J. Rossant, and T.W. Mak. 1996. The tumor suppressor gene Brca1 is required for embryonic cellular proliferation in the mouse. *Cell*. 85:1009-1023.

Hanada, K., M. Budzowska, S.L. Davies, E. van Drunen, H. Onizawa, H.B. Beverloo, A. Maas, J. Essers, I.D. Hickson, and R. Kanaar. 2007. The structure-specific endonuclease Mus81 contributes to replication restart by generating double-strand DNA breaks. *Nat Struct Mol Biol*. 14:1096-1104.

Hashimoto, Y., A. Ray Chaudhuri, M. Lopes, and V. Costanzo. 2010. Rad51 protects nascent DNA from Mre11-dependent degradation and promotes continuous DNA synthesis. *Nat Struct Mol Biol*. 17:1305-1311.

Hershko, A., and A. Ciechanover. 1998. The ubiquitin system. *Annual review of biochemistry*. 67:425-479.

Higgs, M.R., J.J. Reynolds, A. Winczura, A.N. Blackford, V. Borel, E.S. Miller, A. Zlatanou, J. Nieminuszczy, E.L. Ryan, N.J. Davies, T. Stankovic, S.J. Boulton, W. Niedzwiedz, and G.S. Stewart. 2015. BOD1L Is Required to Suppress Deleterious Resection of Stressed Replication Forks. *Mol Cell*. 59:462-477.

Hira, A., H. Yabe, K. Yoshida, Y. Okuno, Y. Shiraishi, K. Chiba, H. Tanaka, S. Miyano, J. Nakamura, S. Kojima, S. Ogawa, K. Matsuo, M. Takata, and M. Yabe. 2013. Variant ALDH2 is associated with accelerated progression of bone marrow failure in Japanese Fanconi anemia patients. *Blood*. 122:3206-3209.

Hira, A., K. Yoshida, K. Sato, Y. Okuno, Y. Shiraishi, K. Chiba, H. Tanaka, S. Miyano, A. Shimamoto, H. Tahara, E. Ito, S. Kojima, H. Kurumizaka, S. Ogawa, M. Takata, H. Yabe, and M. Yabe. 2015. Mutations in the gene encoding the E2 conjugating enzyme UBE2T cause Fanconi anemia. *American journal of human genetics*. 96:1001-1007.

Ho, G.P., S. Margossian, T. Taniguchi, and A.D. D'Andrea. 2006. Phosphorylation of FANCD2 on two novel sites is required for mitomycin C resistance. *Molecular and cellular biology*. 26:7005-7015.

Hodson, C., A. Purkiss, J.A. Miles, and H. Walden. 2014. Structure of the human FANCL RING-Ube2T complex reveals determinants of cognate E3-E2 selection. *Structure*. 22:337-344.

Howlett, N.G., T. Taniguchi, S. Olson, B. Cox, Q. Waisfisz, C. De Die-Smulders, N. Persky, M. Grompe, H. Joenje, G. Pals, H. Ikeda, E.A. Fox, and A.D. D'Andrea. 2002. Biallelic inactivation of BRCA2 in Fanconi anemia. *Science*. 297:606-609.

Hu, J., L. Sun, F. Shen, Y. Chen, Y. Hua, Y. Liu, M. Zhang, Y. Hu, Q. Wang, W. Xu, F. Sun, J. Ji, J.M. Murray, A.M. Carr, and D. Kong. 2012. The intra-S phase checkpoint targets Dna2 to prevent stalled replication forks from reversing. *Cell*. 149:1221-1232.

Huang, J., S. Liu, M.A. Bellani, A.K. Thazhathveetil, C. Ling, J.P. de Winter, Y. Wang, W. Wang, and M.M. Seidman. 2013. The DNA translocase FANCM/MHF promotes replication traverse of DNA interstrand crosslinks. *Mol Cell*. 52:434-446.

Huang, M., J.M. Kim, B. Shiotani, K. Yang, L. Zou, and A.D. D'Andrea. 2010. The FANCM/FAAP24 complex is required for the DNA interstrand crosslink-induced checkpoint response. *Mol Cell*. 39:259-268.

Ishiai, M., H. Kitao, A. Smogorzewska, J. Tomida, A. Kinomura, E. Uchida, A. Saberi, E. Kinoshita, E. Kinoshita-Kikuta, T. Koike, S. Tashiro, S.J. Elledge, and M. Takata. 2008. FANCI phosphorylation functions as a molecular switch to turn on the Fanconi anemia pathway. *Nature structural & molecular biology*. 15:1138-1146.

Itan, Y., L. Shang, B. Boisson, M.J. Ciancanelli, J.G. Markle, R. Martinez-Barricarte, E. Scott, I. Shah, P.D. Stenson, J. Gleeson, D.N. Cooper, L. Quintana-Murci, S.Y. Zhang, L. Abel, and J.L. Casanova. 2016. The mutation significance cutoff: gene-level thresholds for variant predictions. *Nature methods*. 13:109-110.

Jacquinet, A., L. Brown, J. Sawkins, P. Liu, D. Pugash, M.I. Van Allen, and M.S. Patel. 2018. Expanding the FANCO/RAD51C associated phenotype: Cleft lip and palate and lobar holoprosencephaly, two rare findings in Fanconi anemia. *Eur J Med Genet*. 61:257-261.

Jasin, M., and R. Rothstein. 2013. Repair of strand breaks by homologous recombination. *Cold Spring Harb Perspect Biol*. 5:a012740.

Jaspers, J.E., A. Kersbergen, U. Boon, W. Sol, L. van Deemter, S.A. Zander, R. Drost, E. Wientjens, J. Ji, A. Aly, J.H. Doroshow, A. Cranston, N.M. Martin, A. Lau, M.J. O'Connor, S. Ganesan, P. Borst, J. Jonkers, and S. Rottenberg. 2013. Loss of 53BP1 causes PARP inhibitor resistance in Brca1-mutated mouse mammary tumors. *Cancer Discov*. 3:68-81.

Jensen, R.B. 2013. BRCA2: one small step for DNA repair, one giant protein purified. *Yale J Biol Med*. 86:479-489.

Jensen, R.B., A. Carreira, and S.C. Kowalczykowski. 2010. Purified human BRCA2 stimulates RAD51-mediated recombination. *Nature*. 467:678-683.

Kalb, R., K. Neveling, H. Hoehn, H. Schneider, Y. Linka, S.D. Batish, C. Hunt, M. Berwick, E. Callen, J. Surralles, J.A. Casado, J. Bueren, A. Dasi, J. Soulier, E. Gluckman, C.M. Zwaan, R. van Spaendonk, G. Pals, J.P. de Winter, H. Joenje, M. Grompe, A.D. Auerbach, H. Hanenberg, and D. Schindler. 2007. Hypomorphic mutations in the gene encoding a key Fanconi anemia protein, FANCD2, sustain a significant group of FA-D2 patients with severe phenotype. *American journal of human genetics*. 80:895-910.

Karanja, K.K., S.W. Cox, J.P. Duxin, S.A. Stewart, and J.L. Campbell. 2012. DNA2 and EXO1 in replication-coupled, homology-directed repair and in the interplay between HDR and the FA/BRCA network. *Cell cycle*. 11:3983-3996.

Karanja, K.K., E.H. Lee, E.A. Hendrickson, and J.L. Campbell. 2014. Preventing over-resection by DNA2 helicase/nuclease suppresses repair defects in Fanconi anemia cells. *Cell cycle*. 13:1540-1550.

Kehrli, K.R., and J.M. Sidorova. 2014. Mitomycin C reduces abundance of replication forks but not rates of fork progression in primary and transformed human cells. *Oncoscience*. 1:540-555.

Kelsall, I.R., J. Langenick, C. MacKay, K.J. Patel, and A.F. Alpi. 2012. The Fanconi anaemia components UBE2T and FANCM are functionally linked to nucleotide excision repair. *PLoS One*. 7:e36970.

Khincha, P.P., and S.A. Savage. 2013. Genomic characterization of the inherited bone marrow failure syndromes. *Semin Hematol*. 50:333-347.

Kienker, L.J., E.K. Shin, and K. Meek. 2000. Both V(D)J recombination and radioresistance require DNA-PK kinase activity, though minimal levels suffice for V(D)J recombination. *Nucleic acids research*. 28:2752-2761.

Kile, A.C., D.A. Chavez, J. Bacal, S. Eldirany, D.M. Korzhnev, I. Bezsonova, B.F. Eichman, and K.A. Cimprich. 2015. HLTF's Ancient HIRAN Domain Binds 3' DNA Ends to Drive Replication Fork Reversal. *Mol Cell*. 58:1090-1100.

Kim, J., J.H. Kim, S.H. Lee, D.H. Kim, H.Y. Kang, S.H. Bae, Z.Q. Pan, and Y.S. Seo. 2002. The novel human DNA helicase hFBH1 is an F-box protein. *J Biol Chem*. 277:24530-24537.

Kim, T.M., M.Y. Son, S. Dodds, L. Hu, and P. Hasty. 2014. Deletion of BRCA2 exon 27 causes defects in response to both stalled and collapsed replication forks. *Mutat Res*. 766-767:66-72.

Kim, Y., F.P. Lach, R. Desetty, H. Hanenberg, A.D. Auerbach, and A. Smogorzewska. 2011. Mutations of the SLX4 gene in Fanconi anemia. *Nature genetics*. 43:142-146.

Kim, Y., G.S. Spitz, U. Veturi, F.P. Lach, A.D. Auerbach, and A. Smogorzewska. 2013. Regulation of multiple DNA repair pathways by the Fanconi anemia protein SLX4. *Blood*. 121:54-63.

King, M.C. 2014. "The race" to clone BRCA1. *Science (New York, N.Y.)*. 343:1462-1465.

Kircher, M., D.M. Witten, P. Jain, B.J. O'Roak, G.M. Cooper, and J. Shendure. 2014. A general framework for estimating the relative pathogenicity of human genetic variants. *Nature genetics*. 46:310-315.

Klein Douwel, D., R.A. Boonen, D.T. Long, A.A. Szypowska, M. Raschle, J.C. Walter, and P. Knipscheer. 2014. XPF-ERCC1 acts in Unhooking DNA interstrand crosslinks in cooperation with FANCD2 and FANCP/SLX4. *Mol Cell*. 54:460-471.

Knipscheer, P., M. Raschle, A. Smogorzewska, M. Enoiu, T.V. Ho, O.D. Scharer, S.J. Elledge, and J.C. Walter. 2009. The Fanconi anemia pathway promotes replication-dependent DNA interstrand cross-link repair. *Science*. 326:1698-1701.

Kolinjivadi, A.M., V. Sannino, A. De Antoni, K. Zadorozhny, M. Kilkenny, H. Techer, G. Baldi, R. Shen, A. Ciccia, L. Pellegrini, L. Krejci, and V. Costanzo. 2017. Smarcal1-Mediated Fork Reversal Triggers Mre11-Dependent Degradation of Nascent DNA in the Absence of Brca2 and Stable Rad51 Nucleofilaments. *Mol Cell*. 67:867-881 e867.

Kottemann, M.C., and A. Smogorzewska. 2013. Fanconi anaemia and the repair of Watson and Crick DNA crosslinks. *Nature*. 493:356-363.

Kratz, K., B. Schopf, S. Kaden, A. Sendoel, R. Eberhard, C. Lademann, E. Cannavo, A.A. Sartori, M.O. Hengartner, and J. Jiricny. 2010. Deficiency of FANCD2-associated nuclease KIAA1018/FAN1 sensitizes cells to interstrand crosslinking agents. *Cell*. 142:77-88.

Kumagai, A., J. Lee, H.Y. Yoo, and W.G. Dunphy. 2006. TopBP1 activates the ATR-ATRIP complex. *Cell*. 124:943-955.

Kurimasa, A., S. Kumano, N.V. Boubnov, M.D. Story, C.S. Tung, S.R. Peterson, and D.J. Chen. 1999. Requirement for the kinase activity of human DNA-dependent protein kinase catalytic subunit in DNA strand break rejoining. *Molecular and cellular biology*. 19:3877-3884.

Kutler, D.I., A.D. Auerbach, J. Satagopan, P.F. Giampietro, S.D. Batish, A.G. Huvos, A. Goberdhan, J.P. Shah, and B. Singh. 2003. High incidence of head and neck squamous cell carcinoma in patients with Fanconi anemia. *Arch Otolaryngol Head Neck Surg*. 129:106-112.

Kutler, D.I., K.R. Patel, A.D. Auerbach, J. Kennedy, F.P. Lach, E. Sanborn, M.A. Cohen, W.I. Kuhel, and A. Smogorzewska. 2016. Natural history and management of Fanconi anemia patients with head and neck cancer: A 10-year follow-up. *Laryngoscope*. 126:870-879.

Langevin, F., G.P. Crossan, I.V. Rosado, M.J. Arends, and K.J. Patel. 2011. Fancd2 counteracts the toxic effects of naturally produced aldehydes in mice. *Nature*. 475:53-58.

Lee, J., and W.G. Dunphy. 2013. The Mre11-Rad50-Nbs1 (MRN) complex has a specific role in the activation of Chk1 in response to stalled replication forks. *Mol Biol Cell*. 24:1343-1353.

Lek, M., K.J. Karczewski, E.V. Minikel, K.E. Samocha, E. Banks, T. Fennell, A.H. O'Donnell-Luria, J.S. Ware, A.J. Hill, B.B. Cummings, T. Tukiainen, D.P. Birnbaum, J.A. Kosmicki, L.E. Duncan, K. Estrada, F. Zhao, J. Zou, E. Pierce-Hoffman, J. Berghout, D.N. Cooper, N. Deflaux, M. DePristo, R. Do, J. Flannick, M. Fromer, L. Gauthier, J. Goldstein, N. Gupta, D. Howrigan, A. Kiezun, M.I. Kurki, A.L. Moonshine, P. Natarajan, L. Orozco, G.M. Peloso, R. Poplin, M.A. Rivas, V. Ruano-Rubio, S.A. Rose, D.M. Ruderfer, K. Shakir, P.D. Stenson, C. Stevens, B.P. Thomas, G. Tiao, M.T. Tusie-Luna, B. Weisburd, H.H. Won, D. Yu, D.M. Altshuler, D. Ardissino, M. Boehnke, J. Danesh, S. Donnelly, R. Elosua, J.C. Florez, S.B. Gabriel, G. Getz, S.J. Glatt, C.M. Hultman, S. Kathiresan, M. Laakso, S. McCarroll, M.I. McCarthy, D. McGovern, R. McPherson, B.M. Neale, A. Palotie, S.M. Purcell, D. Saleheen, J.M. Scharf, P. Sklar, P.F. Sullivan, J. Tuomilehto, M.T. Tsuang, H.C. Watkins, J.G. Wilson, M.J. Daly, D.G. MacArthur, and C. Exome Aggregation. 2016. Analysis of protein-coding genetic variation in 60,706 humans. *Nature*. 536:285-291.

Lemacon, D., J. Jackson, A. Quinet, J.R. Brickner, S. Li, S. Yazinski, Z. You, G. Ira, L. Zou, N. Mosammaparast, and A. Vindigni. 2017. MRE11 and EXO1

nucleases degrade reversed forks and elicit MUS81-dependent fork rescue in BRCA2-deficient cells. *Nat Commun*. 8:860.

Leuzzi, G., V. Marabitti, P. Pichierri, and A. Franchitto. 2016. WRNIP1 protects stalled forks from degradation and promotes fork restart after replication stress. *EMBO J*. 35:1437-1451.

Li, H., and R. Durbin. 2009. Fast and accurate short read alignment with Burrows-Wheeler transform. *Bioinformatics*. 25:1754-1760.

Litman, R., M. Peng, Z. Jin, F. Zhang, J. Zhang, S. Powell, P.R. Andreassen, and S.B. Cantor. 2005. BACH1 is critical for homologous recombination and appears to be the Fanconi anemia gene product FANCJ. *Cancer cell*. 8:255-265.

Liu, C.Y., A. Flesken-Nikitin, S. Li, Y. Zeng, and W.H. Lee. 1996. Inactivation of the mouse Brca1 gene leads to failure in the morphogenesis of the egg cylinder in early postimplantation development. *Genes & development*. 10:1835-1843.

Liu, S., S. Bekker-Jensen, N. Mailand, C. Lukas, J. Bartek, and J. Lukas. 2006. Claspin operates downstream of TopBP1 to direct ATR signaling towards Chk1 activation. *Molecular and cellular biology*. 26:6056-6064.

Liu, T., G. Ghosal, J. Yuan, J. Chen, and J. Huang. 2010. FAN1 acts with FANCI-FANCD2 to promote DNA interstrand cross-link repair. *Science*. 329:693-696.

Lo Ten Foe, J.R., M.L. Kwee, M.A. Rooimans, A.B. Oostra, A.J. Veerman, M. van Weel, R.M. Pauli, N.T. Shahidi, I. Dokal, I. Roberts, C. Altay, E. Gluckman, R.A. Gibson, C.G. Mathew, F. Arwert, and H. Joenje. 1997. Somatic mosaicism in Fanconi anemia: molecular basis and clinical significance. *European journal of human genetics : EJHG*. 5:137-148.

Long, D.T., M. Raschle, V. Joukov, and J.C. Walter. 2011. Mechanism of RAD51-dependent DNA interstrand cross-link repair. *Science (New York, N.Y.)*. 333:84-87.

Longerich, S., Y. Kwon, M.S. Tsai, A.S. Hlaing, G.M. Kupfer, and P. Sung. 2014. Regulation of FANCD2 and FANCI monoubiquitination by their interaction and by DNA. *Nucleic acids research*. 42:5657-5670.

Longerich, S., J. San Filippo, D. Liu, and P. Sung. 2009. FANCI binds branched DNA and is monoubiquitinated by UBE2T-FANCL. *The Journal of biological chemistry*. 284:23182-23186.

Lord, C.J., and A. Ashworth. 2016. BRCAness revisited. *Nat Rev Cancer*. 16:110-120.

Lord, C.J., and A. Ashworth. 2017. PARP inhibitors: Synthetic lethality in the clinic. *Science*. 355:1152-1158.

Ludwig, T., D.L. Chapman, V.E. Papaioannou, and A. Efstratiadis. 1997. Targeted mutations of breast cancer susceptibility gene homologs in mice: lethal phenotypes of Brca1, Brca2, Brca1/Brca2, Brca1/p53, and Brca2/p53 nullizygous embryos. *Genes Dev*. 11:1226-1241.

Lundin, C., K. Erixon, C. Arnaudeau, N. Schultz, D. Jenssen, M. Meuth, and T. Helleday. 2002. Different roles for nonhomologous end joining and homologous recombination following replication arrest in mammalian cells. *Mol Cell Biol*. 22:5869-5878.

Lv, Z., K.A. Rickman, L. Yuan, K. Williams, S.P. Selvam, A.N. Woosley, P.H. Howe, B. Ogretmen, A. Smogorzewska, and S.K. Olsen. 2017. S. pombe Uba1-Ubc15 Structure Reveals a Novel Regulatory Mechanism of Ubiquitin E2 Activity. *Molecular cell*. 65:699-714 e696.

Machida, Y.J., Y. Machida, Y. Chen, A.M. Gurtan, G.M. Kupfer, A.D. D'Andrea, and A. Dutta. 2006. UBE2T is the E2 in the Fanconi anemia pathway and undergoes negative autoregulation. *Molecular cell*. 23:589-596.

MacKay, C., A.C. Declais, C. Lundin, A. Agostinho, A.J. Deans, T.J. MacArtney, K. Hofmann, A. Gartner, S.C. West, T. Helleday, D.M. Lilley, and J. Rouse. 2010. Identification of KIAA1018/FAN1, a DNA repair nuclease recruited to DNA damage by monoubiquitinated FANCD2. *Cell*. 142:65-76.

Matsuoka, S., B.A. Ballif, A. Smogorzewska, E.R. McDonald, 3rd, K.E. Hurov, J. Luo, C.E. Bakalarski, Z. Zhao, N. Solimini, Y. Lerenthal, Y. Shiloh, S.P. Gygi, and S.J. Elledge. 2007. ATM and ATR substrate analysis reveals extensive protein networks responsive to DNA damage. *Science*. 316:1160-1166.

McPherson, J.P., B. Lemmers, R. Chahwan, A. Pamidi, E. Migon, E. Matysiak-Zablocki, M.E. Moynahan, J. Essers, K. Hanada, A. Poonepalli, O. Sanchez-Sweatman, R. Khokha, R. Kanaar, M. Jasin, M.P. Hande, and R. Hakem. 2004. Involvement of mammalian Mus81 in genome integrity and tumor suppression. *Science (New York, N.Y.)*. 304:1822-1826.

Meetei, A.R., J.P. de Winter, A.L. Medhurst, M. Wallisch, Q. Waisfisz, H.J. van de Vrugt, A.B. Oostra, Z. Yan, C. Ling, C.E. Bishop, M.E. Hoatlin, H. Joenje, and W. Wang. 2003a. A novel ubiquitin ligase is deficient in Fanconi anemia. *Nature genetics*. 35:165-170.

Meetei, A.R., M. Levitus, Y. Xue, A.L. Medhurst, M. Zwaan, C. Ling, M.A. Rooimans, P. Bier, M. Hoatlin, G. Pals, J.P. de Winter, W. Wang, and H. Joenje.

2004. X-linked inheritance of Fanconi anemia complementation group B. *Nature genetics*. 36:1219-1224.

Meetei, A.R., S. Sechi, M. Wallisch, D. Yang, M.K. Young, H. Joenje, M.E. Hoatlin, and W. Wang. 2003b. A multiprotein nuclear complex connects Fanconi anemia and Bloom syndrome. *Molecular and cellular biology*. 23:3417-3426.

Mehmet Demirel, U.S., Gumruk Fatma, Akarsu Nurten Ayse. 2016. A Homozygous Germ Line Nonsense Mutation in BRCA1 Leading Fanconi Anemia and Neuroblastoma. *Blood*. 128.

Mijic, S., R. Zellweger, N. Chappidi, M. Berti, K. Jacobs, K. Mutreja, S. Ursich, A. Ray Chaudhuri, A. Nussenzweig, P. Janscak, and M. Lopes. 2017. Replication fork reversal triggers fork degradation in BRCA2-defective cells. *Nat Commun*. 8:859.

Mimitou, E.P., and L.S. Symington. 2008. Sae2, Exo1 and Sgs1 collaborate in DNA double-strand break processing. *Nature*. 455:770-774.

Mirzoeva, O.K., and J.H. Petrini. 2003. DNA replication-dependent nuclear dynamics of the Mre11 complex. *Mol Cancer Res*. 1:207-218.

Moder, M., G. Velimezi, M. Owusu, A. Mazouzi, M. Wiedner, J. Ferreira da Silva, L. Robinson-Garcia, F. Schischlik, R. Slavkovsky, R. Kralovics, M. Schuster, C.

Bock, T. Ideker, S.P. Jackson, J. Menche, and J.I. Loizou. 2017. Parallel genome-wide screens identify synthetic viable interactions between the BLM helicase complex and Fanconi anemia. *Nature communications*. 8:1238.

Montillo, M., F. Ricci, and A. Tedeschi. 2006. Role of fludarabine in hematological malignancies. *Expert Rev Anticancer Ther*. 6:1141-1161.

Mordes, D.A., G.G. Glick, R. Zhao, and D. Cortez. 2008. TopBP1 activates ATR through ATRIP and a PIKK regulatory domain. *Genes & development*. 22:1478-1489.

Motegi, A., H.J. Liaw, K.Y. Lee, H.P. Roest, A. Maas, X. Wu, H. Moinova, S.D. Markowitz, H. Ding, J.H. Hoeijmakers, and K. Myung. 2008. Polyubiquitination of proliferating cell nuclear antigen by HLTF and SHPRH prevents genomic instability from stalled replication forks. *Proc Natl Acad Sci U S A*. 105:12411-12416.

Moynahan, M.E., J.W. Chiu, B.H. Koller, and M. Jasin. 1999. Brca1 controls homology-directed DNA repair. *Mol Cell*. 4:511-518.

Moynahan, M.E., A.J. Pierce, and M. Jasin. 2001. BRCA2 is required for homology-directed repair of chromosomal breaks. *Mol Cell*. 7:263-272.

Murfuni, I., S. Nicolai, S. Baldari, M. Crescenzi, M. Bignami, A. Franchitto, and P. Pichierri. 2013. The WRN and MUS81 proteins limit cell death and genome instability following oncogene activation. *Oncogene*. 32:610-620.

Myers, K., S.M. Davies, R.E. Harris, S.L. Spunt, T. Smolarek, S. Zimmerman, R. McMasters, L. Wagner, R. Mueller, A.D. Auerbach, and P.A. Mehta. 2012. The clinical phenotype of children with Fanconi anemia caused by biallelic FANCD1/BRCA2 mutations. *Pediatric blood & cancer*. 58:462-465.

Naim, V., T. Wilhelm, M. Debatisse, and F. Rosselli. 2013. ERCC1 and MUS81-EME1 promote sister chromatid separation by processing late replication intermediates at common fragile sites during mitosis. *Nat Cell Biol*. 15:1008-1015.

Nalepa, G., and D.W. Clapp. 2018. Fanconi anaemia and cancer: an intricate relationship. *Nat Rev Cancer*. 18:168-185.

Neelsen, K.J., I.M. Zanini, R. Herrador, and M. Lopes. 2013. Oncogenes induce genotoxic stress by mitotic processing of unusual replication intermediates. *J Cell Biol*. 200:699-708.

Ng, B.G., L.A. Wolfe, M. Ichikawa, T. Markello, M. He, C.J. Tifft, W.A. Gahl, and H.H. Freeze. 2015. Biallelic mutations in CAD, impair de novo pyrimidine

biosynthesis and decrease glycosylation precursors. *Hum Mol Genet*. 24:3050-3057.

Ng, S.B., K.J. Buckingham, C. Lee, A.W. Bigham, H.K. Tabor, K.M. Dent, C.D. Huff, P.T. Shannon, E.W. Jabs, D.A. Nickerson, J. Shendure, and M.J. Bamshad. 2010. Exome sequencing identifies the cause of a mendelian disorder. *Nature genetics*. 42:30-35.

Niedernhofer, L.J., H. Odijk, M. Budzowska, E. van Drunen, A. Maas, A.F. Theil, J. de Wit, N.G. Jaspers, H.B. Beverloo, J.H. Hoeijmakers, and R. Kanaar. 2004. The structure-specific endonuclease Ercc1-Xpf is required to resolve DNA interstrand cross-link-induced double-strand breaks. *Molecular and cellular biology*. 24:5776-5787.

Nielsen, F.C., T. van Overeem Hansen, and C.S. Sorensen. 2016. Hereditary breast and ovarian cancer: new genes in confined pathways. *Nat Rev Cancer*. 16:599-612.

Norquist, B., K.A. Wurz, C.C. Pennil, R. Garcia, J. Gross, W. Sakai, B.Y. Karlan, T. Taniguchi, and E.M. Swisher. 2011. Secondary somatic mutations restoring BRCA1/2 predict chemotherapy resistance in hereditary ovarian carcinomas. *J Clin Oncol*. 29:3008-3015.

O'Donnell, M., L. Langston, and B. Stillman. 2013. Principles and concepts of DNA replication in bacteria, archaea, and eukarya. *Cold Spring Harb Perspect Biol*. 5.

Oberbeck, N., F. Langevin, G. King, N. de Wind, G.P. Crossan, and K.J. Patel. 2014. Maternal aldehyde elimination during pregnancy preserves the fetal genome. *Molecular cell*. 55:807-817.

Olson, E., C.J. Nievera, A.Y. Lee, L. Chen, and X. Wu. 2007. The Mre11-Rad50-Nbs1 complex acts both upstream and downstream of ataxia telangiectasia mutated and Rad3-related protein (ATR) to regulate the S-phase checkpoint following UV treatment. *J Biol Chem*. 282:22939-22952.

Oostra, A.B., A.W. Nieuwint, H. Joenje, and J.P. de Winter. 2012. Diagnosis of fanconi anemia: chromosomal breakage analysis. *Anemia*. 2012:238731.

Orthwein, A., S.M. Noordermeer, M.D. Wilson, S. Landry, R.I. Enchev, A. Sherker, M. Munro, J. Pinder, J. Salsman, G. Dellaire, B. Xia, M. Peter, and D. Durocher. 2015. A mechanism for the suppression of homologous recombination in G1 cells. *Nature*. 528:422-426.

Patch, A.M., E.L. Christie, D. Etemadmoghadam, D.W. Garsed, J. George, S. Fereday, K. Nones, P. Cowin, K. Alsop, P.J. Bailey, K.S. Kassahn, F. Newell, M.C. Quinn, S. Kazakoff, K. Quek, C. Wilhelm-Benartzi, E. Curry, H.S. Leong, G.

Australian Ovarian Cancer Study, A. Hamilton, L. Mileshkin, G. Au-Yeung, C. Kennedy, J. Hung, Y.E. Chiew, P. Harnett, M. Friedlander, M. Quinn, J. Pyman, S. Cordner, P. O'Brien, J. Leditschke, G. Young, K. Strachan, P. Waring, W. Azar, C. Mitchell, N. Traficante, J. Hendley, H. Thorne, M. Shackleton, D.K. Miller, G.M. Arnau, R.W. Tothill, T.P. Holloway, T. Semple, I. Harliwong, C. Nourse, E. Nourbakhsh, S. Manning, S. Idrisoglu, T.J. Bruxner, A.N. Christ, B. Poudel, O. Holmes, M. Anderson, C. Leonard, A. Lonie, N. Hall, S. Wood, D.F. Taylor, Q. Xu, J.L. Fink, N. Waddell, R. Drapkin, E. Stronach, H. Gabra, R. Brown, A. Jewell, S.H. Nagaraj, E. Markham, P.J. Wilson, J. Ellul, O. McNally, M.A. Doyle, R. Vedururu, C. Stewart, E. Lengyel, J.V. Pearson, N. Waddell, A. deFazio, S.M. Grimmond, and D.D. Bowtell. 2015. Whole-genome characterization of chemoresistant ovarian cancer. *Nature*. 521:489-494.

Patel, K.J., V.P. Yu, H. Lee, A. Corcoran, F.C. Thistlethwaite, M.J. Evans, W.H. Colledge, L.S. Friedman, B.A. Ponder, and A.R. Venkitaraman. 1998. Involvement of Brca2 in DNA repair. *Molecular cell*. 1:347-357.

Pepe, A., and S.C. West. 2014. MUS81-EME2 promotes replication fork restart. *Cell Rep*. 7:1048-1055.

Petermann, E., M.L. Orta, N. Issaeva, N. Schultz, and T. Helleday. 2010. Hydroxyurea-stalled replication forks become progressively inactivated and

require two different RAD51-mediated pathways for restart and repair. *Mol Cell*. 37:492-502.

Petryk, A., R. Kanakatti Shankar, N. Giri, A.N. Hollenberg, M.M. Rutter, B. Nathan, M. Lodish, B.P. Alter, C.A. Stratakis, and S.R. Rose. 2015. Endocrine disorders in Fanconi anemia: recommendations for screening and treatment. *J Clin Endocrinol Metab*. 100:803-811.

Pettitt, S.J., F.L. Rehman, I. Bajrami, R. Brough, F. Wallberg, I. Kozarewa, K. Fenwick, I. Assiotis, L. Chen, J. Campbell, C.J. Lord, and A. Ashworth. 2013. A genetic screen using the PiggyBac transposon in haploid cells identifies Parp1 as a mediator of olaparib toxicity. *PLoS One*. 8:e61520.

Phelan, C.M., J. Iqbal, H.T. Lynch, J. Lubinski, J. Gronwald, P. Moller, P. Ghadirian, W.D. Foulkes, S. Armel, A. Eisen, S.L. Neuhausen, L. Senter, C.F. Singer, P. Ainsworth, C. Kim-Sing, N. Tung, M. Llacuachaqui, G. Chornokur, S. Ping, S.A. Narod, and G. Hereditary Breast Cancer Study. 2014. Incidence of colorectal cancer in BRCA1 and BRCA2 mutation carriers: results from a follow-up study. *Br J Cancer*. 110:530-534.

Pichierri, P., A. Franchitto, and F. Rosselli. 2004. BLM and the FANC proteins collaborate in a common pathway in response to stalled replication forks. *EMBO J*. 23:3154-3163.

Pinder, J., J. Salsman, and G. Dellaire. 2015. Nuclear domain 'knock-in' screen for the evaluation and identification of small molecule enhancers of CRISPR-based genome editing. *Nucleic acids research*. 43:9379-9392.

Poole, L.A., and D. Cortez. 2017. Functions of SMARCAL1, ZRANB3, and HLTF in maintaining genome stability. *Crit Rev Biochem Mol Biol*. 52:696-714.

Poole, L.A., R. Zhao, G.G. Glick, C.A. Lovejoy, C.M. Eischen, and D. Cortez. 2015. SMARCAL1 maintains telomere integrity during DNA replication. *Proc Natl Acad Sci U S A*. 112:14864-14869.

Postow, L., E.M. Woo, B.T. Chait, and H. Funabiki. 2009. Identification of SMARCAL1 as a component of the DNA damage response. *J Biol Chem*. 284:35951-35961.

Prakash, R., Y. Zhang, W. Feng, and M. Jasin. 2015. Homologous recombination and human health: the roles of BRCA1, BRCA2, and associated proteins. *Cold Spring Harb Perspect Biol*. 7:a016600.

Quinet, A., D. Lemacon, and A. Vindigni. 2017. Replication Fork Reversal: Players and Guardians. *Molecular cell*. 68:830-833.

Rahman, N., S. Seal, D. Thompson, P. Kelly, A. Renwick, A. Elliott, S. Reid, K. Spanova, R. Barfoot, T. Chagtai, H. Jayatilake, L. McGuffog, S. Hanks, D.G. Evans, D. Eccles, D.F. Easton, and M.R. Stratton. 2007. PALB2, which encodes a BRCA2-interacting protein, is a breast cancer susceptibility gene. *Nature genetics*. 39:165-167.

Rainger, J., H. Bengani, L. Campbell, E. Anderson, K. Sokhi, W. Lam, A. Riess, M. Ansari, S. Smithson, M. Lees, C. Mercer, K. McKenzie, T. Lengfeld, B. Gener Querol, P. Branney, S. McKay, H. Morrison, B. Medina, M. Robertson, J. Kohlhase, C. Gordon, J. Kirk, D. Wieczorek, and D.R. Fitzpatrick. 2012. Miller (Genee-Wiedemann) syndrome represents a clinically and biochemically distinct subgroup of postaxial acrofacial dysostosis associated with partial deficiency of DHODH. *Hum Mol Genet*. 21:3969-3983.

Rajendra, E., V.H. Oestergaard, F. Langevin, M. Wang, G.L. Dornan, K.J. Patel, and L.A. Passmore. 2014. The genetic and biochemical basis of FANCD2 monoubiquitination. *Molecular cell*. 54:858-869.

Raschle, M., P. Knipscheer, M. Enoiu, T. Angelov, J. Sun, J.D. Griffith, T.E. Ellenberger, O.D. Scharer, and J.C. Walter. 2008. Mechanism of replication-coupled DNA interstrand crosslink repair. *Cell*. 134:969-980.

Raschle, M., G. Smeenk, R.K. Hansen, T. Temu, Y. Oka, M.Y. Hein, N. Nagaraj, D.T. Long, J.C. Walter, K. Hofmann, Z. Storchova, J. Cox, S. Bekker-Jensen, N. Mailand, and M. Mann. 2015. DNA repair. Proteomics reveals dynamic assembly of repair complexes during bypass of DNA cross-links. *Science*. 348:1253671.

Ratajska, M., E. Antoszewska, A. Piskorz, I. Brozek, A. Borg, H. Kusmierek, W. Biernat, and J. Limon. 2012. Cancer predisposing BARD1 mutations in breast-ovarian cancer families. *Breast cancer research and treatment*. 131:89-97.

Ray Chaudhuri, A., E. Callen, X. Ding, E. Gogola, A.A. Duarte, J.E. Lee, N. Wong, V. Lafarga, J.A. Calvo, N.J. Panzarino, S. John, A. Day, A.V. Crespo, B. Shen, L.M. Starnes, J.R. de Ruiter, J.A. Daniel, P.A. Konstantinopoulos, D. Cortez, S.B. Cantor, O. Fernandez-Capetillo, K. Ge, J. Jonkers, S. Rottenberg, S.K. Sharan, and A. Nussenzweig. 2016. Replication fork stability confers chemoresistance in BRCA-deficient cells. *Nature*. 535:382-387.

Ray Chaudhuri, A., Y. Hashimoto, R. Herrador, K.J. Neelsen, D. Fachinetti, R. Bermejo, A. Cocito, V. Costanzo, and M. Lopes. 2012. Topoisomerase I poisoning results in PARP-mediated replication fork reversal. *Nat Struct Mol Biol*. 19:417-423.

Regairaz, M., Y.W. Zhang, H. Fu, K.K. Agama, N. Tata, S. Agrawal, M.I. Aladjem, and Y. Pommier. 2011. Mus81-mediated DNA cleavage resolves replication forks stalled by topoisomerase I-DNA complexes. *J Cell Biol*. 195:739-749.

Ren, X., Z. Ji, C.M. McHale, J. Yuh, J. Bersonda, M. Tang, M.T. Smith, and L. Zhang. 2013. The impact of FANCD2 deficiency on formaldehyde-induced toxicity in human lymphoblastoid cell lines. *Archives of toxicology*. 87:189-196.

Rickman, K.A., F.P. Lach, A. Abhyankar, F.X. Donovan, E.M. Sanborn, J.A. Kennedy, C. Sougnez, S.B. Gabriel, O. Elemento, S.C. Chandrasekharappa, D. Schindler, A.D. Auerbach, and A. Smogorzewska. 2015. Deficiency of UBE2T, the E2 Ubiquitin Ligase Necessary for FANCD2 and FANCI Ubiquitination, Causes FA-T Subtype of Fanconi Anemia. *Cell reports*. 12:35-41.

Ridpath, J.R., A. Nakamura, K. Tano, A.M. Luke, E. Sonoda, H. Arakawa, J.M. Buerstedde, D.A. Gillespie, J.E. Sale, M. Yamazoe, D.K. Bishop, M. Takata, S. Takeda, M. Watanabe, J.A. Swenberg, and J. Nakamura. 2007. Cells deficient in the FANC/BRCA pathway are hypersensitive to plasma levels of formaldehyde. *Cancer research*. 67:11117-11122.

Roach, J.C., G. Glusman, A.F. Smit, C.D. Huff, R. Hubley, P.T. Shannon, L. Rowen, K.P. Pant, N. Goodman, M. Bamshad, J. Shendure, R. Drmanac, L.B.

Jorde, L. Hood, and D.J. Galas. 2010. Analysis of genetic inheritance in a family quartet by whole-genome sequencing. *Science (New York, N.Y.)*. 328:636-639.

Robison, J.G., J. Elliott, K. Dixon, and G.G. Oakley. 2004. Replication protein A and the Mre11.Rad50.Nbs1 complex co-localize and interact at sites of stalled replication forks. *J Biol Chem*. 279:34802-34810.

Rondinelli, B., E. Gogola, H. Yucel, A.A. Duarte, M. van de Ven, R. van der Sluijs, P.A. Konstantinopoulos, J. Jonkers, R. Ceccaldi, S. Rottenberg, and A.D. D'Andrea. 2017. EZH2 promotes degradation of stalled replication forks by recruiting MUS81 through histone H3 trimethylation. *Nat Cell Biol*. 19:1371-1378.

Rottenberg, S., J.E. Jaspers, A. Kersbergen, E. van der Burg, A.O. Nygren, S.A. Zander, P.W. Derksen, M. de Bruin, J. Zevenhoven, A. Lau, R. Boulter, A. Cranston, M.J. O'Connor, N.M. Martin, P. Borst, and J. Jonkers. 2008. High sensitivity of BRCA1-deficient mammary tumors to the PARP inhibitor AZD2281 alone and in combination with platinum drugs. *Proc Natl Acad Sci U S A*. 105:17079-17084.

Roy, R., J. Chun, and S.N. Powell. 2012. BRCA1 and BRCA2: different roles in a common pathway of genome protection. *Nature reviews. Cancer*. 12:68-78.

Rustgi, A.K. 2014. Familial pancreatic cancer: genetic advances. *Genes & development*. 28:1-7.

Saeki, H., N. Siaud, N. Christ, W.W. Wiegant, P.P. van Buul, M. Han, M.Z. Zdzienicka, J.M. Stark, and M. Jasin. 2006. Suppression of the DNA repair defects of BRCA2-deficient cells with heterologous protein fusions. *Proceedings of the National Academy of Sciences of the United States of America*. 103:8768-8773.

Sakai, W., E.M. Swisher, B.Y. Karlan, M.K. Agarwal, J. Higgins, C. Friedman, E. Villegas, C. Jacquemont, D.J. Farrugia, F.J. Couch, N. Urban, and T. Taniguchi. 2008. Secondary mutations as a mechanism of cisplatin resistance in BRCA2-mutated cancers. *Nature*. 451:1116-1120.

Saldivar, J.C., D. Cortez, and K.A. Cimprich. 2017. The essential kinase ATR: ensuring faithful duplication of a challenging genome. *Nat Rev Mol Cell Biol*. 18:622-636.

Santos, C., A. Peixoto, P. Rocha, P. Pinto, S. Bizarro, M. Pinheiro, C. Pinto, R. Henrique, and M.R. Teixeira. 2014. Pathogenicity evaluation of BRCA1 and BRCA2 unclassified variants identified in Portuguese breast/ovarian cancer families. *J Mol Diagn*. 16:324-334.

Sarbajna, S., and S.C. West. 2014. Holliday junction processing enzymes as guardians of genome stability. *Trends Biochem Sci*. 39:409-419.

Sartori, A.A., C. Lukas, J. Coates, M. Mistrik, S. Fu, J. Bartek, R. Baer, J. Lukas, and S.P. Jackson. 2007. Human CtIP promotes DNA end resection. *Nature*. 450:509-514.

Sato, K., K. Toda, M. Ishiai, M. Takata, and H. Kurumizaka. 2012. DNA robustly stimulates FANCD2 monoubiquitylation in the complex with FANCI. *Nucleic acids research*. 40:4553-4561.

Sawyer, S.L., L. Tian, M. Kahkonen, J. Schwartzentruber, M. Kircher, G. University of Washington Centre for Mendelian, F.C. Consortium, J. Majewski, D.A. Dyment, A.M. Innes, K.M. Boycott, L.A. Moreau, J.S. Moilanen, and R.A. Greenberg. 2015. Biallelic mutations in BRCA1 cause a new Fanconi anemia subtype. *Cancer discovery*. 5:135-142.

Schlacher, K., N. Christ, N. Siaud, A. Egashira, H. Wu, and M. Jasin. 2011. Double-strand break repair-independent role for BRCA2 in blocking stalled replication fork degradation by MRE11. *Cell*. 145:529-542.

Schlacher, K., H. Wu, and M. Jasin. 2012. A distinct replication fork protection pathway connects Fanconi anemia tumor suppressors to RAD51-BRCA1/2. *Cancer Cell*. 22:106-116.

Schubert, L., T. Ho, S. Hoffmann, P. Haahr, C. Guerillon, and N. Mailand. 2017. RADX interacts with single-stranded DNA to promote replication fork stability. *EMBO Rep*.

Schwab, R.A., A.N. Blackford, and W. Niedzwiedz. 2010. ATR activation and replication fork restart are defective in FANCM-deficient cells. *The EMBO journal*. 29:806-818.

Scully, R., J. Chen, A. Plug, Y. Xiao, D. Weaver, J. Feunteun, T. Ashley, and D.M. Livingston. 1997. Association of BRCA1 with Rad51 in mitotic and meiotic cells. *Cell*. 88:265-275.

Semlow, D.R., J. Zhang, M. Budzowska, A.C. Drohat, and J.C. Walter. 2016. Replication-Dependent Unhooking of DNA Interstrand Cross-Links by the NEIL3 Glycosylase. *Cell*. 167:498-511 e414.

Sharan, S.K., M. Morimatsu, U. Albrecht, D.S. Lim, E. Regel, C. Dinh, A. Sands, G. Eichele, P. Hasty, and A. Bradley. 1997. Embryonic lethality and radiation hypersensitivity mediated by Rad51 in mice lacking Brca2. *Nature*. 386:804-810.

Shen, S.X., Z. Weaver, X. Xu, C. Li, M. Weinstein, L. Chen, X.Y. Guan, T. Ried, and C.X. Deng. 1998. A targeted disruption of the murine Brca1 gene causes gamma-irradiation hypersensitivity and genetic instability. *Oncogene*. 17:3115-3124.

Shimelis, H., R.L.S. Mesman, C. Von Nicolai, A. Ehlen, L. Guidugli, C. Martin, F. Calleja, H. Meeks, E. Hallberg, J. Hinton, J. Lilyquist, C. Hu, C.M. Aalfs, K. Aittomaki, I. Andrulis, H. Anton-Culver, V. Arndt, M.W. Beckmann, J. Benitez, N.V. Bogdanova, S.E. Bojesen, M.K. Bolla, A.L. Borresen-Dale, H. Brauch, P. Brennan, H. Brenner, A. Broeks, B. Brouwers, T. Bruning, B. Burwinkel, J. Chang-Claude, G. Chenevix-Trench, C.Y. Cheng, J.Y. Choi, J.M. Collee, A. Cox, S.S. Cross, K. Czene, H. Darabi, J. Dennis, T. Dork, I. Dos-Santos-Silva, A.M. Dunning, P.A. Fasching, J. Figueroa, H. Flyger, M. Garcia-Closas, G.G. Giles, G. Glendon, P. Guenel, C.A. Haiman, P. Hall, U. Hamann, M. Hartman, F.B. Hogervorst, A. Hollestelle, J.L. Hopper, H. Ito, A. Jakubowska, D. Kang, V.M. Kosma, V. Kristensen, K.N. Lai, D. Lambrechts, L.L. Marchand, J. Li, A. Lindblom, A. Lophatananon, J. Lubinski, E. Machackova, A. Mannermaa, S. Margolin, F. Marme, K. Matsuo, H. Miao, K. Michailidou, R.L. Milne, K. Muir, S.L. Neuhausen, H. Nevanlinna, J.E. Olson, C. Olswold, J.J.C. Oosterwijk, A. Osorio, P. Peterlongo, J. Peto, P.D.P. Pharoah, K. Pylkas, P. Radice, M.U. Rashid, V. Rhenius, A. Rudolph, S. Sangrajrang, E.J. Sawyer, M.K. Schmidt, M.J. Schoemaker, C. Seynaeve, M. Shah, C.Y. Shen, M. Shrubsole, et al. 2017. BRCA2 Hypomorphic

Missense Variants Confer Moderate Risks of Breast Cancer. *Cancer research*. 77:2789-2799.

Siaud, N., M.A. Barbera, A. Egashira, I. Lam, N. Christ, K. Schlacher, B. Xia, and M. Jasin. 2011. Plasticity of BRCA2 function in homologous recombination: genetic interactions of the PALB2 and DNA binding domains. *PLoS genetics*. 7:e1002409.

Singh, T.R., A.M. Ali, M. Paramasivam, A. Pradhan, K. Wahengbam, M.M. Seidman, and A.R. Meetei. 2013. ATR-dependent phosphorylation of FANCM at serine 1045 is essential for FANCM functions. *Cancer research*. 73:4300-4310.

Smogorzewska, A., R. Desetty, T.T. Saito, M. Schlabach, F.P. Lach, M.E. Sowa, A.B. Clark, T.A. Kunkel, J.W. Harper, M.P. Colaiacovo, and S.J. Elledge. 2010. A genetic screen identifies FAN1, a Fanconi anemia-associated nuclease necessary for DNA interstrand crosslink repair. *Molecular cell*. 39:36-47.

Smogorzewska, A., S. Matsuoka, P. Vinciguerra, E.R. McDonald, 3rd, K.E. Hurov, J. Luo, B.A. Ballif, S.P. Gygi, K. Hofmann, A.D. D'Andrea, and S.J. Elledge. 2007a. Identification of the FANCI protein, a monoubiquitinated FANCD2 paralog required for DNA repair. *Cell*. 129:289-301.

Smogorzewska, E.M., L. Dukes, L. Kuo, and N. Kapoor. 2007b. Nucleated red blood cells in normal bone marrow for transplantation. *Medycyna wieku rozwojowego*. 11:7-11.

Snouwaert, J.N., L.C. Gowen, A.M. Latour, A.R. Mohn, A. Xiao, L. DiBiase, and B.H. Koller. 1999. BRCA1 deficient embryonic stem cells display a decreased homologous recombination frequency and an increased frequency of non-homologous recombination that is corrected by expression of a brca1 transgene. *Oncogene*. 18:7900-7907.

Somyajit, K., S. Saxena, S. Babu, A. Mishra, and G. Nagaraju. 2015. Mammalian RAD51 paralogs protect nascent DNA at stalled forks and mediate replication restart. *Nucleic Acids Res*. 43:9835-9855.

Sonoda, E., M.S. Sasaki, C. Morrison, Y. Yamaguchi-Iwai, M. Takata, and S. Takeda. 1999. Sister chromatid exchanges are mediated by homologous recombination in vertebrate cells. *Molecular and cellular biology*. 19:5166-5169.

Sorensen, C.S., R.G. Syljuasen, J. Lukas, and J. Bartek. 2004. ATR, Claspin and the Rad9-Rad1-Hus1 complex regulate Chk1 and Cdc25A in the absence of DNA damage. *Cell cycle*. 3:941-945.

Soulier, J., T. Leblanc, J. Larghero, H. Dastot, A. Shimamura, P. Guardiola, H. Esperou, C. Ferry, C. Jubert, J.P. Feugeas, A. Henri, A. Toubert, G. Socie, A. Baruchel, F. Sigaux, A.D. D'Andrea, and E. Gluckman. 2005. Detection of somatic mosaicism and classification of Fanconi anemia patients by analysis of the FA/BRCA pathway. *Blood*. 105:1329-1336.

Stivaros, S.M., R. Alston, N.B. Wright, K. Chandler, D. Bonney, R.F. Wynn, A.M. Will, M. Punekar, S. Loughran, J.P. Kilday, D. Schindler, L. Patel, and S. Meyer. 2015. Central nervous system abnormalities in Fanconi anaemia: patterns and frequency on magnetic resonance imaging. *Br J Radiol*. 88:20150088.

Stone, R.L., J. Aimi, B.A. Barshop, J. Jaeken, G. Van den Berghe, H. Zalkin, and J.E. Dixon. 1992. A mutation in adenylosuccinate lyase associated with mental retardation and autistic features. *Nature genetics*. 1:59-63.

Suhasini, A.N., and R.M. Brosh, Jr. 2012. Fanconi anemia and Bloom's syndrome crosstalk through FANCJ-BLM helicase interaction. *Trends in genetics : TIG*. 28:7-13.

Swisher, E.M., W. Sakai, B.Y. Karlan, K. Wurz, N. Urban, and T. Taniguchi. 2008. Secondary BRCA1 mutations in BRCA1-mutated ovarian carcinomas with platinum resistance. *Cancer Res*. 68:2581-2586.

Sy, S.M., M.S. Huen, and J. Chen. 2009. PALB2 is an integral component of the BRCA complex required for homologous recombination repair. *Proceedings of the National Academy of Sciences of the United States of America*. 106:7155-7160.

Symington, L.S. 2014. End resection at double-strand breaks: mechanism and regulation. *Cold Spring Harb Perspect Biol*. 6.

Taglialatela, A., S. Alvarez, G. Leuzzi, V. Sannino, L. Ranjha, J.W. Huang, C. Madubata, R. Anand, B. Levy, R. Rabadan, P. Cejka, V. Costanzo, and A. Ciccia. 2017. Restoration of Replication Fork Stability in BRCA1- and BRCA2-Deficient Cells by Inactivation of SNF2-Family Fork Remodelers. *Mol Cell*. 68:414-430 e418.

Tamary, H., R. Bar-Yam, L. Shalmon, G. Rachavi, M. Krostichevsky, R. Elhasid, Y. Barak, J. Kapelushnik, I. Yaniv, A.D. Auerbach, and R. Zaizov. 2000. Fanconi anaemia group A (FANCA) mutations in Israeli non-Ashkenazi Jewish patients. *British journal of haematology*. 111:338-343.

Tang, J., N.W. Cho, G. Cui, E.M. Manion, N.M. Shanbhag, M.V. Botuyan, G. Mer, and R.A. Greenberg. 2013. Acetylation limits 53BP1 association with damaged chromatin to promote homologous recombination. *Nature structural & molecular biology*. 20:317-325.

Thangavel, S., M. Berti, M. Levikova, C. Pinto, S. Gomathinayagam, M. Vujanovic, R. Zellweger, H. Moore, E.H. Lee, E.A. Hendrickson, P. Cejka, S. Stewart, M. Lopes, and A. Vindigni. 2015. DNA2 drives processing and restart of reversed replication forks in human cells. *J Cell Biol*. 208:545-562.

Thongthip, S., M. Bellani, S.Q. Gregg, S. Sridhar, B.A. Conti, Y. Chen, M.M. Seidman, and A. Smogorzewska. 2016. Fan1 deficiency results in DNA interstrand cross-link repair defects, enhanced tissue karyomegaly, and organ dysfunction. *Genes & development*. 30:645-659.

Timmers, C., T. Taniguchi, J. Hejna, C. Reifsteck, L. Lucas, D. Bruun, M. Thayer, B. Cox, S. Olson, A.D. D'Andrea, R. Moses, and M. Grompe. 2001. Positional cloning of a novel Fanconi anemia gene, FANCD2. *Molecular cell*. 7:241-248.

Tischkowitz, M., and B. Xia. 2010. PALB2/FANCN: recombining cancer and Fanconi anemia. *Cancer research*. 70:7353-7359.

Toledo, L.I., M. Altmeyer, M.B. Rask, C. Lukas, D.H. Larsen, L.K. Povlsen, S. Bekker-Jensen, N. Mailand, J. Bartek, and J. Lukas. 2013. ATR prohibits replication catastrophe by preventing global exhaustion of RPA. *Cell*. 155:1088-1103.

Trapnell, C., A. Roberts, L. Goff, G. Pertea, D. Kim, D.R. Kelley, H. Pimentel, S.L. Salzberg, J.L. Rinn, and L. Pachter. 2012. Differential gene and transcript expression analysis of RNA-seq experiments with TopHat and Cufflinks. *Nature protocols*. 7:562-578.

Trenz, K., E. Smith, S. Smith, and V. Costanzo. 2006. ATM and ATR promote Mre11 dependent restart of collapsed replication forks and prevent accumulation of DNA breaks. *EMBO J*. 25:1764-1774.

Unk, I., I. Hajdu, K. Fatyol, J. Hurwitz, J.H. Yoon, L. Prakash, S. Prakash, and L. Haracska. 2008. Human HLTF functions as a ubiquitin ligase for proliferating cell nuclear antigen polyubiquitination. *Proc Natl Acad Sci U S A*. 105:3768-3773.

Vaz, F., H. Hanenberg, B. Schuster, K. Barker, C. Wiek, V. Erven, K. Neveling, D. Endt, I. Kesterton, F. Autore, F. Fraternali, M. Freund, L. Hartmann, D. Grimwade, R.G. Roberts, H. Schaal, S. Mohammed, N. Rahman, D. Schindler, and C.G. Mathew. 2010. Mutation of the RAD51C gene in a Fanconi anemia-like disorder. *Nature genetics*. 42:406-409.

Venkitaraman, A.R. 2014. Cancer suppression by the chromosome custodians, BRCA1 and BRCA2. *Science (New York, N.Y.)*. 343:1470-1475.

Vindigni, A., and M. Lopes. 2017. Combining electron microscopy with single molecule DNA fiber approaches to study DNA replication dynamics. *Biophys Chem*. 225:3-9.

Vujanovic, M., J. Krietsch, M.C. Raso, N. Terraneo, R. Zellweger, J.A. Schmid, A. Taglialatela, J.W. Huang, C.L. Holland, K. Zwicky, R. Herrador, H. Jacobs, D. Cortez, A. Ciccia, L. Penengo, and M. Lopes. 2017. Replication Fork Slowing and Reversal upon DNA Damage Require PCNA Polyubiquitination and ZRANB3 DNA Translocase Activity. *Mol Cell*. 67:882-890 e885.

Wagner, J.E., J. Tolar, O. Levran, T. Scholl, A. Deffenbaugh, J. Satagopan, L. Ben-Porat, K. Mah, S.D. Batish, D.I. Kutler, M.L. MacMillan, H. Hanenberg, and A.D. Auerbach. 2004. Germline mutations in BRCA2: shared genetic susceptibility to breast cancer, early onset leukemia, and Fanconi anemia. *Blood*. 103:3226-3229.

Waisfisz, Q., N.V. Morgan, M. Savino, J.P. de Winter, C.G. van Berkel, M.E. Hoatlin, L. Ianzano, R.A. Gibson, F. Arwert, A. Savoia, C.G. Mathew, J.C. Pronk, and H. Joenje. 1999. Spontaneous functional correction of homozygous fanconi anaemia alleles reveals novel mechanistic basis for reverse mosaicism. *Nature genetics*. 22:379-383.

Walden, H., and A.J. Deans. 2014. The Fanconi anemia DNA repair pathway: structural and functional insights into a complex disorder. *Annu Rev Biophys*. 43:257-278.

Waltes, R., R. Kalb, M. Gatei, A.W. Kijas, M. Stumm, A. Sobeck, B. Wieland, R. Varon, Y. Lerenthal, M.F. Lavin, D. Schindler, and T. Dork. 2009. Human RAD50 deficiency in a Nijmegen breakage syndrome-like disorder. *American journal of human genetics*. 84:605-616.

Wamelink, M.M., R.J. Ramos, A.P. van den Elzen, G.J. Ruijter, R. Bonte, L. Diogo, P. Garcia, N. Neves, B. Nota, A. Haschemi, I. Tavares de Almeida, and G.S. Salomons. 2015. First two unrelated cases of isolated sedoheptulokinase deficiency: A benign disorder? *J Inherit Metab Dis*. 38:889-894.

Wang, A.T., T. Kim, J.E. Wagner, B.A. Conti, F.P. Lach, A.L. Huang, H. Molina, E.M. Sanborn, H. Zierhut, B.K. Cornes, A. Abhyankar, C. Sougnez, S.B. Gabriel, A.D. Auerbach, S.C. Kowalczykowski, and A. Smogorzewska. 2015. A Dominant Mutation in Human RAD51 Reveals Its Function in DNA Interstrand Crosslink Repair Independent of Homologous Recombination. *Mol Cell*. 59:478-490.

Wang, A.T., and A. Smogorzewska. 2015. SnapShot: Fanconi anemia and associated proteins. *Cell*. 160:354-354 e351.

Wang, W. 2008. A major switch for the Fanconi anemia DNA damage-response pathway. *Nature structural & molecular biology*. 15:1128-1130.

Weston, R., H. Peeters, and D. Ahel. 2012. ZRANB3 is a structure-specific ATP-dependent endonuclease involved in replication stress response. *Genes Dev*. 26:1558-1572.

Wijker, M., N.V. Morgan, S. Herterich, C.G. van Berkel, A.J. Tipping, H.J. Gross, J.J. Gille, G. Pals, M. Savino, C. Altay, S. Mohan, I. Dokal, J. Cavenagh, J. Marsh, M. van Weel, J.J. Ortega, D. Schuler, E. Samochatova, M. Karwacki, A.N. Bekassy, M. Abecasis, W. Ebell, M.L. Kwee, T. de Ravel, C.G. Mathew, and et al. 1999. Heterogeneous spectrum of mutations in the Fanconi anaemia group A gene. *European journal of human genetics : EJHG*. 7:52-59.

Willis, N.A., G. Chandramouly, B. Huang, A. Kwok, C. Follonier, C. Deng, and R. Scully. 2014. BRCA1 controls homologous recombination at Tus/Ter-stalled mammalian replication forks. *Nature*. 510:556-559.

Wilson, J.B., K. Yamamoto, A.S. Marriott, S. Hussain, P. Sung, M.E. Hoatlin, C.G. Mathew, M. Takata, L.H. Thompson, G.M. Kupfer, and N.J. Jones. 2008. FANCG promotes formation of a newly identified protein complex containing BRCA2, FANCD2 and XRCC3. *Oncogene*. 27:3641-3652.

Wong, M.W., C. Nordfors, D. Mossman, G. Pecenpetelovska, K.A. Avery-Kiejda, B. Talseth-Palmer, N.A. Bowden, and R.J. Scott. 2011. BRIP1, PALB2, and RAD51C mutation analysis reveals their relative importance as genetic susceptibility factors for breast cancer. *Breast cancer research and treatment*. 127:853-859.

Wu, K., S.R. Hinson, A. Ohashi, D. Farrugia, P. Wendt, S.V. Tavtigian, A. Deffenbaugh, D. Goldgar, and F.J. Couch. 2005. Functional evaluation and cancer risk assessment of BRCA2 unclassified variants. *Cancer research*. 65:417-426.

Xia, B., J.C. Dorsman, N. Ameziane, Y. de Vries, M.A. Rooimans, Q. Sheng, G. Pals, A. Errami, E. Gluckman, J. Llera, W. Wang, D.M. Livingston, H. Joenje, and J.P. de Winter. 2007. Fanconi anemia is associated with a defect in the BRCA2 partner PALB2. *Nature genetics*. 39:159-161.

Xia, B., Q. Sheng, K. Nakanishi, A. Ohashi, J. Wu, N. Christ, X. Liu, M. Jasin, F.J. Couch, and D.M. Livingston. 2006. Control of BRCA2 cellular and clinical functions by a nuclear partner, PALB2. *Molecular cell*. 22:719-729.

Xu, G., J.R. Chapman, I. Brandsma, J. Yuan, M. Mistrik, P. Bouwman, J. Bartkova, E. Gogola, D. Warmerdam, M. Barazas, J.E. Jaspers, K. Watanabe, M. Pieterse, A. Kersbergen, W. Sol, P.H.N. Celie, P.C. Schouten, B. van den Broek, A. Salman, M. Nieuwland, I. de Rink, J. de Ronde, K. Jalink, S.J. Boulton, J. Chen, D.C. van

Gent, J. Bartek, J. Jonkers, P. Borst, and S. Rottenberg. 2015. REV7 counteracts DNA double-strand break resection and affects PARP inhibition. *Nature*. 521:541-544.

Xu, S., X. Wu, L. Wu, A. Castillo, J. Liu, E. Atkinson, A. Paul, D. Su, K. Schlacher, Y. Komatsu, M.J. You, and B. Wang. 2017. Abro1 maintains genome stability and limits replication stress by protecting replication fork stability. *Genes Dev*. 31:1469-1482.

Yang, H., P.D. Jeffrey, J. Miller, E. Kinnucan, Y. Sun, N.H. Thoma, N. Zheng, P.L. Chen, W.H. Lee, and N.P. Pavletich. 2002. BRCA2 function in DNA binding and recombination from a BRCA2-DSS1-ssDNA structure. *Science (New York, N.Y.)*. 297:1837-1848.

Yang, H., Q. Li, J. Fan, W.K. Holloman, and N.P. Pavletich. 2005. The BRCA2 homologue Brh2 nucleates RAD51 filament formation at a dsDNA-ssDNA junction. *Nature*. 433:653-657.

Ying, S., F.C. Hamdy, and T. Helleday. 2012. Mre11-dependent degradation of stalled DNA replication forks is prevented by BRCA2 and PARP1. *Cancer Res*. 72:2814-2821.

Ying, S., S. Minocherhomji, K.L. Chan, T. Palmai-Pallag, W.K. Chu, T. Wass, H.W. Mankouri, Y. Liu, and I.D. Hickson. 2013. MUS81 promotes common fragile site expression. *Nat Cell Biol*. 15:1001-1007.

Young, N.S., P. Scheinberg, and R.T. Calado. 2008. Aplastic anemia. *Curr Opin Hematol*. 15:162-168.

Yuan, J., G. Ghosal, and J. Chen. 2009. The annealing helicase HARP protects stalled replication forks. *Genes Dev*. 23:2394-2399.

Yuan, J., G. Ghosal, and J. Chen. 2012. The HARP-like domain-containing protein AH2/ZRANB3 binds to PCNA and participates in cellular response to replication stress. *Mol Cell*. 47:410-421.

Yusufzai, T., and J.T. Kadonaga. 2008. HARP is an ATP-driven annealing helicase. *Science*. 322:748-750.

Yusufzai, T., and J.T. Kadonaga. 2010. Annealing helicase 2 (AH2), a DNA-rewinding motor with an HNH motif. *Proc Natl Acad Sci U S A*. 107:20970-20973.

Zellweger, R., D. Dalcher, K. Mutreja, M. Berti, J.A. Schmid, R. Herrador, A. Vindigni, and M. Lopes. 2015. Rad51-mediated replication fork reversal is a global response to genotoxic treatments in human cells. *J Cell Biol*. 208:563-579.

Zeman, M.K., and K.A. Cimprich. 2014. Causes and consequences of replication stress. *Nat Cell Biol*. 16:2-9.

Zhang, F., Q. Fan, K. Ren, and P.R. Andreassen. 2009a. PALB2 functionally connects the breast cancer susceptibility proteins BRCA1 and BRCA2. *Mol Cancer Res*. 7:1110-1118.

Zhang, F., J. Ma, J. Wu, L. Ye, H. Cai, B. Xia, and X. Yu. 2009b. PALB2 links BRCA1 and BRCA2 in the DNA-damage response. *Curr Biol*. 19:524-529.

Zhang, J., J.M. Dewar, M. Budzowska, A. Motnenko, M.A. Cohn, and J.C. Walter. 2015. DNA interstrand cross-link repair requires replication-fork convergence. *Nature structural & molecular biology*. 22:242-247.

Zhang, J., and J.C. Walter. 2014. Mechanism and regulation of incisions during DNA interstrand cross-link repair. *DNA Repair (Amst)*. 19:135-142.

Zhang, Y., X. Zhou, L. Zhao, C. Li, H. Zhu, L. Xu, L. Shan, X. Liao, Z. Guo, and P. Huang. 2011. UBE2W interacts with FANCL and regulates the monoubiquitination of Fanconi anemia protein FANCD2. *Molecules and cells*. 31:113-122.

Zhou, W., E.A. Otto, A. Cluckey, R. Airik, T.W. Hurd, M. Chaki, K. Diaz, F.P. Lach, G.R. Bennett, H.Y. Gee, A.K. Ghosh, S. Natarajan, S. Thongthip, U. Veturi, S.J.

Allen, S. Janssen, G. Ramaswami, J. Dixon, F. Burkhalter, M. Spoendlin, H. Moch, M.J. Mihatsch, J. Verine, R. Reade, H. Soliman, M. Godin, D. Kiss, G. Monga, G. Mazzucco, K. Amann, F. Artunc, R.C. Newland, T. Wiech, S. Zschiedrich, T.B. Huber, A. Friedl, G.G. Slaats, J.A. Joles, R. Goldschmeding, J. Washburn, R.H. Giles, S. Levy, A. Smogorzewska, and F. Hildebrandt. 2012. FAN1 mutations cause karyomegalic interstitial nephritis, linking chronic kidney failure to defective DNA damage repair. *Nature genetics*. 44:910-915.

Zhu, Z., W.H. Chung, E.Y. Shim, S.E. Lee, and G. Ira. 2008. Sgs1 helicase and two nucleases Dna2 and Exo1 resect DNA double-strand break ends. *Cell*. 134:981-994.

Zou, L., and S.J. Elledge. 2003. Sensing DNA damage through ATRIP recognition of RPA-ssDNA complexes. *Science (New York, N.Y.)*. 300:1542-1548.